Systematics and ecology of the New Zealand Mastigoteuthidae (Cephalopoda, Oegopsida)

Heather Elizabeth Braid

A thesis submitted through the
Earth & Oceanic Sciences Research Institute,
Auckland University of Technology

in partial fulfilment of the
requirements for the degree of
Masters of Applied Science (MAppSc)

supervised by Dr Kathrin Bolstad

2013

TABLE OF CONTENTS

ATTESTATION OF AUTHORSHIP

I hereby declare that this submission is my own work and that, to the best of my knowledge and belief, it contains no material previously published or written by another person (except where explicitly defined in the acknowledgements), nor material that to a substantial extent has been submitted for the award of any other degree or diploma of a university or other institution of higher learning.

_____

Heather E. Braid

LIST OF FIGURES

LIST OF TABLES

MATERIAL EXAMINED ACRONYMS

CAML—Census of Antarctic Marine Life

FV—fisheries vessel

IORAS—P. P. Shirshov Institute of Oceanology of the Russian Academy of Sciences

IPY—International Polar Year

MWT—midwater trawl

NIWA—National Institute of Water and Atmospheric Research, Ltd

NMNZ—Museum of New Zealand Te Papa Tongarewa

NORFANZ—New Zealand and Australia Norfolk Ridge and Lord Howe Rise Biodiversity Voyage

RNZFA—Royal New Zealand Fleet Auxiliary

RV—research vessel

Stn—station

USNM—Smithsonian National Museum of Natural History, USA

ZMB— Zoologisches Museum, Museum für Naturkunde der Humboldt-Universitat, Berlin

ZMBN—University Museum of Bergen

ZIN— Zoological Institute, Russian Academy of Sciences

SPECIMEN MEASUREMENT ACRONYMS

ML—mantle length (dorsal)

MW / MWI—mantle width / index as % of ML

FL / FLI—fin length / index (measured from anterior edge of fin to end of tail)

FW / FWI—fin width / index

HL / HLI—head length / index (measured from anterior tip of nuchal cartilage to separation of Arms I)

HW / HWI—head width / index

ED / EDI—eye diameter / index

ALI—arm length index (arms measured from most-proximal sucker to arm tip)

TL—total length including tentacles

TLA—total length from mantle tip to tip of longest arms

MLC / MLCI—mantle-locking cartilage / index

TnL/ TnLI—tentacle length / index

CL / CLI—tentacle club length / index as % of TnL

GL—gladius length

LRL—lower rostral length

URL—upper rostral length

DEDICATION

To Steve O'Shea, for inspiring my love of squids.

ACKNOWLEDGEMENTS

Most of all, I would like to thank Kat Bolstad for teaching me everything about squid taxonomy, but also for her patience and guidance throughout this process. Thanks to Steve O'Shea for always being available for taxonomic help. Special thanks to my roommate, Aaron Boyd Evans, for making the Apartment of Awesome live up to its name. Thanks to my other lab mate, Jesse Kelly, for late nights in the lab, squid adventures, and encouraging me to look at beaks.

I am grateful to my undergraduate mentor, Bob Hanner, for reagents, lab space, and stories throughout my time in New Zealand—even after I left his DNA barcoding lab to learn traditional taxonomy. There are many people in the Hanner Lab who have assisted me: Amanda Naaum, for a place to crash in Guelph during the completion of my lab work; Andrew Frewin, for his assistance in the lab; and Taryn Athey, for help with lab access. Also at the University of Guelph, I am grateful to Sandy Smith, for helping with critical-point drying of formalin-fixed tissue, Tyler Tunney, for stable isotope advice, Royce Steeves, for advice on difficult DNA extractions, and Jeff Gross for sequencing my DNA extra fast and for the most beautiful sequences.

Thanks to my family, especially Mum and Dad, Wendy and Andy Braid, for all their support while I left to follow my dreams; my sister Debbie Harn, who is always there to talk to; my Granny, Audrey Braid, who never tires of hearing about my adventures in science; and to my Granddad, Philip Braid, who always encouraged my pursuit of science. I am grateful to many friends have provided emotional support. To Katie Arnup, the better half of Trent, who made it all the way here and for making business good. To Natasha Serrao for reassurance, understanding, and sequencing. To Kareen Drot for helping me through the difficult parts. To Justin Scott for being my family in New Zealand. Also to John Wilson, Ariel Levitsky, Chris Ho, and Neil deJong. And also to Gary Peebles, Chris Pook, and Jess Kniller for helping me get through the final stages.

I would like to thank Adrian Turner at the Auckland University for assistance with critical-point drying, and Patrick Conor at AUT for platinum plating, imaging assistance, and sharing in the excitement of looking at squid bits. Histology would not have been possible without Adam Rusk, who taught me the necessary skills, and Karin Lohrmann, who provided me with staining protocols. Thanks to Bríd Lorigan for all of her help with everything from card access to finding funding for stable isotope work. To Matt Jones for input on the morphological identification of stomach contents. And to Paul McBride for help with tree building, and for reassurance that *Idioteuthis cordiformis* is making the story more interesting, rather than painful.

I would like to thank the museums and institutions that made this study possible. The Smithsonian, particularly Tyjuana Nickens, for technical help, and Mike Vecchione, for his time and tissue samples, which made the genetics chapter possible, and for assistance in comparing species in the *magna* group. I would also like to thank Dick Young for his input on the *magna* group as well. At the IORAS, I would like to thank Andrey Gebruk for his assistance with collection data. NIWA, especially Darren Stevens for tissue samples and beaks, Sadie Mills and Kareen Schnabel who were always fast to provide specimen data, and Dean Stotter and Mark Fenwick. Te Papa, particularly Bruce Marshall for samples, assistance, and extensive taxonomic insight.

And to the squids that were used in this study.

ABSTRACT

Mastigoteuthid squids are ecologically important, being prey to many apex predators, yet the diversity and systematics of the family remain poorly understood. Delicate by nature, they are often damaged during capture; this has led to a controversial and unstable taxonomy for this family. Recent reviews have accepted one or two genera, and eight to 17 species. A complete taxonomic review of the New Zealand mastigoteuthids is undertaken here first time. A morphological revision of New Zealand material was completed to identify and describe locally occurring species, and to re-evaluate the status of the genera in this family. Morphological examinations focused on both internal and external anatomy. A set of morphological characters have been identified to distinguish five genera: *Mastigoteuthis* [*Mt*.]*, Idioteuthis, Mastigopsis* [*Mp*.]*, Echinoteuthis,* and *Magnoteuthis* [*Mg*.]. Eight species were identified: *Mt. dentata*, *Mt. psychrophila*, *Mt.* sp. X, *Mt.* sp. Y, *I. cordiformis*, *Mp. hjorti*, *Mg*. sp. nov., and *E. famelica*. The Mastigoteuthidae now appears to be second most diverse squid family in New Zealand waters.

Three mitochondrial genes (16S rRNA, 12S rRNA and cytochrome *c* oxidase subunit I [COI]) were analysed for eight different species, in order to assess the utility of DNA barcodes to differentiate between species and to test the morphological hypothesis for the division of the five genera. Genetic evidence was found that supports *Mg.* sp. nov. as a distinct species that has been previously misidentified as the morphologically similar species *Mg. magna*. Each species analysed herein exhibited unique mitochondrial DNA haplotypes for all genes, and the morphological distinction between the genera was strongly supported using a combined phylogeny with all genes. However, *I. cordiformis* grouped with the chiroteuthids. Of the three genes examined, the DNA barcode region shows the greatest divergence between species and should be used in future systematic work on the Mastigoteuthidae.

Because most mastigoteuthid specimens are badly damaged, integrative taxonomy is especially important for this family. Unfortunately, most specimens are formalin fixed, rendering DNA extraction difficult or impossible. Therefore, some preliminary tests were conducted on DNA from formalin-fixed museum specimens. Two sequences were recovered out of eight specimens tested using a silica-gel column-based extraction, with critical-point-dried tissue and a DNA purification protocol. The third sequence was

recovered using an alkaline lysis extraction, with non-critical-point-dried tissue and without DNA purification. The sequences that were recovered showed a close relationship between *Mt. agassizii*, *Mt. dentata*, and *Mt*. sp. X.

Idioteuthis cordiformis is the largest mastigoteuthid squid species and may currently be facing the potential of a local extinction in New Zealand; however, its ecology has not been previously studied. Therefore, stable isotopes ^{15}N and ^{13}C were analysed to find the trophic position and the source of carbon, respectively, and gut contents were examined using DNA barcoding. Stable isotopes revealed a correlation between $\delta^{15}N$ and $\delta^{13}C$ values, and *I. cordiformis* $\delta^{15}N$ indicated that it occupies a high trophic position. Morphological analysis was not successful in identifying prey items below class, while DNA barcoding was able to identify two prey species: snapper (*Lutjanus* sp.), and birdbeak dogfish (*Deania calcea*).

Although a review of the systematics of the New Zealand Mastigoteuthidae has been completed, a full review of this family is still required; an integrative taxonomic approach will be essential because there is often low interspecific and high intraspecific morphological variation. This will require continued collection efforts for new specimens, along with further research into DNA extraction from formalin-fixed tissue. In addition, future studies should also focus on the dietary habits and trophic position of mastigoteuthids in order to better understand their ecological importance.

CHAPTER 1: General introduction

The squid family Mastigoteuthidae, commonly known as whip-lash squid, was first established by Verrill in 1881 with the type genus and species *Mastigoteuthis agassizii*. Members of this meso- to bathypelagic family have been recorded from all oceans except for the Arctic; some species have circumglobal distributions, while others are endemic to certain regions. Mastigoteuthids are not commercially valuable; however, like many species not specifically targeted by fisheries, they can still be affected by anthropogenic disturbances (Hitchmough, Bull, & Cromarty, 2005). They have been found in the diets of a variety of marine predators including marine mammals (Santos et al., 2001; Evans & Hindell, 2004; Mintzer et al., 2008), seabirds (Cherel, Weimerskirch, & Trouvé, 2002; Xavier, Croxall, Trathan, & Rodhouse, 2003; Wienecke & Robertson, 2006), and commercially important fishes (Horn & Dunn, 2010; Rosecchi, Tracey, & Webber, 1988). As predators, mastigoteuthids are likely passive, drifting in the water column with their tentacles hanging down, and relying primarily on their fins, rather than jet-propulsion, for motion (Dilly, Nixon, & Young, 1977; Roper & Vecchione, 1997). Very little is known about the diet of mastigoteuthids, but *Mt. psychrophila* has been found to consume euphausiids (Kear, 1992).

Mastigoteuthids are characterised by long, whip-like tentacles that do not expand into well-defined clubs and are covered with hundreds of microscopic suckers in most species. The arms bear two series of suckers, and Arms IV are enlarged. The funnel-locking cartilage morphology varies between species, and can be oval, ear, or flask shaped. The buccal formula is DDVV. Eye photophores are present in *Mt. cordiformis*, *Mt. hjorti, Mt.* sp. Y, *Idioteuthis okutanii*, and potentially *Magnoteuthis* sp. nov.; however, they are believed to be absent in all other species. Some species have integumental photophores, while photophores are entirely absent in others. Most species in this family mature at a mantle length (ML) of less than 250mm, but one species, *I. cordiformis*, attains mantle lengths greater than 1000mm.

Although they are ubiquitous in the ocean, mastigoteuthids are deep-sea squid rarely caught in large numbers, and usually badly damaged by capture; this has contributed to the taxonomic confusion in this family. Most species have been described from single, juvenile, and/or badly damaged specimens (Roper, Young, & Voss, 1969). Furthermore, cephalopod species descriptions were not standardised until Roper and Voss (1983)

published a list of recommended characters. Unfortunately, most mastigoteuthid species descriptions were published prior to this and therefore are lacking important details.

No complete review of this family has ever been undertaken. Out of the 21 named species and three genera, recent reviews have accepted the number of genera and species as two and eight, respectively (Salcedo-Vargas & Okutani, 1994), one and 13 (Vecchione, Young, & Lindgren, 2007), two and 14–18 (Nesis, 1987), and two and 17 (Salcedo-Vargas, 1997). Here, a local systematic review of mastigoteuthids found around New Zealand and adjacent waters has been undertaken for the first time.

Family and generic nomenclature

The Chiroteuthidae and Mastigoteuthidae, currently grouped together informally in the 'chiroteuthid families' (Young & Vecchione, 2008) along with the Batoteuthidae, Magnapinnidae, and Joubiniteuthidae, share many characters and have, at times, been classified as a single family. Both families have enlarged fourth arms, ear-shaped funnel-locking cartilage in some species, and photophores in most species. Pfeffer (1900) suggested that Mastigoteuthidae should be a subfamily under Chiroteuthidae. Chun (1908) agreed, but divided Chiroteuthidae into three subfamilies: Mastigoteuthinae, Chiroteuthinae, and Grimalditeuthinae. Mastigoteuthids' status as a subfamily was maintained by Pfeffer (1912), Grimpe (1922), Naef (1921–1923), Sasaki (1916, 1929), Joubin (1924), Thiele (1935), Voss (1956), Clarke (1966), and Rancurel (1972). However, the full family status of Mastigoteuthidae was supported by Roper et al. (1969), Young (1972), Nesis (1987), and Clarke & Trueman (1988).

Three genera have been described within the Mastigoteuthidae: *Mastigoteuthis* Verrill, 1881, *Idioteuthis* Sasaki, 1916, and *Echinoteuthis* Joubin, 1933; however, only one (Young, 1991; Vecchione et al., 2007) or two (Salcedo-Vargas & Okutani, 1994; Salcedo-Vargas 1997) are currently accepted. The second genus, *Idioteuthis*, was established by Sasaki (1916) when he described *I. latipinna*. However, shortly thereafter, Sasaki (1929) synonymised *Idioteuthis* with *Mastigoteuthis*. Salcedo-Vargas (1993) resurrected *Idioteuthis* when he revised the species found in the northwestern Pacific, and Salcedo-Vargas & Okutani (1994) described several morphological characters that separate these two genera and placed *Mt. hjorti*, *Mt. cordiformis*, and *Mt. magna* in *Idioteuthis*. Subsequently, Salcedo-Vargas (1997) moved *Mt. magna* into

Mastigoteuthis, despite the presence of characters used in his study that could classify this species as *Idioteuthis*. The third genus, *Echinoteuthis*, was established by Joubin (1933) when he described *E. danae*, because of the presence of skin tubercles; this character had been previously reported for *Mt. cordiformis* (Chun, 1910; Sasaki, 1929) but this seems to have been overlooked by Joubin (1933). Young (1991) synonymised *Echinoteuthis* with *Mastigoteuthis* because skin tubercles are, in fact, found in species that he believed belong in *Mastigoteuthis*, such as *Mt. famelica*. Salcedo-Vargas later (1997) transferred both *E. danae* and *Mt. famelica* into *Idioteuthis* due to the presence of skin tubercles.

At times, subgenera have also been described within the Mastigoteuthidae. Grimpe (1922) added the subgenus *Mastigopsis* for *Mt. hjorti*. Nesis (1987) maintained that *Mastigoteuthis* was divided into two subgenera: *Mastigoteuthis* (s. str.), which consisted of most species, and *Mastigopsis* (Grimpe, 1922), which only consisted of *Mt. hjorti* (Nesis, 1987). Salcedo-Vargas and Okutani (1994) divided *Mastigoteuthis* into the subgenera *Echinoteuthis* (for *Mt. famelica*, *Mt. glaukopis, Mt. atlantica, and Mt. pyrodes*), and *Mastigoteuthis* (for *Mt. agassizii*). They also divided *Idioteuthis* into *Idioteuthis* (for *Mt. cordiformis* and *Mt. hjorti*) and *Magnoteuthis* (for *Mt. magna*). However, Salcedo-Vargas (1997) rearranged the taxonomy considerably and did not maintain any subgenera, but rather arranged sets of species together into 'groups'. Recently, certain species have been placed into groups based on morphological similarities including the *Mt. agassizii* group, the *Mt. glaukopis* group, and the *Mt. magna* group (Vecchione et al., 2007).

Interfamily confusion

The morphological similarities among the 'chiroteuthid families' have occasionally led to confusion and caused species to be attributed to incorrect families. True members of the Chiroteuthidae are differentiated by tentacle morphology and the 'doratopsis' stage (Young & Roper, 2011a); however, without a complete ontogenetic series or tentacles, the classification is easily confused. This has led to species being originally described within one family, and later being re-classified into another. Both *Mt. grimaldii* Joubin, 1895, and *Mt. famelica* Berry, 1909, were originally placed in *Chiroteuthis*. Pfeffer (1900) named a new genus, *Chiroteuthopsis*, for *Mt. grimaldii,* based on the funnel-locking cartilage and gladius morphology. However, he later synonymised this genus

with *Mastigoteuthis* (Pfeffer, 1912). Fischer and Joubin (1907) described *Chiroteuthopsis talismani* from a single, badly damaged specimen. Chun (1910) synonymised *Chiroteuthopsis* with *Mastigoteuthis* after examining the tentacles on an intact *Mt. grimaldii* specimen; Sasaki (1929) supported *Chiroteuthopsis* as a synonym of *Mastigoteuthis*. Young (1972) and Nesis (1987) classified *C. talismani* within *Mastigoteuthis*, but it was later transferred to the genus *Magnapinna* in the family Magnapinnidae Vecchione and Young, 1998 (Vecchione & Young, 2006a). Lönnberg (1896) described *'Mastigoteuthis' levimana*, which was later transferred to the genus *Valbyteuthis* in Chiroteuthidae (Young, 1972); this genus was subsequently synonymised to *Planctoteuthis* (Young, 1991). Berry (1920) described *'Chiroteuthoides' hastula* from a paralarva before distinguishing characters were recognised that placed it in *Mastigoteuthis* (Young, 1991).

Descriptions based on paralarvae

Descriptions based on paralarvae have created further confusion. Because full ontogenetic series are not available for most species, the status of taxa known from limited life stages remains unclear, as some may represent previously named species that are only known from more mature specimens. The first species described from a paralarva was *'Chiroteuthoides' hastula* (Berry, 1920) from the Northwest Atlantic and, as noted above, the genus was erected specifically for this species. It was recognised as a paralarval *Mastigoteuthis* by Naef (1921–1923) but Nesis (1987) considered it a valid genus. Young (1991) stated that *Mt. hastula* is not a doratopsis, and therefore not a chiroteuthid, and possesses characteristics of mastigoteuthid paralarvae (long Arms IV, extremely short Arms III); however, it is unlikely that *Mt. hastula* can ever be identified to species because it lacks chromatophore patterns. It is therefore generally considered a *species dubium* (Young & Vecchione, 2004). Joubin (1933) described *Echinoteuthis danae* from three young specimens total length (TL) 17 and 45mm, and one 61mm from tail to arm tip, from the North Atlantic, and Salcedo-Vargas (1997) has recently reported this species from the Indian Ocean near Somalia; however, it has been considered a junior synonym of *Mt. famelica* (Salcedo-Vargas & Okutani, 1994), while Vecchione and Young (2007a) suggested that *E. danae* could be a young specimen of another species, possibly *Mt. atlantica*.

In addition to reporting paralarval *E. danae* from the Indian Ocean, Salcedo-Vargas (1997) added two new species to this family based on paralarvae from the Western Indian Ocean, off the coast of Somalia. *Idioteuthis okutanii* is characterised by having two eye photophores and oval funnel-locking cartilage; however, both these characteristics are shared with *Mt. hjorti*. *Idioteuthis okutanii* can reportedly be differentiated from *Mt. hjorti* of a similar size by the smaller eyes, narrower fin, and shorter tail. However, due to the similarities between the two species, and because the paralarval *Mt. hjorti* was discussed but not described by Salcedo-Vargas (1997), *I. okutanii* has been considered a junior synonym of *Mt. hjorti* (Young & Vecchione, 2004). Additionally, Salcedo-Vargas (1997) described *I. tyroi* from a single paralarva; this species is distinct from previously described mastigoteuthid paralarvae because it possesses expanded tentacle clubs (Salcedo-Vargas & Young, 2007). *Mastigoteuthis cordiformis* is the only other species known to have slightly expanded tentacle clubs, but it has not been found in the Indian Ocean, which is the type locality of *I. tyroi* (Salcedo-Vargas & Young, 2007).

The Mt. grimaldii *complex*

The *Mt. grimaldii* complex consists of several species that are very similar morphologically, including members of the *Mt. agassizii* group, many of which currently have an uncertain status (Young & Vecchione, 2007a). *Mastigoteuthis agassizii* is the oldest described species in this group, and was described based on two damaged specimens from the Northwest Atlantic (Verrill, 1881). Shortly thereafter, *'Chiroteuthis' grimaldii* was described by Joubin (1895) from a single damaged specimen from the Azores. Salcedo-Vargas (1993) suggested that *Mt. grimaldii* and *Mt. agassizii* were the same species, but later (1997) considered both to be valid. Hoyle (1904) described *Mt. dentata* from two specimens caught in the Pacific Ocean, near the Galapagos Islands, stating that it differed from *Mt. agassizii* in the dentition of the arm-sucker rings. However, Vecchione and Young (2006b) stated that, contrary to the original description, the type for *Mt. agassizii* does not have smooth sucker rings, and that reliable characters have not yet been found to separate these two species. After *Mt. dentata*, *Mt. flammea* Chun, 1908 was the next species to be described, based on two specimens from the Guinea Current in the Atlantic that were lacking tentacles. According to Chun (1908), *Mt. flammea* differs from previously named species by the small size of the eyes, and the presence of an antitragus in the funnel-locking cartilage.

Nesis (1987) considered *Mt. flammea* a valid species, while Salcedo-Vargas (1997) synonymised *Mt. flammea* with *Mt. grimaldii*. However, Vecchione and Young (2007b) suggested that these two species may both be junior synonyms of *Mt. agassizii*. Degner (1925) described *Mt. schmidti* from a single specimen in relatively good condition caught in the Eastern North Atlantic in the Bay of Biscay. Nesis (1987) suggested that *Mt. schmidti* was likely a junior synonym of *Mt. grimaldii*; Salcedo-Vargas (1997) suggested that *Mt. schmidti* is a junior synonym for *Mt. agassizii*; and Vecchione and Young (2007b) considered both species to be junior synonyms of *Mt. agassizii* because there are no reliable characters for their separation.

Nesis (1977) added the latest member to this species complex, *Mt. psychrophila*, based on several specimens caught in sub-Antarctic waters. This species is distinguished from other members of the *Mt. grimaldii* complex by a strong antitragus in the funnel-locking cartilage and the dentition on the arm-sucker rings (Nesis, 1977). Although this species has been synonymised with *Mt. agassizii* (Salcedo-Vargas & Okutani, 1994) and suggested for re-evaluation (Salcedo-Vargas, 1997) some recent authors consider it valid (Young & Vecchione, 2010). Two additional species have been considered part of the *Mt. grimaldii* complex, but not the *Mt. agassizii* group because they can be reliably distinguished from the others. Young (1972) described *Mt. pyrodes* from specimens caught in the Northeast Pacific, off the coast of California, and it is the only *Mastigoteuthis* species known from this area. Nesis (1977) considered *Mt. pyrodes* part of the *Mt. grimaldii* complex, but it has distinctive features that separate it from the complex: the eye-sinus photophores are larger than the integumental photophores, the chromatophores are more abundant, the photophore structure is unique, and the mantle-locking cartilage is not nose shaped (Young & Vecchione, 2007b).

The Mt. glaukopis *group*

Three species are included in the *Mt. glaukopis* group: *Mt. glaukopis*, *Mt. famelica*, and *Mt. atlantica* (Young & Vecchione, 2007c). This group is characterised by a relatively large eye-sinus photophore and the lack of any other photophores. Chun (1908) described the first species, *Mt. glaukopis*, from a single immature specimen of ML 37mm caught from the Indian Ocean by the East African coast. Joubin (1933) then described the subspecies *Mt. glaukopis atlantica*, based on a specimen from the Atlantic. However, it was elevated to full species status by Young (1972). The best-

known species in this group is *'Chiroteuthis' famelica* Berry, 1909, which was described from a single immature ML 39mm specimen caught near Kauai in the central Pacific. Nesis (1980) incorrectly synonymised this species with *'Chiroteuthis' acanthoderma* and placed them both in the new genus *Asperoteuthis*. Young (1991) identified this error after examining adult *Mt. famelica* specimens whose features place it in *Mastigoteuthis*. MacDonald and Clench (1934) described *Mt. iselini* from a single, ML 52mm, damaged specimen missing both tentacles from the Northwest Atlantic; this species was supposedly distinguished by fin length (~67% ML), and an apparent complete lack of photophores, but its gladius structure was similar to that of *Mt. grimaldii*. *Mastigoteuthis iselini* has since been synonymised with *Mt. glaukopis* (Salcedo-Vargas & Okutani, 1994) and with *Mt. atlantica* (Nesis, 1987), suggested to be re-evaluated (Salcedo-Vargas, 1997), and considered a *species dubium* (Young, 1972; Young & Vecchione, 2004). Salcedo-Vargas (1997) grouped *Mt. glaukopis*, *Mt. atlantica*, *Mt. iselini*, and *Mt. psychrophila* together under *Mastigoteuthis*, while he grouped *Mt. famelica* with *Mt. danae* and *I. tyroi* under *Idioteuthis*.

The Mt. magna *group*

The *Mt. magna* group consists of four species that all share flask-shaped funnel-locking cartilage and microscopic tentacular suckers (even smaller than those of other species in this family) (Young & Vecchione, 2007d). *Mastigoteuthis magna* was described by Joubin (1913) from a single specimen that had lost its tentacles, from the Sargasso Sea in the North Atlantic. The second species in this group, described by Rancurel (1972), was *Mt. inermis* from the Eastern North Atlantic near the Ivory Coast off Africa. *Mastigoteuthis inermis* has an undulating fin that is narrower than *Mt. magna* (53% and 79.5% respectively) (Rancurel, 1972), and has been considered a junior synonym of *Mt. magna* by some authors (Young & Vecchione, 2004; Salcedo-Vargas & Okutani, 1994), while others maintain its validity (Nesis, 1987; Salcedo-Vargas, 1997). The most recently described mastigoteuthid species is *Mastigoteuthis microlucens* (Young, Lindgren, & Vecchione, 2008). Paralarvae found near Hawaii were initially identified as *Mt. inermis* by Young (1991), but later found to be *Mt. microlucens* (Young, Vecchione, & Lindgren, 2008). The characteristic microscopic photophores of *Mt. microlucens* were initially overlooked because of their small size and the morphological similarities of species in the *Mt. magna* group (Young, Lindgren, & Vecchione, 2008). A potential third species in this family, *Mt.* 'type beta', is only known from a single

specimen caught from sub-Antarctic waters, but has not been formally described (Young & Vecchione, 2007e).

Other mastigoteuthids

Mastigoteuthis cordiformis was described by Chun (1908) from a single juvenile specimen, ML 83mm, caught in the Indian Ocean near Sumatra, and named for its heart-shaped fins. This is the largest species in the family, attaining ML >1m and weights of over 75kg (Steve O'Shea, pers. comm.). The status of this species, the only mastigoteuthid whose potential endangered status has been assessed, is considered nationally critical in New Zealand waters because of its greatly reduced occurrence as bycatch in commercial fishing nets (Freeman, 2010). The exact time frame for the decline in the *Mt. cordiformis* population is unclear because there are no specific records for *Mt. cordiformis* in the Ministry of Primary Industries trawl database. This is because specimen identifications rely on the taxonomic knowledge of the crew, who are not taxonomists. However, the first local record of a mastigoteuthid in this database is in 1985; due to the high weight (~5kg) of the specimen, it was likely *Mt. cordiformis*.

Sasaki (1916) described *I. latipinna* from a single specimen ML 238mm that happened to be the largest mastigoteuthid ever reported at the time. *Idioteuthis latipinna* has been maintained by Young (1972), Nesis (1987), and Salcedo-Vargas (1997), but it was considered a junior synonym of *Mt. cordiformis* by Salcedo-Vargas and Okutani (1994) and Young and Vecchione (2004). Chun (1910) described *Mastigoteuthis hjorti* from several damaged specimens caught in the North Atlantic. The most striking features of this new species were the two round photophores on each eye, while all other known mastigoteuthids lacked eye photophores, and the rhombic sculpture on the skin, which resembled scales. No additional specimens were reported until Rancurel (1973), who determined that the skin 'sculpture' was actually impressions left by the nets during capture.

The extensive taxonomic uncertainty within this family has resulted from species being misclassified within the chiroteuthid families, described from paralarvae, and inadequately described. The phylogenetic relationships among species and the validity of the different genera are uncertain; even the number of valid species is considerably debated. These taxonomic problems are a hindrance to ecology and conservation. The

dietary habits of mastigoteuthids remain largely unknown because few studies have been conducted, and most knowledge is based on speculation. One species in New Zealand, *Mt. cordiformis*, has been classified as nationally critical (Freeman, 2010); however, the impact of its decline on the ecosystem remains uncertain because its ecology has been poorly studied. In addition, the true diversity of New Zealand mastigoteuthid species remains unknown, with new or unrecorded species likely to exist since this family has not been previously been reviewed in this region. For these reasons, this regional review has been undertaken.

Objectives

The overall goal of this project was to increase the knowledge of the Mastigoteuthidae occurring in New Zealand, using three specific objectives:

1. Redescribe known species, and identify and describe potentially new species locally occurring around New Zealand, in accordance with modern systematic standards, and incorporating genetics when possible, including attempts to extract DNA from formalin-fixed tissue.
2. Resolve the higher classification in this family using combined morphology and genetics.
3. Increase ecological knowledge of this family.

Thesis organisation

The present study is an investigation of the squid family Mastigoteuthidae with an emphasis on the New Zealand region, with tissue from additional specimens from the Northwest Atlantic opportunistically included for a more robust molecular examination. This thesis is divided into four parts. First (Chapter 2), a morphological revision of New Zealand material is completed to identify and describe locally occurring species. Second (Chapter 3), the inter- and intraspecific divergences for COI, 16S rRNA, and 12S rRNA are evaluated for their ability to identify species and investigate the morphological divisions found between genera. Third (Chapter 4), some preliminary tests are conducted to attempt to extract DNA from formalin-fixed museum specimens. Fourth (Chapter 5), insight into the ecology of this family is obtained from stomach contents and stable isotopes for ^{13}C and ^{15}N are evaluated for *I. cordiformis* and one specimen of *Magnoteuthis* sp. nov. from New Zealand waters.

CHAPTER 2: Systematics of New Zealand Mastigoteuthidae (Cephalopoda, Oegopsida)

INTRODUCTION

A meso- and bathypelagic family, mastigoteuthids are distinguished from other squids by their long whip-like tentacles. Characters that have previously been relied upon heavily for species identification are mostly lost or damaged during capture, rendering identification difficult. Additional difficulties include species being described only from paralarvae, single damaged specimens, and descriptions that lack adequate detail. Because specimens are frequently damaged and rarely caught in large numbers, there has been a great deal of confusion in their taxonomy. Higher taxonomy also remains unstable with several genera and subgenera named but currently debated.

Within New Zealand waters, mastigoteuthid squids have been found in the diets of a variety of marine predators, including sperm whales, *Physeter macrocephalus* (Clark & Roper, 1998), orange roughy, *Hoplostethus atlanticus* (Rosecchi, Tracey, & Webber, 1988), hoki, *Macruronus novaezelandiae* (Horn & Dunn, 2010), and black oreo, *Allocyttus niger* (*Mastigoteuthis* sp., NIWA 84373). Interestingly, several local species of birds also consume mastigoteuthids, including sooty shearwaters, *Puffinus griseus* (Cruz et al., 2001), Buller's mollymawk, *Diomedea bulleri* (West & Imber, 1986), Providence Petrel, *Pterodroma solandri* (Bester, Priddel, & Klomp, 2010), southern Buller's albatross, *Diomedea bulleri bulleri* (James & Stahl, 2000), and the Snares Penguin, *Eudyptes robustus* (Mattern, Houston, Lalas, Setiawan, & Davis, 2009). Because mastigoteuthids are trophically important in local ecosystems, it is important to determine their true local diversity and how best to identify these species.

Very little is known about the mastigoteuthid squids in New Zealand; they were first reported from local waters just 50 years ago by Dell (1959), who identified three specimens from Cook Strait as *Mt. flammea*. Unfortunately, his illustration of this material lacked detail and the specimens were not described. During a review of the biodiversity of New Zealand, Spencer, Marshall, and Willan (2009) compiled a list of mastigoteuthids in New Zealand identified from previous works consisting of : *Idioteuthis cordiformis*, *I. magna*, *Mastigoteuthis agassizii*, and *Mt.* sp. 1 and *Mt.* sp. 2. The taxonomic classifications were based on Salcedo-Vargas and Okutani (1994) and

these species were identified from specimens found in the collections of the Museum of New Zealand Te Papa Tongarewa and the National Institution of Water and Atmospheric Research, Ltd (NIWA). A more recent list of New Zealand mastigoteuthids reported three species: *I. cordiformis* and *I. magna* as cited in Spencer, Marshall, and Willan (2009), and *Mt. agassizii* (which were synonymised with *Mt. dentata* and *Mt. flammea* following Salcedo-Vargas & Okutani, 1994). In addition to identifying *Mt. dentata* as occurring in New Zealand, Nesis (1987) identified *Mt. magna*, *Mt. hjorti* and *Echinoteuthis* sp. as occurring in the Tasman Sea, and *Mt. psychrophila* as having a circumglobal Antarctic distribution.

Reviewing the taxonomy of the Mastigoteuthidae around New Zealand is essential in order to make informed decisions about the management of anthropogenic threats to their habitat. These are meso- and bathypelagic species that have the potential to be affected by trawling activity (Freeman et al., 2010). The local population of one species, *I. cordiformis* (the largest, most easily recognisable species in this family), has already been classified as nationally critical (Freeman et al., 2010). However, the threat status for other locally occurring species has not been evaluated.

Much of the work on the Mastigoteuthidae has focused on species found around the United States (*e.g.* Young, 1972; Young, 1991; Vecchione et al., 2007). In addition, Salcedo-Vargas (1993) reviewed the Mastigoteuthidae from the northwestern Pacific. However, the taxonomy of the New Zealand mastigoteuthids has not been previously reviewed. The purpose of this study is to identify species of mastigoteuthid squid that occur locally, and evaluate their higher taxonomic classifications.

MATERIALS & METHODS

Materials examined

Original type descriptions for all mastigoteuthid species were reviewed. Type specimens from the Smithsonian National Museum of Natural History, USA (USNM) were examined for *Mt. agassizii*, *Mt. dentata*, *Mt. hastula*, *Mt. microlucens*, and *Mt. famelica*. The entire national collections of mastigoteuthid specimens were loaned and examined from Museum of New Zealand Te Papa Tongarewa (NMNZ) and the National Institute of Water and Atmospheric Research, Ltd (NIWA), in Wellington.

Species synonymies are limited to citations that provide morphological species descriptions and/or images, and descriptions based on type specimens.

Collection data for some of the specimens were not available (mostly ex-gut-content material). A distribution map shows the location for all New Zealand specimens of Mastigoteuthidae used in this study (Fig. 1). Collection dates are listed as dd/mm/yyyy. Specimens are listed by order of decreasing latitude, and secondarily by dorsal mantle length (ML). Specimens were sexed except juveniles and those where the viscera were damaged (indicated 'sex indet.'). Specimens that were too damaged to be identified to species morphologically, and where no tissue was available for DNA analysis, were excluded from this study (four out of 98 available specimens).

Morphological examination

Species descriptions were made in accordance with the guidelines provided by Roper and Voss (1983) with some modification. Morphological descriptions focus on both internal (beak, gladius, radula, and palatine palps) and external anatomy. The latter characters include mantle shape; fin shape, width, and length; head shape; presence/absence of funnel pocket; funnel-locking cartilage shape, presence/absence of tragus and antitragus (Fig. 2A); mantle-locking cartilage shape; nuchal cartilage shape; arm length relative to ML; presence/absence of arm keels; arm- and tentacle-sucker ultrastructure (Fig. 2B, C); and presence/absence and position of photophores. Fin margin undulation was observed as either undulating ('wavy') or planar (flat). The funnel pocket is a depression between the bridles of the funnel. The eye-sinus photophore is embedded in the tissue just ventral to the eye sinus, while the eye photophore is situated on the eye itself, and integumental photophores are situated on any external surface of the body (mantle, arms, fins, head, or funnel).

Measurements (Fig. 3) were taken from the more complete side of the specimen (indicated in tables by R or L). Indices are based on the feature's dimension as a percentage of the mantle length; specific definitions are given below. Measurement ranges are given in the format of lowest value (X), mean (*Y*), and largest value (Z) in the format of X–*Y*–Z; where less than three specimens were available for a species, or when the range was less than 5% ML, only the mean is provided. Measurements of damaged features are indicated by a star (*).

Beaks were described following Clarke (1986), and drawn using a camera lucida (or when too large, from photographs) (Fig. 4A–D). For scanning electron microscopy (SEM), specimens were critical-point dried at the University of Auckland, then platinum plated and imaged at the Auckland University of Technology. Sucker descriptions were based on Salcedo-Vargas (1995) with some modifications (Fig. 2B, C). Palatine teeth on the lateral buccal palps are described following Bolstad (2010). Radular tooth descriptions followed Bolstad (2010) with some modifications (Fig. 4E).

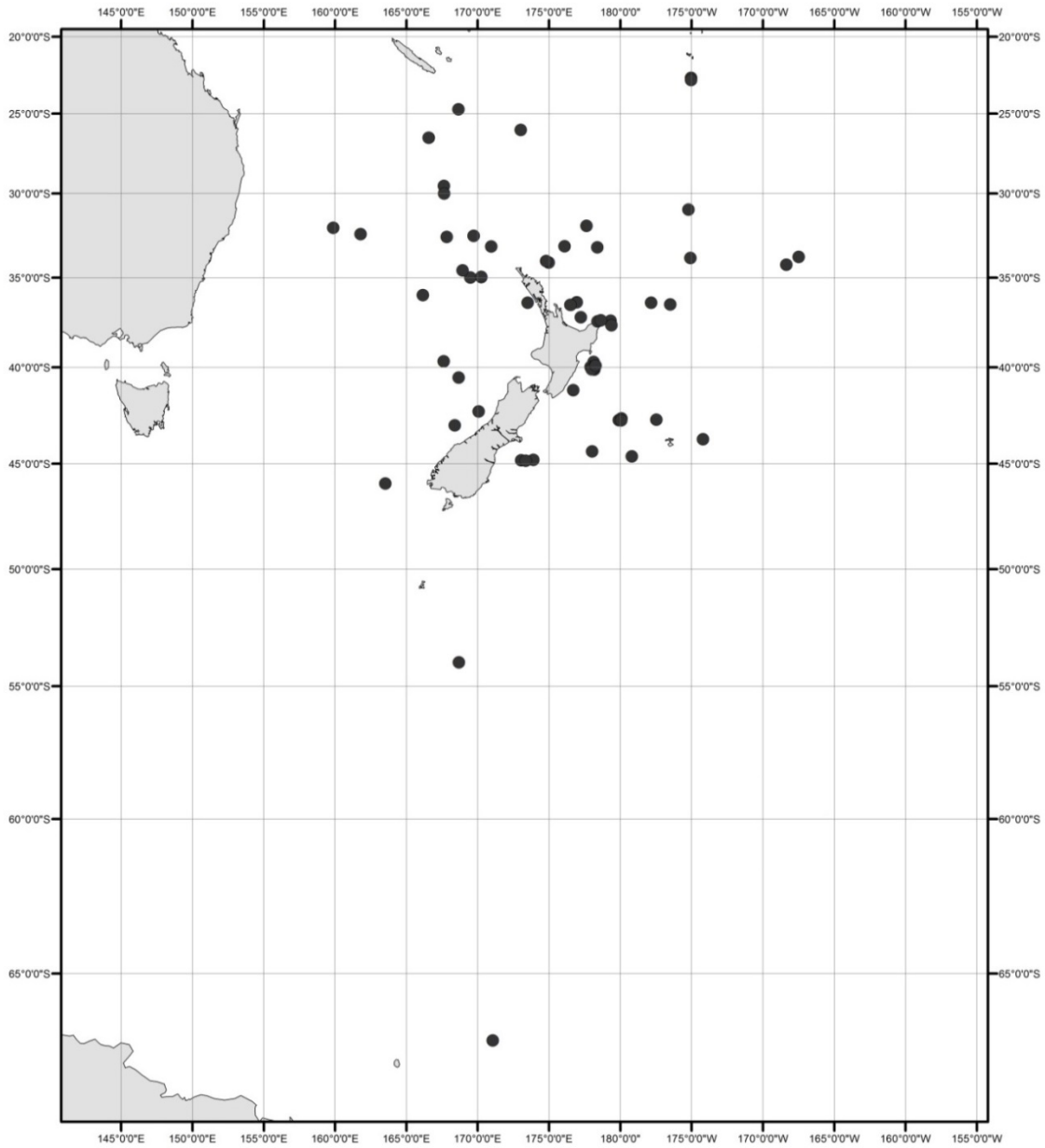

Fig. 1—Geographic distribution of New Zealand mastigoteuthid specimens examined in this study.

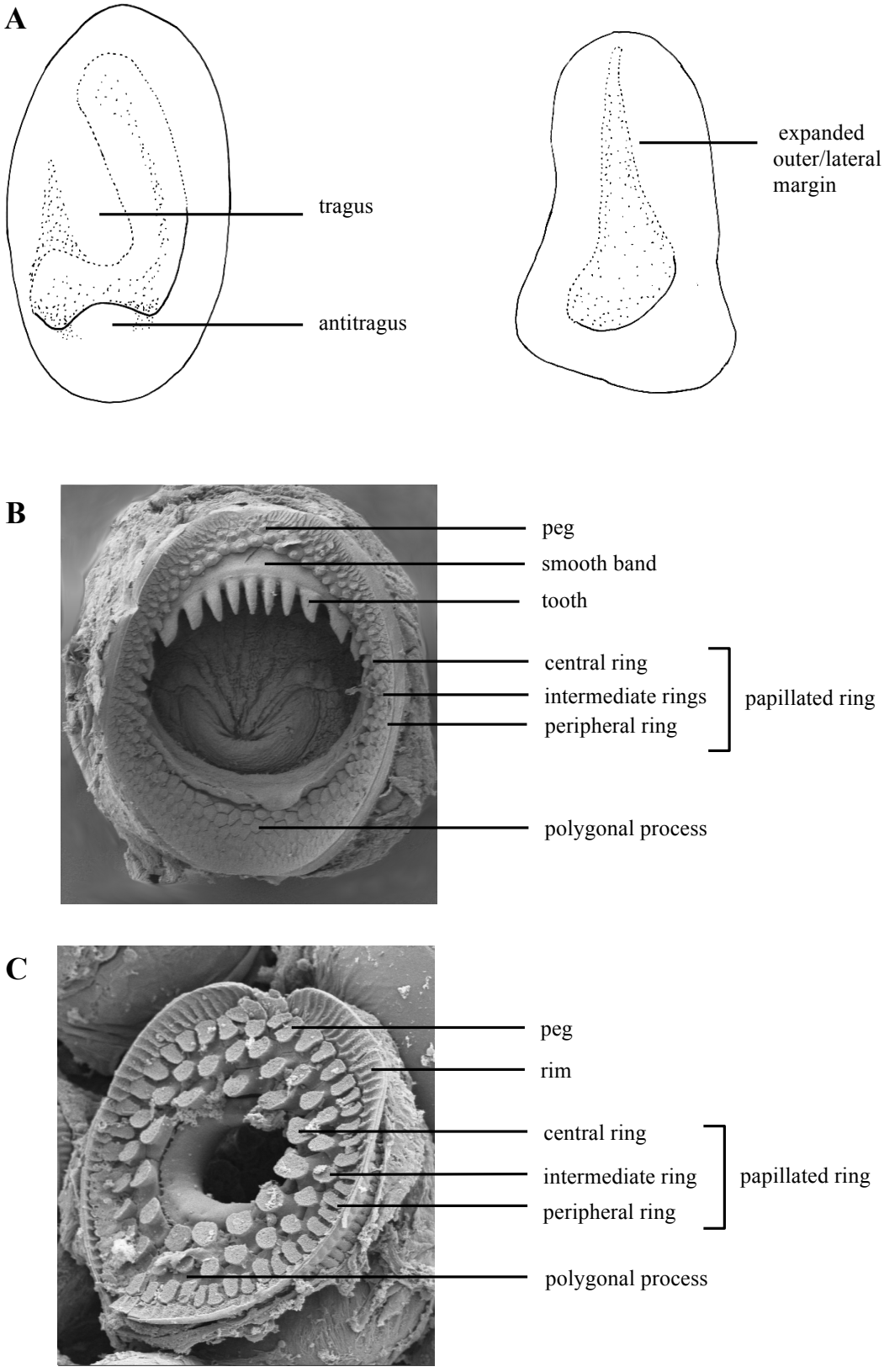

Fig. 2—Terminology for mastigoteuthid funnel-locking cartilage and suckers. A) funnel-locking cartilage; B) arm-sucker morphology; C) tentacle-sucker morphology.

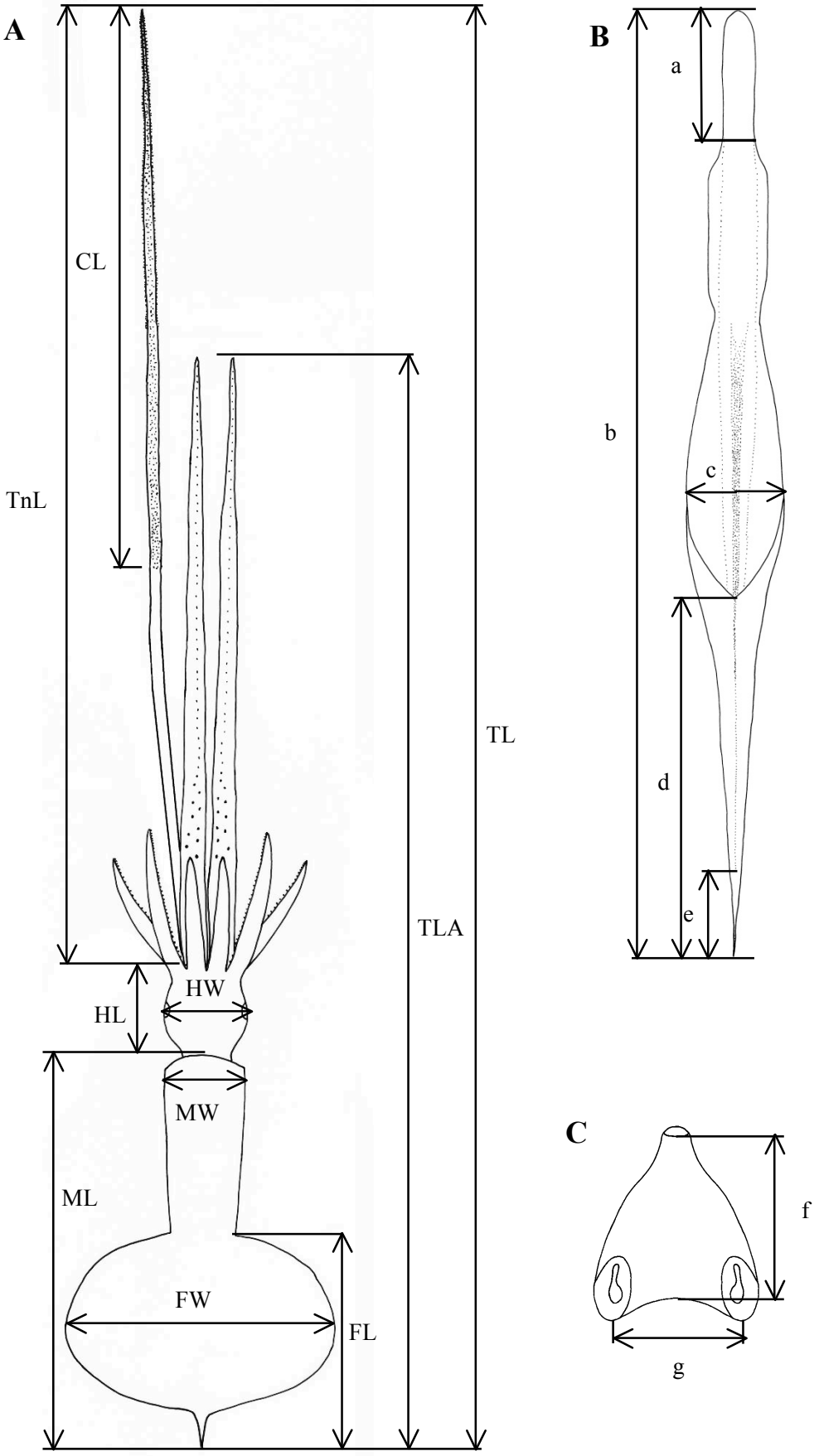

Fig. 3—Mastigoteuthid measurements and acronyms as defined in text. A) specimen measurements; B) gladius measurements: (a) free rachis, (b) gladius length, (c) maximum width, (d) secondary conus, (e) rostrum; C) funnel measurements: (f) funnel length, (g) funnel width.

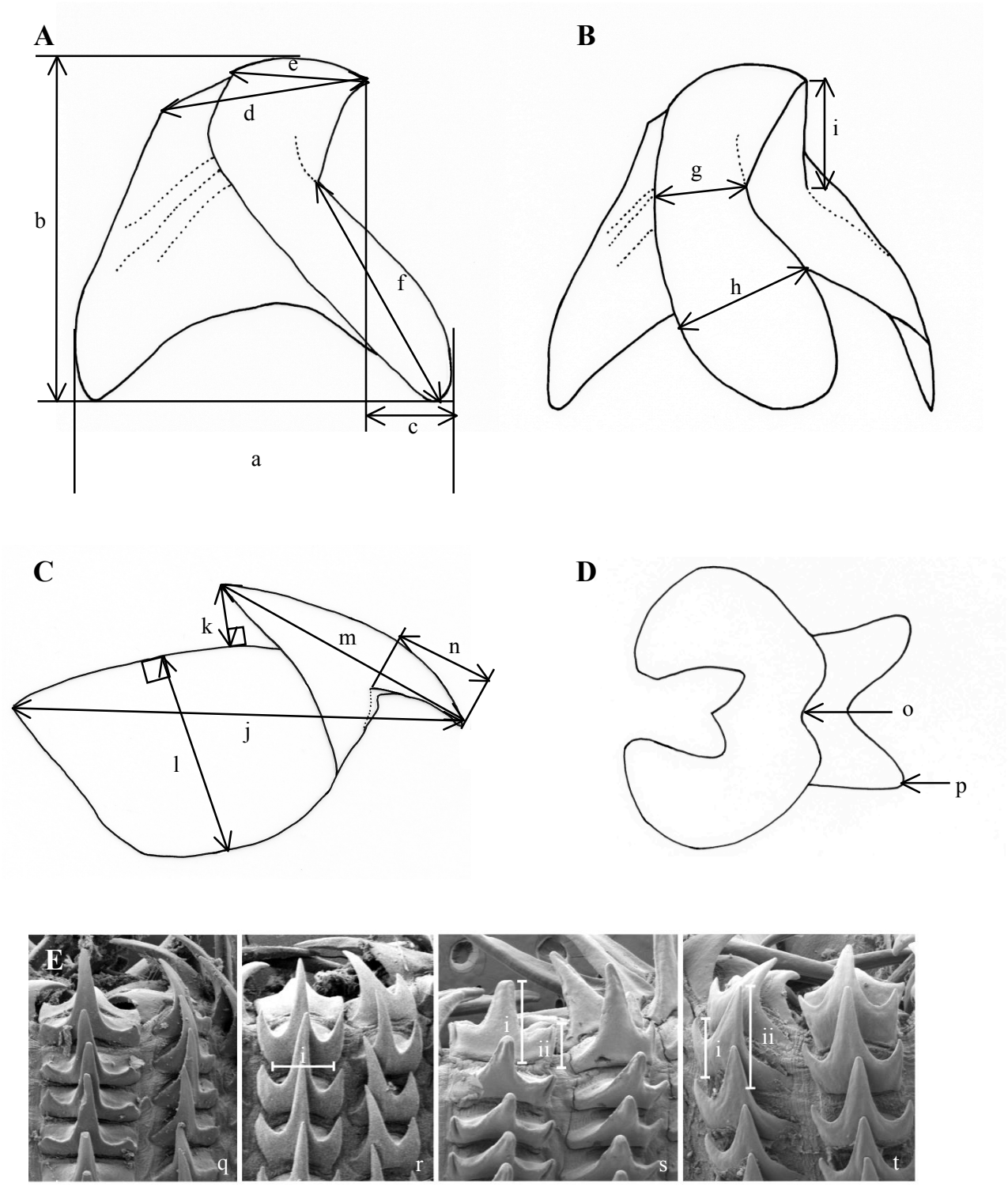

Fig. 4—Mastigoteuthid beak and radular tooth measurements. A) lower beak, profile view: (a) baseline, (b) beak height, (c) rostral tip behind leading edge of wing, (d) crest length, (e) hood length, (f) wing length; B) lower beak, oblique view: (g) minimum wing width, (h) maximum wing width, (i) lower rostral length; C) upper beak, profile view: (j) beak length, (k) hood height, (l) beak width, (m) hood length, (n) upper rostral length; D) lower beak, ventral view: (o) notch in hood, (p) free corner; E) radular tooth measurements and types: (q) rachidian with narrow, sharp, triangular mesocone and small lateral cusps, base rectangular and weakly bicuspid first lateral, (r) rachidian with narrow, sharp, triangular mesocone and sharp lateral cusps, base concave and strongly bicuspid first lateral (i, base width), (s) rachidian with broad, blunt, triangular mesocone and broad lateral cusps, base rectangular, bicuspid first lateral (i, mesocone height, ii lateral cusp height), (t) rachidian with broad, sharp triangular mesocone and sharp lateral cusps, base concave; strongly bicuspid first lateral (i, first lateral outer cusp height, ii inner cusp height).

Histological examination

Formalin-fixed, ethanol-preserved museum specimens were used for histology. A piece of tissue was sourced from the ventral side of the eye for each species (except for *E. famelica* and *Mp. hjorti* due to limited material). Tissue was embedded using a ThremoScientific Shandon Citadel 1000 following the protocol in Table 1. Five-micrometer sections were cut and stained with Mallory's trichrome following Lormann (2008) (Table 2). Acid fuchsin solution contained 0.5g acid fuchsin in 100mL tap water. Aniline blue and orange G contained 0.5g water-soluble aniline blue, 2g orange G, and 1g phosphotungstic acid in 100mL distilled water.

Table 1—Embedding protocol for histology.

Step	Solution	Time
1	90% EtOH	1 h
2	100% EtOH	1 h
3	100% EtOH	2 h
4	100% EtOH	2 h
5	Xylol	1 h
6	Xylol	1.5 h
7	Xylol	1.5 h
8	Paraffin	2 h
9	Paraffin	3 h

Table 2—Staining protocol for Mallory's trichrome.

Step	Solution	Time
1	Xylol	5 min
2	Xylol	5 min
3	100% EtOH	1 min
4	95% EtOH	1 min
5	95% EtOH	1 min
6	70% EtOH	1 min
7	Water	20 sec
8	Acid fuchsin	5 min
9	Aniline blue orange G	45 min
10	95% EtOH	1 min
11	95% EtOH	2 min
12	95% EtOH	2 min
13	95% EtOH	2 min
14	100% EtOH	1 min
15	50% EtOH/50% Xylol	20 sec
16	Xylol	1 min
17	Xylol	1 min

SYSTEMATICS

Family Mastigoteuthidae Verrill, 1881

Diagnosis: Medium- to large-bodied deep-sea squids (ML ~130 mm to > 1 m at maturity). Fins heart shaped, circular, elliptical, or lanceolate in outline when considered together. Ventral anterior margin produced into two points indicating underlying mantle-locking cartilage. Funnel-locking cartilage generally ovate, with tragus and/or antitragus in some species; mantle-locking cartilage ovate, flask, C or nose shaped; buccal formula DDVV. Arm suckers arranged in two series on most arms; oral faces of arms bordered by wide protective membranes. Arms IV generally longer and thicker than other arms, with strong lateral keels. Hectocotylus absent. Tentacles whip-like, often lost, club elongate and cylindrical; most tentacular suckers minute and densely set. Integumental photophores variably present; eye or eye-sinus photophores present in some species. Skin tubercles may be present on mantle, fins, arms, head and funnel. Gladius with secondary conus.

Table 3—Morphological characters for the mastigoteuthid species examined in this study. Acronyms indicate fin-length index (FLI), funnel-locking cartilage (FLC), and mantle-locking cartilage (MLC).

Character	*Mt. dentata*	*Mt. psychrophila*	*Mt.* sp. X	*Mt.* sp. Y	*I. cordiformis*	*Mp. hjorti*	*E. famelica*	*Mg.* sp. nov.
FLI	51–*61*–70	~*63*	53–*63*–75	~64	72–*81*–92	~89[a]	~55	60–*64*–70
Fin shape	elliptical	elliptical	elliptical	heart	heart or elliptical	heart	lanceolate	heart
FLC shape	ear	ear	ear	ear	ear	oval	ear	flask
Tragus	present	present	present	present	present	absent	present	present
Antitragus	weak	strong	strong	weak	weak	absent	absent	absent
MLC shape	nose	nose	nose	nose	nose	oval	C-shaped	flask
Arm sucker teeth	sharp	sharp	sharp	small, sharp	adentate/blunt	long, blunt	sharp	adentate/indistinct
Tentacle suckers	minute	minute	minute	unknown[b]	large to minute	minute[a]	minute	microscopic
Skin tubercles	absent	absent	absent	absent	present	present	present	absent
Photophores								
Integumental	present	present	present	present	absent	absent	absent	absent
Eye sinus	small	small	small	small	absent	absent	large	absent
Eye	absent	absent	absent	one band	ventral patch	two ventral	absent	absent

[a] From type description (Chun, 1913) and Rancurel (1973)
[b] Damaged in sole known specimen

Table 4—Arm length index for mastigoteuthids examined in this study.

Character	*Mt. dentata*	*Mt. psychrophila*	*Mt.* sp. X	*Mt.* sp. Y	*I. cordiformis*	*Mp. hjorti*	*E. famelica*	*Mg.* sp. nov.
A1LI	32–*52*–72	38–*48*–64	43–*50*–64	~56	54–*68*–75	33–*40*–48[a]	~13	58–*66*–75
A2LI	54–*71*–83	57–*66*–87	62–*69*–97	~69	62–*77*–84	~75	~19	76–*89*–108
A3LI	43–*62*–80	50–*58*–76	54–*62*–73	~62	58–*71*–80	~63	~14	56–*72*–85
A4LI	128–*163*–186	104–*119*–131	125–*157*–186	unknown[b]	65–*77*–91	~80[a]	~54	107–*118*–138

[a] From type description (Chun, 1913) and Rancurel (1973)
[b] Damaged in sole known specimen

Species found in New Zealand:

Family Mastigoteuthidae Verrill, 1881

- Genus *Mastigoteuthis* Verrill, 1881
  - *Mastigoteuthis dentata* Hoyle, 1904
  - *Mastigoteuthis psychrophila* Nesis, 1977
  - *Mastigoteuthis* sp. X
  - *Mastigoteuthis* sp. Y
- Genus *Idioteuthis* Sasaki, 1916
  - *Idioteuthis cordiformis* (Chun, 1908)
- Genus *Mastigopsis* Grimpe 1922
  - *Mastigopsis hjorti* (Chun, 1910)
- Genus *Echinoteuthis* Joubin 1933
  - *Echinoteuthis famelica* (Berry, 1909)
- Genus *Magnoteuthis* Salcedo-Vargas & Okutani 1994
  - *Magnoteuthis* sp. nov.

Genus *Mastigoteuthis* Verrill, 1881

Mastigoteuthis Verrill, 1881: 100. Type species *Mastigoteuthis agassizii* Verrill, 1881, by original designation.

Chiroteuthopsis Pfeffer, 1900: 187. Type species *Chiroteuthis grimaldii* Joubin, 1895, by monotypy.

Diagnosis: Mantle length at maturity ~130–200 mm. Fins circular or elliptical in outline when considered together; fin length ~64% ML. Funnel widely conical with recurved end. Funnel-locking cartilage ear shaped with tragus and antitragus present; funnel pocket present. Mantle-locking cartilage nose shaped, posteriorly undercut in profile. Arm suckers arranged in two distinct series but appearing to merge into single series midway on Arms IV; arm suckers with sharp teeth; Arms IV ~137% ML, 'minute trabeculate protective membrane is present' (*fide* Young, 1972). Tentacular suckers minute; club not expanded protective membranes without trabeculae. Small eye-sinus photophore present, diameter ~9% eye diameter. Eye photophore absent in most species. Integumental photophores present, skin tubercles absent. Gladius narrow (greatest width ~3% GL).

***Mastigoteuthis dentata* Hoyle, 1904** (Tables 3–6, Figs 5–11)

Mastigoteuthis dentata Hoyle, 1904: 34, 35, pl. 6 figs 8–11; Young (1972): 66, pl. 26 T, S.

Type material examined: **USNM 00574643,** lectotype, ♂, ML 60*mm, 7.35°N, 79.58°W, 10/03/1891, RV *Albatross*, large beam trawl, Stn 3394.

Additional material examined (21 specimens): **NMNZ M.172934**, 4 ♂, ML 43*–78mm, 26.52°S, 166.57°E, 2000m, 18/05/2003, RV *Tangaroa*, NORFANZ Stn 45; **NMNZ M.074540**, sex indet., ML 32mm, 30.97°S, 172.21°W, 971m over 5000m, 15/12/1976, RV *James Cook*, MWT, Stn J17/76/76; **NMNZ M.172936**, ♀, ML 81mm, 32.07°S, 159.88°E, 1920–1934m, 24/05/2003, RV *Tangaroa*, NORFANZ Stn 71; **NMNZ M.172963**, ♂, ML 54mm, 32.43°S, 161.79°E, 1132–1197m, 24/05/2003, RV *Tangaroa*, NORFANZ Stn 73; **NMNZ M.172944**, ♀, ML 98mm, ♂, ML 76mm, sex indet., ML 70mm, 32.61°S, 167.84°E, 1303–1313m, 30/05/2003, RV *Tangaroa*, NORFANZ Stn 120; **NMNZ M.074172**, sex indet., ML 47mm, 33.15°S, 176.10°E, 183m over 1980–4000m, 23/07/1962, RNZFA *Tui*, MWT; **NMNZ M.091520**, ♀, ML 58mm, 33.17°S, 170.96°E, 600m over 1900m, 25/10/1985, RV *James Cook*, MWT, Stn J16/28/85; **NMNZ M.287218**, ♀, ML 46mm, 33.22°S, 178.40°E, 640–823m, over 2213–2304m, 02/08/1962, MWT, Stn Z87218; **NMNZ M.172955**, ♂, ML 71mm, 34.98°S, 169.49°E, 1288–1294m, 04/06/2003, RV *Tangaroa*, NORFANZ Stn 160; **NMNZ M.287217**, sex indet., ML 29mm, 39.70°S, 178.13°E, 790–928m, 11/10/1988, RV *James Cook*, Stn J12/31/88; **NMNZ M.287214**, ♂, ML 85mm, 41.22°S, 176.70°E, 918–970m, 24/10/1988, RV *James Cook*, bottom trawl, Stn J12/56/88; **NIWA 48885**, ♀, ML 55mm, 42.69°S, 179.93°W, 920m, 06/07/1996, TAN9608/374, Stn Z9926; **NIWA 71720**, sex indet., ML 24mm, 42.78°S, 179.90°E, 950–0m, 08/07/1996, TAN9608/447; **NIWA 75806**, ♂, fins missing, 44.80°S, 173.90°E, 899–973m, 28/11/2011, TRIP3415/31; **NMNZ M.091649**, ♀, ML 81mm, 45.96°S, 163.54°E, 480–80m over 4570m, 28/07/1985, RV *Kaiyo Maru*, Stn KM/110B/85; **NMNZ M.091723**, ♀, ML 93*mm, New Zealand, *Macruronus novaezelandiae* stomach content, FV *Wanaka*, years 1985–1986; **CH-LIA-01**, sex indet., ML 69.2mm, no data.

Distribution (Fig. 5): 26–46°S, 159°E –172°W (near New Zealand); elsewhere reported from tropical and subtropical Indo-Pacific (except the California Current) (Nesis, 1987).

Diagnosis: Fins elliptical in outline when considered together, length 57–*62*–71% ML, width 59–*70*–80% ML; integumental photophores present, eye-sinus photophore diameter ~9% ED, Arms IV with two main series of photophores along length; skin tubercles absent; funnel-locking cartilage ear shaped with weak tragus and antitragus; arm suckers with long, sharp teeth.

Description (ML 46–85mm, Figs 6A, 7–11): Mantle cone-shaped anteriorly, with mantle cavity extending to ~30% FL from anterior of fins (thereafter gladius and surrounding musculature continue as narrow cylinder) widest (~26% ML) at anterior margin; dorsal anterior mantle margin nearly straight. Fins elliptical in outline when considered together, length 57–*62*–71% ML, width 59–*70*–80% ML; anterior lobes absent; posterior margin at tail concave. Photophores present on all external surfaces of head, fins, mantle, funnel, and aboral surface of arms; Arms IV photophore pattern with two distinct series of large photophores (Fig. 7E), with smaller photophores scattered; eye-sinus photophore diameter ~9% ED.

Head cylindrical, length ~31% ML, width ~19% ML. Olfactory papilla cylindrical. Eye diameter ~12% ML. Eye photophore absent. Funnel width ~11% ML, length ~9% ML; aperture approximately level with posterior margin of eye; funnel pocket present. Funnel-locking cartilage ear shaped (Fig. 7A), ~6% ML; anterior groove slightly concave due to weak antitragus; tragus present along inner/medial margin, extending approximately to midline of groove; concave along outer/lateral margin. Mantle-locking cartilage nose shaped (Fig. 7B, C), ~4% ML; posteriorly undercut in profile.

Arm formula IV>II>III>I; arm length 52–*87*–163% ML (Tables 4, 5); Arms I–III all of subequal thickness with aboral keels present; Arms IV thicker with expanded lateral membrane. At ML ~55–81mm, 100–128 suckers present on each arm; largest suckers overall located at base of Arm IV (~30% arm width).

Arm-sucker rings (Fig. 8) proximally with 8–14 short, blunt, rectangular teeth, distally with 7–15 sharp, conical teeth. Polygonal processes on oral surface of sucker in 2–5 concentric rings; distally, central and intermediate rings with cylindrical, pitted, porous pegs; proximally, central and intermediate rings nearly flat; peripheral ring with flat, rectangular processes.

At ML 24mm (sole tentacle available for examination), tentacle length ~308% ML, club ~46% TnL (~142% ML), not expanded. Suckers minute, covering majority of tentacle surface apart from narrow aboral strip; where tentacle club begins, width of sucker-covered surface is less than half of stalk circumference, broadening distally to cover nearly entire stalk circumference. Tentacular suckers not examined due to lack of adult material.

Lower beak (Fig. 9), lateral profile: lower rostral length 30–*37*–52% wing length, rostral edge moderately curved, rostral tip without hook, rostral tip behind leading edge of wing by 9–*30*–38% of baseline; wing angle obtuse, jaw angle obscured by low wing fold, shoulder groove absent; beak height 83–*88*–97% baseline; hood close to crest, hood length 50–*57*–68% crest length, crest length 51–*56*–65% baseline, visible portion of crest nearly straight; lateral wall fold present, thickened into ridge, lateral wall fold extends to posterior edge of lateral wall; no notch in lateral wall. Lateral oblique view with wing narrowest level with jaw angle, 53–*60*–70% greatest wing width. Ventral

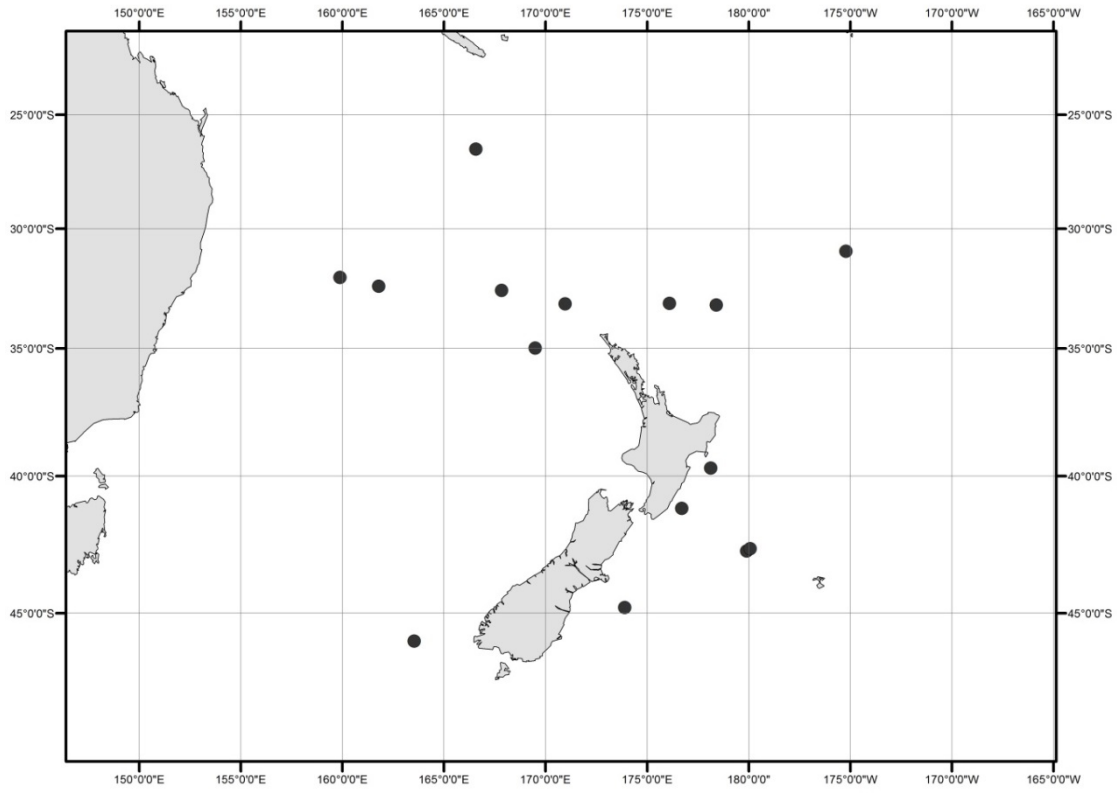

Fig. 5—Distribution of *Mastigoteuthis dentata* specimens examined in this study.

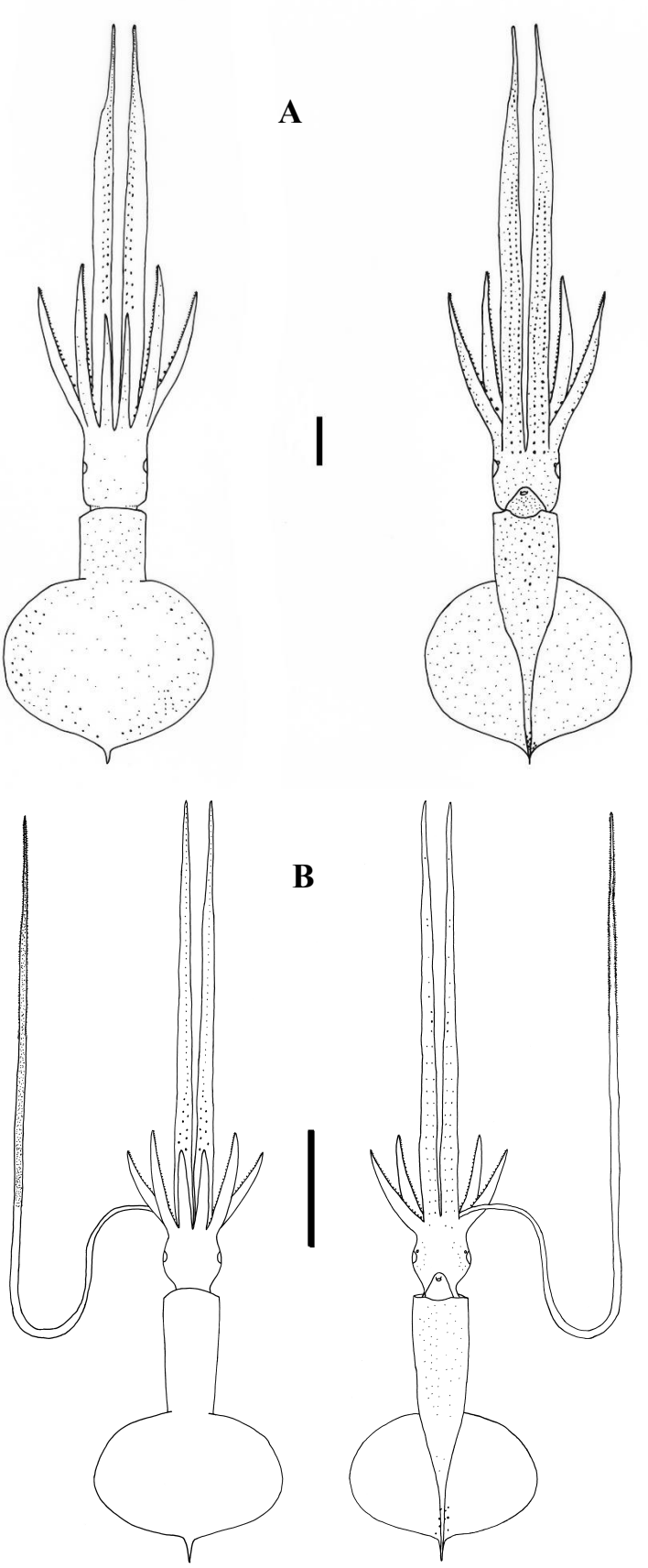

Fig. 6—*Mastigoteuthis dentata*. A) NIWA 48885, ♀, ML 55mm, photophore pattern on dorsal fins based on NMNZ M.091520, ♀, ML 58mm; B) NIWA 71720, sex indet., ML 24mm. Scale bars = 10mm.

view with broad notch in hood, free corners well separated. Wing entirely unpigmented at LRL 2.11mm (ML 54mm); midline of wing pigmented at LRL 3.08mm (ML 81mm); posterior edge, and anterior edge below shoulder of wing remains clear at LRL 3.65–3.87mm. Regression equation (Fig. 10F) ML = $0.0275(\text{LRL})^{1.0801}$ ($R^2 = 0.9222$) (N=9).

Upper beak, lateral profile (Fig. 10A–E): upper rostral length ~37% hood length; hood length 61–*67*–71% beak length; hood height ~28% beak width. Lateral wall fold absent; shoulder produced into point; jaw edge curved; jaw angle nearly 90°.

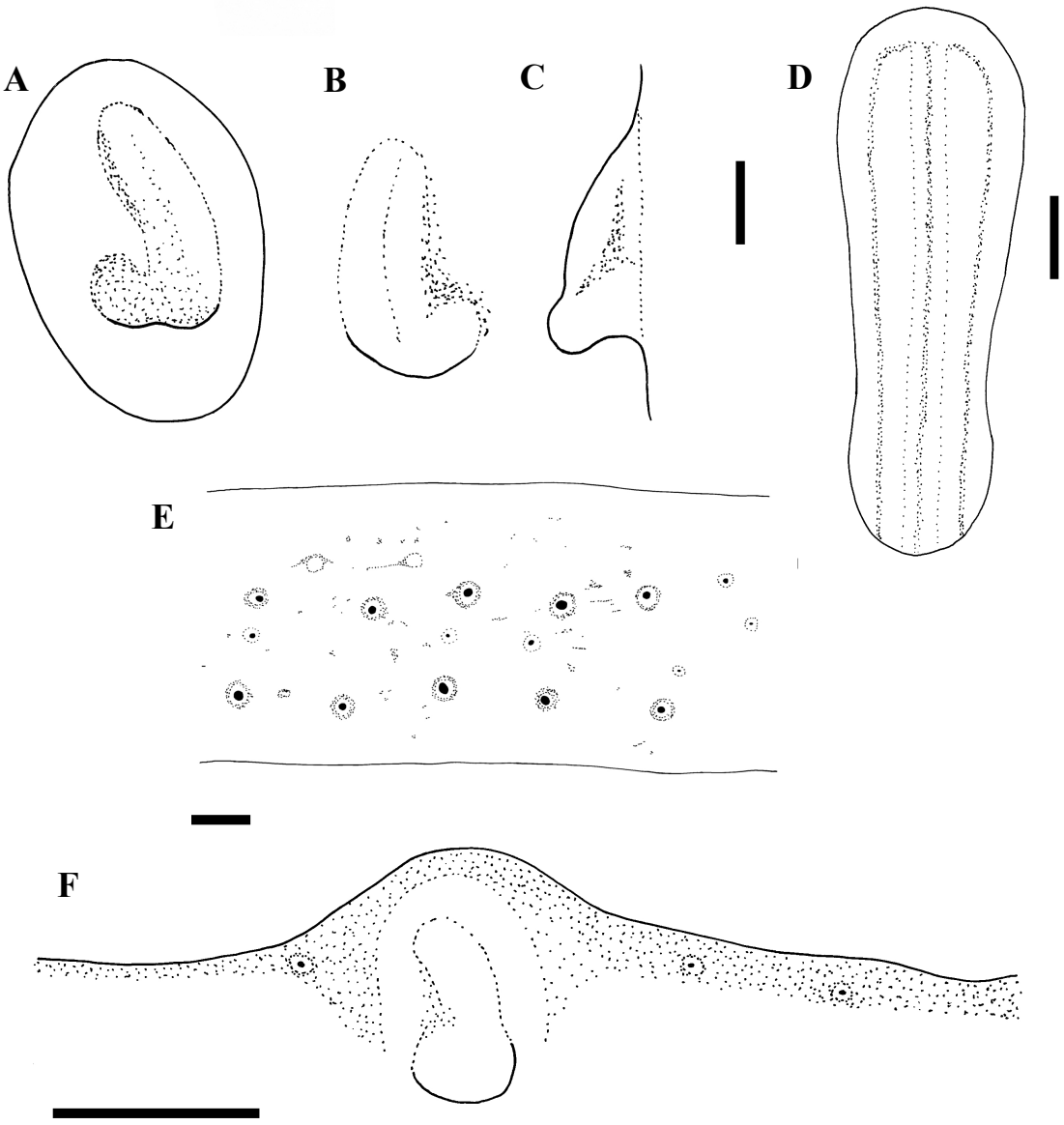

Fig. 7—*Mastigoteuthis dentata*. A–E) NIWA 48885, ♀, ML 55mm; F) NIWA 75806, ♂, ML unknown (damaged; LRL 3.34mm); A) left funnel-locking cartilage; B) left mantle-locking cartilage; C) left mantle-locking cartilage profile view; D) nuchal cartilage; E) proximal view of aboral photophores on Arms IV; F) internal mantle pigmentation. Scale bars = A–D, E) 1mm; F) 5mm.

Radula (Fig. 11A) with tricuspid rachidian, base width ~110% height, proximal margin of base rectangular, with narrow, sharp, triangular mesocone and small, pointed lateral cusps, laterally directed, their height ~25% mesocone height. First lateral tooth weakly bicuspid; inner cusp narrow, triangular, slightly curved towards rachidian, its height ~80% that of overall rachidian; outer cusp blunt, medially directed, its height ~30% that of inner cusp. Second lateral tooth simple, curving slightly towards rachidian, ~195% rachidian height. Marginal tooth simple, straight, ~290% rachidian height. Marginal plate absent (Fig. 11B). Palatine palp (Fig. 11E) with ~50 narrow, flat teeth, each ~60–200% rachidian height, evenly distributed over palp.

Gladius (Fig. 11F) with greatest width (~3% GL) attained at 5% GL; free rachis ~4% GL; secondary conus ~50% GL, rostrum ~5% GL, approximately triangular with rounded corners in cross section.

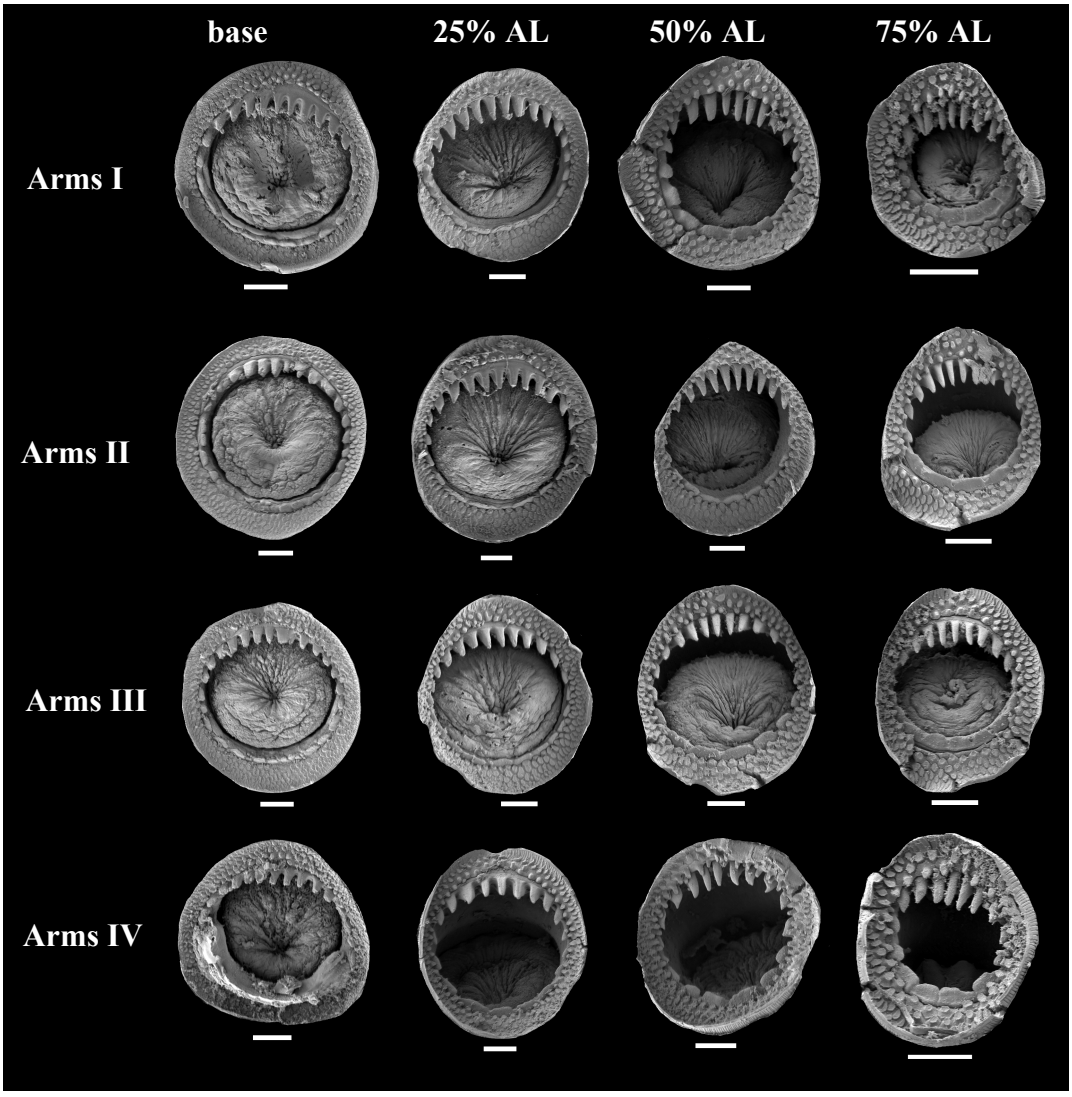

Fig. 8—*Mastigoteuthis dentata* arm suckers, NMNZ M.091649, ♀, ML 81mm. Scale bars = 100µm.

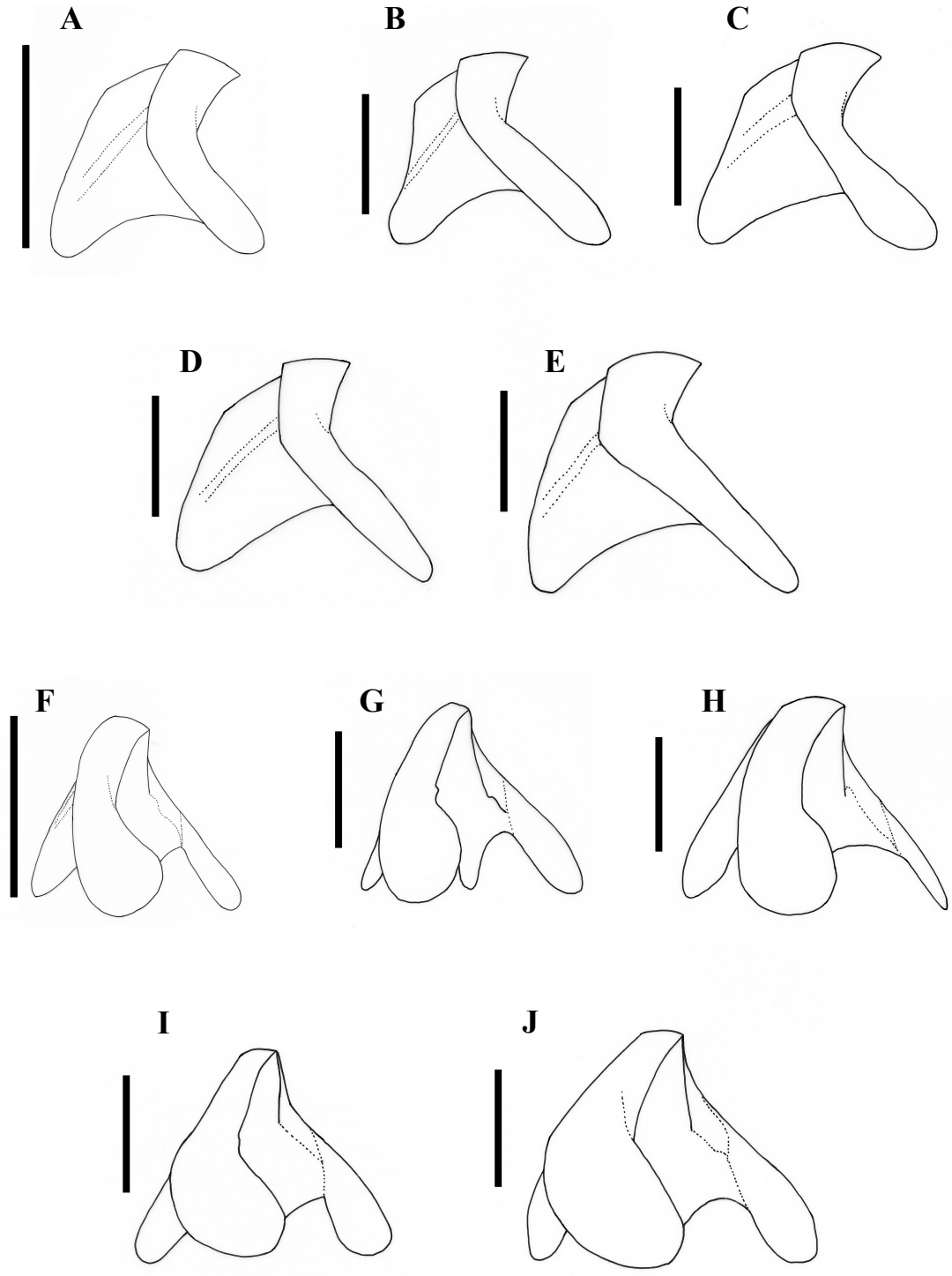

Fig. 9—*Mastigoteuthis dentata* lower beaks. A, F) NMNZ M.172963, ♂, ML 54mm, LRL 2.11mm; B, G) NMNZ M.287214, ♂, ML 85mm, LRL 3.39mm; C, H) M.172936, ♀, ML 81mm, LRL 3.46mm; D, I) NIWA 75806, ♂, ML unknown, LRL 3.34mm; E, J) NMNZ M.091723, ♀, ML 92.3*mm, LRL 3.96mm. A–E) lateral profile view; F–J) lateral oblique view. Scale bars = 5mm.

Epidermis damaged on all examined material. Integumental photophores present. Colour (preserved) dark purple to pink; chromatophores overlying integumental photophores; pigmentation on interior mantle wall with some small photophores extending to the anterior margin of locking cartilage (Fig. 7F); scattered chromatophores present on aboral surface of arms, oral surface of arms darkly pigmented but individual chromatophores not readily discernible.

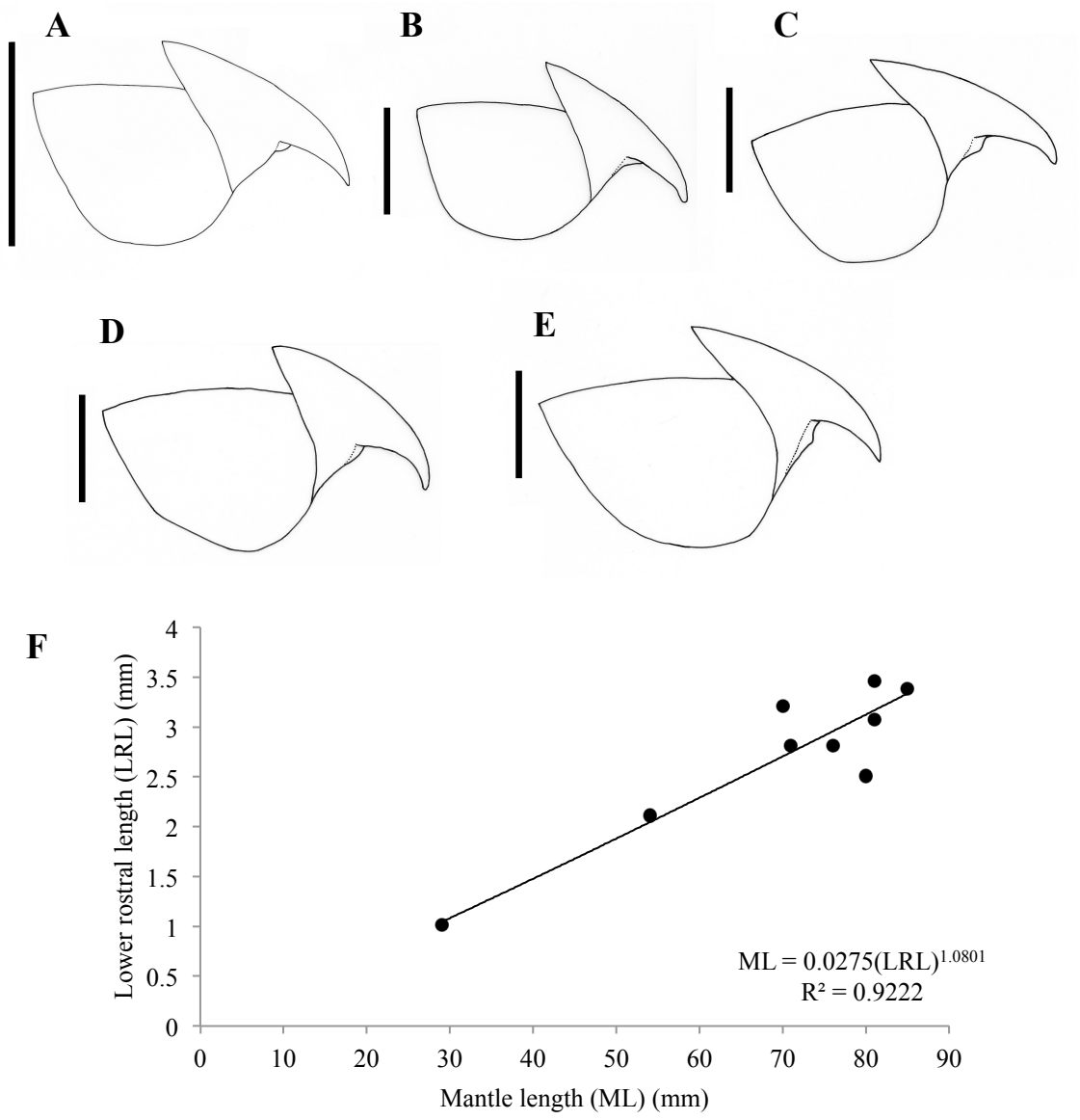

Fig. 10—*Mastigoteuthis dentata*. A) NMNZ M.172963, ♂, ML 54mm; B) NMNZ M.287214, ♂, ML 85mm; C) M.172936, ♀, ML 81mm; D) NIWA 75806, ♂,LRL 3.34mm; E) NMNZ M.091723, ♀, ML 92.3*mm. A–E) upper beaks; F) regression equation for mantle length (ML) and lower rostral length (LRL). Scale bars = 5mm.

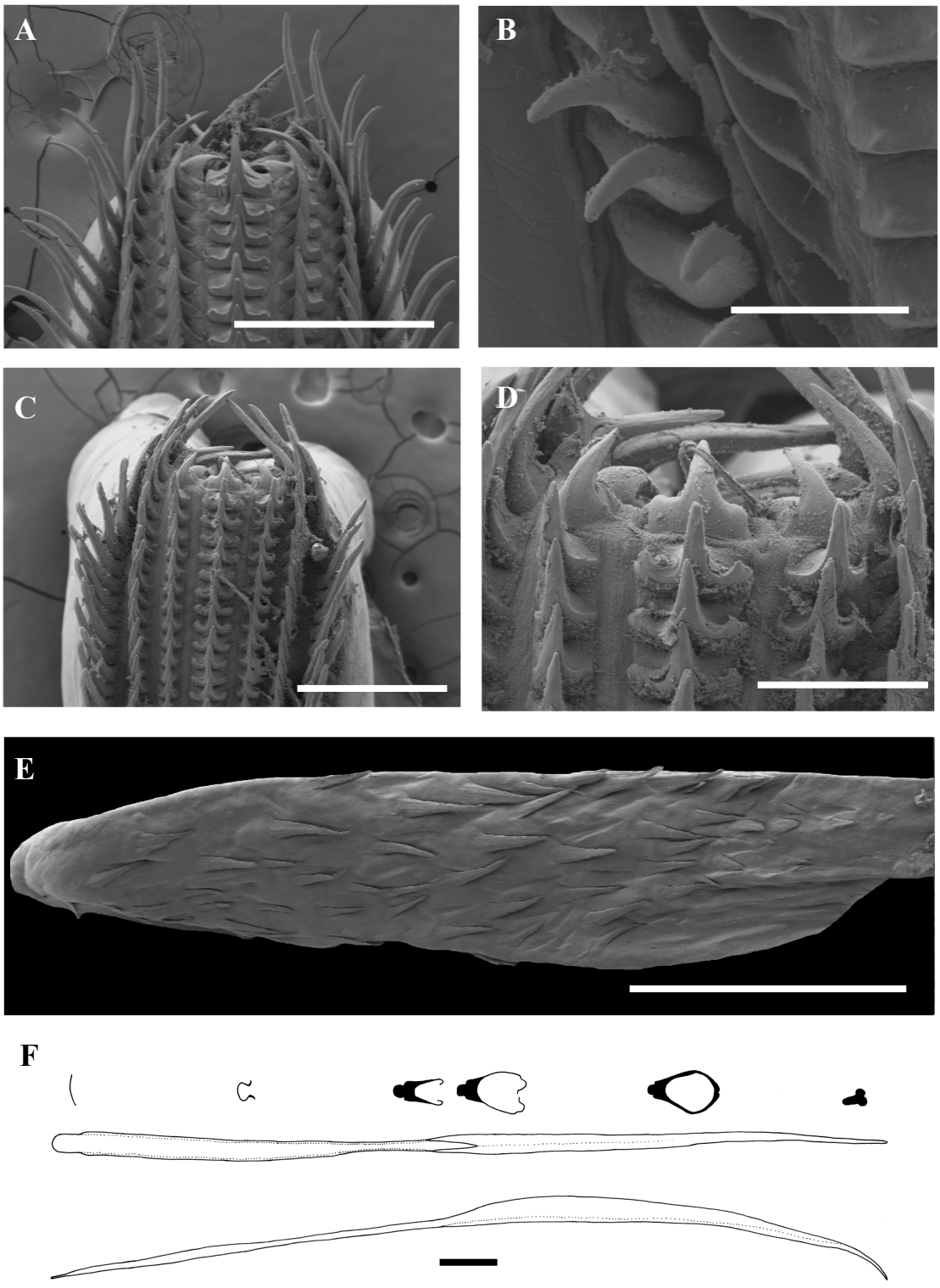

Fig. 11—*Mastigoteuthis dentata*. A, B) NMNZ M.287214, ♂, ML 85mm; C–E) NMNZ M.091649, ♀, ML 81mm; F) CH-LIA-01, ♂, ML 70mm. A) radula; B) radula margin; C) asymmetrical radula; D) asymmetrical radula rachidian and first lateral teeth; E) palatine palp; F) gladius. Scale bars = A, C) 500µm; B) 100µm; D) 200µm; E) 1mm; F) 5mm.

Smaller specimens (ML 24–32mm, Fig. 6B) differ from above descriptions only as follows: fin length 54–*57*–63% ML, fin width 66–*68*–72% ML. Head length 21–*28*–34% ML. Arms I ~30% ML, Arms II 38–*54*–63% ML, Arms III 33–*45*–55% ML, Arms IV 150–*184*–220% ML; with 44–100 suckers present on each arm.

Remarks: Three locally occurring species closely resemble *Mt. dentata*: *Mt. psychrophila*, *Mt.* sp. X, and *Mt.* sp. Y. These species are all approximately the same size at maturity (ML~150mm), with many small integumental photophores, arm suckers with sharp teeth, and a funnel pocket. *Mastigoteuthis psychrophila* can be distinguished from *Mt. dentata* by the photophore pattern on Arms IV, gladius cross sections, and the funnel-locking cartilage morphology. The photophore pattern on *Mt. psychrophila* Arms IV is widely spaced discrete clusters of larger photophores (Fig. 14A), while *Mt. dentata* has two main series along the entire arm length (Fig. 7E). In *Mt. psychrophila*, the cross-section of the gladius rostrum is tear-drop shaped (Fig. 17G); in *Mt. dentata,* the cross section is approximately triangular with rounded corners (Fig. 11F). The funnel-locking cartilage of *Mt. psychrophila* (Fig. 13B) has a much stronger antitragus than that of *Mt. dentata* (Fig. 7A). In addition, these species can be separated genetically (Chapter 4). The eye photophore present on *Mt.* sp. Y (Fig. 28A) differentiates it readily from *Mt. dentata*, which has no eye photophores.

Out of all the local mastigoteuthids, the two most similar species are *Mt. dentata* and *Mt.* sp. X. They can, however, be distinguished by the funnel-locking cartilage, photophore patterns on Arms IV, arm-sucker morphology, and beak morphology. In general, the funnel-locking cartilage of *Mt.* sp. X (Fig. 20B) has a stronger antitragus than that of *Mt. dentata* (Fig. 7A), but this is not apparent in all specimens (Fig. 20A). The photophore pattern on Arms IV of *Mt.* sp. X is proximally scattered (Fig. 20H), and distally in two rows; this contrasts with *Mt. dentata*, which has two main series of photophores for the entire length of Arms IV (Fig. 7E). The arm suckers of *Mt. dentata* (Fig. 8) have more distal teeth than those of *Mt.* sp. X (Fig. 21), and lack the smooth band between the polygonal processes and teeth, a feature present in all *Mt.* sp. X arm suckers. The beaks of *Mt.* sp. X (Fig. 22E–I) can be differentiated from those of *Mt. dentata* (Fig. 9A–E) by the angle of the lower rostrum to the baseline: there is an approximate right angle in *Mt.* sp. X, but a more acute angle in *Mt. dentata*. It is possible that *Mt. dentata* and *Mt.* sp. X are a single species and that the differences found herein represent natural intraspecific variation. Unfortunately, the intraspecific

variation found in mastigoteuthids has not been well studied because specimens are almost always badly damaged and rarely caught in large numbers. Preliminary results have indicated that these species cannot be distinguished with 16S rRNA or 12S rRNA (Chapter 4), but a more extensive study, on a variety of loci, with better quality tissue, and with a larger sample size, is necessary for these species.

Hoyle (1904) distinguished *Mt. dentata* from *Mt. agassizii* by the sucker dentition: *Mt. dentata* arm suckers possessed teeth. Verrill (1881) reported that the arm suckers of *Mt. agassizii* were adentate, but re-examination of the type specimen revealed that the suckers were degraded, but some dentition could be seen (Vecchione & Young, 2006b). In addition, specimens of *Mt. agassizii* from the type locality all have arm suckers with sharp teeth (Vecchione & Young, 2006b). The sucker illustrated by Hoyle (1904) appears similar to those observed herein for *Mt. dentata*. Young (1972) suggested that Hoyle (1904) may have described *Mt. dentata* from two specimens that belonged to different species because of the differences in fin length. Therefore, he declared the syntype from Cape Mala (male, ML 72mm) as the lectotype. Hoyle (1904) did not comment on the photophore pattern or draw the whole specimen; however, two main series of photophores on Arms IV are apparent on the lectotype. The FLI for this specimen is within the range found herein, while the other specimen described had a much smaller FLI. Although Young (1972) added information focused on the tentacles and tentacle-sucker ultrastructure, this cannot be compared here because no tentacles from New Zealand material were available for examination.

Within *Mastigoteuthis*, *Mt. dentata* is most morphologically similar to *Mt. agassizii*. The type locality of *Mt. agassizii* is the North Atlantic (Verrill, 1881), and *Mt. dentata* was described from the equatorial Pacific (Hoyle, 1904). These species share the same photophore pattern on Arms IV, funnel-locking cartilage morphology, arm-sucker morphology, presence of a funnel pocket, and similar beak morphology. Currently, there are no reliable morphological characters to separate these two species (Young & Vecchione, 2007a). However, some genetic evidence suggests a potential divergence between them (Chapter 4). Several other morphologically similar species have been described from the North Atlantic, which are not clearly distinguished from *Mt. agassizii*: *Mt. grimaldii* (Joubin, 1895), *Mt. flammea* Chun, 1908, and *Mt. schmidti* Degner, 1925 (Vecchione & Young, 2007b). Because these specimens were described

from the North Atlantic, and *Mt. dentata* is found in the Pacific, it is likely that these species are more closely related to (or synonymous with) *Mt. agassizii* than *Mt. dentata*.

As frequently found in mastigoteuthids herein (see Discussion), the radula morphology of one specimen appeared unusual (Fig. 11C, D) as follows: left first lateral tooth unicuspid; its height equal to that of rachidian. Right first lateral tooth bicuspid; its height equal to that of rachidian; outer cusp sharp.

Table 5—Measurements (mm) of *Mastigoteuthis dentata* Hoyle, 1904 of larger specimens (ML 46–85mm), all measured on right side except CH-LIA-01 and NMNZ M.172955.

Specimen ID:	**NMNZ M.287218**	**NMNZ M.074172**	**NMNZ M.172963**	**NMNZ M.172944**	**NMNZ M.172944**	**NMNZ M.287214**
Sex	F	Indet.	M	Indet.	M	M
ML	46	47	54	70	76	85
MW	12	13	15	17	17	21
FL	28	31	31	42	43	51
FW	27	33	42	55	51	60
HL	14	14	16	21	25	21
HW	10	10	9	15	13	13
ED	6	6	7*	7*	10*	10
Arm I	15	20	26	40	55	51
Arm II	25	29	37	58	62	60
Arm III	20	27	27	45	58	55
Arm IV	59	71*	84	130	86*	152
TLF	113	120*	148	210	192*	253

*indicates damaged features.

Table 5 (continued)

Specimen ID:	**NMNZ M.172934**	**CH-LIA-01**	**NIWA 48885**	**NMNZ M.091649**	**NMNZ M.172955**	**Mean Indices**	
Sex	M	M	F	F	M		
ML	78	70	55	81	71		
MW	19	20*	15	18	18	MWI	26
FL	49	42	39	52	44	FLI	62
FW	56	48	44	53	43	FWI	70
HL	28	25	16	20	22	HLI	31
HW	15	12	13	13	10	HWI	19
ED	8	6*	8	9	8*	EDI	12
Arm I	38	37	25	43	33	A1LI	52
Arm II	58	56	38	56	49	A2LI	71
Arm III	47	56	34	48	45	A3LI	62
Arm IV	65*	75*	87	140	71*	A4LI	163
TLA	176*	190*	152	235	160*		

*indicates damaged features.

Table 6—Measurements (mm) of small *Mastigoteuthis dentata* Hoyle, 1904 (ML 24–32mm).

Specimen ID:	**NIWA 71720**	**NMNZ M.287217**	**NMNZ M.074540**	**Mean Indices**	
Sex	Indet.	Indet.	Indet.		
ML	24	29	32		
MW	5	7	9	MWI	24
FL	13	16	20	FLI	57
FW	16	21	21	FWI	68
HL	5	10	9	HLI	28
HW	5	5	6	HWI	19
ED	3	4*	4	EDI	13
Side measured	L	R	L		
Arm I	7	7	11	A1LI	30
Arm II	9	18	20	A2LI	54
Arm III	8	16	15	A3LI	45
Arm IV	36	64	58	A4LI	184
TLA	67	102	105		
TF	107	-	-		
TnL	74	-	-	TnLI	308
CL	34	-	-	CLI	142

*indicates damaged features.
-indicates missing features.

***Mastigoteuthis psychrophila* Nesis, 1977** (Tables 3, 4, 7, Figs 12–17)
Mastigoteuthis psychrophila Nesis, 1977: 835–841, fig. 1.

Type material (not examined): **ZIN 60034/1**, holotype, ♂, ML 84mm, 59.43–59.51°S, 158.6–158.48°E, 500–1500m, 01–02/02/1976, RV *Dmitry Mendeleyev*, cruise 16m Isaacs-Kidd MWT, Stn 1309; **IORAS paratype**, 2 ♂, ML 88, 143mm, 54.95–54.87°S, 158.83–159.45°E,1500m, 25/01/1976, *Dmitry Mendeleyev*, pelagic trawl, Stn 1294; **IORAS paratype**, ♂,124mm, 57.18–57.13°S, 26.58–26.37°W, 650m, *Akademik Kurchatov*, Isaacs-Kidd MWT, Stn 883.

Material examined (8 specimens): **NMNZ M.070954** (2 specimens),♀, ML 88mm, ♂, no fins, 54.02°S, 168.69°E, 955m, 12/05/1979, RV *Wesermunde*, Stn W02B/137/79; **NIWA 44277**, 2 ♀, ML 86, 99mm, sex indet., ML 68mm, sex indet., head only, 66.91–66.99°S, 171.06–171.09°E, 1032–50m, 12/03/2008, Stn TAN0802/293. **NIWA 44301**, 2 ♀, ML 84, 96mm, 67.01–66.94°S, 170.70–170.73°E, 1078–100m, 14/03/2008, Stn TAN0802/312.

Beak only: **NIWA 86553**, sex indet., LRL 3.65mm, 43.76°S, 174.20°W, 43.81°S, 174.23°W, 1126–1150m, 10/01/2011, Stn TAN1101/43; **NIWA 86557**, sex indet., LRL 3.90mm, 44.62°S, 179.19°W, 1272–1270m, 14/01/2010, Stn TAN1001/67.

Distribution (Fig. 12): 43–67°S, 168°E –174°W (near New Zealand); elsewhere reported from circumpolar sub-Antarctic waters (Nesis, 1977; 1987).

Diagnosis: Fins circular to elliptical in outline when considered together, length ~63% ML, width 60–*67*–72% ML; integumental photophores present, eye-sinus photophore diameter ~10% ED, Arms IV with widely spaced discrete clusters of photophores; skin tubercles absent; funnel-locking cartilage ear shaped with strong tragus and antitragus; arm suckers with long, sharp teeth.

Description (ML 42–99mm, Figs 13–17): Mantle cone-shaped anteriorly, with mantle cavity extending to ~30% FL from anterior of fins (thereafter gladius and surrounding musculature continue as narrow cylinder), widest (22–*25*–31% ML) at anterior margin; dorsal anterior mantle margin slightly convex. Fins circular to elliptical in outline when

considered together, length ~63% ML, width 60–*67*–72% ML; anterior lobes absent; posterior margin at tail concave. Photophores present on all surfaces of head, funnel, mantle, dorsal surface of fins (ventral surface unknown), and aboral surface of arms; Arms IV photophore pattern with widely spaced discrete clusters of larger photophores distributed along the length of the arm (Fig. 14A); eye-sinus photophore diameter ~10% ED.

Head cylindrical, length ~29% ML, width ~17% ML. Olfactory papilla cylindrical. Eye diameter ~15% ML. Funnel width ~13% ML, length ~10% ML; aperture approximately level with posterior margin of eye; funnel pocket present. Funnel-locking cartilage ear shaped (Fig. 13B), ~6% ML, anterior groove concave due to strong antitragus; strong tragus present along inner/medial margin, extending approximately to midline of groove; concave along outer/lateral margin. Mantle-locking cartilage nose-shaped (Fig. 13C, D), ~4% ML; posteriorly undercut in profile.

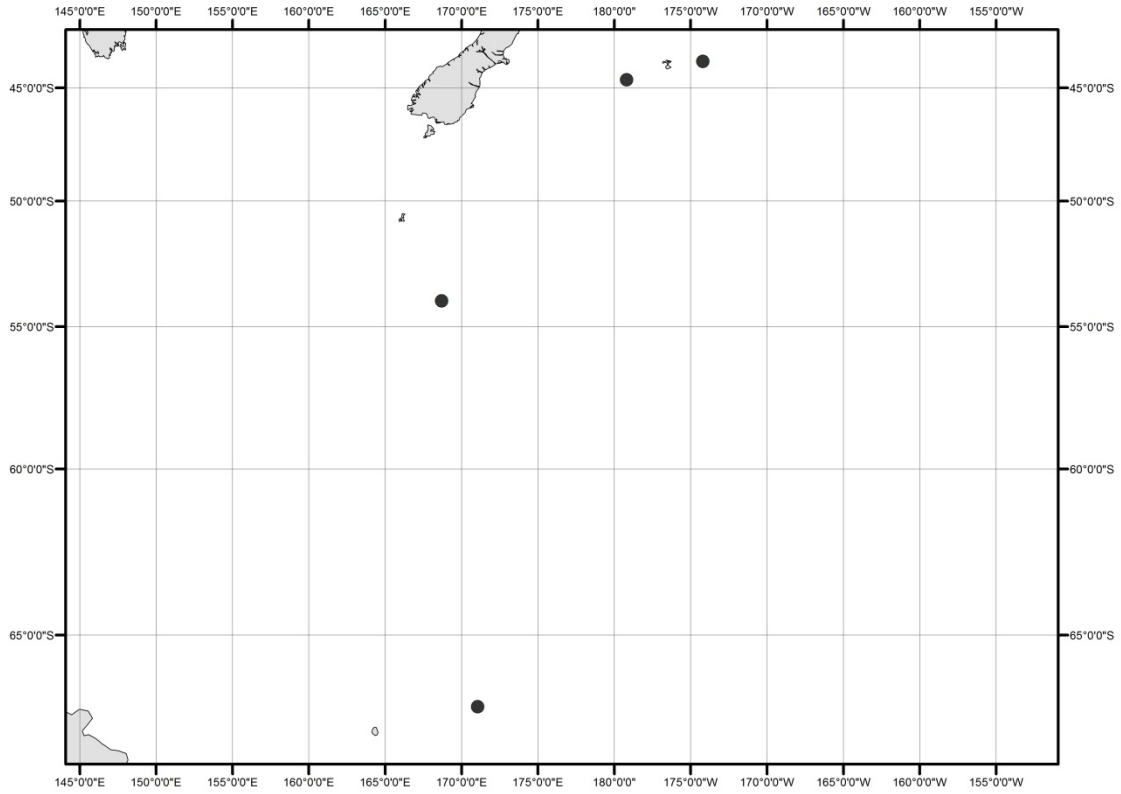

Fig. 12—Distribution of *Mastigoteuthis psychrophila* specimens examined in this study.

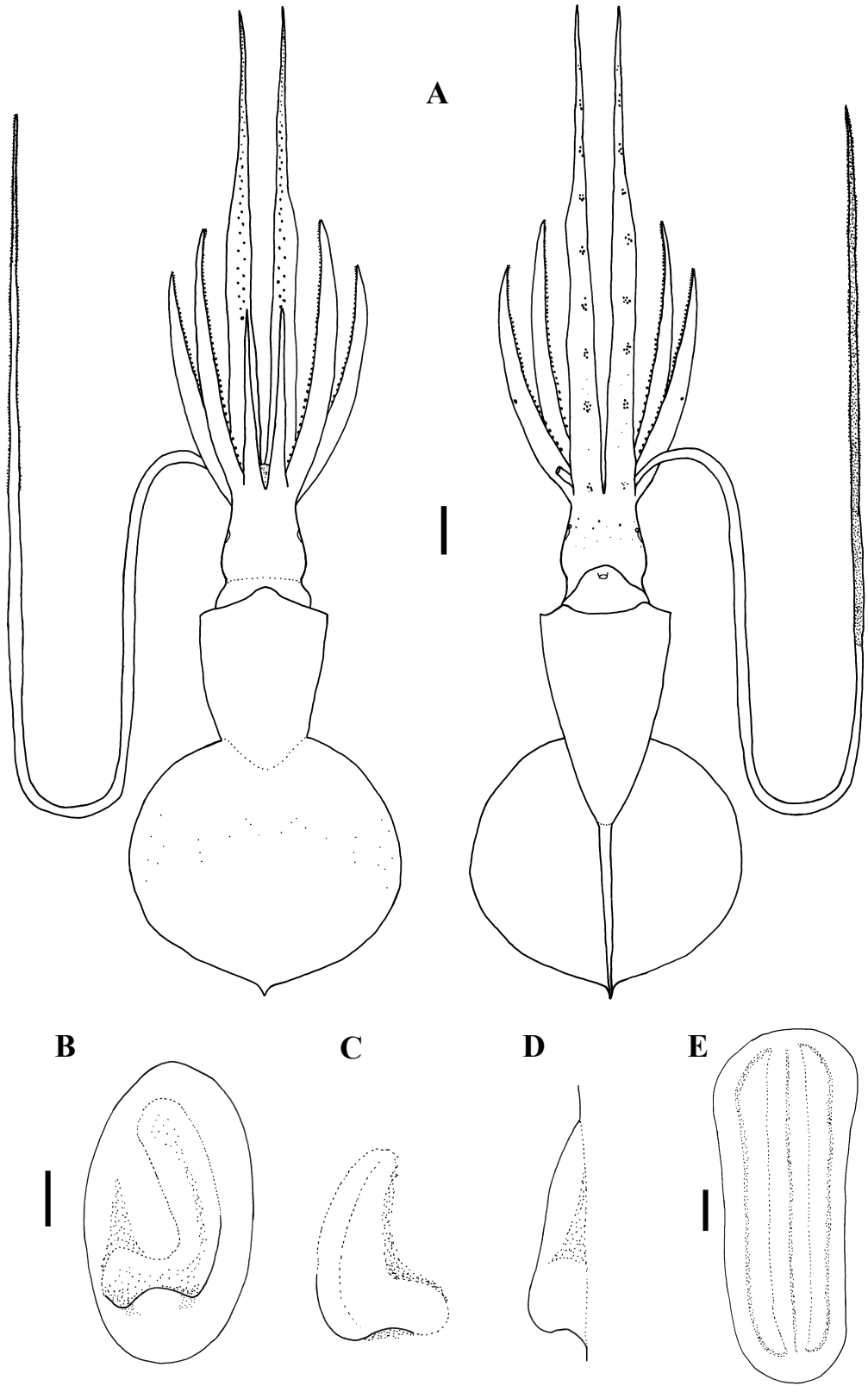

Fig.13—*Mastigoteuthis psychrophila*. A) NMNZ M.070954, ♀, ML 88mm, tentacle based on NIWA 44301, ♀, ML 96mm; B–E) NIWA 44301, ♀, ML 84mm. A) whole specimen; B) left funnel-locking cartilage; C) left mantle-locking cartilage; D) left mantle-locking cartilage, profile view; E) nuchal cartilage. Scale bars = A) 10mm; B–E) 1mm.

Arm formula IV>II>III>I; arm length 48–*75*–127% ML (Tables 4, 7); Arms I–III all of subequal thickness with aboral keels present; Arms IV thicker with expanded lateral membrane; oral faces of arms bordered by wide membranes. At ML ~42–99mm, 86–128 suckers present on each arm; suckers arranged in two distinct series, distally merging into one series on Arms IV; largest suckers overall located at base of Arm IV (~30% arm width).

Arm-sucker rings (Fig. 15) proximally with 8–16 blunt, rectangular teeth, distally with 8–30 sharp, conical teeth. Polygonal processes on oral surface sucker in 4–7 concentric rings; distally, central and intermediate rings with cylindrical, pitted, porous pegs; proximally, central and intermediate rings nearly flat; peripheral ring with flat, rectangular processes.

At 96mm ML (sole tentacle available for examination), tentacle length ~242% ML, club ~52% TnL (~125% ML), not expanded. Suckers minute, covering majority of tentacle surface apart from narrow aboral strip; proximally, width of sucker-covered surface is less than half of stalk circumference, broadening distally to cover nearly entire stalk circumference. Tentacular suckers (Fig. 16A–F) adentate; polygonal processes on oral

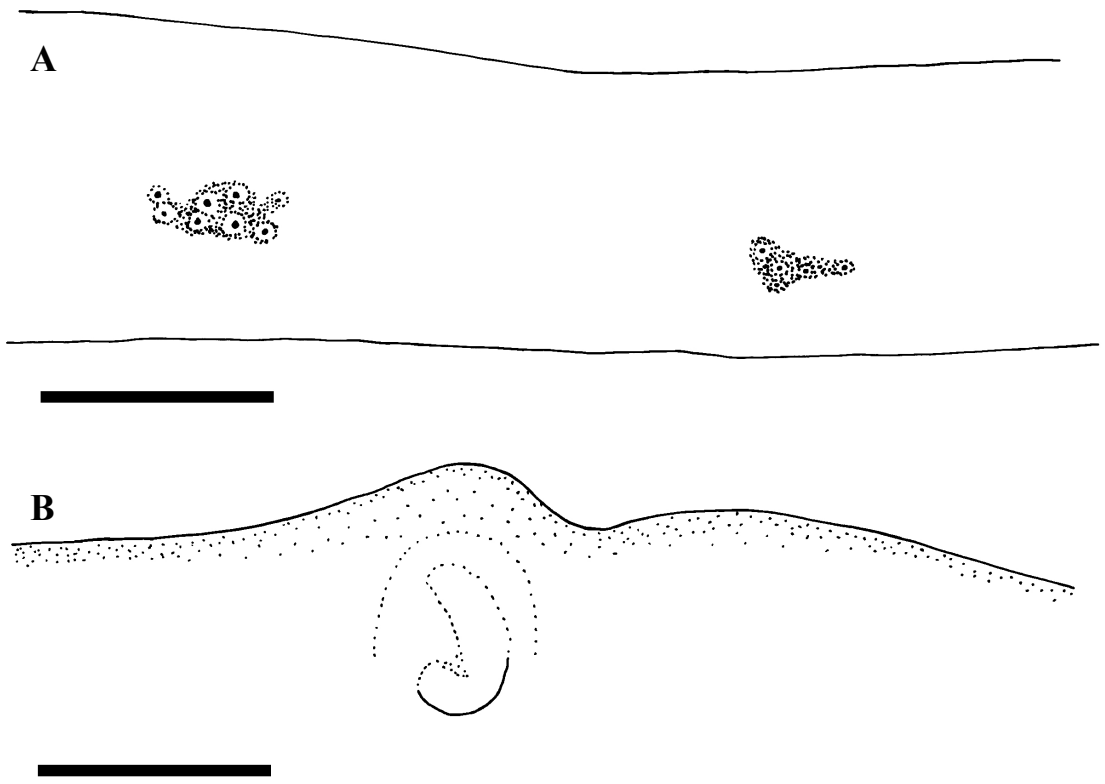

Fig. 14—*Mastigoteuthis psychrophila*. A) NIWA 44301, ♀, ML 84mm; B) NIWA 44277, ♀, ML 78mm. A) proximal view of aboral photophores on Arms IV; B) internal mantle pigmentation. Scale bars = 5mm.

surface of rings in three concentric rings; central ring with 11–12 ovate to circular pegs; intermediate ring with 22–28 smaller, circular pegs; peripheral ring with 40–45 rectangular-faced pegs; rim processes rectangular, pitted, porous. Sucker diameter ~100μm (~4% club width).

Lower beak, lateral profile (Fig. 16G, J): lower rostral length ~60% wing length, rostral edge moderately curved, rostral tip without hook, rostral tip behind leading edge of wing by ~25% baseline; wing angle obtuse, jaw angle obscured by low wing fold, shoulder groove present; beak height ~90% baseline; hood close to crest, hood length ~60% crest length, crest length ~55% baseline, visible portion of crest straight; broad lateral wall fold present, thickened into ridge, lateral wall fold extends to posterior edge

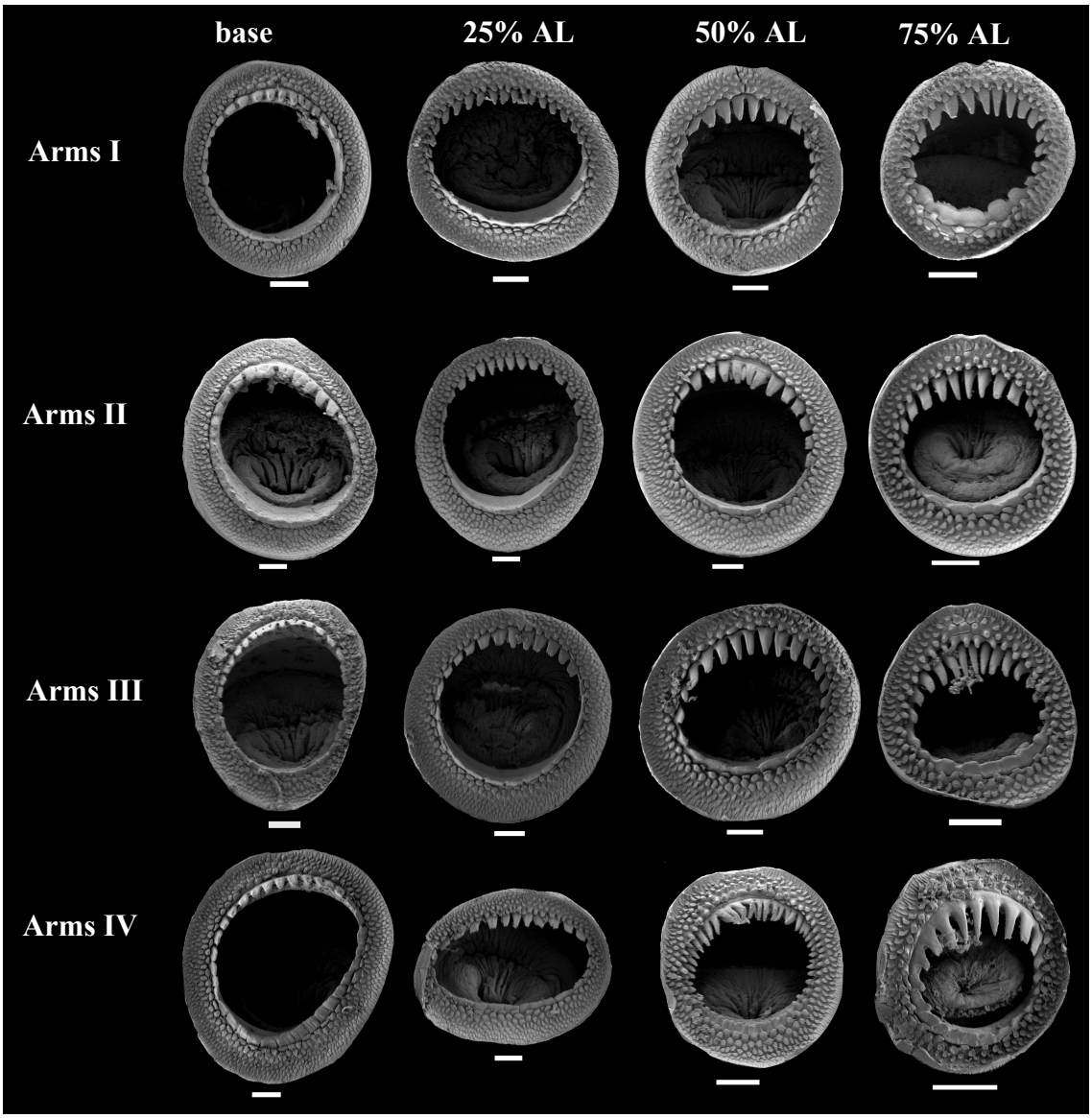

Fig. 15—*Mastigoteuthis psychrophila* arm suckers, NIWA 44277, head only, LRL 3.07mm. Scale bars = 100μm.

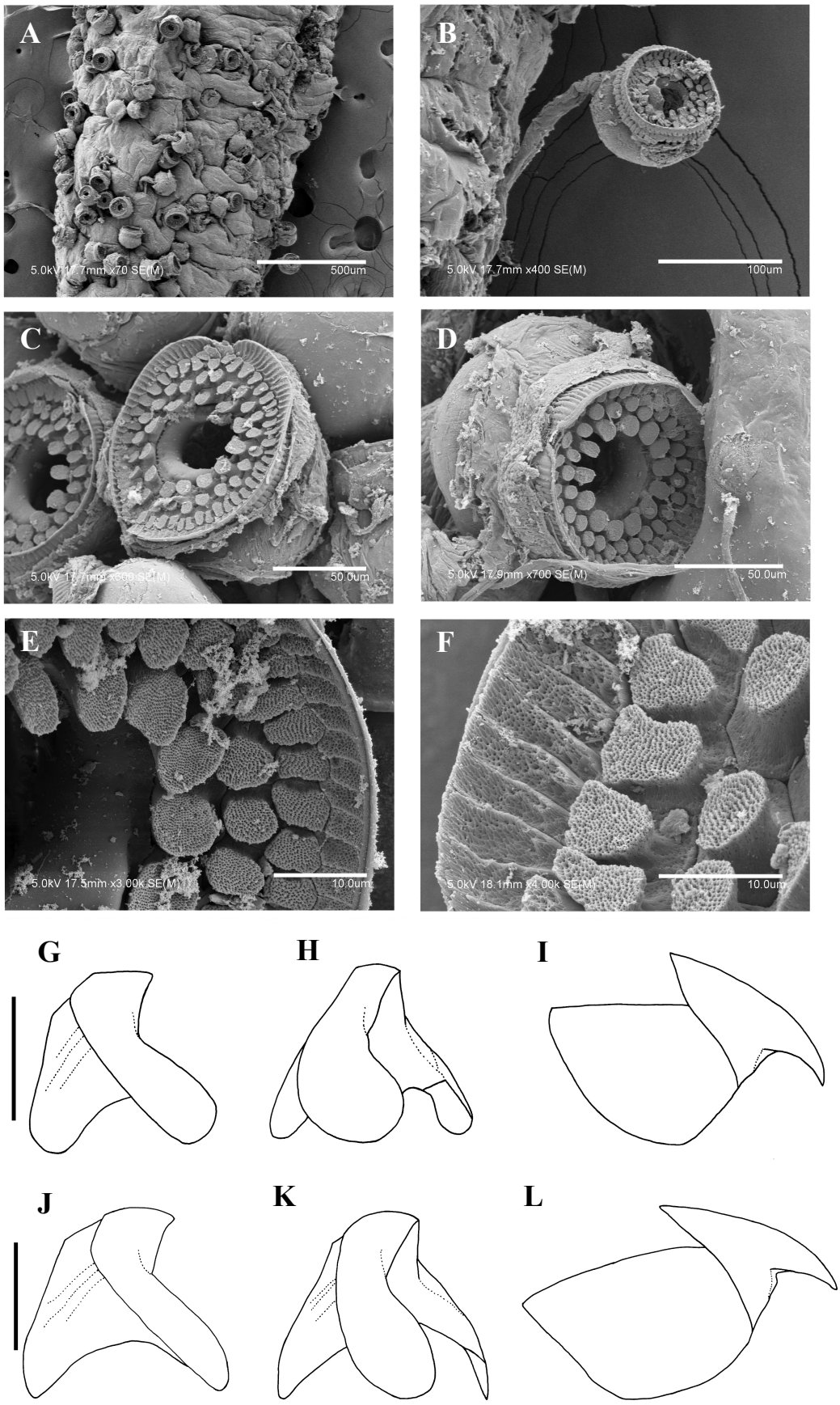

Fig. 16—*Mastigoteuthis psychrophila*. A–F) NIWA 44301, ♀, ML 96mm; G–I) NIWA 44301, ♀, ML 84mm, LRL 2.67mm; J–L) NIWA 44277, head only, LRL 3.07mm. A–F) tentacle suckers; G, J) lower beaks in lateral profile view; H, K) lower beaks in lateral oblique view; I, L) upper beaks. Scale bars = A) 500µm; B) 100µm; C, D) 50µm; E, F) 10µm; G–L) 5mm.

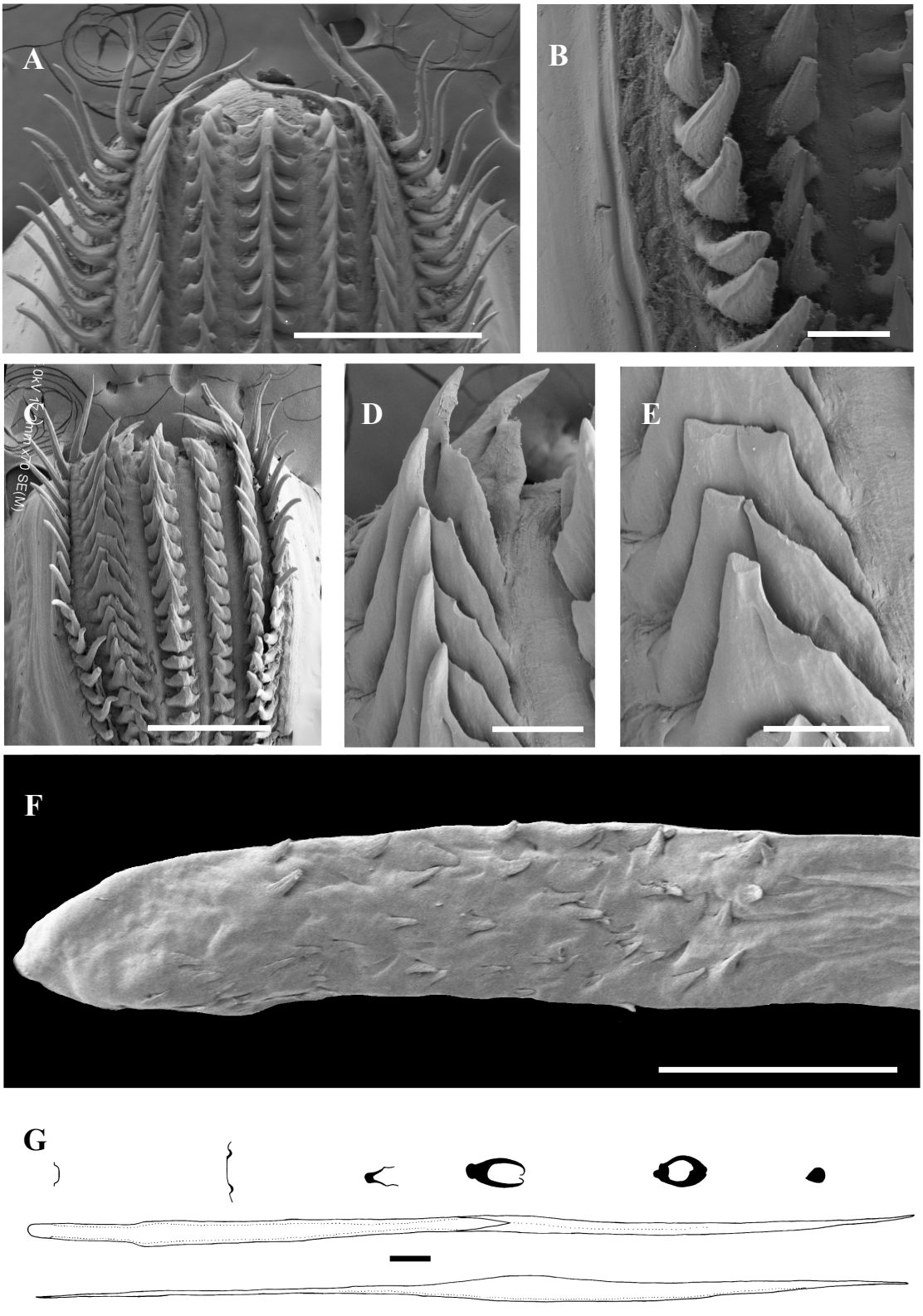

Fig. 17—*Mastigoteuthis psychrophila*. A, B) M.070954, ♂, no fins, LRL 2.89mm; C–F) NIWA 44277, sex indet., ML 86mm; G) NIWA 44301, ♀, ML 96mm. A) radula; B) radula margin; C) asymmetrical radula; D, E) fused lateral teeth of asymmetrical radula; F) palatine palp; G) gladius. Scale bars = A, C) 500µm; B, D, E) 100µm F) 1mm; G) 5mm.

of lateral wall; no notch in lateral wall. Lateral oblique view (Fig. 16H, K) with wing narrowest level with jaw angle, ~70% of greatest width. Ventral view with broad notch in hood, free corners well separated. Wings nearly completely unpigmented at LRL 2.67mm (ML 84mm), shoulder remains clear at LRL 3.03mm, entirely pigmented by LRL 3.07mm.

Upper beak, lateral profile (Fig. 16I, L): upper rostral length ~35% hood length; hood length ~60% beak length; hood height ~30% beak width. Lateral wall fold absent; shoulder produced into point; jaw edge curved; jaw angle obtuse.

Radula (Fig. 17A) with tricuspid rachidian; base width ~130% height; proximal margin of base concave, with broad, sharp, triangular mesocone and small, sharp lateral cusps, slightly laterally directed, their height ~55% mesocone height. First lateral tooth weakly bicuspid; inner cusp broad, triangular, nearly straight, its height ~80% that of overall rachidian; small, blunt outer cusp, laterally directed, its height ~40% that of inner cusp. Second lateral tooth simple, straight, directed lightly towards rachidian, ~120% rachidian height. Marginal tooth simple, curved proximally, straight distally, ~225% rachidian height. Marginal plate absent (Fig. 17B). Palatine palp (Fig. 17F) with ~40 narrow, flat teeth, each ~40–75% rachidian height, evenly distributed over palp.

Gladius (Fig. 17G) with greatest width (~3% GL) attained at 13% GL; free rachis ~12% GL; secondary conus ~45% GL, rostrum ~12% GL, tear-drop-shaped in cross section.

Epidermis damaged on all examined material. Integumental photophores present. Colour (preserved) pink-purple; aboral arms purple; head naturally white; chromatophores overlying integumental photophores; pigmentation on interior mantle wall extending to the anterior margin of locking cartilage (Fig. 14B); scattered chromatophores present on aboral surface of arms; oral surface of arms darkly pigmented but individual chromatophores not readily discernible.

Remarks: *Mastigoteuthis psychrophila* inhabits sub-Antarctic waters of the Southern Ocean, and herein was found to have a northern limit of ~44°S, which overlaps with the distributions of other local mastigoteuthids. The type description for *Mt. psychrophila* only included illustrations of the funnel-locking cartilage, arm suckers, tentacular sucker, and the terminal organ (Nesis, 1977). Unfortunately, the photophore pattern on

Arms IV, which is important for species identification, was not included. However, the specimens identified herein as *Mt. psychrophila* had characteristics consistent with this description as well as a distribution in the sub-Antarctic waters. Nesis (1977) used the strong antitragus in the funnel-locking cartilage of *Mt. psychrophila* to distinguish this species from other members of the *Mt. grimaldii* complex. Morphologically, *Mt. psychrophila* shares some characteristics with the other local *Mastigoteuthis* species—*Mt. dentata*, *Mt.* sp. X, and *Mt.* sp. Y—including the presence of integumental photophores, ear-shaped funnel-locking cartilage, funnel pocket, and arm suckers with sharp teeth.

Two local species that are most morphologically similar to *Mt. psychrophila* are *Mt.* sp. X and *Mt. dentata*. *Mastigoteuthis psychrophila* can be differentiated from *Mt. dentata* by its strong antitragus, gladius cross sections, and the Arms IV photophore pattern (see Remarks for *Mt. dentata*). The funnel-locking cartilage of both *Mt. psychrophila* and *Mt.* sp. X is ear shaped, with a strong tragus and antitragus. These species can be readily differentiated by the photophore pattern on Arms IV: *Mt. psychrophila* has widely spaced discrete clusters of several closely grouped photophores (Fig. 14A), and *Mt.* sp. X has scattered photophores proximally (Fig. 20H). Although the type description did not discuss photophore patterns, a photograph of the holotype (Young & Vecchione, 2010) shows the same pattern found herein. In addition, the specimens of *Mt. psychrophila* in this study have a distribution farther south than *Mt.* sp. X and *Mt. dentata*, which is consistent with the type description. The beaks can also be used to differentiate *Mt.* sp. X and *Mt. psychrophila*: the lower rostrum of the *Mt.* sp. X beak forms an approximate right angle with the baseline (Fig. 22E–I), while the angle is smaller in *Mt. psychrophila* (Fig. 16G, J). In addition, *Mt. psychrophila* is genetically distinct from *Mt.* sp. X and *Mt. dentata* (Chapter 4).

Although *Mt. psychrophila* and *Mt.* sp. Y both have ear-shaped funnel-locking cartilages, *Mt. psychrophila* has a much stronger tragus and antitragus compared to *Mt.* sp. Y (Fig. 26B). The complete photophore pattern of *Mt.* sp. Y is unknown; however, proximally, the Arms IV photophores appear to be scattered (Fig. 28B), which contrasts with the widely spaced distinct clusters of *Mt. psychrophila* (Fig. 14A). The most distinctive feature of *Mt.* sp. Y is the band of photophore around the circumference of the eye (Fig. 28A), which is lacking in *Mt. psychrophila*.

As frequently found in mastigoteuthids herein (see Discussion), the radula morphology of one specimen appeared unusual (Fig. 17C–E) as follows: unicuspid to weakly tricuspid rachidian, base ~65% height, with small, blunt lateral cusps, their height ~40% that of mesocone height. Right first and second lateral teeth fused, triangular, broad sharp, slightly curved; height ~135% that of rachidian; width 120% rachidian. Left first and second lateral teeth separate; first lateral tooth nearly unicuspid with low, rounded outer cusp, its height ~55% that of inner cusp.

Table 7—Measurements (mm) of *Mastigoteuthis psychrophila* Nesis, 1977, all taken on right side except for NIWA 44277.

Specimen ID	**NIWA 44301**	**NIWA 44301**	**NIWA 44277**	**NIWA 44277**	**NMNZ M.070954**	**NMNZ M.012944**	**Mean indices**	
Sex	F	F	Indet.	F	F	F		
ML	96	84	86	99	88	42		
MW	21	20	21	25	28	10	MWI	25
FL	60	53	55	59	56	27	FLI	63
FW	68	51	62	60	60	28	FWI	67
HL	26	23	28	30	28	11	HLI	29
HW	17	13	17	16	14	9	HWI	18
ED	12*	13	12	12*	13*	6	EDI	15
Arm I	45	35*	55	49	36	16	A1LI	48
Arm II	58	50*	75	65	54	24	A2LI	66
Arm III	56	39*	65	52	49	21	A3LI	58
Arm IV	118	90*	108*	103*	94*	55	A4LI	127
TLA	228	190*	205*	230	203*	110		
TL	352	-	-	-	-	-		
TnL	232	-	-	-	-	-	TnLI	242
CL	120	-	-	-	-	-	CLI	125

* indicates damaged features.
- indicates missing features.

***Mastigoteuthis* sp. X** (Table 3, 4, 8, Figs 18–24)

Material examined (14 specimens): **NMNZ M.074544**, ♂, ML 70mm, 22.69°S, 175.03°W, 944m over 3000m,12/12/1976, RV *James Cook*, Stn J17/57/76; **NMNZ M.074197**, 2 sex indet., ML 26, 37mm, 31.95°S, 177.63°E, 869–1006m over 3762m, 24/07/1962, RNZFA *Tui*, MWT; **NMNZ M.172950**, 2 ♀, ML 68,73mm, 32.54°S, 169.73°E, 1257m, 12/05/2003, RV *Tangaroa*, NORFANZ Stn 10; **NMNZ M.150970**, sex indet., ML 62*mm, 39.93°S, 178.2°E, 780–1110m, 26/03/1998, Stn 1097/20; **NMNZ M.100817**, ♀, ML 70mm, 39.97°S, 177.92°E, 1105–1110m, 19/09/1989, RV *James Cook*, bottom trawl, Stn J09/29/89; **NIWA 48870**, ♀, head and mantle lumen only, sex indet., head only, 40.02°S, 178.12°E, 860m, 14/12/1998, Stn Z9573, TRIP 1172/59; **NMNZ M.287213**, ♀, ML 74*mm, 40.55°S, 168.68°E, 937–942m, RV *James Cook*, 09/02/1987, Stn J02/33/87; **NMNZ M.094101**, ♀, ML 85mm, 43.05°S, 168.40°E, 1092m, 14/10/1988, FV *Arrow*, Stn A03/23/83; **NMNZ M.091719**, ♀, ML 90*mm, New Zealand, *Hoplostethus atlanticus* stomach content, Wanakai WK1, 1985 cruise; **NIWA 48865**, ♂, ML 66mm, New Zealand, no data; **NIWA 48864**, ♂, ML 106mm, New Zealand, no data, TAN9306/181.

Beak only: **NIWA 86556**, sex indet., LRL 3.93mm, 42.79–42.80°S, 179.93–179.97°W, 1015–1005m, 17/06/2010, TAN1008/14.

Distribution (Fig. 18): 22–43°S, 168°E–175°W (near New Zealand).

Diagnosis: Fins circular to elliptical in outline when considered together, length 54–*64*–75% ML, width 66–*71*–82% ML; eye-sinus photophore diameter ~9% ED, Arms IV with scattered photophores proximally and two main rows of photophores distally; funnel-locking cartilage ear shaped with strong tragus and strong antitragus; arm suckers with smooth band between teeth and polygonal processes.

Description (ML 37–106mm, Figs 19A, 20–24): Mantle cone-shaped anteriorly, with mantle cavity extending to ~30% of FL from the anterior of fins (thereafter gladius and surrounding musculature continue as narrow cylinder), widest (~24% ML) at anterior margin; dorsal anterior mantle margin slightly convex. Fins circular to elliptical in outline when considered together, length 54–*64*–75% ML, width 66–*71*–82% ML; anterior lobes absent; posterior margin at tail concave. Photophores present on all

external surfaces of fins, mantle, head, funnel, and aboral surface of arms; Arms IV photophore pattern with scattered photophores proximally and two main rows of photophores distally (Fig. 20H); eye-sinus photophore diameter ~9% ED.

Head cylindrical, length ~29% ML, width ~21% ML. Olfactory papilla cylindrical. Eye diameter ~13% ML. Funnel width ~12% ML, length ~10% ML; aperture approximately level with posterior margin of eye; funnel pocket present. Funnel-locking cartilage ear shaped (Fig. 20B), ~6% ML; anterior groove concave due to strong antitragus; strong tragus along inner/medial margin, extending approximately to midline of groove; concave along outer/lateral margin. Mantle-locking cartilage nose shaped (Fig. 20C, D), ~4% ML; posteriorly undercut in profile.

Arm formula IV>II>III>I; arm length 50–*85*–157% ML (Tables 4, 8); Arms I–III all of subequal thickness with aboral keels present; Arms IV thicker with expanded lateral membrane. At ML ~70–106mm, 100–130 suckers present on each arm; largest suckers overall located at base of Arms IV (~30% arm width).

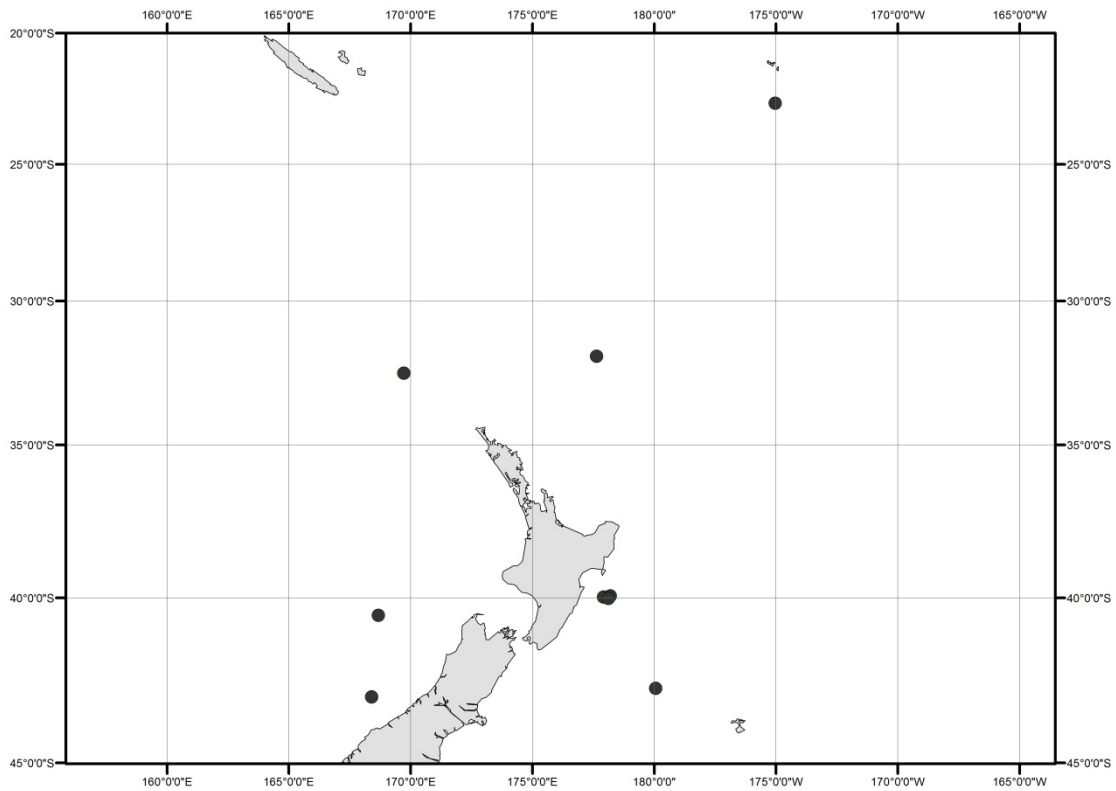

Fig. 18—Distribution of *Mastigoteuthis* sp. X specimens examined in this study.

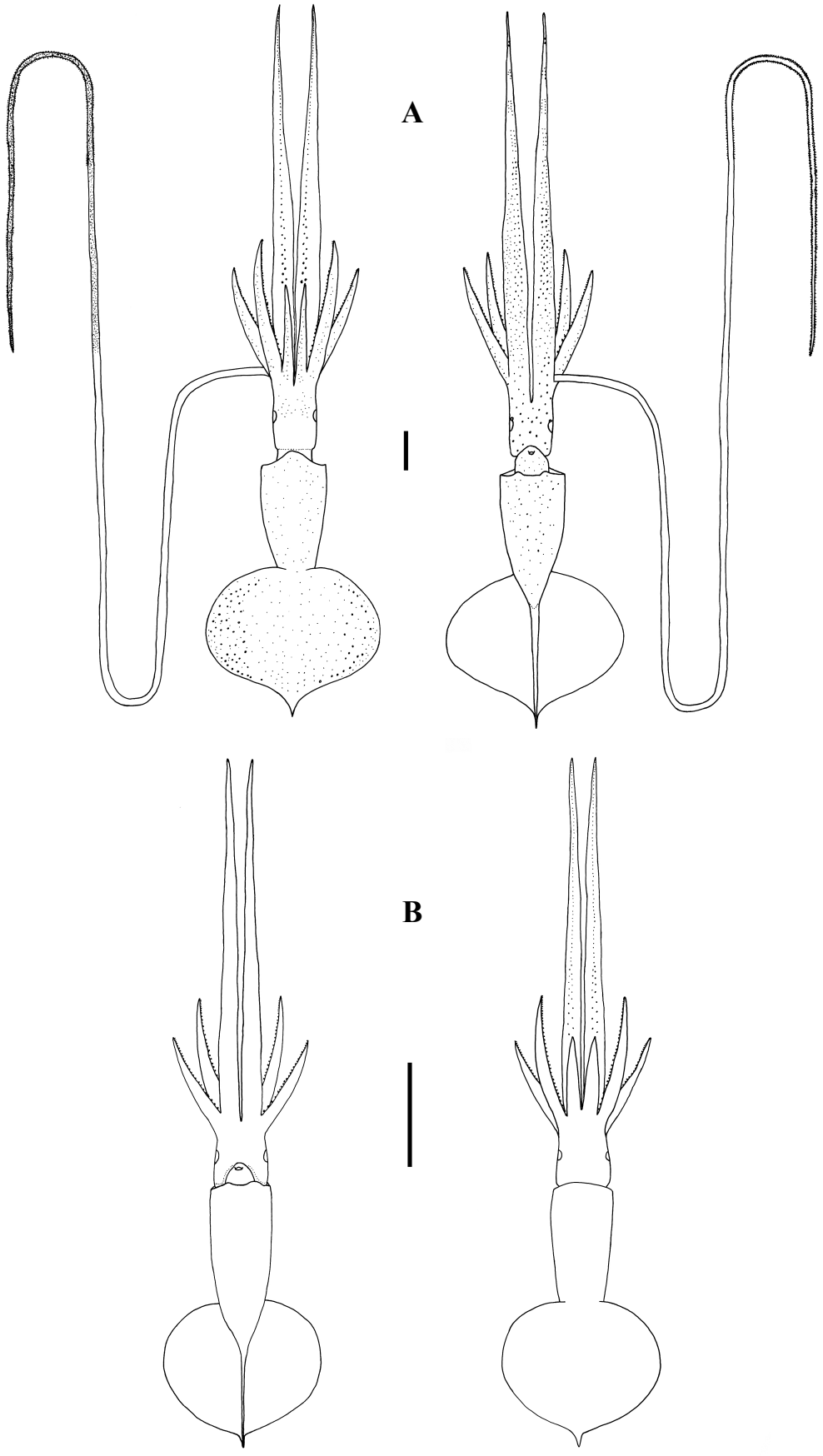

Fig. 19—*Mastigoteuthis* sp. X. A) NMNZ M.172950, ♀, ML 68mm; photophore pattern based on NMNZ M.172950 and NMNZ M.074544, ♂, ML 70mm; tentacle based on NMNZ M.100817, ♀, ML 70mm; B) NMNZ M.074197, sex indet., ML 26mm. Scale bars = 10mm.

Arm-sucker rings (Fig. 21) proximally adentate or with 8–15 short, blunt, rectangular teeth, distally with 5–12 sharp, conical teeth. Polygonal processes on oral surface sucker in 2–6 concentric rings; distally, central and intermediate rings with cylindrical, pitted, porous pegs; proximally, central and intermediate rings nearly flat; peripheral ring with flat, rectangular processes.

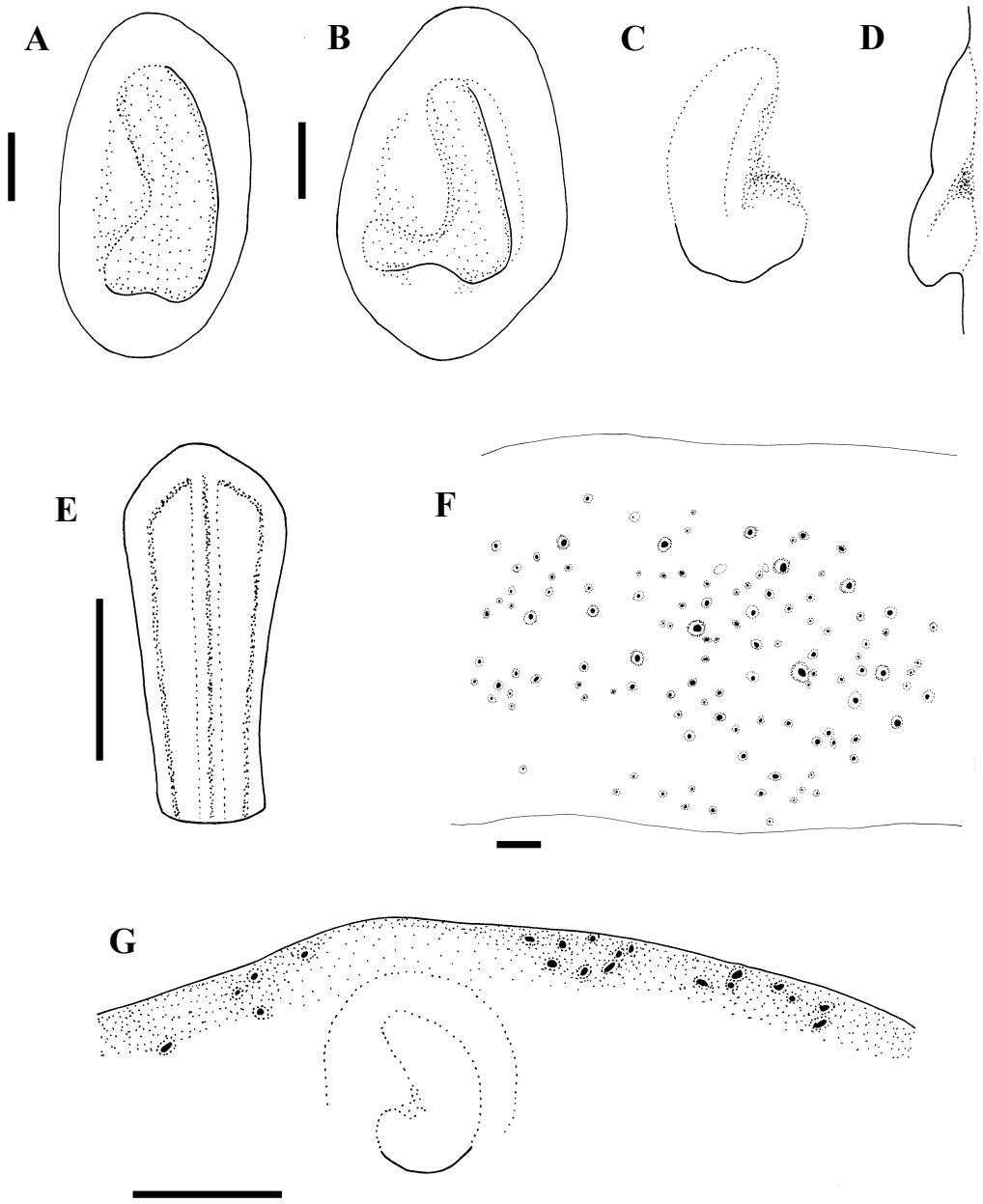

Fig. 20—*Mastigoteuthis* sp. X. A) NMNZ M.172950, ♀, ML 73mm; B–D) NMNZ M.172950, ♀, ML 68mm; E) NIWA 48864, ♂, ML 106mm; F) M.094101, ♀, ML 85mm; G) NIWA 48865, ♂, ML 66mm. A, B) left funnel-locking cartilage; C) left mantle-locking cartilage; D) left mantle-locking cartilage, profile view; E) nuchal cartilage; F) proximal view of aboral photophores on Arms IV; G) internal mantle pigmentation. Scale bars = A–D, F) 1mm; E, G) 5mm.

At ML 70mm (sole tentacle available for examination), tentacle length ~586% ML, club ~56% TnL (~329% ML), not expanded; stalk without keel. Suckers minute, covering majority of tentacle surface apart from narrow aboral strip; proximally, width of sucker-covered surface is less than half of stalk circumference, broadening distally to cover nearly entire stalk circumference. Tentacular suckers (Fig. 22A–D) adentate; polygonal processes on oral surface of suckers in three concentric rings; central ring with 12–13 circular to ovate pegs; intermediate ring with 24–27 smaller, circular pegs; peripheral ring with 45–54 rectangular-faced pegs; rim processes rectangular. Sucker diameter ~100µm (~5% club width).

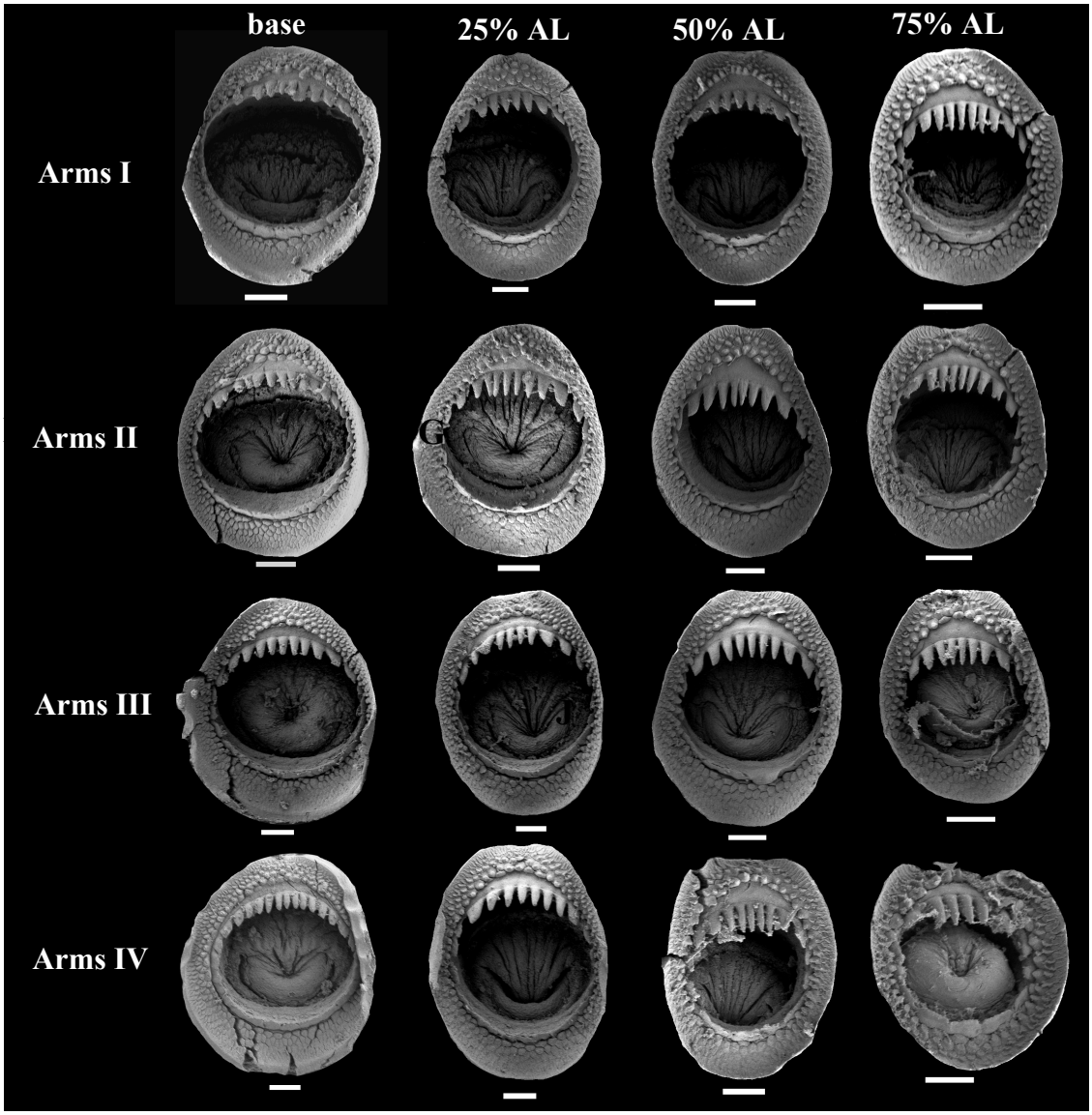

Fig. 21—*Mastigoteuthis* sp. X arm suckers, NIWA 48864, ♂, ML 106mm. Scale bars = 100µm.

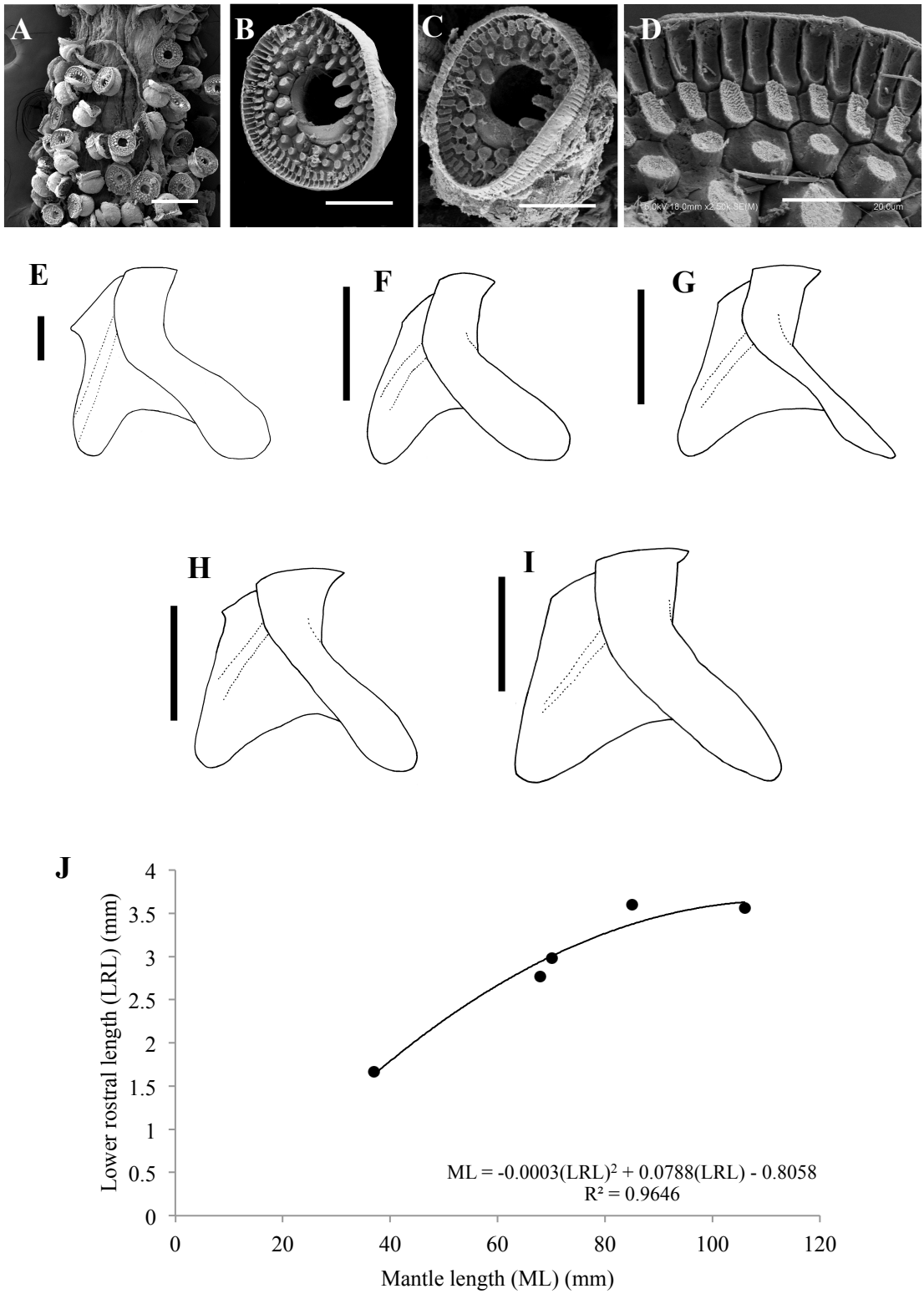

Fig. 22—*Mastigoteuthis* sp. X. A–D, F) NMNZ M.100817, ♀, ML 70mm, LRL 2.98mm; E) M.074197, ML sex indet., 37mm, LRL 1.67mm; G) NIWA 94101, ♀, ML 85mm, LRL 3.60mm; H) NIWA 48864, ♂, ML 106mm, LRL 3.56mm; I) NIWA 48870, ♀, ML unknown, LRL 4.16mm. A–D) tentacle suckers; E–I) lower beaks in profile; J) regression equation for ML and LRL. Scale bars = A) 200µm; B, C) 50µm; D) 20µm; E) 1mm; F–I) 5mm.

Lower beak, lateral profile (Fig. 22E–I): lower rostral length 38–*50*–55% wing length, rostral edge forms nearly right angle to baseline, rostral edge nearly straight, rostral tip hooked, rostral tip behind leading edge of wing by 34–*38*–47% of baseline; wing angle obtuse, low wing fold obscures jaw angle in profile, shoulder groove present; beak height ~91% baseline; hood slightly above crest, hood length 42–*60*–70% crest length, crest length ~54% baseline, visible portion of crest slightly curved; broad lateral wall fold present, thickened into a ridge, lateral wall fold extends to posterior edge of lateral wall; slight notch in lateral wall. Lateral oblique view (Fig. 23A–E) with wing

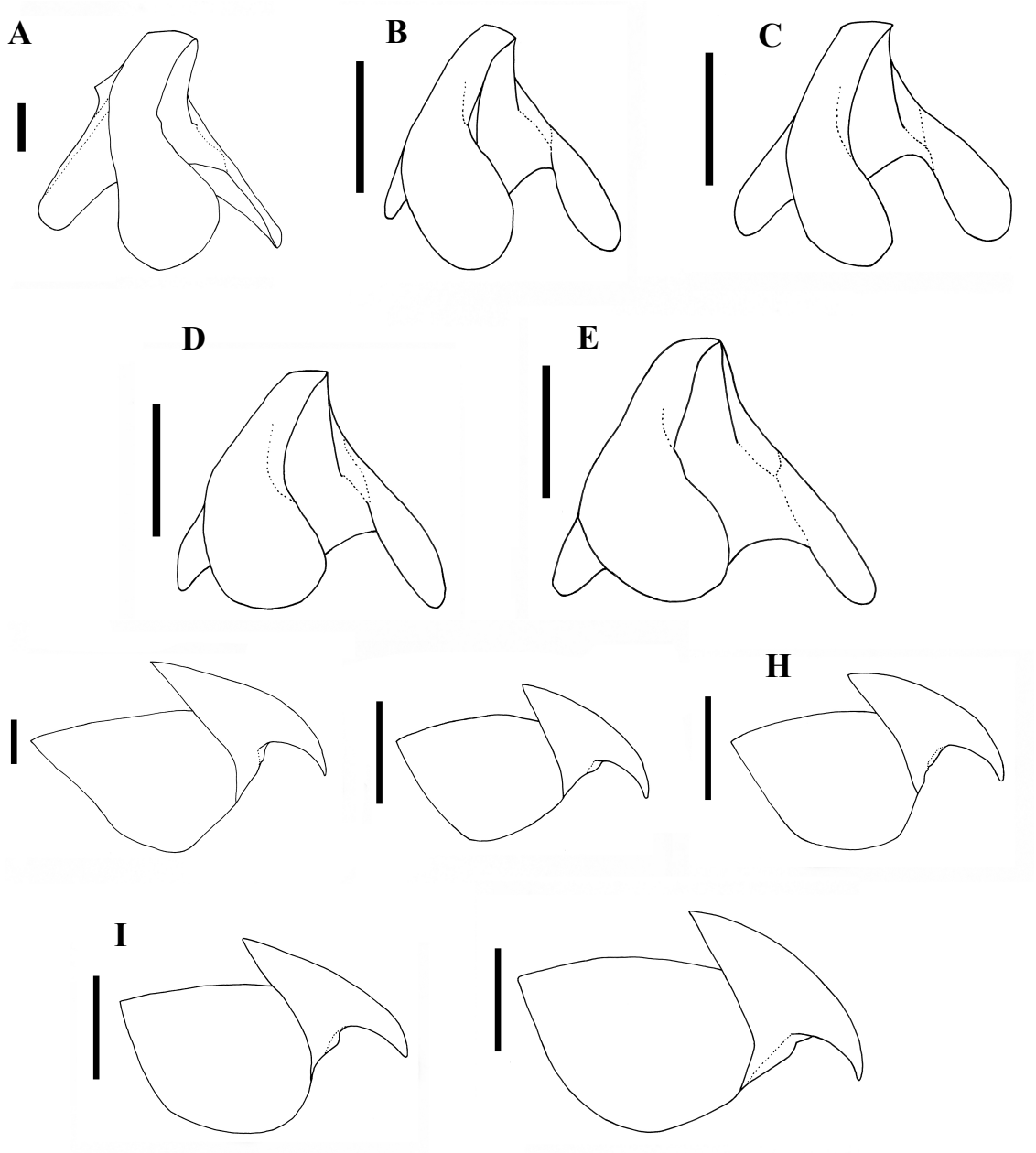

Fig. 23—*Mastigoteuthis* sp. X beaks. A, F) NMNZ M.100817, ♀, ML 70mm; B, G) M.074197, ML sex indet., 37mm; C, H) NIWA 94101, ♀, ML 85mm; D, I) NIWA 48864, ♂, ML 106mm; E, J) NIWA 48870, ♀, ML unknown, LRL 4.16mm. A–E) lower beaks in lateral oblique view; F–J) upper beaks. Scale bars = A, F) 1mm; B–E, G–J) 5mm.

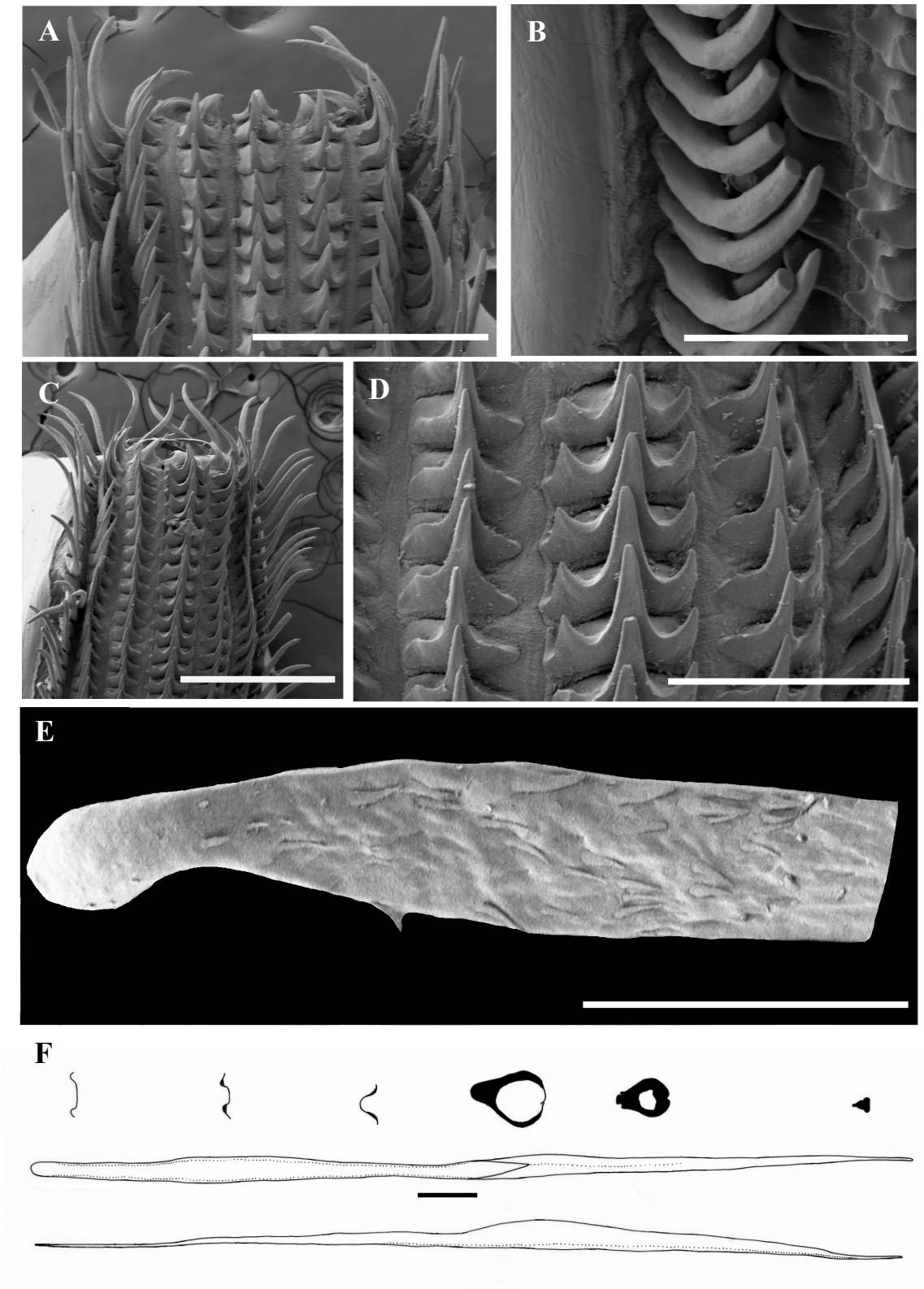

Fig. 24—*Mastigoteuthis* sp. X. A, B) NIWA 48864, ♂, ML 106mm; C–F) NMNZ M.172950, ♀, ML 68mm. A) radula; B) radula margin; C) asymmetrical radula; D) asymmetrical radula rachidian and first lateral teeth; E) palatine palp; F) gladius. Scale bars = A, C) 500µm; B, D) 200µm; E) 1mm; F) 5mm.

narrowest level with jaw angle, 50–*57*–67% of greatest width. Ventral view with shallow, broad notch in hood wing structure, free corners well separated. Anterior shoulder and wing with clear cartilage and wing unpigmented at LRL 2.63mm, wing only pigmented in mid region of distal wing at LRL 2.98mm (ML 70mm), clear cartilage only present at junction of lateral wall and shoulder at LRL 3.64mm (ML 85mm), posterior edge, and anterior edge below shoulder of wing remains clear at LRL 3.76mm (ML 106mm), fully pigmented by LRL 4.45mm. Regression equation (Fig. 22J) $ML = -0.0003(LRL)^2 + 0.0788(LRL) - 0.8058$ ($R^2 = 0.9646$) (N=5).

Upper beak, lateral profile (Fig. 23F–J): upper rostral length ~35% hood length, hood ~68% beak length, hood height 26–*32*–37% beak width. Lateral wall fold absent; shoulder not produced into point; jaw edge curved, jaw angle acute.

Radula (Fig. 24A) with tricuspid rachidian, base ~95% height, proximal margin of base slightly concave, with broad, sharp, triangular mesocone and small, pointed lateral cusps, slightly laterally directed, their height ~20% mesocone height. First lateral tooth weakly bicuspid; inner cusp broad, triangular, nearly straight, its height ~120% that of rachidian; small, blunt outer cusp, laterally directed, its height ~25% that of inner cusp. Second lateral tooth simple, curving slightly towards rachidian, ~170% height of rachidian. Marginal tooth simple, slightly curved, ~260% height of rachidian. Faint marginal plate present (Fig. 24B). Palatine palp (Fig. 24E) with ~35 narrow, flat teeth, each ~80–220% rachidian height, sparsely distributed over palp.

Gladius (Fig. 24F) with greatest width (3% GL) attained at ~20% GL; free rachis ~15% GL; secondary conus ~45% GL, rostrum 6% GL, approximately triangular with rounded corners in cross section.

Epidermis nearly always damaged. Integumental photophores present. Colour (preserved) dark purple to pink-purple; aboral arm surfaces dark; head with lighter pigmentation; chromatophores overlying integumental photophores; pigmentation on interior mantle wall with small photophores extending to the anterior margin of locking cartilage (Fig. 20G); scattered chromatophores present on aboral surface of arms; oral surface of arms darkly pigmented but individual chromatophores not readily discernible.

Smaller specimens (ML 26mm, Fig. 19B) differ from above descriptions only as follows: fin width ~58% ML. Arms I ~27% ML with , Arms II ~46% ML, Arms III ~35% ML, Arms IV ~127% ML; with 48–112 suckers present on each arm.

Remarks: *Mastigoteuthis* sp. X belongs in *Mastigoteuthis* as defined herein, which has the same characteristics as the *Mt. agassizii* group: ear-shaped funnel-locking cartilage, integumental photophores, a small eye-sinus photophore, funnel pocket, and arm suckers with sharp teeth. There are four local species in this group: *Mt. dentata*, *Mt. psychrophila*, *Mt.* sp. X, and *Mt.* sp. Y. Although *Mt.* sp. X and *Mt.* sp. Y both appear to have scattered photophores proximally on Arms IV (Figs 20F, 28B), *Mt.* sp. X has a stronger tragus and antitragus in the funnel-locking cartilage (Fig. 28A). In addition, *Mt.* sp. X lacks eye photophores, while *Mt.* sp. Y has a photophore forming a single band around the circumference of the eye. *Mastigoteuthis* sp. X can be differentiated from *Mt. psychrophila* by the photophore patterns on Arms IV, gladius cross sections, arm-sucker rings, and beaks (see Remarks for *Mt. psychrophila*). In addition, *Mt.* sp. X is genetically distinct from *Mt. psychrophila* (Chapter 4).

Mastigoteuthis sp. X most closely resembles *Mt. dentata* and *Mt. agassizii*. Proximally, the Arms IV of *Mt.* sp. X have scattered photophores (Fig. 20F), while *Mt. dentata* (Fig. 7E) and *Mt. agassizii* have two distinct series. Distally, however, these species all have two distinct series of photophores. The arm suckers of *Mt.* sp. X all appear to have a smooth band between the polygonal processes and the teeth (Fig. 21), which is lacking in *Mt. dentata* (Fig. 8). The beaks can be readily differentiated by the angle of the jaw to the baseline, which forms an approximate right angle in *Mt.* sp. X (Fig. 22E–I), and a smaller angle in *Mt. dentata* (Fig. 9A–E) and *Mt. agassizii* (*fide* Young & Vecchione, 2007f). The funnel-locking cartilage of *Mt.* sp. X generally has a strong antitragus (Fig. 20B), but in some specimens the antitragus may appear weaker (Fig. 20A) and closely resemble that of *Mt. dentata* (Fig. 7A) or *Mt. agassizii*. Genetically, *Mt.* sp. X can be differentiated from *Mt. agassizii*, but they are very closely related (Chapter 4). However, *Mt. dentata* and *Mt.* sp. X cannot be distinguished with 16S rRNA or 12S rRNA (Chapter 4), but more quickly evolving genes should be investigated in the future.

Mastigoteuthis flammea Chun, 1908, which was described from the North Atlantic, also shares some morphological similarities with *Mt.* sp. X. Both have funnel-locking

cartilage with a strong tragus and antitragus. However, the arm suckers of *Mt. flammea* have 3–5 small, sharp teeth (Chun, 1910), while *Mt.* sp. X has 5–12 long, sharp teeth. Additionally, *Mt. flammea* is distinguished by the small size of the eyes (~10% ML), compared with the larger eyes of *Mt.* sp. X (~13% ML). However, because no specimens of *Mt. flammea* were available, no statistical significance could be determined. Nesis (1977) suggested that the specimens identified as *Mt. flammea* from New Zealand waters by Dell (1959) were likely *Mt. dentata*. However, without details of the funnel-locking cartilage, photophore patterns, arm suckers, and beak morphology, it is possibly that Dell's specimens could have been either *Mt. dentata* or *Mt.* sp. X. Previous authors have considered *Mt. flammea* a junior synonym of *Mt. grimaldii* (Salcedo-Vargas, 1997) or *Mt. agassizii* (Salcedo-Vargas & Okutani, 1994; Vecchione & Young, 2006b).

Mastigoteuthis schmidti Degner, 1925 is another member of the *Mt. agassizii* group described from the North Atlantic. This species can be differentiated from *Mt.* sp. X by the photophore pattern on Arms IV; *Mt. schmidti* has two main series of photophores, in contrast to the proximal scattered pattern of *Mt.* sp. X. In addition, previous authors have considered *Mt. schmidti* a junior synonym of *Mt. agassizii* (Salcedo-Vargas & Okutani, 1994; Salcedo-Vargas, 1997; Young & Vecchione, 2006b).

Mastigoteuthis grimaldii (Joubin, 1895) was described from the Azores. Unfortunately, the photophore pattern on Arms IV was not described. However, Salcedo-Vargas (1997) reported specimens of *Mt. grimaldii* from the Indian Ocean, and found two main series of photophores on Arms IV, contrasting with the scattered photophore pattern found on *Mt.* sp. X. The funnel-locking cartilage of *Mt. grimaldii* lacks an antitragus (Joubin, 1895), which contrasts with the strong antitragus of *Mt.* sp. X. Some previous authors have considered *Mt. grimaldii* a junior synonym of *Mt. agassizii* (Salcedo-Vargas & Okutani, 1994; Young & Vecchione, 2006b).

Rancurel (1971) described specimens he identified as *Mt. grimaldii* from the Gulf of Guinea, and this description has many similarities with *Mt.* sp. X. The photophore pattern on Arms IV was described as having approximately three series of photophores proximally on Arms IV and two series distally, which is similar to *Mt.* sp. X. His beak description is also morphologically similar to *Mt.* sp. X. Furthermore, the arm suckers had a smooth band between the teeth and polygonal processes, which is characteristic of

Mt. sp. X. Although the species described by Rancurel (1971) cannot be differentiated from *Mt.* sp. X, it is not clear that the species he described was *Mt. grimaldii*. The presence of a clear antitragus in Rancurel's specimens contrasts with the type description for *Mt. grimaldii*, where the funnel-locking cartilage lacked an antitragus.

As frequently found in mastigoteuthids herein (see Discussion), the radula morphology of one specimen appeared unusual (Fig. 24C, D) as follows: rachidian with sharp lateral cusps, slightly laterally directed, their height ~55% that of mesocone height. Right first lateral tooth unicuspid, its height 90% that of rachidian. Left first lateral tooth strongly bicuspid, its height 80% that of rachidian; sharp outer cusp, slightly laterally directed, its height ~80% that of inner cusp.

Table 8—Measurements (mm) of *Mastigoteuthis* sp. X.

Specimen ID:	**NMNZ M.074197**	**NMNZ M.074197**	**NMNZ M.172950**	**NMNZ M.172950**	**NIWA 48864**	**NIWA 48865**	**NMNZ M.100817**	**NMNZ M.94101**	**NMNZ M.074544**	**Mean Indices**	
Sex	Indet.	Indet.	F	F	M	M	F	F	M		
ML	26	37	68	73	106	66	70	85	70		
MW	6	8	17	19	22	16	15	20	18	MWI	24
FL	14	21	41	49	74	42	48	64	38	FLI	64
FW	15	25	48	55	70	44	52	70	46	FWI	71
HL	7	11	20	23	25	20	20	25	19	HLI	29
HW	5	8	14	16	18	13	15	14*	18	HWI	21
ED	3	5	8	11	13	10	8*	-	9	EDI	13
Side measured	R	R	L	R	L	L	L	L	R		
Arm I	7	18	30	37	50	31	45	49	30	A1LI	50
Arm II	12	25	45	47	66	41	68	64	42	A2LI	69
Arm III	9	20	42	47	58	37	51	61	40	A3LI	62
Arm IV	33	52	107	113	132	120	130	148	95	A4LI	157
TLA	65	95	197	205	252	203	205	259	180		
TL	-	-	-	-	-	-	500	-	-		
TnL	-	-	-	-	-	-	410	-	-	TnLI	586
CL	-	-	-	-	-	-	230	-	-	CLI	56

*indicates damaged features.
-indicates missing features.

***Mastigoteuthis* sp. Y** (Table 3, 4, 9, Figs 25–28)

Material examined: **NIWA 71721**, ♀, ML 124mm, 44.82–44.82°S, 173.05–173.04°E, 1053–1052m, 13/04/1997, Stn TAN9705/3.

Distribution (Fig. 25): 44–45°S, 173°E–174°W (near New Zealand).

Diagnosis: Fins heart shaped in outline when considered together, length ~64% ML, width ~73% ML; integumental photophores present, eye-sinus photophore diameter ~6% ED, eye photophore single band around circumference of eye; skin tubercles absent; funnel-locking cartilage ear shaped with tragus and weak antitragus; arm suckers with small, sharp teeth.

Description (ML 124mm, Figs 26–28): Mantle cone-shaped anteriorly, with mantle cavity extending to ~30% FL from anterior of fins (thereafter gladius and surrounding musculature continue as narrow cylinder), widest (~31% ML) at anterior margin; dorsal mantle margin nearly straight. Fins heart shaped in outline when considered together, length ~65% ML, width ~73% ML; rounded anterior lobes present; posterior margin at tail convex. Photophores present on all external surfaces of head, funnel, and aboral arms (fins and mantle unknown); Arms IV photophore pattern scattered (Fig. 28B); eye-sinus photophore diameter ~6% ED.

Head boxy, length ~20% ML, width ~19% ML. Olfactory papilla slim, long with expanded bulb. Eye diameter ~11% ML. Single photophore band around circumference of eye (Fig. 28A). Funnel width ~16% ML, length ~12% ML; aperture approximately level with midpoint of eye; funnel pocket present. Funnel-locking cartilage ear shaped (Fig. 26B), ~6% ML, anterior groove nearly flat with weak antitragus; tragus along inner/medial margin extending to midline by ~30% of groove width; nearly straight along outer/lateral margin. Mantle-locking cartilage nose shaped (Fig. 26C, D), ~4% ML; posteriorly undercut in profile.

Arm formula II>III>I (Arms IV unknown); Arms I–III range from 56–*62*–69% ML (Tables 4, 9) and of subequal thickness; Arms I and III with oral faces bordered by wide membranes, aboral keels present (Arms II keels and membranes unknown); Arms IV thicker, with expanded lateral membrane. Trabeculae absent. At ML 124mm, 50–55

pairs of suckers present on each arm (Arms IV unknown), arranged in two distinct series; largest suckers overall located on Arms II (~50% arm width) at about third pair.

Arm-sucker rings (Fig. 27) proximally with 12–16 blunt, rectangular teeth, distally with 8–14 small, sharp teeth. Polygonal processes on oral surface of sucker in 4–8 concentric rings; distally, central and intermediate rings with cylindrical to conical, pitted, porous pegs; proximally, central and intermediate rings nearly flat; peripheral ring with flat, rectangular processes.

Tentacles absent from sole known specimen.

Lower beak, lateral profile (Fig. 28F): lower rostral length ~40% wing length, rostral edge moderately curved, rostral tip without hook, rostral tip behind leading edge of wing by ~30% of baseline; wing angle obtuse, jaw angle obscured by low wing fold, shoulder groove present; beak height ~85% baseline; hood close to crest, hood length ~55% crest length, crest length ~55% baseline, visible portion of crest slightly curved; broad lateral wall fold extending to posterior edge of lateral wall; no notch in lateral wall. Lateral oblique view (Fig. 28G) with wing narrowest level with jaw angle, ~70% of greatest width. Ventral view with narrow notch in hood, free corners separated

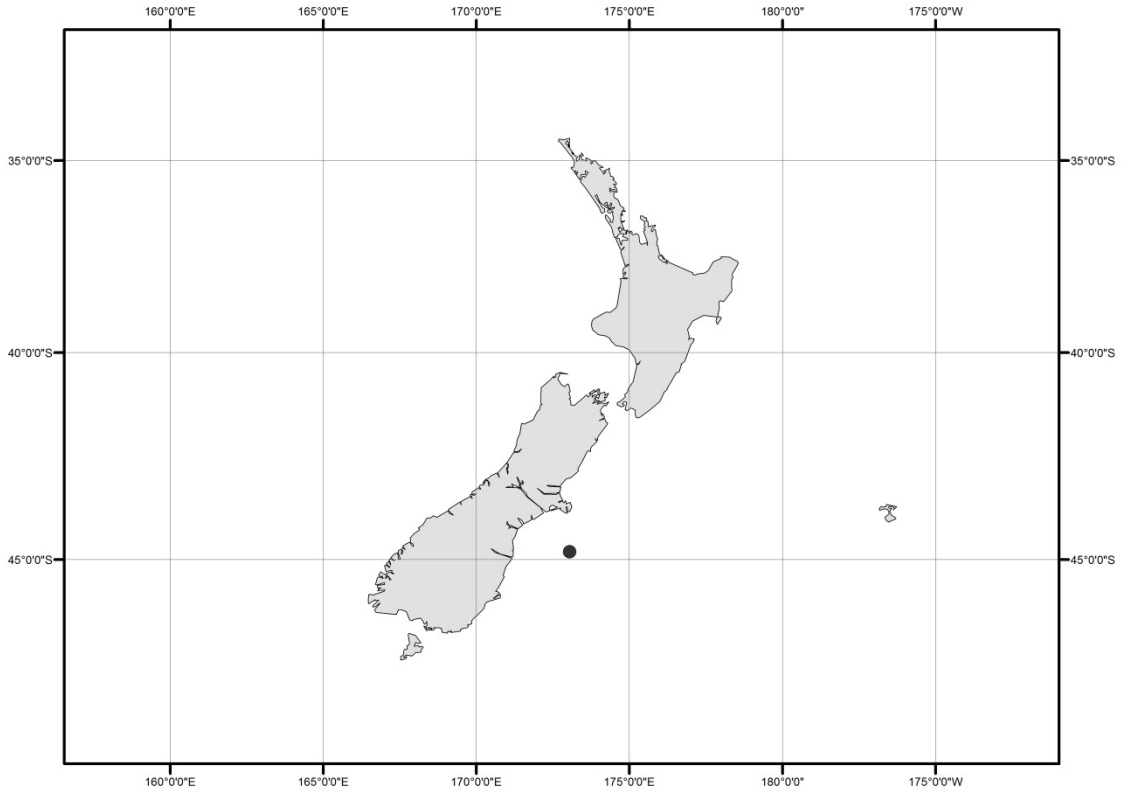

Fig. 25—Collection location of the *Mastigoteuthis* sp. Y specimen examined in this study.

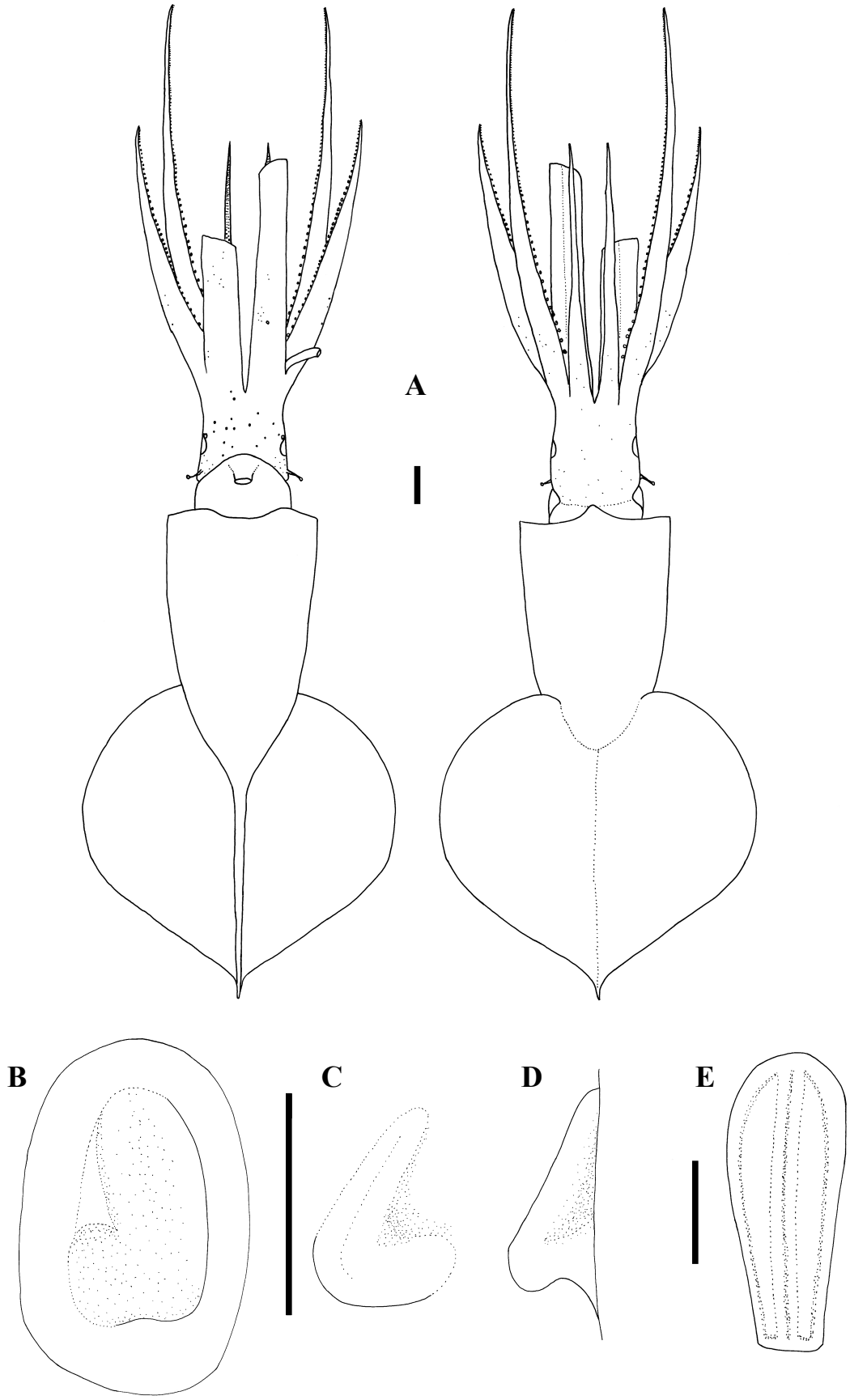

Fig. 26—*Mastigoteuthis* sp. Y, NIWA 71721, ♀, ML 124mm. A) whole specimen; B) left funnel-locking cartilage; C) left mantle-locking cartilage; D) left mantle-locking cartilage profile view; E) nuchal cartilage. Scale bars = A) 1cm; B–E) 5mm.

slightly. Posterior edge of wing, and anterior edge of wing below shoulder, remain clear through at least ML 124mm (LRL 3.70mm).

Upper beak, lateral profile (Fig. 28H): upper rostral length ~25% hood length; hood length ~65% beak length; hood height ~30% beak width. Lateral wall fold absent; shoulder produced into small point; jaw edge curved; jaw angle nearly 90°.

Radula (Fig. 28D) with tricuspid rachidian, base width ~80% height, proximal margin of base rectangular, with broad, sharp, triangular mesocone and small, sharp lateral cusps, laterally directed, their height ~60% mesocone height. First lateral tooth bicuspid; inner cusp broad, triangular, slightly curved away from rachidian, its height ~90% that of overall rachidian; outer cusp sharply pointed, medially directed, its height

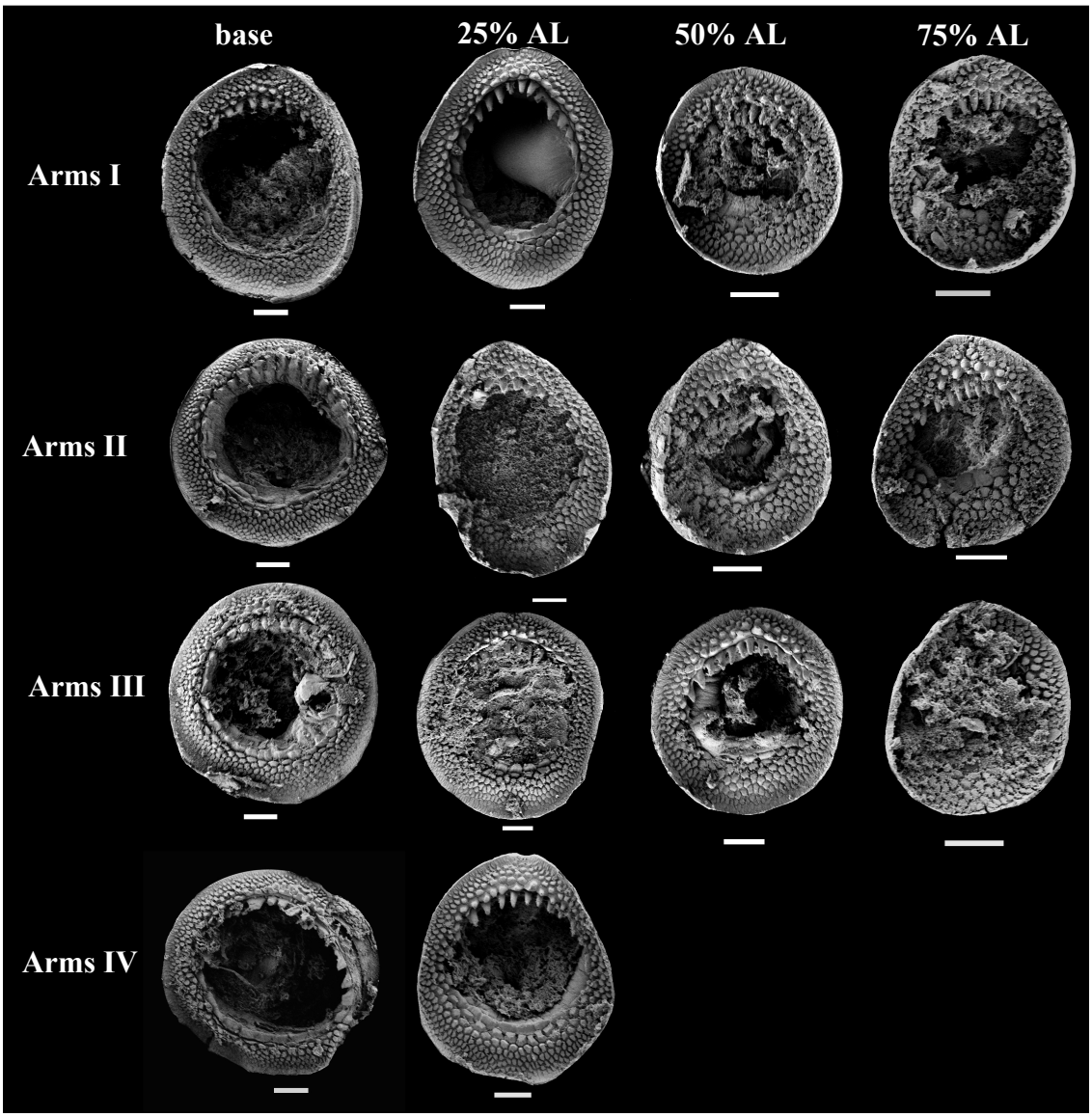

Fig. 27—*Mastigoteuthis* sp. Y arm suckers, NIWA 71721, ♀, ML 124mm. Scale bars = 100µm.

~70% that of inner cusp. Second lateral tooth simple, curving slightly away from rachidian, ~140% height of rachidian. Marginal tooth simple, slightly curved, ~280% height of rachidian. Marginal plate absent. Palatine palp (Fig. 28E) with ~80 broad, flat teeth, each 30–250% rachidian height, densely distributed over palp.

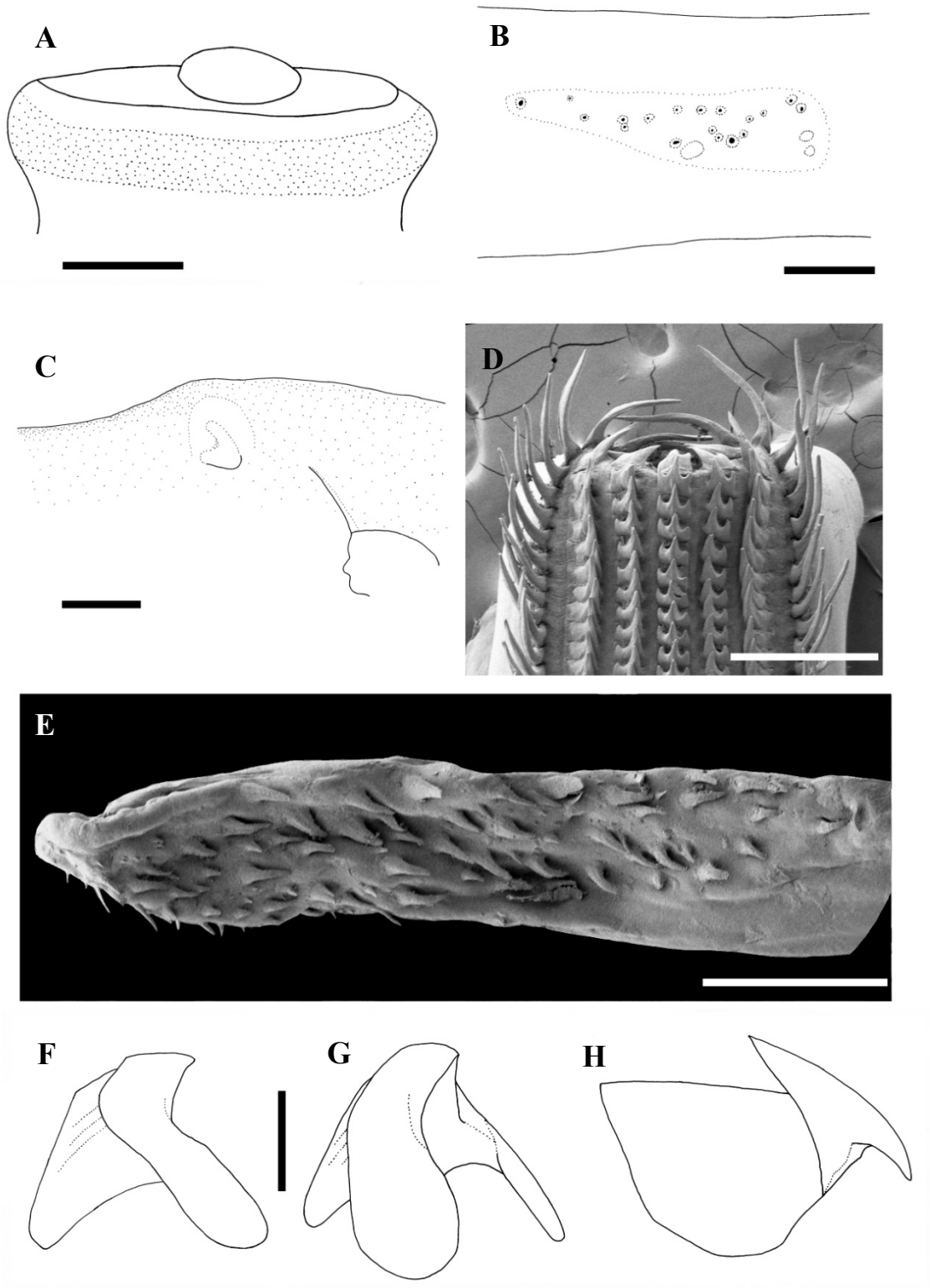

Fig. 28—*Mastigoteuthis* sp. Y, NIWA 71721, ♀, ML 124mm, LRL 3.70mm. A) eye photophore; B) proximal Arms IV; C) internal mantle pigmentation; D) radula; E) palatine palp; F) lower beak, profile view; G) lower beak, lateral profile view; H) upper beak. Scale bars = A–D, F–H) 5mm; E) 1mm.

Gladius not dissected due to limited material.

Epidermis extensively damaged on single specimen available; integument absent from Arms II, and dorsal and ventral mantle and fins. Integumental photophores present. Colour (preserved) pinkish-purple; posterior region of head white, with pronounced darkening around eye sinus; pigmentation on anterior edge of mantle interior extending approximately to level of gills (Fig. 28C); chromatophores present on aboral surface of arms with underlying photophores, arm oral surface darkly pigmented but individual chromatophores not readily discernible.

Remarks: *Mastigoteuthis* sp. Y is similar to members of the *Mt. agassizii* group (species considered herein as *Mastigoteuthis*) because of the ear-shaped funnel-locking cartilage, small integumental photophores, small eye-sinus photophore, funnel pocket, and arm suckers with sharp teeth. However, *Mt.* sp. Y can be distinguished from all other mastigoteuthids by the single photophore band around the circumference of the eye.

Within Mastigoteuthidae, eye photophores are also found in *Mp. hjorti* (Fig. 41E, F), *I. cordiformis* (Fig. 32), *I. okutanii* (Salcedo-Vargas, 1997), and potentially in *Mg*. sp. nov. (Fig. 50). However, the morphology of the eye photophore of *Mt.* sp. Y is unique (Fig. 28A). *Mastigopsis hjorti* and *I. okutanii* each have two round, ventral eye photophores, *I. cordiformis* has a single, crescent-shaped photophore on the ventral side of the eye (Fig. 31G, H), and *Mt*. sp. Y has a single photophore band around the entire circumference of the eye. *Idioteuthis okutanii* is found in the Indian Ocean, and is only known from paralarvae (Salcedo-Vargas, 1997). Although *Mp. hjorti* and *I. cordiformis* also occur locally, they can be differentiated from *Mt.* sp. Y by the larger fin (nearly as long as the mantle length), lack of integumental photophores, lack of funnel pocket, and presence of skin tubercles. Although this species can be distinguished from all other mastigoteuthids, it is currently only known from a single, badly damaged specimen with no tissue available for DNA analysis.

Table 9—Measurements (mm) of *Mastigoteuthis* sp. Y, recorded from right side of specimen.

Specimen ID:	**NIWA 71721**	**Indices**	
Sex	F		
ML	124		
MW	39	MWI	31
FL	80	FLI	65
FW	91	FWI	73
HL	25	HLI	20
HW	23	HWI	19
ED	14	EDI	11
Arm I	70	A1LI	56
Arm II	86	A2LI	69
Arm III	77	A3LI	62
Arm IV	55*	A4LI	>44
TLA	265*		

* indicates damaged features.

Genus *Idioteuthis* Sasaki, 1916

Idioteuthis Sasaki, 1916: 108. Type species *Idioteuthis latipinna* Sasaki, 1916, by monotypy.

Iridioteuthis [sic] Sasaki, 1929: 310.

Diagnosis: Mantle length at maturity 450 mm to > 1 m. Fins heart shaped or elliptical in outline when considered together; fin length ~81% ML. Funnel bulbous posteriorly, anteriorly cylindrical. Funnel-locking cartilage ear shaped, tragus, and antitragus present; funnel pocket absent. Mantle-locking cartilage nose shaped, posteriorly undercut in profile. Arm suckers adentate or possess blunt teeth, arranged in two distinct series; arm length subequal, Arms II (~77% ML) often slightly longer than Arms IV (~77% ML); trabeculae present on arms' protective membranes. Tentacular suckers proximally large, distally minute; club slightly expanded with trabeculate membrane. Eye-sinus photophore absent. Single crescent-shaped photophore present on ventral surface of eye. Integumental photophores absent, skin tubercles present. Gladius broad (greatest width ~10% GL).

Remarks: The status of *I. cordiformis* in the family Mastigoteuthidae is presently unclear. This species shares some characteristics with other mastigoteuthids such ear-shaped funnel-locking cartilage and whip-like tentacles with minute suckers distally. However, in contrast to other mastigoteuthids, the tentacles of *I. cordiformis* are slightly expanded and the proximal suckers are large and have a similar morphology to arm suckers. Additionally, *I. cordiformis* has subequal arms, with Arms II often being longer than Arms IV, while Arms IV in other mastigoteuthids are much longer than the other arms. Furthermore, the mantle length of large *I. cordiformis* individuals is at least five times larger than that of any other mastigoteuthid squid at maturity. Although, out of all species in the chiroteuthid families, the most similar to *I. cordiformis* is *Mp. hjorti*. Both species have large fins, similar skin tubercles, eye photophores, and lack integumental photophores.

***Idioteuthis cordiformis* (Chun, 1908)** (Tables 3, 4, 10, Figs 29–38)

Mastigoteuthis cordiformis Chun, 1908: 88; Chun (1910): 177–180, pl. 34, 35 figs 1, 5,6, 8, 10–14, pl. 36 fig. 3–5, pl. 37 fig. 5; Sasaki (1929): 310–312, pl. 24 figs 15–20; Adam (1954): 159–161, fig. 25, pl. 2 fig. 1; Voss (1963): p. 140–142, fig. 30 B–H; Young (1972): 67.

Idioteuthis cordiformis (Chun, 1908) — Salcedo-Vargas (1993): 155–170, figs 169–222; Salcedo-Vargas & Okutani (1994): 124, fig. 1, 2, 5.

Type material (not examined): **ZMB/Moll 46096**, holotype, ♂, ML 83mm, 0.25°N, 98.13°E, 614m.

Material examined (28 specimens): **NMNZ M.181333**, ♂, ML 181mm, 24.72°S, 168.65°E, 18/11/1996, 720–1048m, RV *Tangaroa*, Stn HALIPRO2 BT62; **NMNZ M.274092**, ♀, ML 205mm, 26.04°S, 173.03°E, 956m, 20/06/2007, FV *Ocean Fresh* with Sanford Limited; **NMNZ M.306358**, ♂, ML 549mm, 33.78°S, 167.49°E, 29/05/2003, RV *Tangaroa*, Stn TAN308/103; **NIWA 71655**, ♀, ML 320mm, 34.02°S, 174.80°E, 780m, 10/07/1999, Stn Z9784; **NIWA 71651**, ♂, ML 251*mm, 34.10°S, 174.91°E, 862m, 08/07/1999, Stn Z9785; **NMNZ M.306356**, sex indet., ML 405mm, 34.24°S, 168.35°E, 03/06/2003, RV *Tangaroa*, Stn TAN308/146; **NMNZ M.306355**, ♂, ML 513mm, 34.57°S, 168.94°E, 03/06/2003, RV *Tangaroa*, Stn TAN308/151; **NIWA 71437**, ♂, ML 608mm, 34.94°S, 170.25°E, 820m, 17/01/2002, Stn Z11003; **NMNZ M.174313**, ♀, ML 654mm, 34.95°S, 170.25°E, 1105m, 08/10/2003, FV *Seamount Explorer* with Thickpenny, Stn 1828/11; **NIWA 71653**, ♂, ML 428mm, 35.98°S, 166.17°E, 1000m, 07/03/1999, Stn Z9723; **NIWA 71661**, ♀, ML 620mm, 36.40–36.40°S, 176.95–176.94°E, 940–1175m, 17/06/1995, Stn Z8292; **NMNZ M.298936**, ♀, ML 620*mm, 36.42°S, 177.83°E, 1177m, FV *Seamount Explorer* with Rattray, Stn 2268; **NIWA 71665**, ♂, ML 286mm, 36.54°S, 176.51°E, 909m, 24/06/1998, Stn Z9158; **NIWA 71664**, ♀, ML 344mm, 36.54°S, 176.51°E, 899m, 19/06/1998, Stn Z9157; **NIWA 71659**, ♀, ML 520mm, 36.54°S, 176.52°E, 913–920m, 25/06/1995, Stn Z8291; **NIWA 71663**, ♀, ML 286mm, ♂, ML 342mm, 37.24°S, 177.23°E, 800m, 28/03/2000, Stn Z10079; **NIWA 71656**, ♀, ML 434mm, 37.40°S, 178.64°E, 37.41°S, 178.64°E, 783–1050m, 19/05/1995, Stn Z8415; **NMNZ M.118004**, ♀, ML 715mm, 37.44°S, 179.32°E, 1095–1193m, 25/03/1992, RV *Tangaroa*, Stn TAN9203/138; **NMNZ M.274094**, ♀, ML 284mm, 37.68°S, 179.38°E, 778m, 21/06/2007, FV *San Rakaia*; **NIWA 71666**, ♀, ML 380*mm, ♂, ML 463*mm, 39.90°S,

178.27°E, 1187m, 20/09/1995, Stn Z8380; **NIWA 71654**, ♀, ML 530mm, 40.00°S, 178.15°E, 40.08°S, 178.12°E, 730–1350m, 20/09/1995, Stn Z8381; **NIWA 71658**, ♀, ML 466mm, 40.10°S, 178.00°E, 750m, 19/08/1995, Stn Z8324; **NMNZ M.117572**, ♀, ML 840*mm, 40.11°S, 178.18°E, 857m, 10/04/1993, RV *Tangaroa*, Stn TAN9303/220; **NMNZ M.299012,** ♀, ML 930mm, New Zealand, no data; **NIWA 71668**, ♀, ML 475*mm, New Zealand, no data; **NIWA 84390**, ♀, ML 820mm, New Zealand, no data; **NIWA 71652**, ♂, ML 248mm, New Zealand, no data, Stn Z10282; **NIWA 71660**, ♀, ML 503mm, New Zealand, no data, Stn Z1972.

Distribution (Fig. 29): 24–40°S, 166–170°E (near New Zealand); elsewhere reported from the Pacific Ocean near the Philippines (Voss, 1963), Japan (Salcedo-Vargas, 1993), Indonesia (Adam, 1954), and the Indian Ocean near Sumatra (Chun, 1910; Sasaki, 1929).

Diagnosis: Fins heart shaped to elliptical in outline when considered together, length 66–*81*–86% ML, width 72–*90*–105% ML; integumental photophores absent; skin tubercles present, single crescent-shaped photophore on ventral surface of eye; funnel-locking cartilage ear shaped; largest suckers of all located mid Arms II, trabeculate membranes present on membranes of arms and tentacles; tentacle suckers proximally large, distally minute.

Description (ML 181–930mm, Figs 30–38): Mantle goblet shaped, tapering gradually towards tail, widest (29–*37*–43% ML) around viscera; dorsal anterior mantle margin slightly convex. Fins heart shaped to elliptical in outline when considered together, length 66–*81*–86% ML, width 72–*90*–105% ML; rounded anterior lobes present; posterior margin at tail concave. Photophores absent from integument; skin tubercles (Fig. 31I) present on dorsal surface of fins, aboral surface of arms, and all external surfaces of mantle, head, and funnel (absent from collar).

Head boxy, length 23–*32*–52% ML, width 17–*23*–30% ML. Olfactory papilla cylindrical. Eye diameter 10–*15*–23% ML. One crescent-shaped photophore on ventral surface of eye (Figs 31G, H, 32). Funnel bulbous posteriorly, anteriorly cylindrical, width ~18% ML, length ~12% ML; aperture approximately level with posterior margin of eyelid; funnel pocket absent. Funnel-locking cartilage ear shaped (Fig. 31A–C), ~7% ML; anterior groove slightly concave due to weak antitragus; weak tragus along

inner/medial margin that extends approximately to midline of groove; outer/lateral margin nearly straight, angled towards midline. Mantle-locking cartilage nose shaped (Fig. 31D, E), ~5% ML; posteriorly undercut in profile.

Arm formula IV≥II>III≥I; arm length 68–*73*–77% ML (Tables 4, 10); Arms IV thickest followed by Arms II; oral faces of arms bordered by wide trabeculate membranes, trabeculae present at level of every sucker row; aboral keels present on Arms I–III; expanded lateral membrane present on Arms IV. Each arm with 56–78 suckers in two series; largest suckers of all located on Arms II (~100% arm width) at about row 13–15 (~30–50% arm length).

Arm-sucker rings (Fig. 33) proximally adentate, distally adentate or with 6–14 blunt, rectangular teeth, with smooth band between teeth and polygonal processes; proximal suckers adentate, more teeth in distal suckers. Polygonal processes on oral surface of sucker in 4–8 concentric rings; distally, central and intermediate rings with rounded, pitted pegs; proximally, central and intermediate rings nearly flat; peripheral ring with flat, rectangular processes.

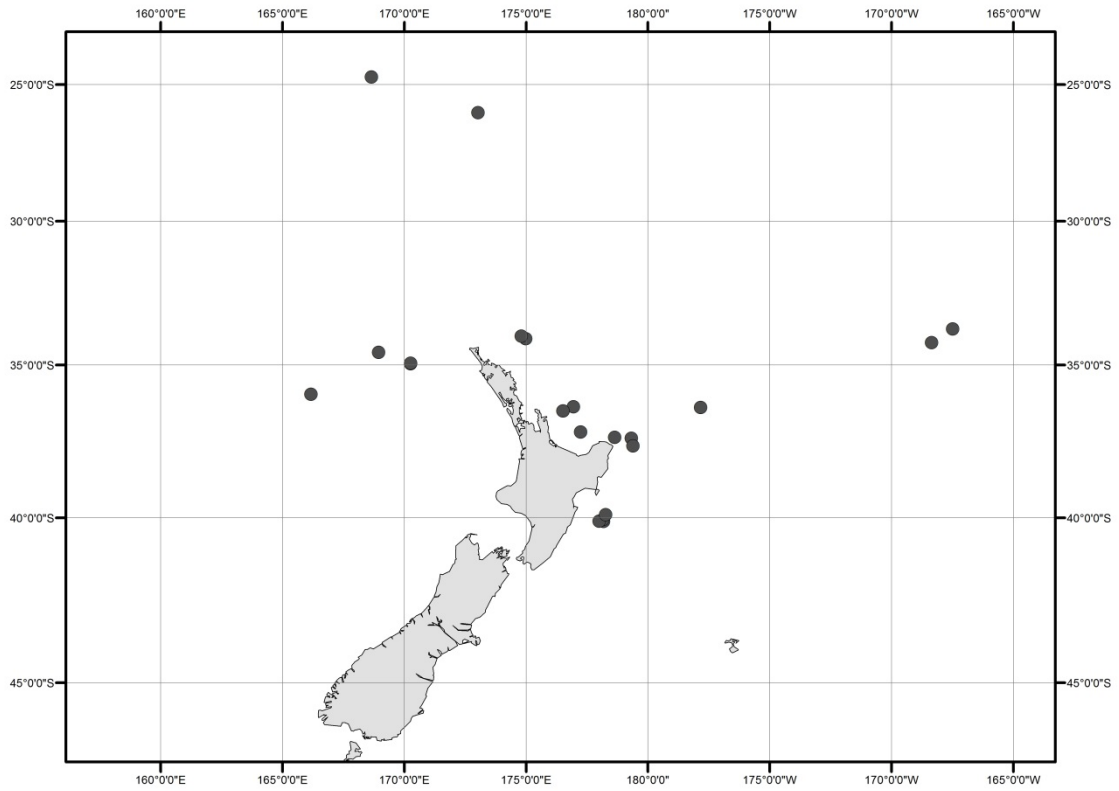

Fig. 29—Distribution of *Idioteuthis cordiformis* specimens examined in this study.

Tentacle length 153–*240*–326% ML, club 41–*52*–63% TnL (84–*123*–164% ML), expanded to 125–*187*–300% stalk width; wide trabeculate membrane bordering club, distally decreasing in width, nearly absent distally. Proximal suckers in two series for ~12–23 pairs, three series for ~12–16 rows, then series number increases gradually with row; proximal ~50–60% CL with large suckers (their diameter ~30% club width), gradually decreasing in size, while increasing in density distally, with minute suckers covering majority of tentacle surface apart from narrow aboral strip. Proximal tentacle suckers (Fig. 34A–C) proximally adentate, distally with 7–22 blunt, conical teeth; polygonal processes on oral surface of sucker in 7–12 concentric rings; distally, central and intermediate rings with cylindrical pegs; proximally, central and intermediate rings nearly flat; peripheral ring with flat, rectangular processes. Distal tentacle suckers (Fig. 34D) minute, proximally adentate, distally with ~6 long, conical teeth; polygonal processes on oral surface of suckers in ~6 concentric rings; distally, central and intermediate rings with long, cylindrical to conical pegs; proximally, central and intermediate rings conical to nearly flat; peripheral ring with flat rectangular processes. Distal-most tentacle suckers (Fig. 34E–H) with ~12 blunt, conical teeth, 'cushions' (Fig. 34F–H), polygonal processes on oral face of suckers in 3–4 concentric rings; central ring with ~22 round pegs; intermediate rings with 35–55 smaller, round pegs; peripheral ring with flat, rectangular-faced processes.

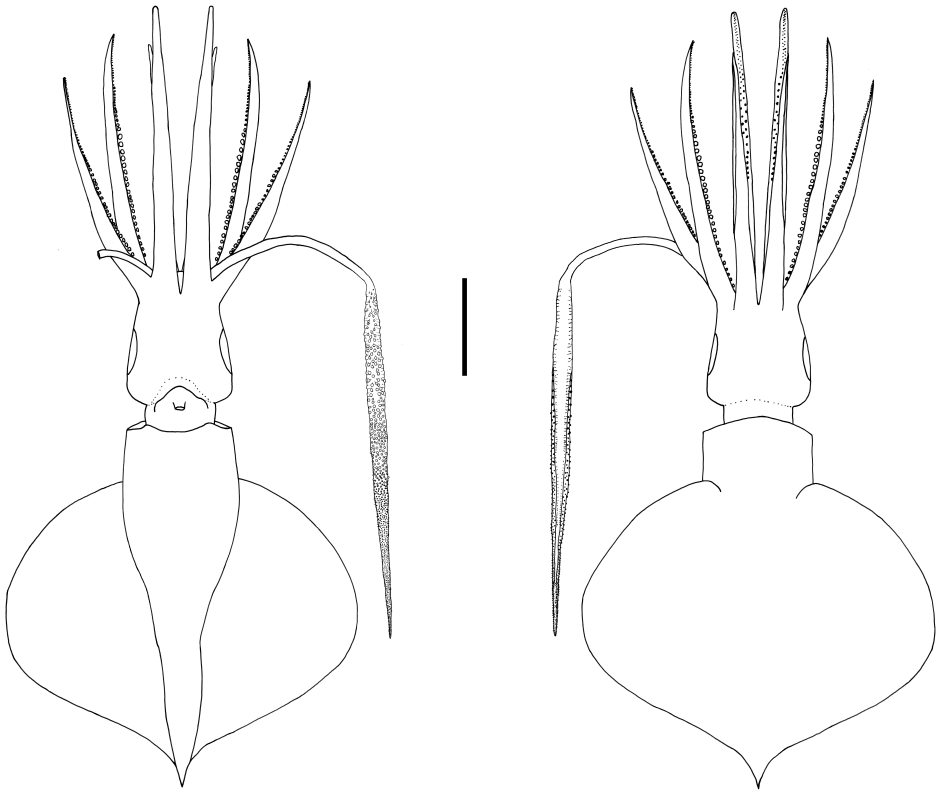

Fig. 30—*Idioteuthis cordiformis*, NMNZ M.171893, ♀, ML 299mm. Scale bar = 100mm.

Lower beak, lateral profile (Fig. 35): lower rostral length ~35% wing length, rostral edge nearly straight to curved or S shaped, rostral tip often slightly hooked, rostral tip behind leading edge of wing by 26–*32*–40% baseline; wing angle obtuse, jaw angle variably obscured by low wing fold, shoulder groove variably present; height 74–*85*–100% baseline; hood well above crest, hood length ~50% crest length, crest length 57–*67*–73% of baseline, visible portion of crest nearly straight; broad lateral wall fold extending to posterior edge of lateral wall; no notch in lateral wall. Lateral oblique view (Fig. 36) with wing narrowest level with jaw angle, 53–*61*–70% of greatest width. Ventral view with deep, broad notch in hood, free corners separated slightly. Wings remain unpigmented at ML 248mm, darkening in middle of wing at ML ~320mm, edges (~5mm) of wings remain clear at ML 428mm, fully pigmented in male at ML 608mm, posterior edge of wing remains clear in female at ML 930mm. Regression

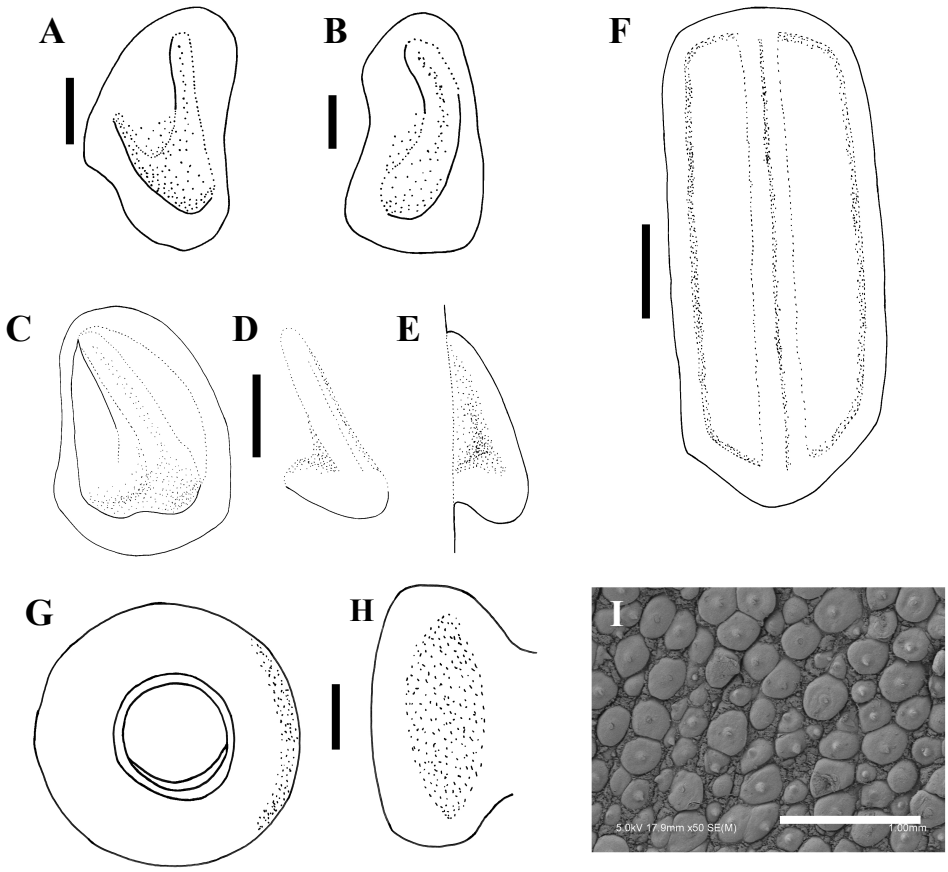

Fig. 31—*Idioteuthis cordiformis*. A) NIWA 71660, ♀, ML 503mm; B) NIWA 71659, ♀, ML 520mm; C–E) NMNZ M.181333, ♂, ML 181mm; F–H) NIWA 71652, ♂, ML 248 mm; I) NMNZ M.171893, ♀, ML 299mm. A–C) left funnel-locking cartilage; D) left mantle-locking cartilage; E) left mantle-locking cartilage profile view; F) nuchal cartilage; G) right eye; H) ventral view of right eye; I) ventral mantle skin tubercles. Scale bars = A, B, G, H) 10mm; C–F) 5mm; I) 1mm.

equation (Fig. 37J): ML = 0.1307(LRL)$^{0.7637}$ (R^2 = 0.9473) (N=13); regression (Fig. 37K) excluding outlier NIWA 71437 (Fig. 35G), which is morphologically distinct from the other beaks: ML = 9.4965ln(LRL) - 43.467 (R^2 = 0.981) (N=12).

Upper beak, lateral profile (Fig. 37A–I): upper rostral length ~25% hood length; hood length ~70% beak length; hood height ~40% beak width. Lateral wall fold variably present; shoulder produced into point; jaw edge slightly curved; jaw angle nearly 90°.

Radula (Fig. 38A, B) with tricuspid rachidian, base width 130% height, proximal margin of base rectangular, with broad, blunt, triangular mesocone and broad, rounded lateral cusps, slightly laterally directed, their height ~45% mesocone height. First lateral tooth bicuspid; inner cusp broad, triangular, slightly curved toward rachidian, its height ~130% that of overall rachidian; small, pointed outer cusp, slightly medially directed, its height ~40% that of inner cusp. Second lateral tooth simple, straight, ~215% height of rachidian. Marginal tooth simple, straight, ~220% height of rachidian. Marginal plate present (Fig. 38C). Palatine palp (Fig. 38D) with ~70 broad, conical teeth, each ~25–125% rachidian height, evenly distributed over palp.

Gladius (Fig. 38E) with greatest width (~10% GL) attained at ~50% GL; free rachis ~10% GL; secondary conus ~35% GL, rostrum ~6% GL, triangular in cross section.

Epidermis damaged on all examined material. Integumental photophores absent. Colour (preserved and fresh) dark purple, chromatophores dense and evenly distributed on all

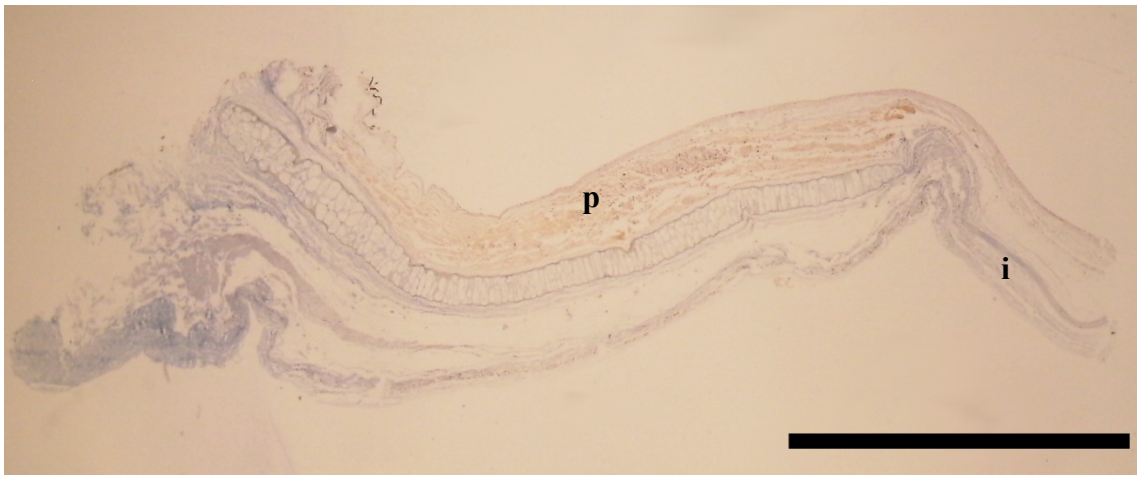

Fig. 32—Cross-section through ventral surface of *Idioteuthis cordiformis* eye photophore stained with Mallory's trichrome; NIWA 71655, ♀, ML 320mm; (p) indicates photophore tissue (in orange), (i) indicates iris. Scale bar = 5mm.

exterior surfaces, sparsely set on internal mantle and funnel surfaces. Subcutaneous chromatophores present on all surfaces, larger and less dense than overlying chromatophores.

Remarks: Three mature males were observed (ML 513–608mm), while the largest female examined herein was still immature (and unmated) at ML 930 mm. Other *I. cordiformis* specimens have been observed at greater than 1m ML (Steve O'Shea, pers. comm.). Salcedo-Vargas (1993) examined a mature male that was 318mm ML, which is far smaller than the mature males examined in this study. The differences in size of maturity along with different locations (New Zealand and Japan) could indicate either different species or that separate populations within this species reach different sizes, as in *Dosidicus gigas* (Nigmatullin, Nesis, & Arkhipkin, 2001).

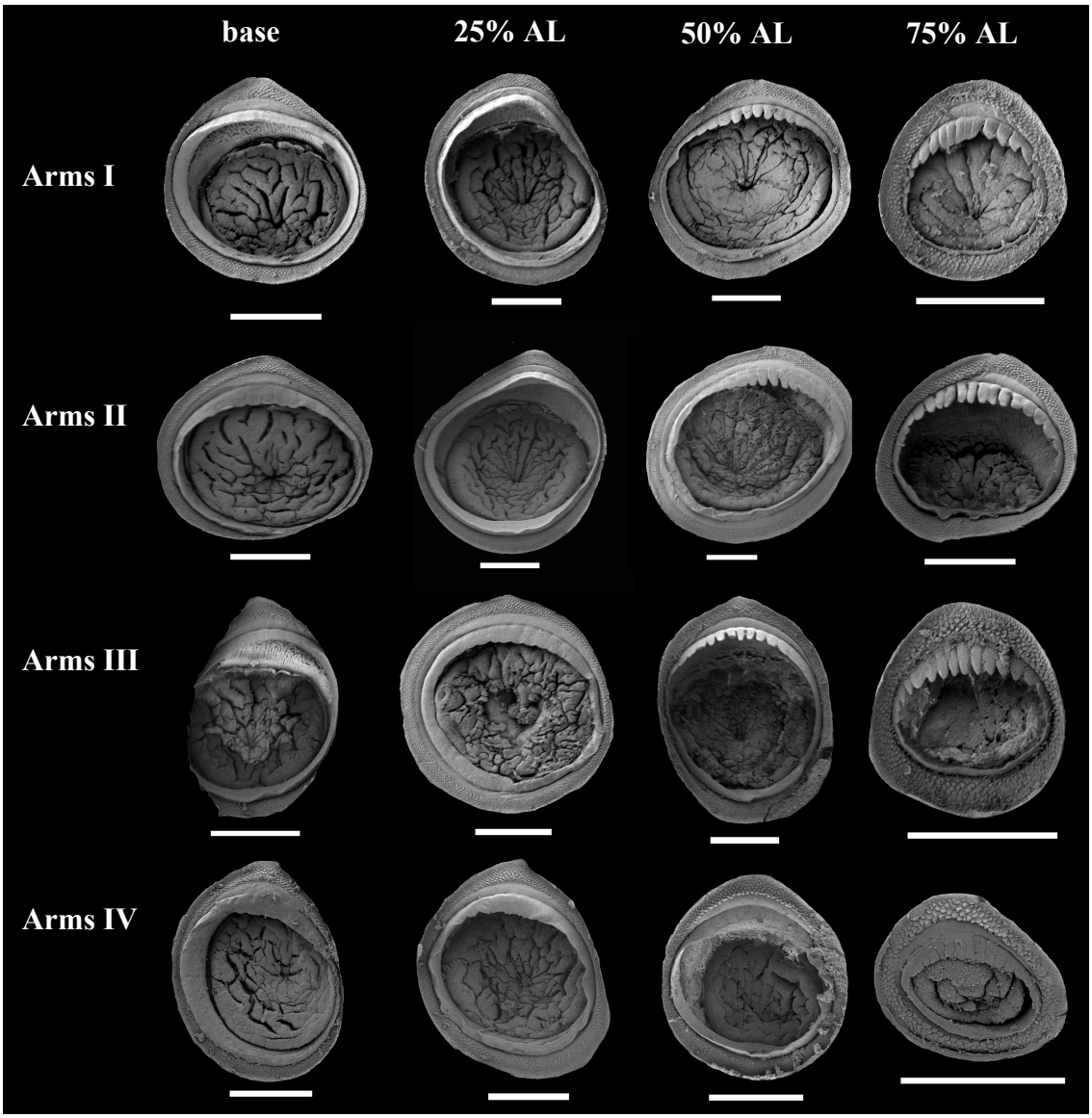

Fig. 33—*Idioteuthis cordiformis* arm suckers, NMNZ M.181333, ♂, ML 181mm. Scale bars = 500µm.

Voss (1963) described several small *I. cordiformis* specimens (36–92mm ML) from the Philippines, with some apparent morphological differences from the material reported here. The fin width was narrower than in the specimens examined in this study. Voss (1963) and Sasaki (1929) found head width slightly greater than mantle width, contrary to what was found herein. They also both noted a distinct eye sinus, which was not found here. The tentacle suckers that Sasaki (1929) examined bore teeth around the circumference, while teeth on tentacle suckers in the New Zealand material were only observed on the distal margin of the sucker ring. Sasaki (1929) found the basal portion of the club to have eight series, while here two or three were found. Sasaki (1929) also found that the teeth on the tentacle suckers were much smaller than those illustrated by Chun (1910). Size difference and damage could account for these discrepancies, but it is also possible that these descriptions refer to different taxa.

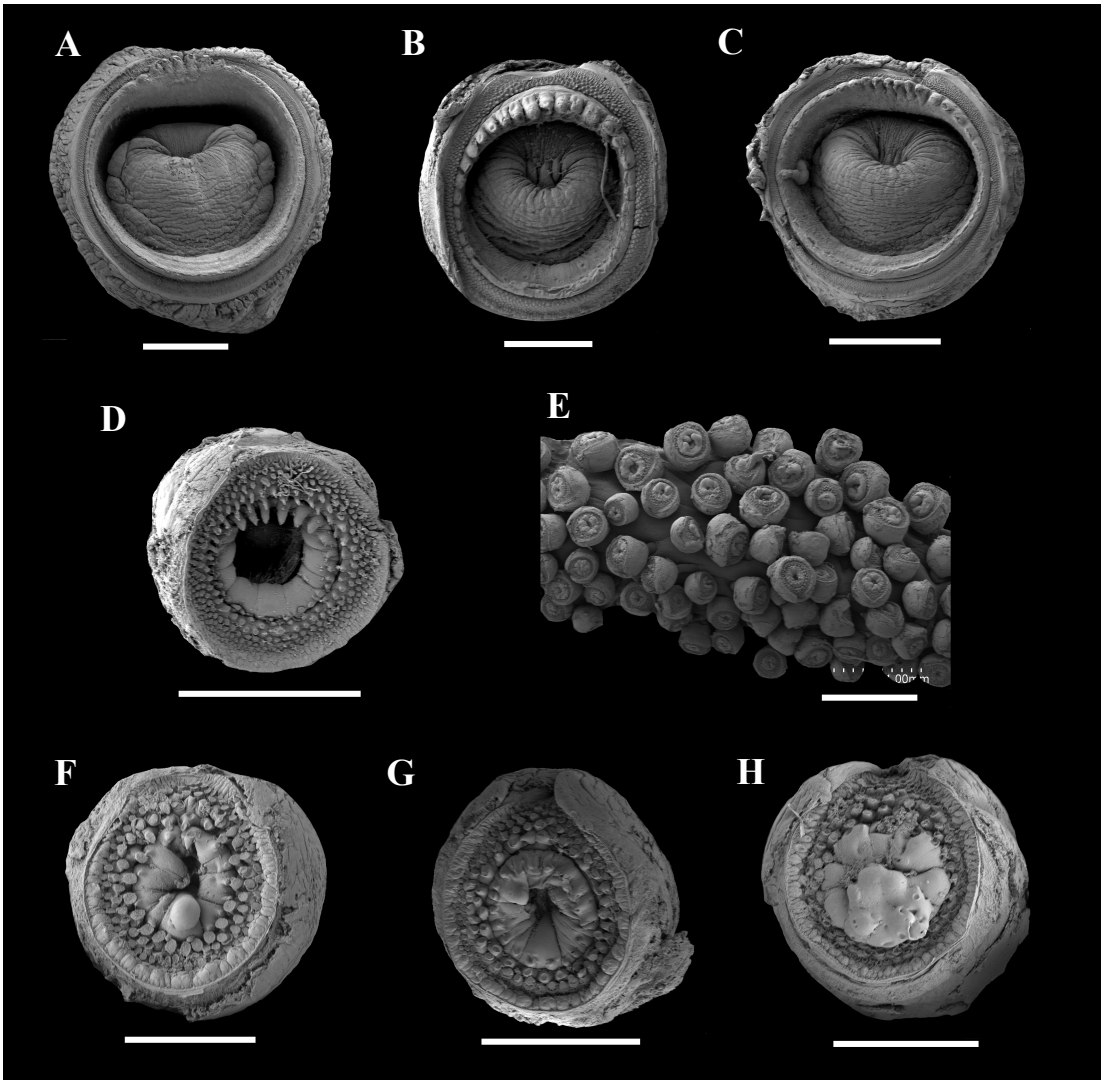

Fig. 34—Tentacle suckers of *Idioteuthis cordiformis*, NMNZ M.171893, ♀, ML 299mm. A) proximal sucker, ~10% CL; B) large proximal sucker, ~20% CL; C) mid-club sucker, ~50% CL; D) distal sucker, ~90% CL; E) tentacle tip suckers; F–H) minute tentacle tip suckers with 'cushions'. Scale bars = A, B, E) 1mm; C, D) 500µm; G) 300µm; F, H) 200µm.

Arm suckers have been reported in varying numbers and dentition for *I. cordiformis*. Herein, arms had 56–78 pairs of suckers, in two series, and were adentate or sometimes possessed 6–14 blunt, rectangular teeth; the sucker shape was globular, similar to the suckers reported by Sasaki (1929). Chun (1910) described one specimen of 83mm ML with 57–59 pairs of 'acorn-shaped' suckers on the ventral arms, and 50 pairs on Arms III. Sasaki (1929) found arm suckers ranging from adentate to possessing 4–11 quadrangular teeth. Young (1972) described arm suckers with 30 small, blunt teeth, while Adam (1945) found 'irregular' teeth on the arm suckers. Approximately half the specimens examined herein had Arms II that exceeded the length of Arms IV, which was also found by Salcedo-Vargas (1993). Voss (1969) reported five or six basal arm

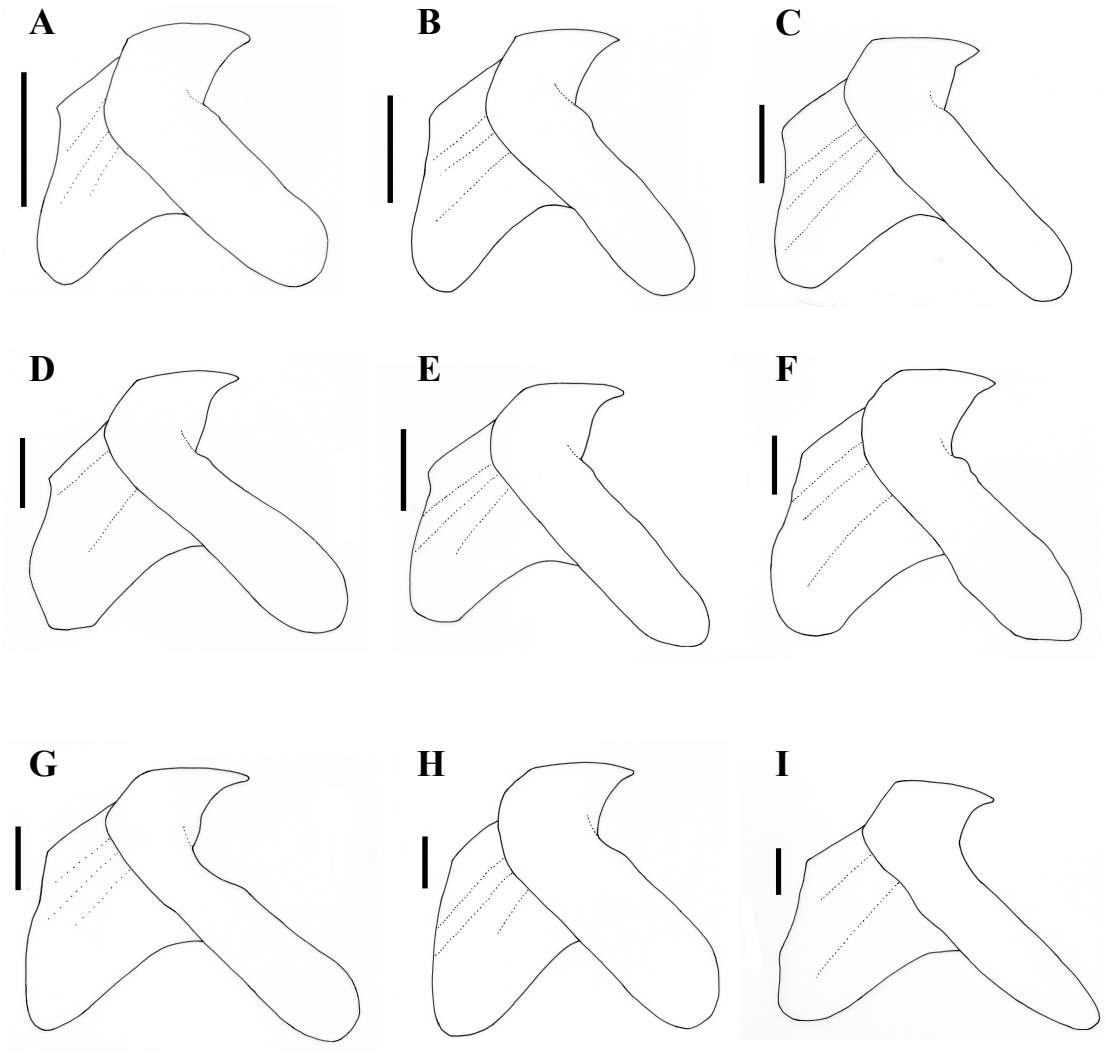

Fig. 35—*Idioteuthis cordiformis* lower beaks, profile view. A) NMNZ M.181333, ♂, ML 181mm, LRL 6.36mm; B) NIWA 71652, ♂, ML 248 mm, LRL 8.31mm; C) NIWA 71655, ♀, ML 320mm, LRL 11.1mm; D) NIWA 71666, ♀, ML 380*mm, LRL 16.98mm; E) NIWA 71653, ♂, ML 428mm, LRL 13.78mm; F) NMNZ M.306358, ♂, ML 549mm, LRL 16.28mm; G) NIWA 71437, ♂, ML 608mm, LRL 20.69mm; H) NMNZ M.118004, ♀, ML 715mm, LRL 18.99mm; I) NIWA 84390, ♀, ML 820mm, LRL 19.28. Scale bars = 10mm.

suckers on Arms IV and III were in a single series, while specimens examined here had two distinct series on all arms. These differences could be due to size or may also indicate different species. However, because of the wide range of morphological variation found within New Zealand material, it is clear that integrative taxonomy will be necessary to determine whether the differences found between these specimens and previous studies represent the same taxa.

The radula illustrated by Adam (1954) is similar to the radula SEMs by Salcedo-Vargas (1993); however, the mesocones for these specimens were relatively much taller than in the specimens examined herein. This difference could be due to growth or geographic area. The specimen examined by Adam (1954) was 96mm ML from Indonesia (7°S, 117°E) and the specimens illustrated by Salcedo-Vargas (1993) were 109 and 318mm

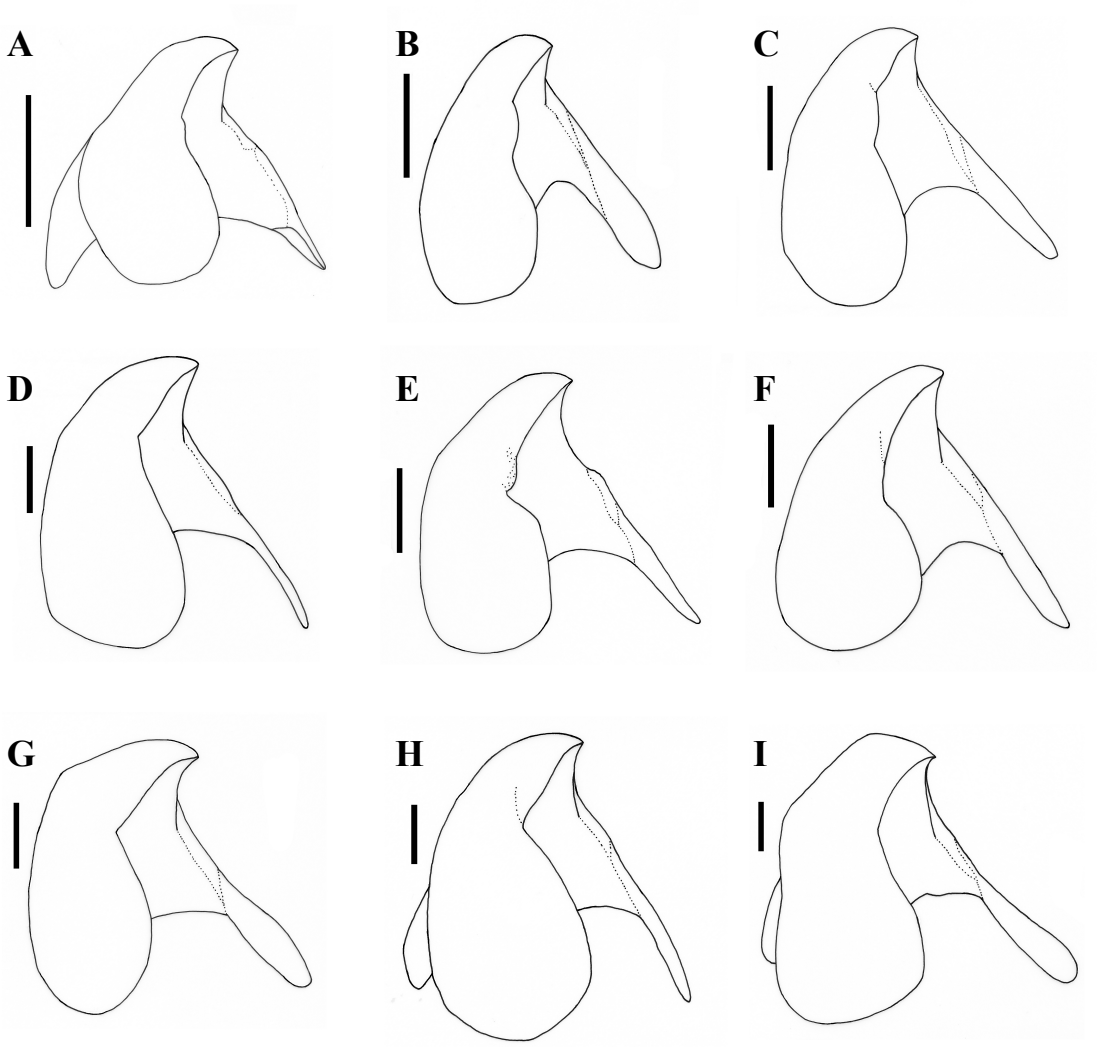

Fig. 36—*Idioteuthis cordiformis* lower beaks, lateral oblique view. A) NMNZ M.181333, ♂, ML 181mm; B) NIWA 71652, ♂, ML 248 mm; C) NIWA 71655, ♀, ML 320mm; D) NIWA 71666, ♀, ML 380*mm; E) NIWA 71653, ♂, ML 428mm; F) NMNZ M.306358, ♂, ML 549mm; G) NIWA 71437, ♂, ML 608mm; H) NMNZ M.118004, ♀, ML 715mm; I) NIWA 84390, ♀, ML 820mm. Scale bars = 10mm.

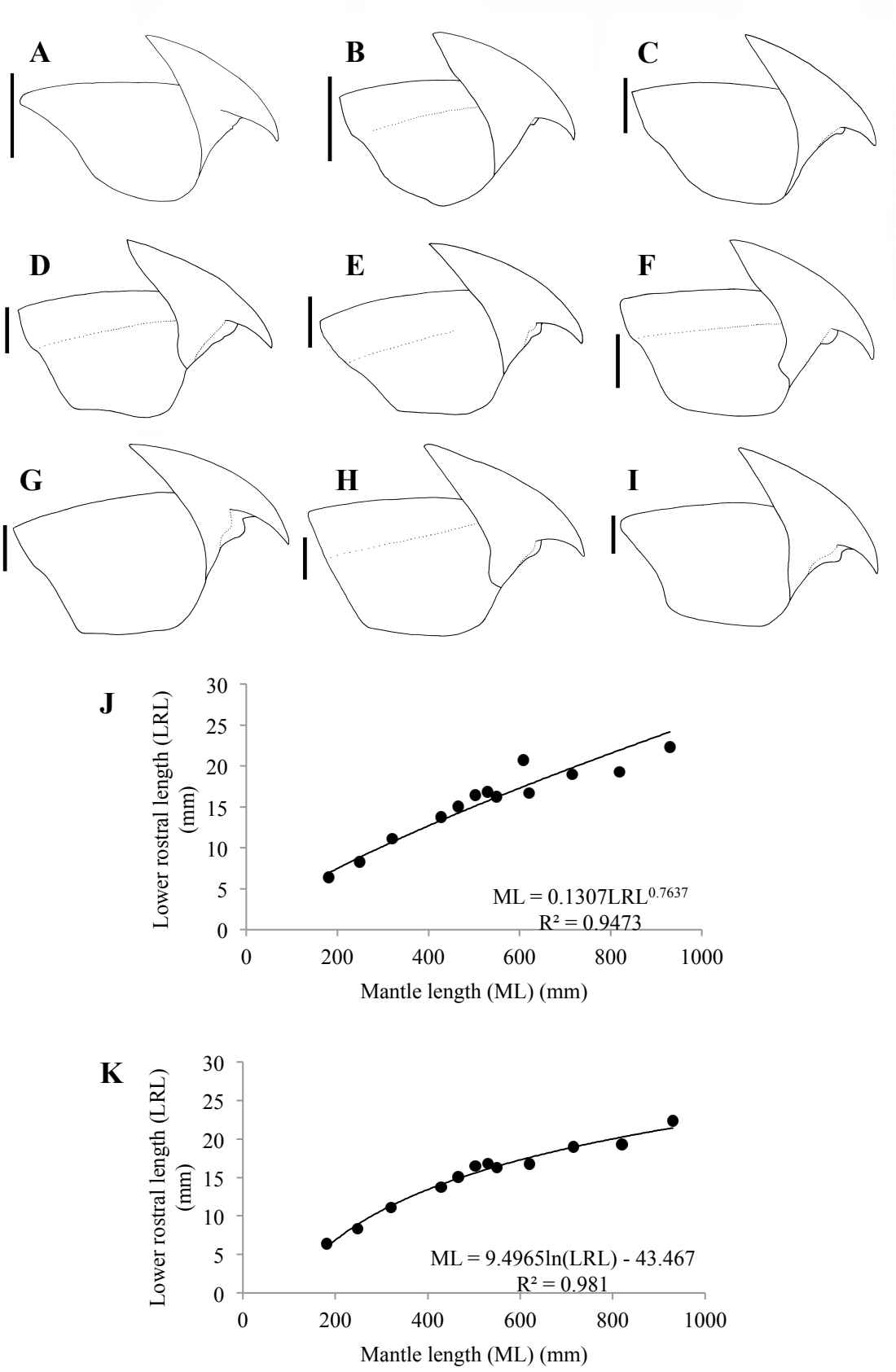

Fig. 37—*Idioteuthis cordiformis.* A) NMNZ M.181333, ♂, ML 181mm; B) NIWA 71652, ♂, ML 248 mm; C) NIWA 71655, ♀, ML 320mm; D) NIWA 71666, ♀, ML 380*mm; E) NIWA 71653, ♂, ML 428mm; F) NMNZ M.306358, ♂, ML 549mm; G) NIWA 71437, ♂, ML 608mm; H) NMNZ M.118004, ♀, ML 715mm; I) NIWA 84390, ♀, ML 820mm. A–I) upper beaks, profile view; J) regression equation for ML and LRL; K) regression equation for ML and LRL without outlier (NIWA 71437). Scale bars = 10mm.

ML from Japan (32–33°N, 133°E). Two specimens with different beak morphologies (Fig. 35G, H) were found herein to have similar radular morphologies (Fig. 38A, B). Although cephalopod radulae have been used widely in taxonomic work, much intraspecific variation has been found (Voss, 1977). In addition, serial repetition in the lateral cusps of the rachidian and asymmetry has been found within single specimens by Nixon (1998), who suggested that radulae should be examined from a full ontogenetic series in a species to determine the degree of intraspecific variation. Unfortunately, this was not possible in the current study because small specimens were not available.

The presence of a photophore on the eye of *I. cordiformis* was first recognised by Salcedo-Vargas (1993); its presence was supported herein with histology (Fig. 32). Salcedo-Vargas (1993) also reported photophores embedded in the protective membrane of the tentacle, which were not found in specimens in this study although

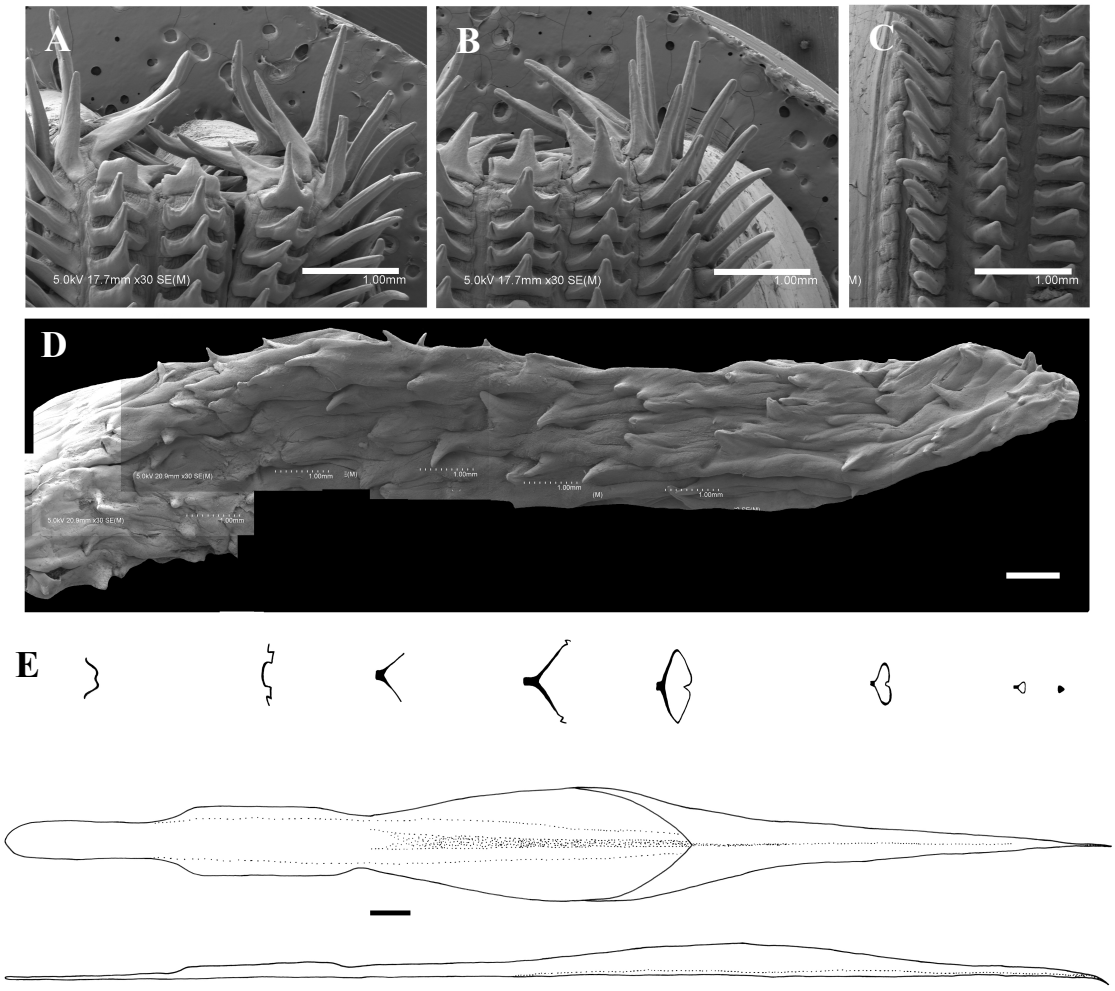

Fig. 38—*Idioteuthis cordiformis*. A) NIWA 71437, ♂, ML 608mm; B–D) NMNZ M.118004, ♀, ML 715mm; E) NIWA 71652, ♂, ML 248 mm. A, B) radula; C) marginal plates of radula; D) palatine palp; E) gladius. Scale bars = A–D) 1mm; E) 10mm.

histological examinations were not undertaken. Young (1972) stated that *I. cordiformis* is covered in small light organs because Chun (1910, Pl. 36) wrote 'luminous organs?' within the figure caption of cross section of an *I. cordiformis* tubercle. However, Chun (1910) stated that he believed that there were no photophores in the integument of *I. cordiformis*. No integumental photophores were observed for *I. cordiformis* herein.

Idioteuthis cordiformis is morphologically similar to *I. latipinna*, which was described from a single specimen from the Sagami Sea in Japan, which was the largest mastigoteuthid specimen known at the time (238mm ML). The eyes of *I. latipinna* are differentiated from *I. cordiformis* by the presence of an eye sinus, and the left eye being approximately twice the size of the right. While this size difference was supported by Salcedo-Vargas (1997), Young and Vecchione (2004) presumed that Sasaki (1929) believed this difference was due to damage because the uneven eyes were not discussed in his comparison with *I. cordiformis*. The tentacles of *I. latipinna* have four series of suckers proximally (Sasaki, 1929), which contrasts with the three proximal series observed herein. The skin of *I. latipinna* is smooth (Sasaki, 1929), while *I. cordiformis* is covered in skin tubercles. Although Sasaki (1929) found that the fins of *I. latipinna* were larger and rounder than those of *I. cordiformis*, this study found that the fin shape of *I. cordiformis* is quite variable. Sasaki (1929) found that the tragus and antitragus was weaker in *I. latipinna*, but here it appears that the funnel- and mantle-locking cartilages are variable in morphology and easily degraded, especially in larger specimens (Fig. 31A–C). Sasaki (1929) found 65–70 suckers on each arm, which falls within the range found herein for *I. cordiformis*. Because of the similarities between the two species, and the potential for the observed differences to be due to damage, some authors have considered *I. latipinna* a junior synonym of *I. cordiformis* (Salcedo-Vargas & Okutani, 1994; Young & Vecchione, 2004). This seems likely due to the commonalities between these species, and the extent variation found within *I. cordiformis* herein; however, genetics will be essential in resolving the status of *I. latipinna*.

There are some morphological similarities between *I. cordiformis* and *Mp. hjorti*, but these two taxa can be readily distinguished. Both species have heart-shaped fins, nearly the length of the mantle. The skin tubercles of both species have similar structure (Roper & Lu, 1990). Eye photophores are present in both species, but *Mp. hjorti* has

two hemispherical photophores (one posterio-ventral, one anterio-ventral; Fig. 41E, F), while *I. cordiformis* has a single, flat, crescent-shaped photophore on the ventral surface of the eye (Fig. 31G, H). The proximal arm suckers of *I. cordiformis* are adentate (Fig. 33), while all arm suckers of *Mp. hjorti* have long, blunt rectangular teeth (Fig. 42). *Idioteuthis cordiformis* has trabeculae on the protective membranes of the arms, while trabeculae are absent from the protective membranes of *Mp. hjorti*. In addition, these species are genetically distinct from each other (Chapter 3).

Extreme morphological variation was found in the beaks of *I. cordiformis* (Fig. 35), although the individuals with different beak shapes were nearly genetically identical (Chapter 3). Variation was found in both upper and lower beaks (Fig. 37A–I). Upper beaks of some specimens possessed a lateral wall groove. In the lower beak, the jaw edge in the lower beak varied from slightly curved to S shaped, and sometimes the rostral tip was slightly hooked. The shoulder varied from a smooth surface leading to the jaw edge in a gentle curve, to a pronounced bump at the wing fold. No consistent differences were found between beak variation and size, sex, or location. The regression equation (Fig. 37K) that was calculated without the LRL of NIWA 71437 (Fig. 37G), which is morphologically distinct from the other beaks, had a higher R^2 value (R^2 = 0.981) than the equation (Fig. 37J) that included this beak (R^2 = 0.9473). Clarke (1980) described beaks of ?*Mastigoteuthis* sp. B from stomach contents of sperm whales from South Africa, that could belong to *I. cordiformis*. He noted that the beaks were similar to other mastigoteuthid beaks, but were much larger (LRL 8–10mm). His description for ?*Mt.* sp. B beak is mostly consistent with the *I. cordiformis* beaks described herein. However, ?*Mt.* sp. B beaks did not have the deep notch in the hood-wing structure, the free corners were closer together, and the rostral tip was closer to the leading edge of the wing.

Table 10—Measurements (mm) of *Idioteuthis cordiformis* (Chun, 1908).

Specimen ID:	**NIWA 71437**	**NIWA 71661**	**NIWA 71654**	**NIWA 71653**	**NIWA 71663**	**NIWA 71663**	**NIWA 71659**	**NIWA 71656**	**NIWA 71665**	**NIWA 71658**	**NIWA 71652**	**NIWA 71660**	**NIWA 71664**
Sex	M	F	F	M	F	M	F	F	M	F	M	F	F
ML	608	620	530	428	286	342	520	434	286	466	248	503	344
MW	225	205	175	148	112	110	210	160	113	195	75	200	125
FL	443	495	437	356	233	289	445	360	235	398	204	415	285
FW	532	514	489	367	272	309	491	418	286	478	231	452	300
HL	174	206	164	140	98	115	138	147	92	139	58	192	120
HW	145	125	125	125	68	90	135	112	90	140	45*	115	80
ED	70	60	50*	50	47	48	70	53	50	65	38	*	65
Side measured	R	R	R	L	R	R	L	R	R	R	R	R	R
Arms I	418	392	361	322	198	237	372	313	173	345	172	352	205
Arms II	305*	423	355	325	213	284	441	354	194	386	201	321	245
Arms III	406	371	357	316	223	271	418	323	166	305	188	322	215
Arms IV	418	401	352	302	259	298	458	355	213	305	221	395	232
TLA	1182	1140	1048	825	666	725	1105	922	622	950	521	1052	703
TL	-	-	1689	1490	1321	1346	1955	1625	-	1768*	922	1552	1250
TnL	-	-	1064	990	932	909	1284	1089	-	1111*	588	906	818
CL	-	-	569	575	469	377	659	586	-	576	330	463	443

* indicates damaged features.
- indicates missing features.

Table 10 (continued)

Specimen ID:	NIWA 71655	NIWA 84390	NMNZ M.274094	NMNZ M.181333	NMNZ M.171893	NMNZ M.306355	NMNZ M.306356	NMNZ M.306358	NMNZ M.174313	NMNZ M.299012	NMNZ M.118004	Mean Indices	
Sex	F	F	F	M	F	M	Indet.	M	F	F	F		
ML	320	820	284	181	299	513	405	549	654	930	715		
MW	125	350	110	54	88	195	160	195	220	320	300	MWI	37
FL	294	630	225	148	237	456	304	445	549	610	595	FLI	81
FW	302	700	298	165	257	439	390	445	510	670	616	FWI	90
HL	165	187	100	61	85	158	145	174	190	217	175	HLI	32
HW	79	165	53	45	73	115	78	105	154	185	120	HWI	23
ED	54	*	45	41	57	*	*	*	*	75*	68	EDI	15
Side measured	R		R	R	R	R	R		L	L	R		
Arms I	231	*	290	98	180	305	302	*	442	590	455	A1LI	68
Arms II	328	*	349	127	195	352	346	*	500	585	518	A2LI	77
Arms III	252	*	307	114	182	304	321	*	468	673	475	A3LI	71
Arms IV	318	*	302*	144	222	374	336	*	*	*	500	A4LI	77
TLA	799	*	716*	398	594	1000	944	*	*	2590	1370		
TL	1618	-	-	-	830	1800	1750	-	-	1790	-		
TnL	1120	-	-	-	458	1168	1121	-	-	1582	-	TnLI	240
CL	456	-	-	-	288		601	-	-	790	-	CLI	123

* indicates damaged features.
- indicates missing features.

Genus *Mastigopsis* Grimpe, 1922

Mastigopsis Grimpe, 1922: 50. Type species *Mastigoteuthis hjorti* Chun, 1913, by monotypy.

Diagnosis: Mantle length at maturity ~180–235 mm. Fins heart shaped in outline when considered together; fin length ~89% ML. Funnel narrowly conical. Funnel-locking cartilage oval with convex protrusion along outer/lateral margin, tragus and antitragus absent; funnel pocket absent. Mantle-locking cartilage ovate, posteriorly undercut in profile. Arm suckers arranged in two distinct series but appearing to merge into single series midway on Arms IV; arm suckers with blunt teeth; Arms IV ~78% ML; protective membranes without trabeculae. Tentacular suckers minute; club not expanded with trabeculate protective membrane (*fide* Chun, 1913). Eye-sinus photophore absent. Two round photophores on each eye (one posterio-ventral, one anterio-ventral). Integumental photophores absent, skin tubercles present. Gladius broad (greatest width ~10% GL).

Remarks: Currently there is only one species in this genus, *Mastigopsis hjorti*. This species appears to have a circumglobal distribution with specimens recorded from the North Atlantic (Chun, 1910; Rancurel, 1973) and the Pacific and Indian Oceans (Nesis, 1987). Although, it has been suggested that specimens from different geographic locations may belong to different species (Nesis, 1987; Vecchione & Young, 2007d).

***Mastigopsis hjorti* (Chun, 1913)** (Tables 3, 4, 11, Figs 39–43)

Mastigoteuthis hjorti Chun, 1913: 6–8, fig. 1, pl. 2; Rancurel (1973): 27–32, figs 1–8; Vecchione et al. (2001): 34–36, fig. 26.

Mastigoteuthis (*Mastigopsis*) *hjorti* (Chun, 1913): Grimpe (1922): 50.

Idioteuthis (*Idioteuthis*) *hjorti* (Chun, 1913): Salcedo-Vargas & Okutani (1994): 124.

Idioteuthis hjorti (Chun, 1913): Salcedo-Vargas (1997): 107.

Type material (not examined): **ZMBN 25906**, syntype, 3 sex indet., ML 71–95mm, 31.40°N, 34.78°W, 06–07/06/1910, RV *Michael Sars*, Stn 52; **ZMBN 25910**, syntype, sex indet., ML 55mm, 36.08°N, 43.97°W, 22/06/1910, RV *Michael Sars*, Stn 63; **ZMBN 25909**, syntype, sex indet., ML 68mm, 36.87°N, 39.92°W, 20–21/06/1910, RV *Michael Sars*, Stn 62.

Material examined (5 specimens): **NMNZ M.172986**, ♂, ML 78mm, 29.53°S, 167.63°E, 200–1200m, 15/05/2003, RV *Tangaroa*, NORFANZ Stn 23, 2003023; **NMNZ M.172921**, ♀, ML 145mm, 29.99°S, 167.65°E, 1245–1285m, 14/05/2003, RV *Tangaroa*, NORFANZ Stn 16, 2003016; **NIWA 48868**, 3 sex indet., ML 24–26mm, 44.84°S, 173.37°E, 44.70°S, 175.38°E, 1000–983m, 16/04/1997, Stn Z8795 TAN9101.

Distribution (Fig. 39): 29–45°S, 167–175°E (near New Zealand); elsewhere reported from North Atlantic (Chun, 1910; Vecchione et al., 2002), Central Pacific (Vecchione & Young, 2007d), off South Africa (Roper & Lu, 1990), Sulu Sea in the Indian Ocean (Nesis, 1987).

Diagnosis: Fins heart shaped in outline when considered together, length ~90% ML, width ~105% ML; integumental photophores absent; two round photophores on each eye (one posterio-ventral, one anterio-ventral); skin tubercles present on mantle, fins, head and arms; funnel-locking cartilage oval shaped; arm suckers with blunt teeth, largest suckers overall located proximally on Arms III; trabeculae absent.

Description (ML ~145mm, Figs 40A, 41–43): Mantle cone shaped, tapering gradually towards tail, widest (~32% ML) at anterior margin; dorsal anterior mantle margin convex. Fins heart shaped in outline when considered together, length ~89% ML, width ~106% ML; rounded anterior lobes present; posterior margin at tail convex.

Photophores absent from integument; skin tubercles (Fig. 41G) present on ventral surface of mantle and fins (dorsal surfaces unknown), and all surfaces of head; overlying gelatinous coating present on posterior half of mantle and on arms.

Head rounded, length ~31% ML, width ~25% ML. Olfactory papilla cylindrical. Eye diameter ~16% ML. Two photophores on ventral surface of eye, one posterio-ventral, one anterio-ventral (Fig. 41E, F). Funnel narrowly conical, width ~15% ML, length ~20% ML; aperture approximately level with posterior margin of eye; funnel pocket absent. Funnel-locking cartilage oval (Fig. 41A), ~8% ML, bulbous posteriorly, narrowing anteriorly; inner/medial margin nearly straight, anterior portion of outer/lateral margin convex. Mantle-locking cartilage approximately oval (Fig. 41B, C), ~6% ML, inner/medial margin concave; posteriorly undercut in profile.

Arm formula unknown due to damage; Arms II ~75% ML, Arms III ~63% ML (Tables 4, 11); Arms I–III all of subequal thickness; Arms IV thicker, with expanded lateral membrane. Trabeculae absent. At ML ~142mm, Arm I suckers in two series (number unknown); Arms II with 236 suckers: proximal 30% of arms with 10 rows in two series, next ~25% with 20 rows in three series, distal portion with 78 rows in two series; Arms

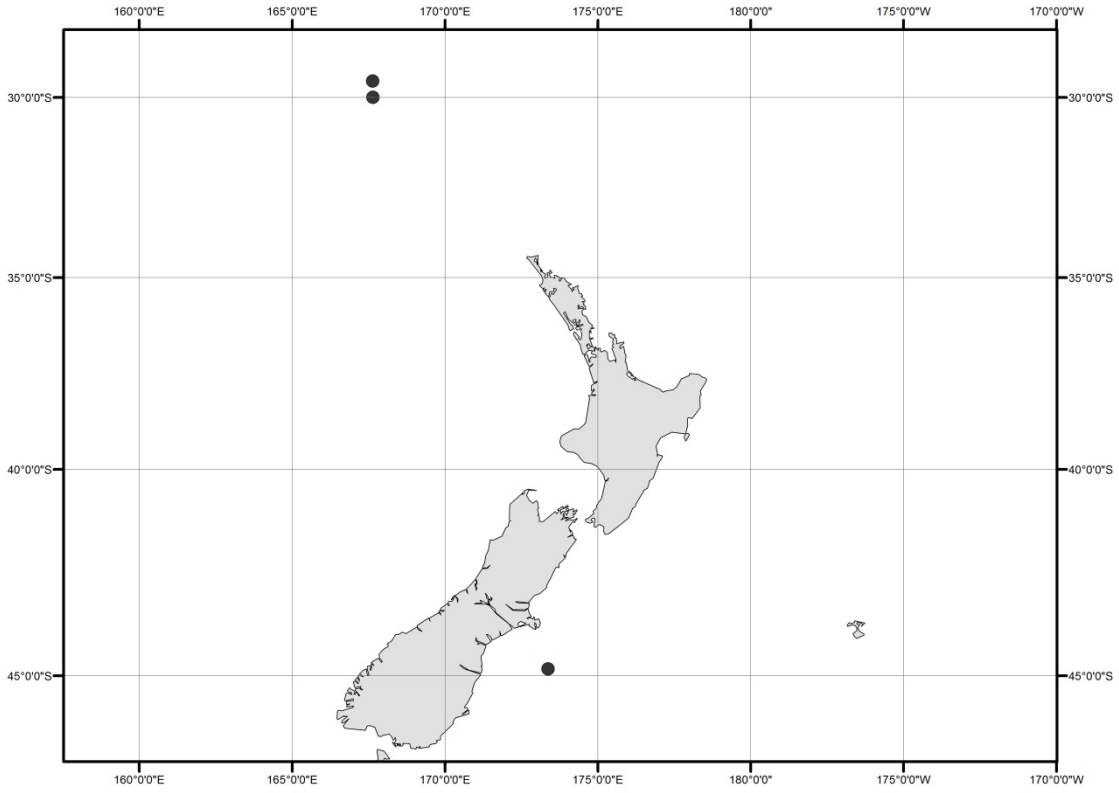

Fig. 39—Distribution of *Mastigopsis hjorti* specimens examined in this study.

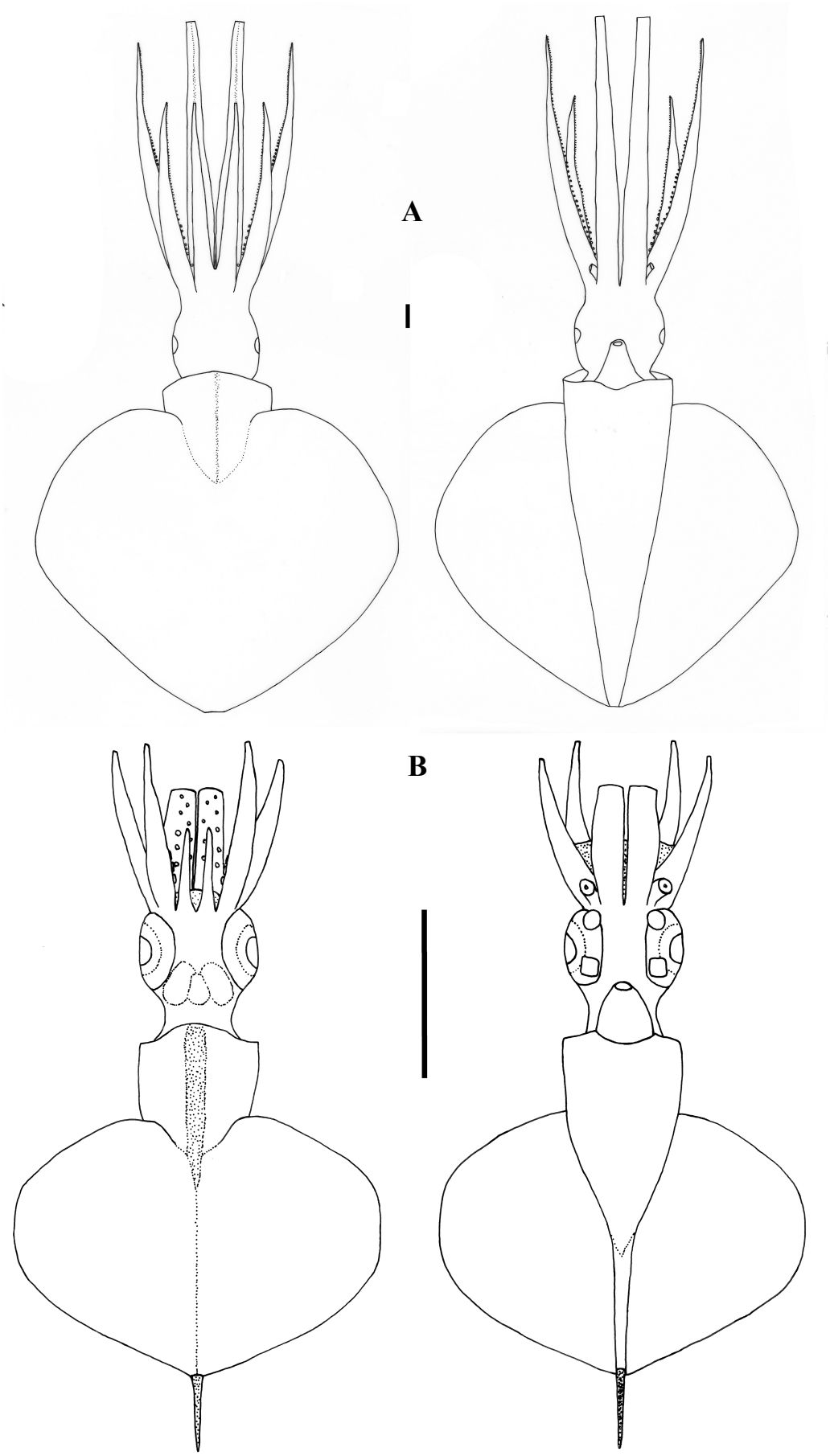

Fig. 40—*Mastigopsis hjorti.* A) NMNZ M.172921, ♀, ML 142*mm; B) NIWA 48868, sex indet., ML 25mm. Scale bars = 10mm.

III with 200 suckers in two series; Arms IV with suckers in two series (number unknown), distally merging into one series; largest suckers overall located on Arms III (~30% arm width) at about second pair.

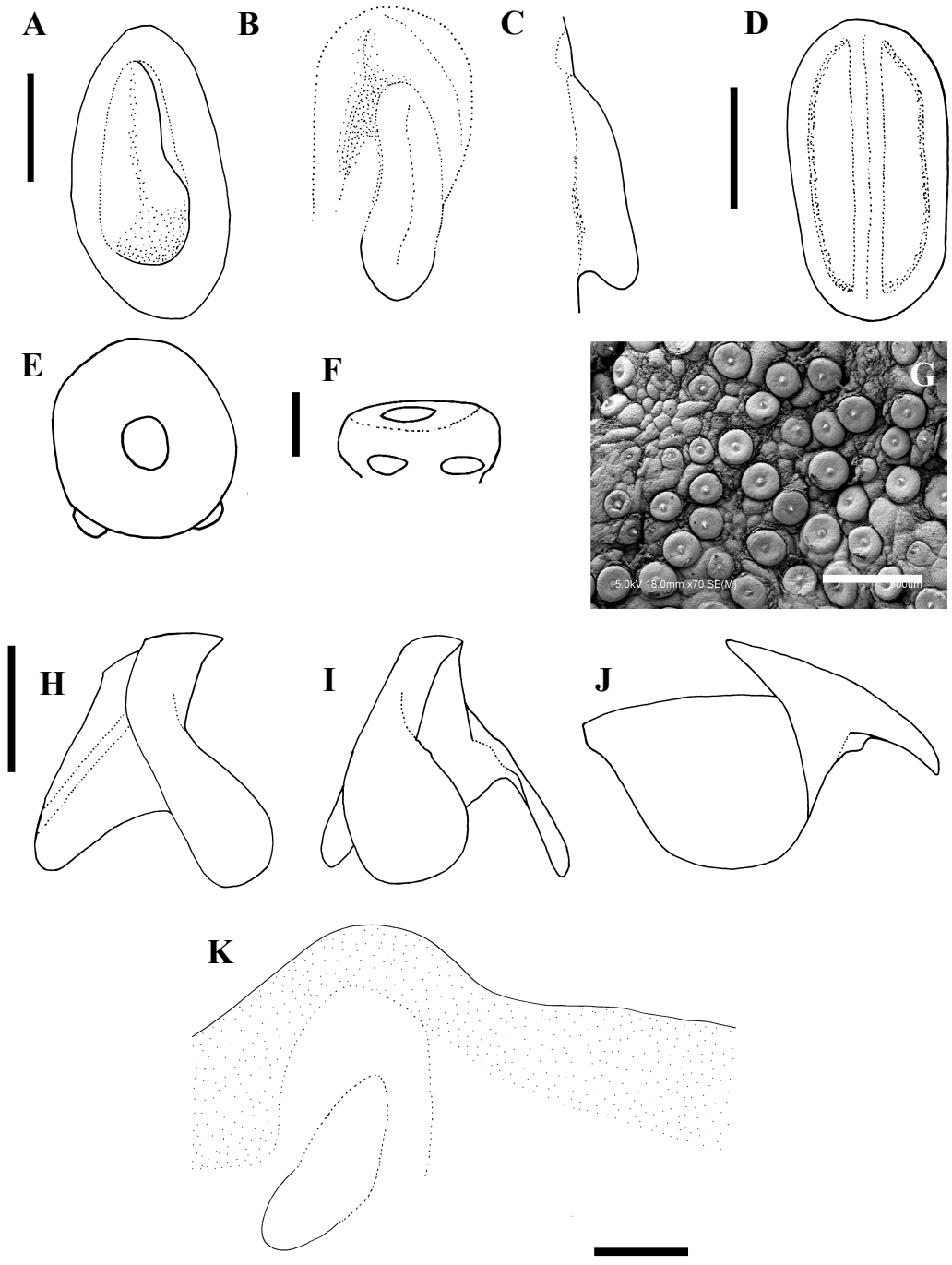

Fig. 41—*Mastigopsis hjorti*. A–C, E–G, K) NMNZ M.172921, ♀, ML 142*mm; D, H–J) M.172986, ♂, ML 78*mm, LRL 4.00mm. A) left funnel-locking cartilage; B) left mantle-locking cartilage; C) left mantle-locking cartilage, profile view; E) right eye; F) ventral view of right eye; G) skin tubercles on ventral surface of mantle; H) lower beak, profile view; I) lower beak, lateral oblique view; J) upper beak; K) internal mantle pigmentation. Scale bars = A–D, H–K) 5mm; E, F) 10mm; G) 500µm.

Arm-sucker rings (Fig. 42) proximally adentate, distally with 8–21 blunt, rectangular teeth; teeth relatively shorter in proximal suckers. Polygonal processes on oral surface of sucker in 3–4 concentric rings; distally, central and intermediate rings with cylindrical, pitted pegs; proximally, central and intermediate rings nearly flat; peripheral ring with flat, rectangular processes.

Tentacles absent from all specimens examined.

Lower beak, lateral profile (Fig. 41H): lower rostral length ~60% wing length, rostral edge nearly straight, rostral tip slightly hooked, rostral tip behind leading edge of wing by ~30% baseline; wing angle obtuse, jaw angle obscured by low wing fold, shoulder groove present; beak slightly taller than deep; hood slightly above crest, hood length

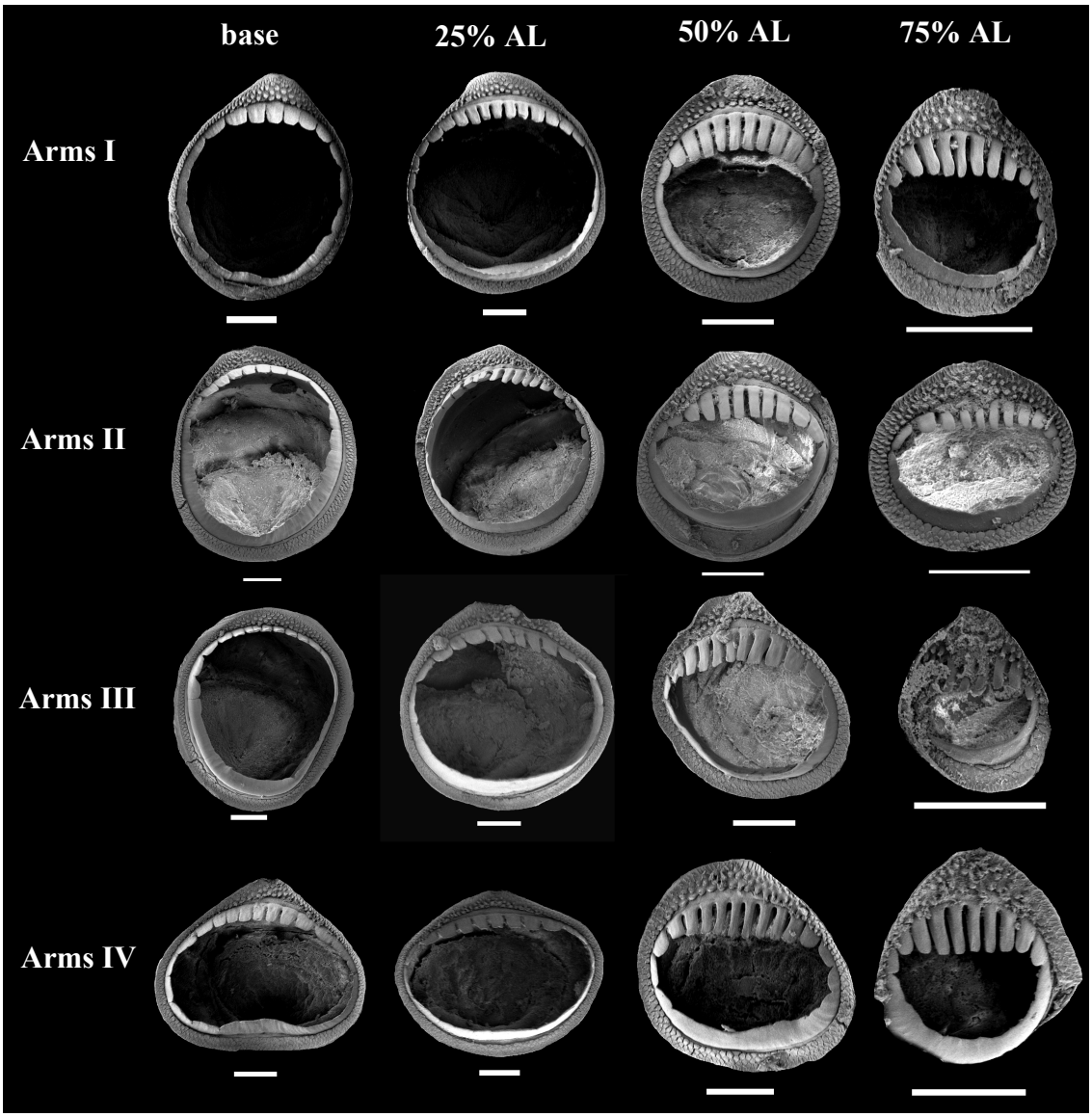

Fig. 42—*Mastigopsis hjorti* arm suckers, NMNZ M.172921, ♀, ML 142*mm. Scale bars = 200µm.

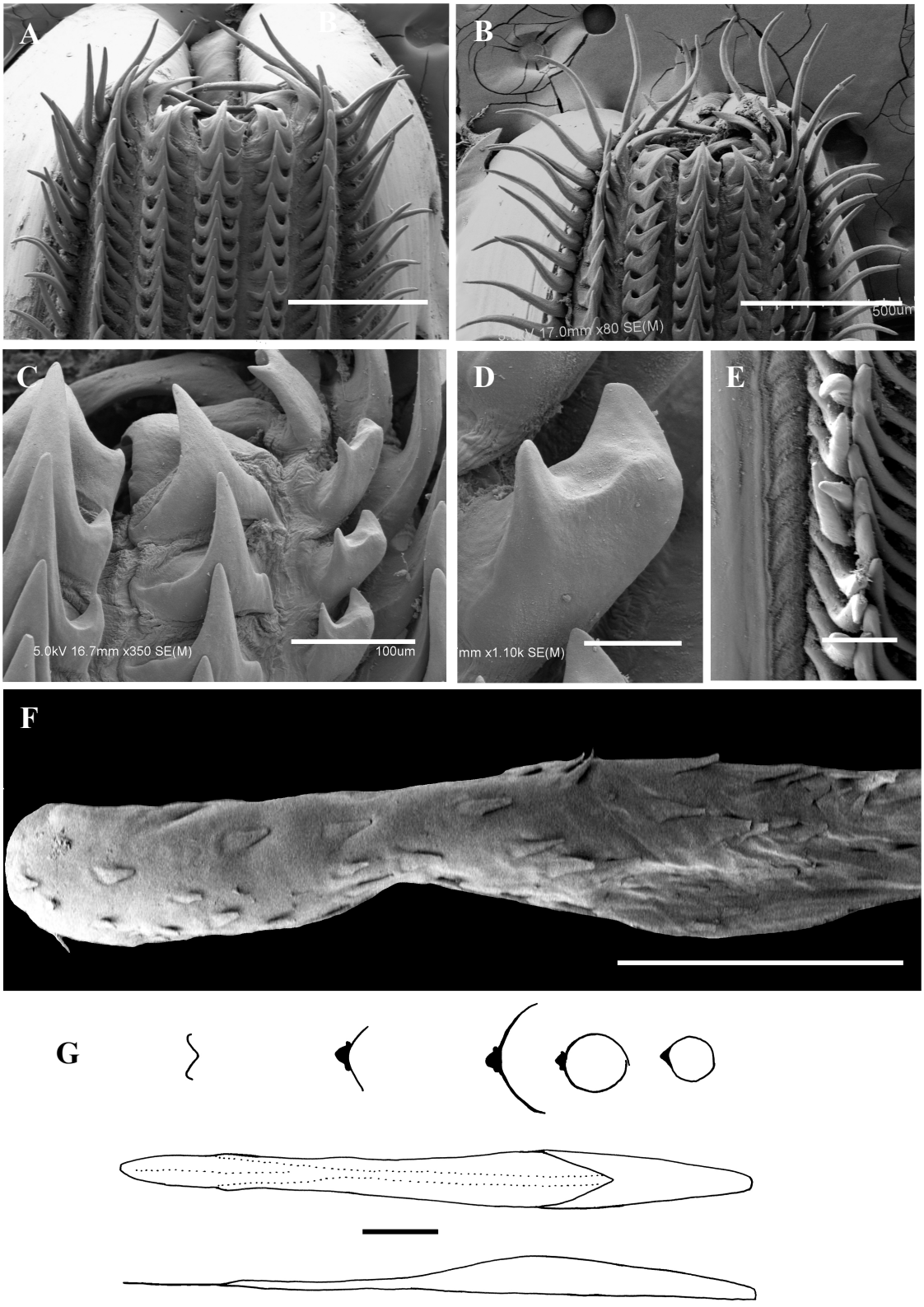

Fig. 43—*Mastigopsis hjorti*. A, E) NMNZ M.172921, ♀, ML 142*mm; B–D, G, H) M.172986, ♂, ML 78*mm. A) radula; B) asymmetrical radula; C) asymmetrical radula rachidian, first lateral tooth, and additional tooth; D) additional tooth of asymmetrical radula; E); radula margin F) palatine palp; G) gladius. Scale bars = A, B) 500µm; C, E) 100µm; D) 20µm; F) 1mm; G) 10mm.

~65% crest length, crest length ~55% of baseline, visible portion of crest straight; lateral wall fold with solid ridge extending to posterior edge of lateral wall; no notch in lateral wall. Lateral oblique view (Fig. 41I) with wing narrowest level with jaw angle, ~70% of greatest wing width. Ventral view with narrow notch in hood, free corners separated slightly. Posterior and anterior edge of wing remains clear through at least ML 78*mm (LRL 4.00mm), beak entirely pigmented at ML 142*mm (LRL 5.26mm).

Upper beak, lateral profile (Fig. 41J): upper rostral length ~30% hood length; hood length ~70% beak length; hood height ~30% beak width. Lateral wall fold absent; shoulder produced into point; jaw edge curved; jaw angle nearly 90°.

Radula (Fig. 43A) with tricuspid rachidian, base width ~75% height, proximal margin of base concave, with broad, sharp triangular mesocone and sharp, lateral cusps, slightly laterally directed, their height ~50% mesocone height. First lateral tooth strongly bicuspid; inner cusp broad, triangular, slightly curved toward rachidian, its height ~80% that of overall rachidian; outer cusp sharply pointed, medially directed, its height ~60% that of inner cusp. Second lateral tooth simple, curved slightly towards rachidian, ~150% rachidian height. Marginal tooth simple, straight, ~190% rachidian height. Poorly defined marginal plate present (Fig. 43E). Palatine palp (Fig. 43F) with ~40 short, flat teeth, each 50–100% rachidian height, sparsely distributed over palp.

Gladius (Fig. 43G) missing rostrum in best available specimen; greatest width (12% GL) attained at 67% [damaged] GL; free rachis 15% GL; secondary conus 22% GL.

Epidermis damaged on all examined material. Integumental photophores not apparent in examined material. Colour (preserved) purple, chromatophores densely and uniformly distributed on mantle, fins, and arms; pigmentation on interior mantle wall extending from anterior margin to approximate level of locking cartilage (Fig. 41K), area around locking cartilages without chromatophores and remainder of inner mantle wall not pigmented; chromatophores present on all surfaces of arms; subcutaneous chromatophores on arm of similar same size and density as overlying chromatophores.

Smaller specimens (ML 24–26mm, Fig. 40B) differ from above only as follows: mantle width ~26% ML, fin length ~79% ML, fin width ~92% ML. Head length ~33% ML, head width ~23% ML; eye diameter ~14% ML; MLC ~5% ML, funnel-locking

cartilage ~6% ML. Arms ~20–25% ML, suckers in two series; with 12–14 pairs of suckers present on each arm.

Remarks: This species appears to have a circumglobal distribution; its type locality is the North Atlantic (Chun, 1910), and specimens have also been reported from the Pacific and Indian Oceans (Nesis, 1987). However, some authors suggest that specimens from different geographic locations may belong to different species (Nesis, 1987; Vecchione & Young, 2007d). The specimens that were available from New Zealand collections all had characteristics that correspond to *Mp. hjorti* (*sensu stricto*, Chun, 1913); however, they did not have the skin sculpture that Chun (1913) described, which Rancurel (1973) determined to be impressions left by the nets during capture, and the triserial suckers on Arms II are an unusual feature. It is not clear whether this arrangement is an illusion resulting from live fixation or characteristic of specimens from this location, because only one specimen with complete Arms II was available for study. No fresh material was available from New Zealand for genetic comparison with *Mp. hjorti* from the North Atlantic.

Mastigopsis hjorti shares some morphological traits with *I. cordiformis*: fin shape, fin length greater than 80% ML, and skin tubercles. However, *Mp. hjorti* beaks are entirely pigmented at LRL 5.26mm, while *I. cordiformis* beaks are still nearly entirely unpigmented at LRL 6.36mm, indicating that *I. cordiformis* grows much larger than *Mp. hjorti*. Additionally, *Mp. hjorti* can be distinguished by the two round eye photophores (*I. cordiformis* has a single, ventral photogenic band), oval funnel-locking cartilage (lacking tragus and antitragus), the lack of trabeculae on the protective membranes of the arms, presence of largest suckers at the arm bases, and beak morphology. The beak of *Mp. hjorti* (Fig. 41H) is taller and narrower than that of *I. cordiformis* (Fig. 35). *Mastigopsis hjorti* and *Mg.* sp. nov. are similar in size and both have funnel-locking cartilage that lacks an antitragus; however, *Mp. hjorti* can be readily distinguished by the larger fin, two eye photophores, and skin tubercles. *Magnoteuthis magna*—the closest genetic relative to, but genetically distinct from—North Atlantic *Mp. hjorti* can be separated by the presence of two eye photophores and larger fins in *Mp. hjorti*.

As frequently found in mastigoteuthids herein (see Discussion), the radula morphology of one specimen appeared unusual (Fig. 43B–D) as follows: rachidian mesocone with

small, sharp lateral cusps, their height ~45% that of mesocone height. Left first lateral tooth unicuspid, broad, triangular, straight, its height ~75% that of rachidian. Additional tooth present between left first lateral tooth and second lateral tooth, elongate with two or three irregular cusps, height ~50% of rachidian, with small sharp lateral cusps slightly anteriorly directed, their height approximately equal to that of mesocone (Fig. 43C, D).

Table 11—Measurements (mm) of *Mastigopsis hjorti* (Chun, 1913), recorded from right side of specimens.

Specimen ID:	**NIWA 48868**	**NIWA 48868**	**NIWA 48868**	**Paralarval mean indices**		**NMNZ M.172986**	**NMNZ M.172921**	**Mean indices**	
Sex	Indet.	Indet.	Indet.			M	F		
ML	25	24	26			78*	142*		
MW	7	5	8	MWI	26	21	45	MWI	32
FL	20	20	19	FLI	79	*	126	FLI	89
FW	21	21	27	FWI	92	92*	150	FWI	106
HL	7	7	11	HLI	33	25*	44	HLI	31
HW	6	4	7	HWI	22	*	35	HWI	25
ED	3	3	4	EDI	14	13*	22	EDI	15
Arm I	5	*	3*	A1LI	20	*	69*	A1LI	>48
Arm II	3*	*	7*	A2LI	>26	*	106	A2LI	73
Arm III	2*	*	5	A3LI	20	*	90	A3LI	62
Arm IV	4*	*	5*	A4LI	>20	*	93*	A4LI	>63
TLA	38	36*	44			113*	264*		

* indicates damage; FL for NMNZ M.172986 and NMNZ M.172921 (non-paralarval) does not include the rostrum, which was missing. Therefore, the mean indices for these specimens are slightly inflated (except for FL which normally includes the rostral length) so they are not directly comparable with other species. Mean indices for paralarvae included only intact features; NMNZ M.172986 was excluded from all mean indices.

Genus *Echinoteuthis* Joubin, 1933

Echinoteuthis Joubin, 1933:13. Type species *Echinoteuthis danae* Joubin, 1933, by monotypy.

Diagnosis: Mantle length at maturity ~240 mm. Fins lanceolate in outline when considered together; fin length ~63% ML. Funnel widely conical with recurved end. Funnel-locking cartilage ear shaped, tragus present, antitragus absent; funnel pocket present. Mantle-locking cartilage C shaped, not posteriorly undercut in profile. Arm suckers arranged in two distinct series but appearing to merge into single series midway on Arms IV; arm suckers with sharp teeth; Arms IV ~73% ML; protective membranes without trabeculae. Tentacular suckers minute; club not expanded, with trabeculate membrane present in some species (*fide* Vecchione & Young, 2007c). Large eye-sinus photophore present, diameter ~24% eye diameter. Eye photophore absent. Integumental photophores absent, skin tubercles variably present. Gladius not examined due to limited material.

Remarks: *Echinoteuthis danae* was described from paralarval specimens and therefore its status remains uncertain. However, Joubin (1933) originally placed both *E. danae* and *E. famelica* into this new genus. Salcedo-Vargas (1997) placed *E. danae* in the same 'group' as *E. famelica* due to morphological similarities, while Vecchione & Young (2007a) suggested that *E. danae* may be a synonym of *E. atlantica*. Because of their similarities, both *E. famelica* and *E. atlantica* are considered *Echinoteuthis* species in this study.

***Echinoteuthis famelica* (Berry, 1909)** (Tables 3, 4, 12, Figs 44, 45)
Chiroteuthis famelica Berry, 1909: 414, 415, fig. 8.
Mastigoteuthis famelica (Berry, 1909)—Young (1991): 176–178, fig. 5.

Type material examined: **USNM neotype**, ♀, ML 241mm, off Oahu, FIDO X, Stn 9.

Additional material examined (2 specimens): **NMNZ M.074535**, 2 sex indet., ML 38, 40mm, 22.83°S, 175.03°W, 377m over 4000m, RV *James Cook*, 12/12/1976, MWT, Stn J17/60/76.

Distribution (Fig. 44): 22–23°S, 175–176°W (near New Zealand); elsewhere reported from the Pacific Ocean, near Hawaii (Berry, 1909; Young, 1991).

Diagnosis: Fins lanceolate in outline when considered together, length ~55% ML, width ~46% ML; integumental photophores absent, eye-sinus photophores diameter ~24% ED, skin tubercles present on mantle; funnel-locking cartilage with tragus, antitragus absent.

Description (ML ~40mm, Fig. 45): Mantle cone shaped anteriorly, with mantle cavity extending to ~20% FL from anterior of fins (thereafter gladius and surrounding musculature continue as narrow cylinder), widest (~18% ML) at anterior margin; ventral anterior mantle margin slightly convex with medial notch; dorsal anterior mantle margin pointed. Fins lanceolate in outline when considered together, length ~55% ML, width ~46% ML; anterior lobes absent; posterior margin at tail convex. Integumental photophores absent; eye-sinus photophore diameter ~24% ED. Skin tubercles present only on mantle.

Head rounded, length ~21% ML, width ~13% ML. Olfactory papilla cylindrical. Eye diameter ~10% ML. Funnel width ~8% ML, length ~6% ML, aperture approximately level with posterior margin of eye; funnel pocket present. Funnel-locking cartilage ear shaped (Fig. 45C), ~4% ML, groove bulbous posteriorly, antitragus absent; strong tragus present along inner/medial margin, extending to midline of groove; concave along outer/lateral margin. Mantle-locking cartilage C shaped (Fig. 45D, E), ~3% ML; not posteriorly undercut in profile.

Arm formula IV>II>III≥I; arm length 13–*25*–54% ML (Tables 4, 12); Arms I–III all of subequal thickness, Arms IV thickest; oral faces of arms bordered by wide membranes; expanded lateral membrane present on Arms IV. Trabeculae absent. Arms I–III with 34–44 suckers arranged in two distinct series; Arms IV damaged on all available material.

Tentacles absent from all specimens examined.

Arm suckers, radula, gladius, and beak not dissected due to limited material.

Colour (preserved) yellow-beige; gladius visible through dorsal surface of fin; chromatophores present but damaged.

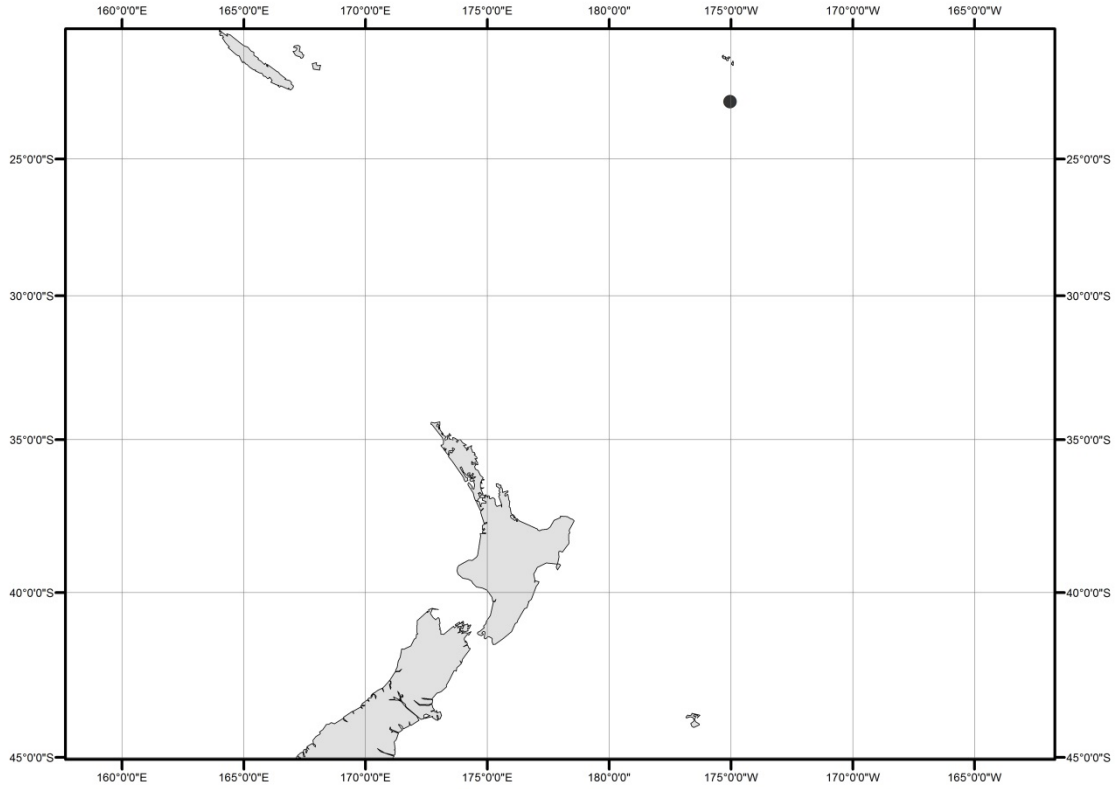

Fig. 44—Distribution of *Echinoteuthis famelica* specimens examined in this study.

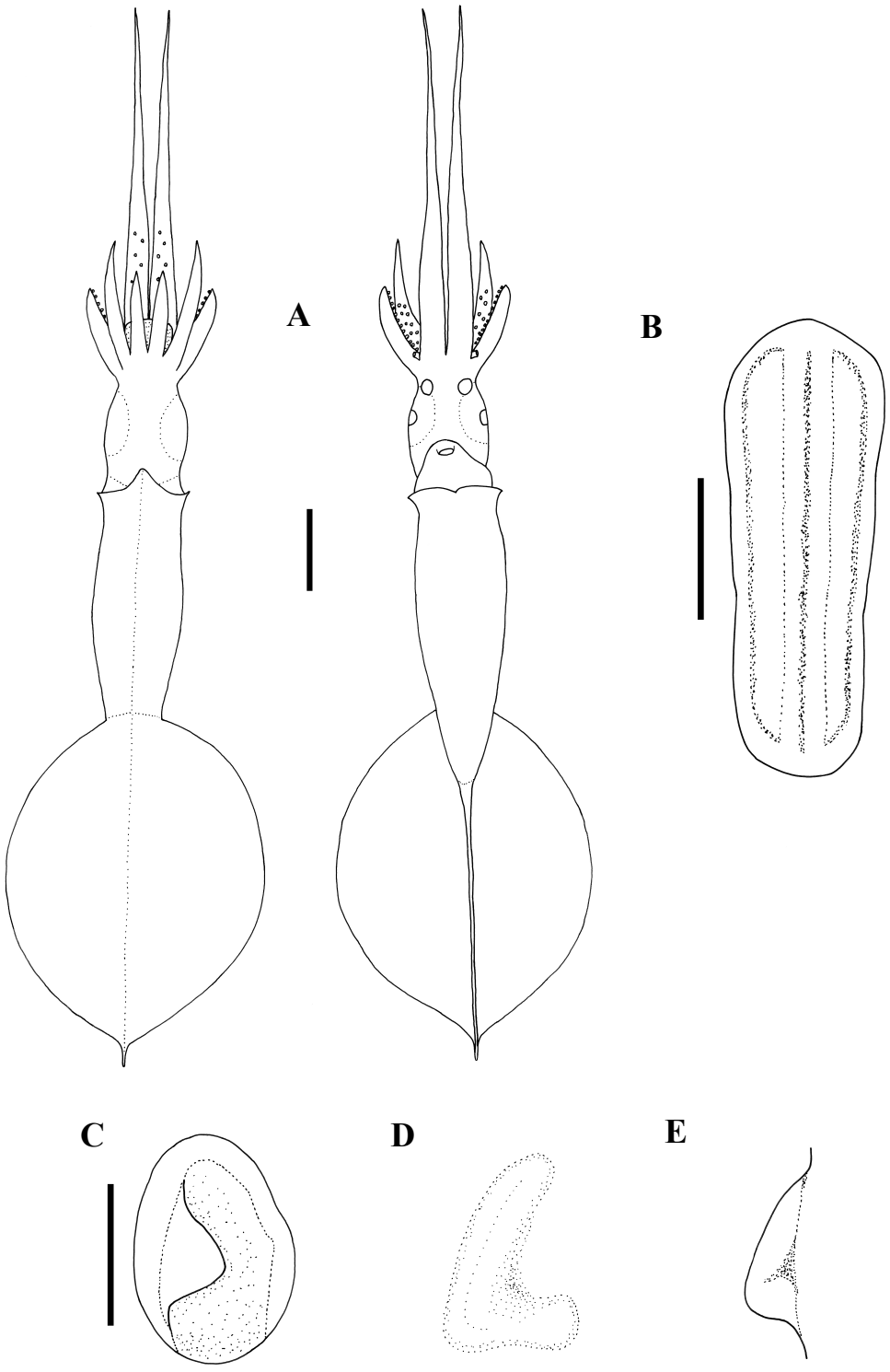

Fig. 45—*Echinoteuthis famelica*. A) NMNZ M.074535, sex indet., ML 38mm; B–E) NMNZ M.074535, sex indet., ML 40mm. A) whole specimen; B) nuchal cartilage; C) left funnel-locking cartilage; D) left mantle-locking cartilage; E) left mantle-locking cartilage, profile view. Scale bars = A) 5mm; B–E) 1mm.

Remarks: This description is limited because only two damaged, juvenile specimens were available from New Zealand collections. Berry's (1909) description was based on a single specimen of a similar size to those examined herein (ML 39mm) and characterised by the lanceolate fins, relatively narrow head, and slender mantle (Berry, 1909); the specimens examined herein agree with this description. Although the original description did not mention the relatively large eye-sinus photophores, they are present on the specimens examined herein and on the *E. famelica* neotype. In addition, this species can be readily distinguished from other local mastigoteuthid species by the lanceolate fin shape, ear-shaped funnel-locking cartilage without an antitragus, C-shaped mantle-locking cartilage, and large eye-sinus photophores (Fig. 45). However, there were no specimens of this size available for *I. cordiformis*, or *Mt.* sp. Y for comparison.

The three members of the *glaukopis* group are believed to occupy different oceans: *E. glaukopis*, Indian Ocean; *E. famelica*, Pacific Ocean; and *E. atlantica*, Atlantic Ocean (Young & Vecchione, 2007c). However, *E. famelica* has only been previously identified from Hawaiian waters, and is known to occur at latitudes as low as 3°S (Young, 2010). *Echinoteuthis glaukopis* is differentiated from *E. atlantica* and *E. famelica* by a rhomboidal fin, the presence of an antitragus in the funnel-locking cartilage, and an undercut mantle-locking cartilage (Chun, 1910). *Echinoteuthis atlantica* can be distinguished from *E. famelica* by the trabeculate membrane present on the tentacles of *E. atlantica* (Vecchione & Young, 2007c).

The characteristics of *E. famelica* are similar to those in published descriptions for *E. danae*; however, they appear to occupy different geographic areas because *E. danae* has been described from the North Atlantic (Joubin, 1933) and the Indian Ocean (Salcedo-Vargas, 1997), while *E. famelica* has only been described from the Pacific Ocean (Berry, 1909; Young, 1991). In addition, the funnel-locking cartilage of *E. danae* has an antitragus, which is not present in *E. famelica*. However, Salcedo-Vargas and Okutani (1994) considered *E. danae* to be a junior synonym of *E. famelica*, while Vecchione and Young (2007) suggest that it may be synonymous with *E. atlantica*. Because very few specimens have been collected, this issue remains unresolved. Genetics indicate that *E. atlantica* is distinct from other mastigoteuthids (Chapter 3), but tissue samples for *E. famelica* were not available.

Echinoteuthis famelica shares some characteristics with *I. tyroi*: lanceolate fin shape, and presence of skin tubercles. However, *I. tyroi* is known from the Indian Ocean near Somalia, and has an ovate funnel-locking cartilage, and lacks photophores (Salcedo-Vargas, 1997). In addition, *I. tyroi* can be separated from all known mastigoteuthid paralarvae by the presence of expanded tentacle clubs (Salcedo-Vargas & Young, 2007). Unfortunately both of the *E. famelica* specimens in this study lacked tentacles.

Table 12—Measurements (mm) of *Echinoteuthis famelica* (Berry, 1909).

Specimen ID:	**NMNZ M.074535**	**NMNZ M.074535**	**Mean indices**	
Sex	Indet.	Indet.		
ML	38	40		
MW	7	8	MWI	18
FL	21	22	FLI	55
FW	17	19	FWI	46
HL	7	9	HLI	21
HW	5	5	HWI	13
ED	3	4	EDI	10
Side measured	R	L		
Arm I	4	7	A1LI	13
Arm II	7	8	A2LI	19
Arm III	5	6	A3LI	14
Arm IV	19	24	A4LI	54
TLA	63	64		

Genus *Magnoteuthis* Salcedo-Vargas & Okutani, 1994

Magnoteuthis Salcedo-Vargas & Okutani, 1994: 125. Type species *Mastigoteuthis magna* Joubin, 1913, by original designation.

Diagnosis: Mantle length at maturity ~220 mm. Fins heart shaped in outline when considered together; fin length ~66% ML. Funnel bulbous posteriorly, cylindrical anteriorly. Funnel-locking cartilage flask shaped, tragus present, antitragus absent, convex protrusion along outer/lateral margin; funnel pocket absent. Mantle-locking cartilage flask shaped, posteriorly undercut in profile. Arm suckers arranged in two distinct series but appearing to merge into single series midway on Arms IV; arm suckers adentate or possess blunt teeth; Arms IV ~110% ML; protective membranes without trabeculae. Tentacular suckers microscopic; club not expanded, protective membranes without trabeculae. Eye-sinus photophore absent. Eye photophore potentially present. Integumental photophores microscopic or absent, skin tubercles absent. Gladius broad (greatest width ~10% GL).

Remarks: The morphological similarities of the species in this genus have lead to much taxonomic confusion. *Magnoteuthis microlucens* has only recently been discovered after careful examination revealed microscopic integumental photophores (Young, Lindgren, & Vecchione, 2008). This species had previously been mistaken for *Mg. inermis* (Young, 1991), a species considered a junior synonym of *Mg. magna* by some authors (Salcedo-Vargas & Okutani, 1994; Young, & Vecchione, 2004).

Salcedo-Vargas and Okutani (1994) created *Magnoteuthis* as a subgenus under *Idioteuthis* for *Mg. magna*. Although subgenera were removed in the classification by Salcedo-Vargas (1997), *Mg. magna* and *Mg. inermis* were included in the same 'group' under *Mastigoteuthis* in this new arrangement. This arrangement is consistent with the *magna* group contains *Mg. magna*, *Mg. microlucens*, and 'type beta', who all share funnel-shaped mantle-locking cartilage and microscopic tentacle suckers (Young & Vecchione, 2007d).

***Magnoteuthis* sp. nov.** (Tables 3, 4, 13, Figs 46–51)

Material examined (9 specimens): **NMNZ M.172975**, sex indet., ML 47mm, 32.54°S, 169.73W, 15/05/2003, RV *Tangaroa*, NORFANZ Stn 10; **NMNZ M.287233**, sex indet., ML 26mm, 33.84°S, 175.08°E, 277m over 5000m, RV *James Cook*, 16/12/1976, MWT, Stn J17/85/76; **NMNZ M.091715**, sex indet., ML 123mm, 36.42°S, 173.50°E, 1024–1045m, FV *Wanaka*, 23/03/1986, Stn WK4/14/86; **NIWA 48866**, ♀, ML 160mm, 36.52°S, 176.50°W, 904–1086m, 24/06/1995, FV *Seamount Enterprise*, Stn Z8289; **NMNZ M.287216**, sex indet., head only, 37.47°S, 178.40°E, 339 over 1350m, 14/12/1975, RV *James Cook*, MWT, Stn J17/69/75; **NMNZ M.287221**, ♀, ML 162.5mm, 39.67°S, 167.63°E, 1072–1102m, 20/07/1990, FV *Will Watch*; **NIWA 76653**, ♂, ML180mm, 39.96°S, 178.18°E, 906m, 23/03/2010, TAN1003/39; **NMNZ M.091708**, ♀, ML 73mm, 42.76°S, 177.47°W, 116–1164m, 09/07/1984, FV *Otago Buccaneer*, Stn B1/6/84; **NMNZ M.091721**, ♀, ML 104.5mm, year 1985–1986, FV *Wanaka*, stomach content of *Hoplostethus atlanticus*.

Distribution (Fig. 46): 32–43°S, 167°E–169°W (near New Zealand).

Diagnosis: Fins heart shaped in outline when considered together, length 60–*65*–72% ML, width 71–*77*–82% ML; integumental photophores and tubercles absent; funnel-locking and mantle-locking cartilage flask shaped; arm suckers adentate or with indistinct teeth, largest arm suckers overall located mid Arms II; trabeculae absent; tentacle suckers microscopic.

Description (ML ~120–180mm, Figs 47A, 48–51): Mantle cone-shaped anteriorly, with mantle cavity terminating beneath midpoint of fins (thereafter gladius and surrounding musculature continue as narrow cylinder), widest (~21% ML) at anterior margin; dorsal anterior mantle margin convex. Fins heart shaped in outline when considered together, length 60–*64*–70% ML, width 71–*79*–82% ML; rounded anterior lobes present; posterior margin at tail concave. Photophores and tubercles absent from integument; overlying gelatinous coating present on posterior half of mantle.

Head cylindrical, length 25–*30*–36% ML, width ~16% ML. Olfactory papilla cylindrical. Eye diameter ~13% ML. Potential inconspicuous eye photophore present (Fig. 50) (see Remarks). Funnel bulbous posteriorly, anteriorly cylindrical, width ~14%

ML, length ~11% ML; aperture approximately level with posterior margin of eye; funnel pocket absent. Funnel-locking cartilage flask shaped (Fig. 48A), ~7% ML, groove bulbous posteriorly; concave along inner/medial margin (due to tragus); convex along outer/lateral margin, with anterior portion narrower, with nearly parallel sides. Mantle-locking cartilage flask shaped (Fig. 48B, C), ~6% ML, approximately hemispherical posteriorly and hemiconical anteriorly; posteriorly undercut in profile.

Arm formula IV>II>III≥I; arm length 98–*116*–138% ML (Tables 4, 13); Arms IV thickest, followed by Arms II; aboral keels present on Arms I–III, expanded lateral membrane present on Arms IV. Trabeculae absent. At ML 160mm, 114–122 suckers present on each arm; suckers arranged in two distinct series, distally merging into one series on Arms IV; largest suckers overall located mid Arms II (~100% arm width) at about pair 17.

Arm-sucker rings (Fig. 49) proximally adentate, distally adentate or with 6–18 indistinct teeth; at ~75% arm, infundibular ring with 7 blunt, conical teeth. Polygonal processes on oral surface of sucker in 4–8 concentric rings; distally, central and intermediate rings with rounded, pitted, porous pegs; proximally, central and intermediate rings nearly flat; peripheral ring with flat, rectangular processes.

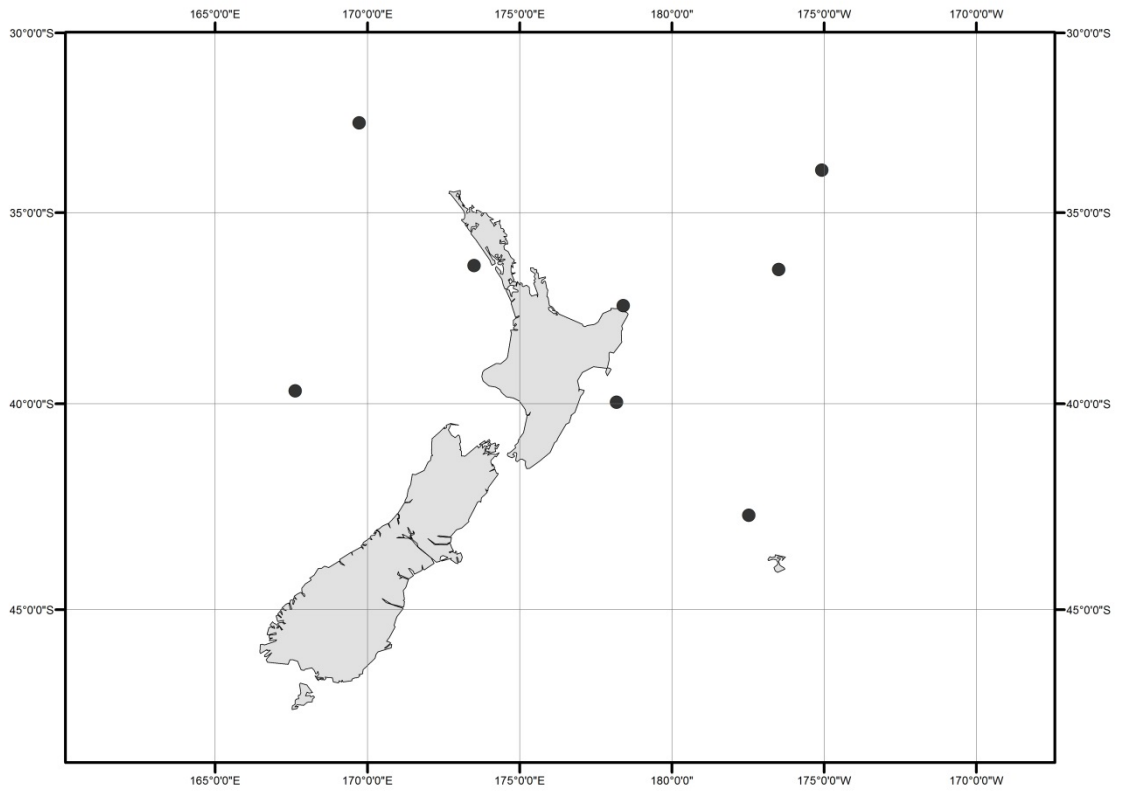

Fig. 46—Distribution of *Magnoteuthis* sp. nov. specimens examined in this study.

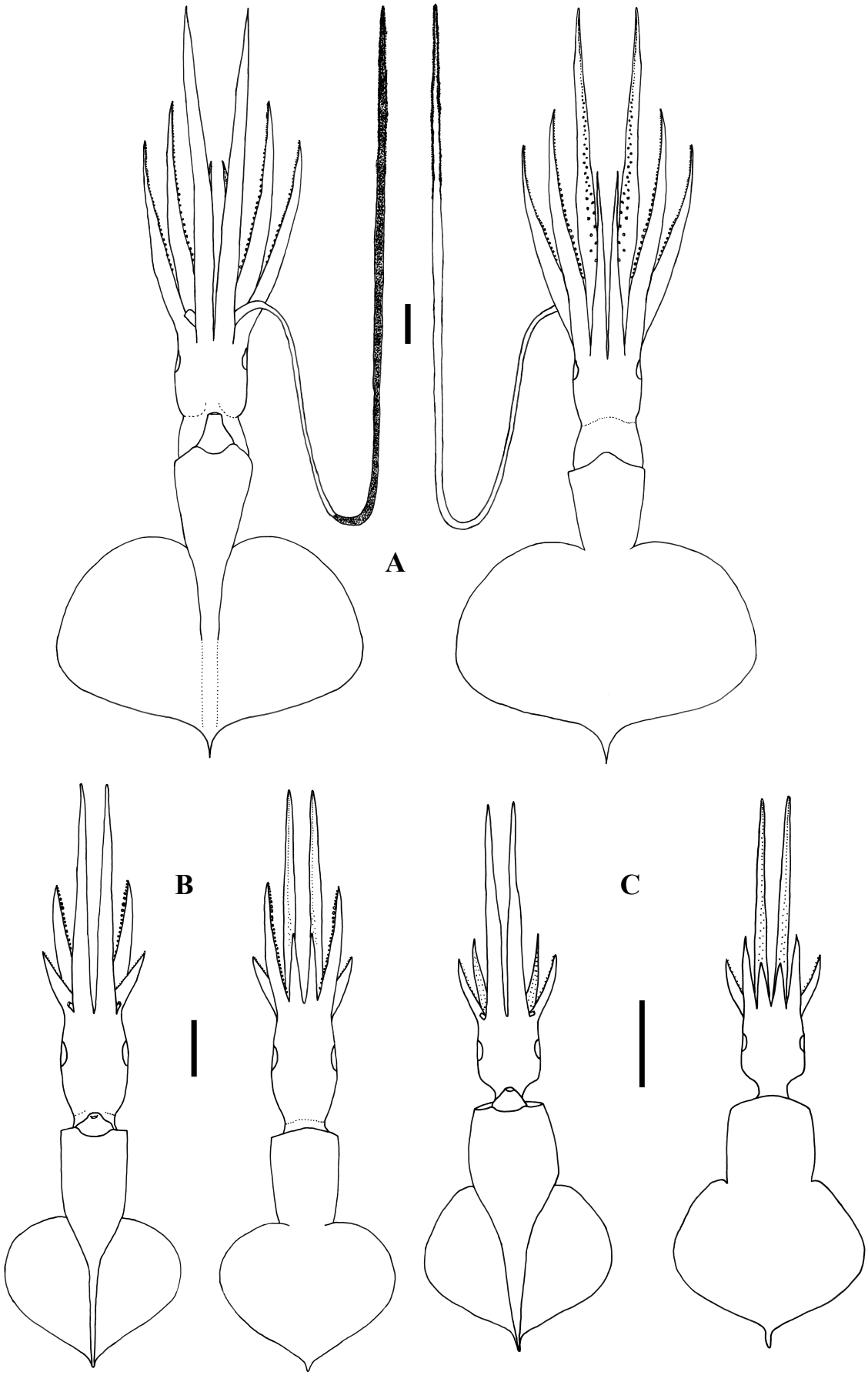

Fig. 47—*Magnoteuthis* sp. nov. A) NMNZ M.287221, ♀, ML 163mm; B) NMNZ M.172945, sex indet., ML 42mm; C) NMNZ M.287233, sex indet., ML 26mm. Scale bars = A) 20mm; B, C) 10mm.

At ML 104.5mm (sole tentacle available for examination), tentacle length ~280% ML, club ~64% TnL (~180% ML), not expanded; stalk without keel. Suckers microscopic (Fig. 51A), covering majority of tentacle surface apart from narrow aboral strip; where tentacle club begins, width of sucker-covered surface is less than half of stalk circumference, broadening distally to cover nearly entire stalk circumference. Tentacle suckers degraded, infundibular rings lost (Fig. 51B); sucker diameter ~40µm, ~3% club width.

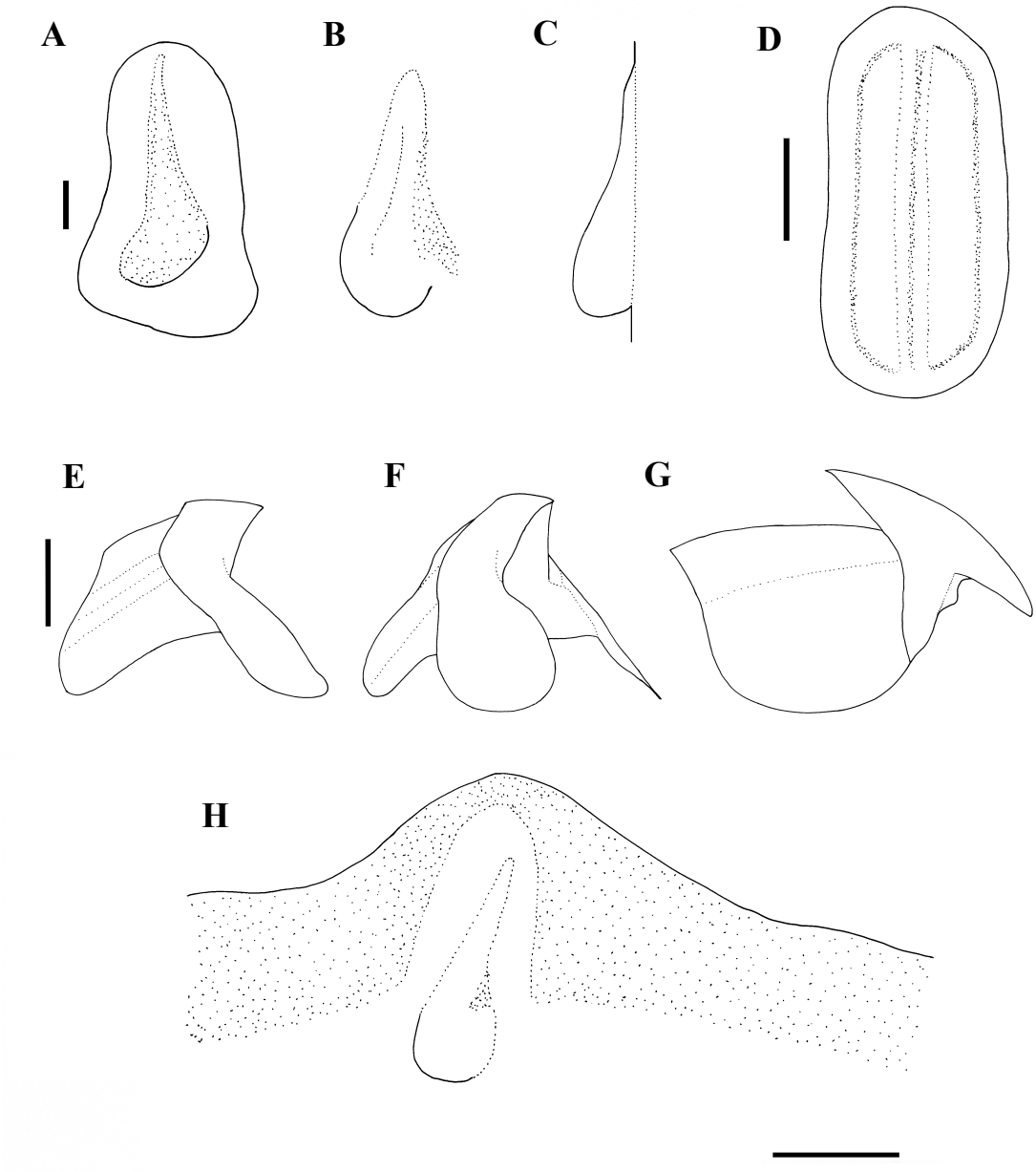

Fig. 48—*Magnoteuthis* sp. nov. A–C, H) NIWA 48866, ♀, ML 160mm; D) NMNZ M.287216, sex indet., head only; E–G) NIWA 76653, ♂, ML 180mm, LRL 4.76mm. A) left funnel-locking cartilage; B) left mantle-locking cartilage; C) left mantle-locking cartilage, profile view; D) nuchal cartilage; E) lower beak, profile view; F) lower beak, lateral oblique view; G) upper beak, profile view; H) internal mantle pigmentation. Scale bars = A–C) 1mm, D) 2mm; E–H) 5mm.

Lower beak, lateral profile (Fig. 48E): lower rostral length ~50% wing length, rostral edge moderately curved, tip without hook, rostral tip behind leading edge of wing by ~25% of baseline; wing angle obtuse, jaw angle obscured by low wing fold, shoulder groove present; beak height ~60% baseline; hood close to crest, hood length ~50% crest length, crest length ~65% baseline, visible portion of crest slightly curved; broad lateral wall fold extends to posterior edge of lateral wall; no notch in lateral wall. Lateral oblique view (Fig. 48F) with wing narrowest level with jaw angle, ~70% of greatest width. Ventral view with narrow notch in hood, free corners separated slightly. Anterior edge of wing below shoulder clear at ML 123mm (LRL 4.00mm), pigmented by ML 180mm (LRL 4.76mm).

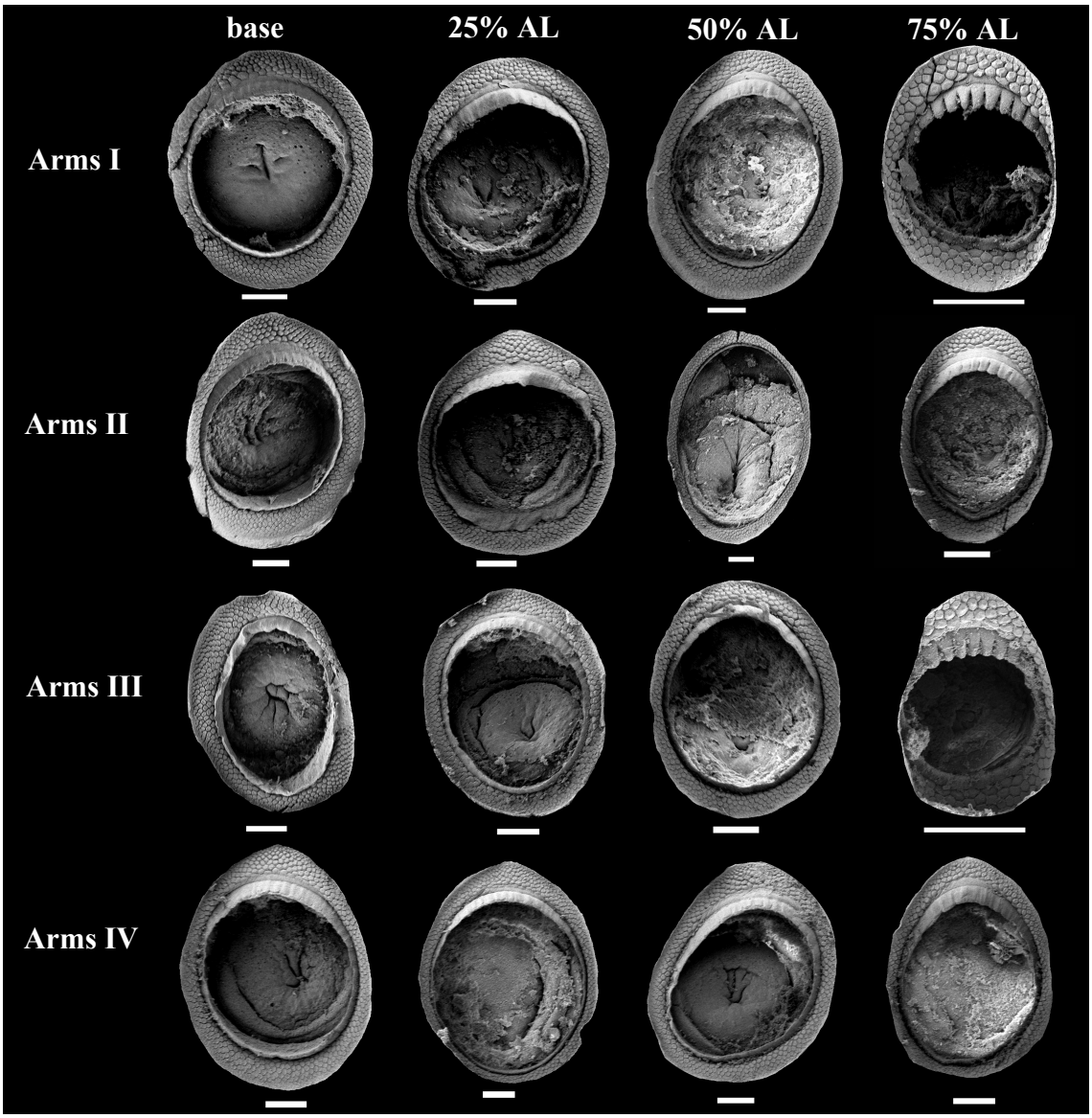

Fig. 49—*Magnoteuthis* sp. nov. arm suckers, NMNZ M.287216, sex indet., head only, LRL 3.09mm. Scale bars = 100µm.

Upper beak, lateral profile (Fig. 48G): upper rostral length ~30% hood length; hood ~70% beak length; hood height ~25% beak width. Lateral wall fold extending to posterior edge of lateral wall; shoulder produced into point; jaw edge nearly straight; jaw angle obtuse.

Radula (Fig. 51C) with tricuspid rachidian, base width ~60% height, proximal margin of base concave, with narrow, sharp, triangular mesocone and sharp lateral cusps, slightly laterally directed, their height ~55% mesocone height. First lateral tooth strongly bicuspid; inner cusp narrow, triangular, slightly curved toward rachidian, its height ~80% that of overall rachidian; outer cusp sharply pointed, medially directed, its height ~65% that of inner cusp. Second lateral tooth simple, curved slightly towards rachidian, ~130% rachidian height. Marginal tooth simple, straight, ~180% rachidian height. Marginal plate present (Fig. 51D). Palatine palp (Fig. 51E) with ~60 narrow, flat teeth, each 30–90% rachidian height, sparsely distributed over palp.

Gladius (Fig. 51F) with greatest width (~10% GL) attained at ~70% GL; free rachis ~13% GL; secondary conus ~25% GL, rostrum ~4% GL, oval in cross section.

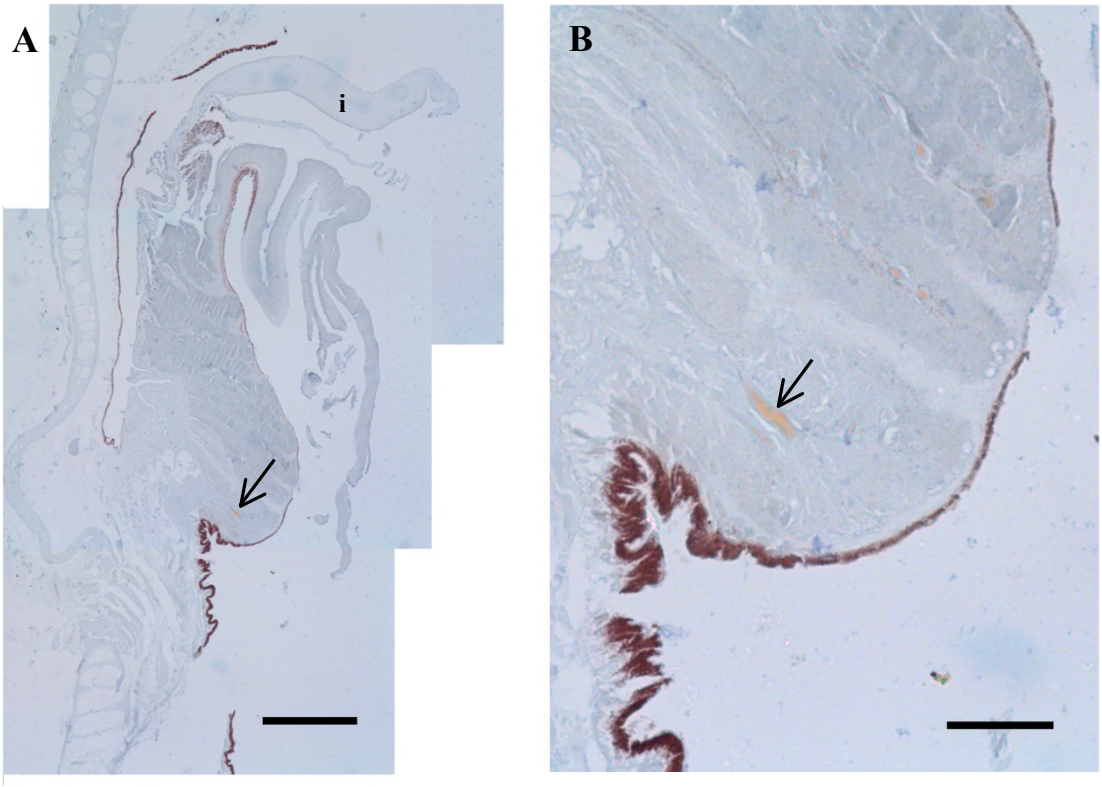

Fig. 50—Cross-section through ventral surface of *Magnoteuthis* sp. nov. eye, stained with Mallory's trichrome; NMNZ M.287216, sex indet., head only. Arrows indicates potential photophore tissue (in orange, with many smaller additional possible minute photophores also staining orange), (i) indicates iris. Scale bars = A) 200 µm; B) 50µm.

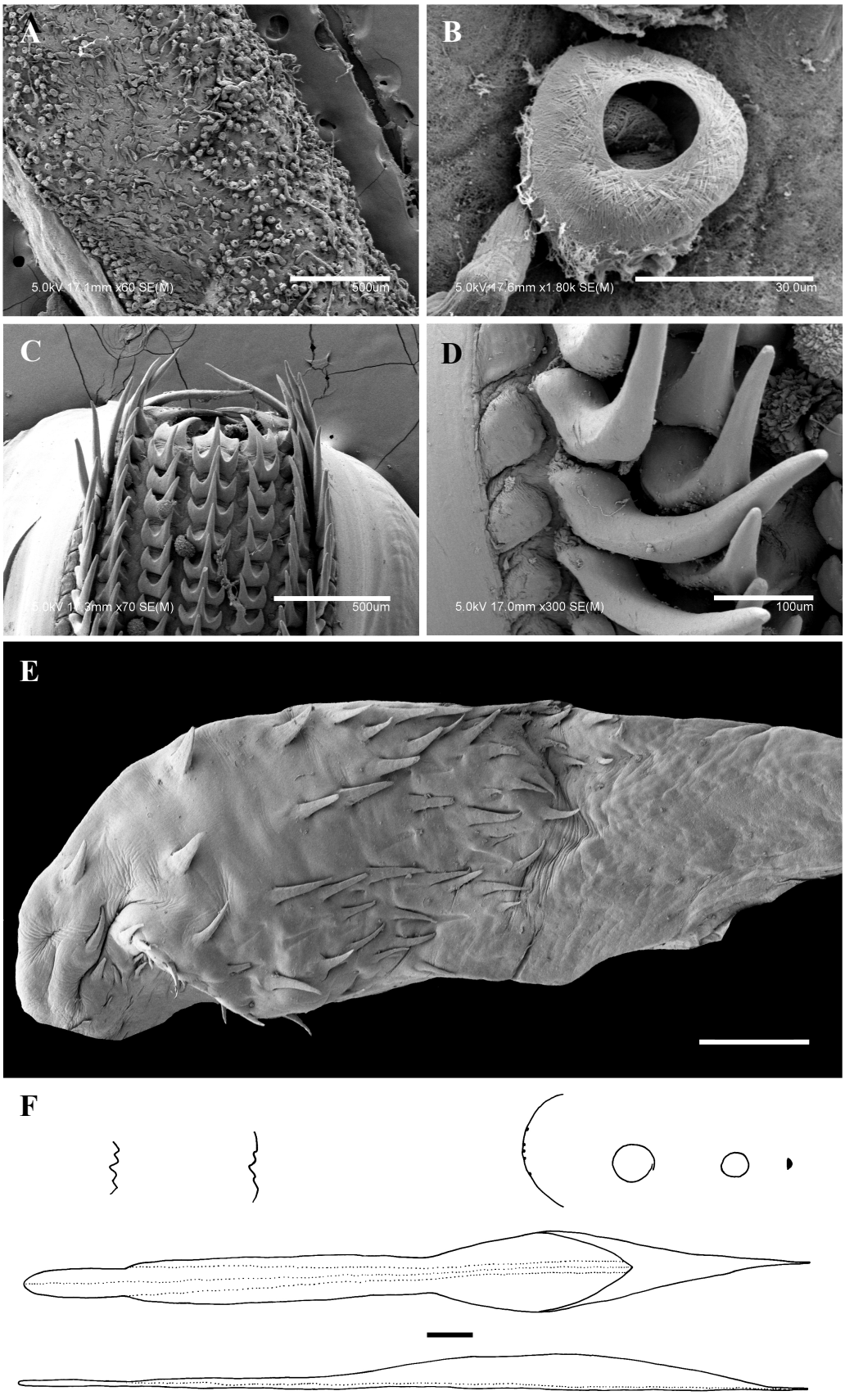

Fig. 51—*Magnoteuthis* sp. nov. A, B) NMNZ M.091708, ♀, ML 73mm; C–E) NMNZ M.287216, sex indet., head only; F) NIWA 76653, ♂, ML 180mm. A) mid-tentacle club; B) degraded microscopic tentacle sucker; C) radula; D) marginal plates of radula; E) palatine palp; F) gladius. Scale bars = A, C) 500µm; B) 30µm; D) 100µm; E) 1mm; F) 10mm.

Epidermis damaged on all examined material. Integumental photophores absent. Colour (preserved) pink or purple, dark red or purple on mantle and fins; head white, with pronounced darkening around eye sinus; chromatophores more densely distributed on fin than head; pigmentation on anterior edge of mantle interior extending approximately to level of locking cartilage (Fig. 48H), area around locking cartilages without chromatophores and remainder of inner mantle wall not pigmented; chromatophores present on aboral surface of arms, arm oral surface darkly pigmented but individual chromatophores not readily discernible; subcutaneous chromatophores on mantle, fins, and funnel; less dense than overlying chromatophores. Colour (fresh) of liver bright red.

Smaller specimens (ML 42–73mm, Fig. 47B) differ from above only as follows: mantle width ~30% ML; fin length ~67% ML, fin width ~74% ML. Head length ~47% ML, head width ~24% ML; MLC ~8% ML, funnel-locking cartilage ~8% ML. Arms I ~42% ML, Arms II ~64% ML, Arms III ~41% ML, Arms IV ~113% ML. At ML 42mm, 24–36 pairs of suckers present on each arm; largest sucker ~75% arm width, appearing in pair 17 at ~70% arm length in Arms II.wjy

Paralarval specimens (ML 25mm, Fig. 47C) differ from adult and 'smaller' specimens only as follows: mantle width ~40% ML; fin width ~86% ML. Head width ~27% ML; eye diameter ~20% ML; MLC ~10% ML, funnel-locking cartilage ~11% ML. Arms I ~31% ML, Arms II ~39% ML, Arms III ~27% ML, Arms IV ~102% ML; 14–35 pairs of suckers present on each arm; largest sucker ~50% arm width, appearing in pair 15 at ~70% arm length in Arms II.

Remarks: The two locally occurring species that most closely resemble *Mg.* sp. nov. are *Mp. hjorti* and *I. cordiformis*, but they can be differentiated as follows. *Magnoteuthis* sp. nov. has a relatively smaller fin and longer arms than *Mp. hjorti* and *I. cordiformis*. Additionally, *Mp. hjorti* has two prominent eye photophores (Fig. 41E, F) and the funnel-locking cartilage lacks a tragus (Fig. 41A). *Idioteuthis cordiformis* reaches a larger size than *Mp.* sp. nov. and the arms have trabeculate membranes. *Magnoteuthis* sp. nov. also appears to have an inconspicuous photophore, with many smaller additional possible minute photophores, embedded within the eye tissue ventral to the lens (Fig. 50); however, the stain that was used turns both photophore tissue and haemocyanin orange. Future testing to assess the presence of an eye photophore could involve *in situ* observation of live specimens or genetic analysis for sequences that code

for photophores. This potential photophore was not observed in the cross section of the eyes of other species examined in this study. Although eye photophores have not been reported in other *Magnoteuthis* species, histology should be performed on them as well.

Magnoteuthis sp. nov. is also morphologically similar to *Mg. magna*, *Mg. inermis*, *Mg.* 'type beta', and *Mg. microlucens*. These species all share the same flask-shaped funnel locking cartilage, largest arm suckers in the middle of the arms, and microscopic tentacular suckers. The distributions of these species are disjunct; however, *Mg.* sp. nov. and *Mg.* 'type beta' are found in the South Pacific around New Zealand (Young & Vecchione, 2007e); *Mg. magna* is known from the Western North Atlantic; the type locality of *Mg. inermis* is in the Eastern North Atlantic, south of Vridi (Abidjan, Ivory Coast); and *Mg. microlucens* is known from the North Pacific, south of Hawaii (Young, Lindgren & Vecchione, 2008). Morphologically, *Mg. microlucens* is distinguished from *Mg.* sp. nov. by the presence of microscopic integumental photophores on the aboral side of the arms, ventral surface of funnel, and dorsal and ventral sides of the mantle, fins, and head. Fin width and undulation are the distinguishing features of *Mg. inermis* and *Mg.* sp. nov; *Mg. inermis* has an undulating fin and FW 53% ML (Rancurel, 1972), while *Mg.* sp. nov. has a planar fin and FW ~79% ML. Because these differences may be due to preservation or damage, some authors consider *Mg. inermis* a junior synonym of *Mg. magna* (Salcedo-Vargas & Okutani, 1994; Young & Vecchione, 2004). Both *Mg.* sp. nov. and *Mg.* 'type beta' are found at the same longitude, but *Mg.* 'type beta' is known from sub-Antarctic waters. The description of 'type beta' is based on a single specimen from the Southern Ocean and is distinguished by an apparent complete lack of chromatophores and by the dentition on the arm suckers, which have small teeth and intermediate between the smooth suckers of *Mg. magna*, and the broad, round teeth of *Mg. microlucens* (Young, Vecchione, & Lindgren, 2008). It is possible that *Mg.* sp. nov. and *Mg*. 'type beta' are the same species; however, all specimens examined for *Mg.* sp. nov. have chromatophores. In *Mg. magna*, the inside of the mantle is darkly pigmented, while *Mg.* sp. nov. lacks this pigmentation (Fig. 48H). The most distinctive feature of *Mg*. sp. nov. is that the largest suckers are located on Arms II, and are twice as large as the largest suckers on other arms, while the largest arm suckers of *Mg. magna* are located on Arms IV and are only slightly larger than those on other arms (Vecchione & Young, 2010). In addition, *Mg. magna*, *Mg. microlucens*, and *Mg.* sp. nov. are genetically distinct (Chapter 3).

Table 13—Measurements (mm) of *Magnoteuthis* sp. nov.

Specimen ID	**NMNZ M.091721**	**NMNZ M.091708**	**NIWA 48866**	**NMNZ M.287216**	**NMNZ M.287221**	**NMNZ M.172975**	**NMNZ M.091715**	**NIWA 76653**	**NMNZ M.287233**	**Mean Indices**	
Sex	F	F	F	Indet.	F	Indet.	Indet.	M	Indet.		
ML	105*	73	160	-	163	42	123	180	26		
MW	26	22	38	-	34	14	22	35	10	MWI	24
FL	69*	53	111	-	98	26	76	101	16	FLI	64
FW	102	52	130	-	134	32	100	143	22	FWI	79
HL	42	31	44	30	48	22	45	45	9	HLI	36
HW	24	14	27	21	28	13	22	25	7	HWI	19
ED	18	12	21	10	23	6	19	21	5	EDI	14
Side Measured	R	R	R	L	L	L	R	R	R		
Arm I	80	37	102	61	95	14	92	30*	8	A1LI	56
Arm II	90	57	128	66	124	21	133	168	10	A2LI	81
Arm III	61	38	125	52	92	13	105	123	7	A3LI	62
Arm IV	140	94	173	105	174	41	170	110*	26	A4LI	116
TLA	260	180	365	-	373	107	320	290*	62		
TL	392	315	-	-	-	-	-	-	-		
TnL	295	190	-	-	-	-	-	-	-	TnLI	270
CL	190	92	-	-	-	-	-	-	-	CLI	56

* indicates damaged features; -indicates missing features; M.091721 (except for the tentacle and club), M.091708, M.172975, M.287233 and M.287216 were excluded from all mean indices.

DISCUSSION

These results suggest that New Zealand mastigoteuthid diversity is higher than has been previously reported. Checklists of local species have listed three (Spencer et al., 2011) or five (Spencer, Marshall, & Willan, 2009) species. However, in this review, eight species were found; five were identified as previously named species, and three potentially new species were also identified. With eight species now identified within in New Zealand waters, Mastigoteuthidae becomes the second most diverse local squid family after Cranchiidae (Spencer et al., 2011).

Many characters were evaluated for their utility in distinguishing species and differentiating genera (Table 3). A subset of these were deemed useful for separating genera and their systematic value is discussed below, with comparison to other chiroteuthid families, which are used to polarise character states to make inferences about higher-level relationships.

Mantle and fins

Mantle shape can be helpful in species identification. In most local mastigoteuthid species, and other members of the chiroteuthid families, the mantle cavity terminates at, or anterior to, the midpoint of the fins (Young & Vecchione, 2008). However, both *Mp. hjorti* and *I. cordiformis* have cone-shaped mantles that gradually narrow towards the fin. This could suggest a common ancestor between *Idioteuthis* and *Mastigopsis*, although the mantle of *I. cordiformis* is widest around the viscera, while in *Mp. hjorti* it is widest at the anterior edge.

Fin size and shape have some value for species identification. While most mastigoteuthids have fins that are wider than long, *E. famelica* can be distinguished by its fins, which are longer than wide (Fig. 45A). Within the Mastigoteuthidae, the lanceolate fin shape is present only in *Echinoteuthis*, while the fin shape varies from heart to elliptical in other mastigoteuthids. *Mastigopsis hjorti* and *I. cordiformis* are distinguished from other species by having fins that are nearly as long as the mantle. A variety of fin lengths are found in other chiroteuthid families; large fins are present in the Magnapinnidae (Vecchione & Young, 2013) and the Promachoteuthidae (Young & Vecchione, 2003); small fins (~20% ML) are present in the Batoteuthidae (Young &

Roper, 2009); and very long, often decorated, tails are present in the Chiroteuthidae (Young & Roper, 2011a) and the Joubiniteuthidae (Young, 2009). However, large fins are present and long tails are absent in the Mastigoteuthidae. The morphological similarities shared between the Chiroteuthidae and the Mastigoteuthidae indicate a common ancestor, but the lack of tail, which could be ancestral because it is also present in the Joubiniteuthidae, suggests that the lack of a tail in the Mastigoteuthidae may be derived.

Locking cartilages

Funnel- and mantle-locking cartilages can be helpful in species identification and provide additional support for the generic divisions proposed herein. The Chiroteuthidae and the Mastigoteuthidae are the only chiroteuthid families to have species with a tragus and antitragus present in the funnel-locking cartilage. This indicates a close relationship between these two families, and suggests that their most recent common ancestor likely had funnel-locking cartilage with a tragus and antitragus. *Mastigoteuthis* and *Idioteuthis* have retained this ancestral form of funnel-locking cartilage. Local species with this ear-shaped funnel-locking cartilage are *I. cordiformis*, *Mt. dentata*, *Mt. psychrophila*, *Mt.* sp. X, and *Mt.* sp. Y. *Mastigoteuthis psychrophila* and *Mt.* sp. X both have a strong antitragus, which distinguishes them from *Mt. dentata*. However, the antitragus strength appears variable within *Mt.* sp. X specimens (Fig. 20A, B), possibly due to degradation or changes during growth; therefore, some can resemble *Mt. dentata* cartilages (Fig. 7A). *Mastigoteuthis* sp. Y is only known from one female specimen, but appears to have a wider groove than the other locally occurring species with ear-shaped funnel-locking cartilage (Fig. 26B). Although the tragus has been retained in *Echinoteuthis*, the antitragus has been lost (Fig. 45C). The unique flask-shaped funnel-locking cartilage in *Magnoteuthis* (Fig. 48A) is synapomorphic, being present only in this genus. In New Zealand waters, *Mg*. sp. nov. can be differentiated from other local mastigoteuthids by the locking cartilage morphology; however, outside of New Zealand waters, *Mg. magna* and *Mg. microlucens* both have similarly shaped locking cartilages. *Mastigopsis* can be distinguished from the other genera in the family by its oval funnel-locking cartilage (Fig. 41A); however, the locking cartilage of damaged/degraded specimens of other species may look approximately oval. Unfortunately, because the morphology of the cartilages can be damaged or degraded, they are not always reliable for species identification (*e.g. I. cordiformis*; Fig. 31A–C).

Arm suckers

Although variation was found in sucker dentition both along the length of the arm and among arms, some consistencies were observed to be useful for species identification and separating the genera. Arm-sucker dentition has been previously suggested as a useful character for separating the genera (Salcedo-Vargas & Okutani, 1994; Salcedo-Vargas, 1995); however, the arm suckers of *Mastigoteuthis* and *Echinoteuthis* bear sharp teeth, while the arm suckers of *Idioteuthis*, *Mastigopsis*, and *Magnoteuthis* are adentate or possess blunt teeth. Within the chiroteuthid families, arm-sucker dentition varies from adentate to sharp teeth, and it is not clear which form is ancestral. The same range of sucker dentition found herein for mastigoteuthids is also found in the Chiroteuthidae (Young & Roper, 2011a). However, sucker morphology can be helpful in species identification. Sucker dentition can be used to separate *Mg.* sp. nov. from the all other species in *Magnoteuthis*; the indistinct teeth of *Mg.* sp. nov. are intermediate between the blunt teeth of *Mg. microlucens* and the adentate suckers of *Mg. magna*. In addition, a smooth band, between the teeth and polygonal processes, was only found in *Mt.* sp. X (Fig. 21) and *I. cordiformis* (Fig. 33). The suckers of *Mt.* sp. Y appear to have relatively smaller teeth compared to other *Mastigoteuthis* species (Fig. 27). The number of papillated rings varies both within and among species, but *Mp. hjorti* has only three to four (Fig. 42), while other species have up to eight (*e.g. I. cordiformis*; Fig. 33) . However, the number of papillated rings is also known to vary ontogenetically (Salcedo-Vargas, 1995). Therefore, arm-sucker ultrastructure seems useful for species-level identification, but appears less useful for higher taxonomy within the Mastigoteuthidae.

Tentacles

The chiroteuthid families are united by the absence of a primary tentacle club, and presence of a secondary tentacle club that is straight and unexpanded (Young & Vecchione, 2008). Although there appear to be many morphological similarities between the Chiroteuthidae and Mastigoteuthidae, their tentacle morphology is quite different. The Chiroteuthidae have a tentacle club with zero to six series of suckers, bordered by wide protective membranes (Young & Roper, 2011a). In contrast, all mastigoteuthid species have a tentacle club with multiple irregular series of suckers with greatly reduced protective membranes. Although tentacles and tentacle-sucker

morphology have been relied on in the past for mastigoteuthid taxonomy and identification, the specimens examined in this study were mostly missing their tentacles. Out of the eight species examined here, only half had specimens with tentacles that could be examined (rarely more than one per species, except *I. cordiformis* where most specimens retain their tentacles), and of those only three had intact sucker rings. Although the tentacular sucker rings were degraded, the microscopic size of *Mg.* sp. nov. sucker rings (Fig. 51A) distinguishes this species from other local mastigoteuthids, and unites it with other species in *Magnoteuthis*. Unlike other mastigoteuthid genera, *Idioteuthis* has an expanded tentacle club and large proximal suckers (Fig. 34B). The large proximal suckers closely resembled arm suckers, with several rows of flat polygonal processes and teeth on the infundibular ring. Distally, the sucker rings were minute and similar to the tentacle suckers of other mastigoteuthids (Fig. 34E–H). Unlike *I. cordiformis*, the tentacle suckers of *Mt. psychrophila* (Fig. 16A–F) and *Mt.* sp. X (Fig. 22A–D) were adentate, and morphologically similar to each other.

Salcedo-Vargas (1995) proposed that 'cushions' be included in evaluations of sucker ultrastructure. He recognised two types of cushions, the 'spongy-type' and the 'horny-type'. Herein, the horny type was observed only in *I. cordiformis* tentacle suckers (Fig. 34F–H) and the arm suckers of larger specimens. It is possible that these cushions are, as proposed by Young and Vecchione (2004) for the 'irregular horny lumps' described for the sucker rings of *I. latipinna* by Sasaki (1929), a preservation artefact. However, Salcedo-Vargas (1995) argued that other scientists have overlooked cushions, considering them pathological malformations, when they are an adaptation to deep-sea life. Cushions were found in all large *I. cordiformis* specimens examined herein. Four specimens examined prior to preservation also had uneven, potentially degraded suckers, indicating that this malformation is not necessarily caused by preservation, but may be due to either freezing, the ammonia in the arm tissue, or possibly an adaption as suggested by Salcedo-Vargas (1995).

Beaks

Both upper and lower beaks of *I. cordiformis* displayed extreme variation (Figs 35–37). Upper beaks appear to have limited use for identifying species because of the lack of any distinguishing characteristics combined with high intraspecific variation; those of some *I. cordiformis* individuals have a lateral groove, which is absent in others

regardless of sex or size; the same variability was found in *Mg.* sp. nov. The lower beaks of *I. cordiformis* show great variation in the jaw edge and shoulder in particular, which does not appear to be correlated with growth or sex (Fig. 35). Locally, variation has been found in the beaks of another species in the chiroteuthid families, *Chiroteuthis veranyi* (Mensch, 2010). Similarly, Voss (1977) found that intraspecific variability can exceed interspecific variability in cephalopods, which may limit beak value for species identification. Variation in beak morphology has implications in particular for ecological studies that rely on morphology to identify species from stomach contents. However, the beaks of *I. cordiformis* (above at least ML 181mm, the smallest specimen observed herein), due to their large size, are not likely to be confused with those of any other mastigoteuthid. Locally, the beaks of *I. cordiformis* are most similar to those of *Mg.* sp. nov, but they are easily distinguished even at small sizes by the larger rostral length to wing length ratio in *Mg.* sp. nov, and the higher beak height to baseline ratio in *I. cordiformis*. Variation was also found in the lower beaks within *Mt. dentata* (Fig. 9) and *Mt.* sp. X (Fig. 23). The difference in the angle of the jaw edge between *Mt.* sp. X and *Mt. dentata* can be used to differentiate these two species at present; however, due to the intraspecific variation found within both species, examination of more individuals may reveal that this difference is part of continuous variation and that they are a single species.

Radulae

Herein, asymmetry of the radula has been found in individuals of half of the species examined. In specimens of both *Mt. dentata* and *Mt.* sp. X, the first lateral tooth was bicuspid on one side and unicuspid on the other (Figs 11C, D, 24C, D). A similar morphology was found in one individual of *Mp. hjorti* (Fig. 43B); however, in addition to the asymmetry of the first lateral tooth, beside the unicuspid tooth, there was an additional row of small, elongate teeth with two or three irregular cusps (Fig. 43C, D). In contrast, one individual of *Mt. psychrophila* had a fusion of the first and second lateral teeth on one side (Fig. 17C–E). This minor and nondirectional deviation from symmetry in a bilaterally symmetrical animal is known as fluctuating asymmetry (Palmer & Strobeck, 1986), which is an epigenetic process that is induced by environmental and genetic stress (Parsons, 1992). Jokela et al. (2001) conducted a study on fluctuating asymmetry in the radulae of freshwater snails (*Potamopyrgus antipodarum*). Measuring both sides of the middle radular teeth, they found the level of

fluctuating asymmetry was higher within populations than between populations. In another gastropod genus, *Peristernia*, Taylor and Lewis (1995) found radular tooth variation among rows on the same radula, and suggested that it may be a form of intra-individual fluctuating asymmetry. Similarly, some taxa in the Octopodidae show asymmetry of the lateral cusps of the rachidian tooth, or serial repetition of asymmetry between rows (Nixon, 1998).

All species examined herein had seven rows of teeth with tricuspid rachidian teeth. Variation among species was found in the tooth shape and relative length, and relative cusp length. Marginal plates were variably present within genera: absent in *Mt. dentata*, *Mt. psychrophila*, and *Mt.* sp. Y; present in *I. cordiformis* and *Mg. sp*. nov.; and poorly defined in *Mt.* sp. X and *Mp. hjorti*. Although differences in the morphology of the radulae of all species were found, due to limited material, the consistency of the radula morphology and occurrence of asymmetry in the Mastigoteuthidae remains unknown. Voss (1977) found great variation in the number and morphology of radular teeth within a single species of octopus, and suggested that there is limited value in the radula for species identification. Therefore, intraspecific variation as well as fluctuating asymmetry in the mastigoteuthid radula should be investigated in the future.

Gladius structure

It appears that the ancestral form of the chiroteuthid family gladius was long and narrow because this trait is present in the Magnapinnidae (Vecchione & Young, 2013), the Promachoteuthidae (Young & Vecchione, 2003), the Batoteuthidae (Young & Roper, 2009), the Chiroteuthidae (Young & Roper, 2011a) and the Joubiniteuthidae (Young, 2009). Therefore, it is likely that the most recent common ancestor between the Chiroteuthidae and the Mastigoteuthidae had a long, narrow gladius, as is found in *Mastigoteuthis* and *Echinoteuthis*, which have a narrow gladius width (~3% GL) and a long secondary conus (~50% GL). The gladius structure of *Idioteuthis*, *Mastigopsis*, and *Magnoteuthis* appears to be more derived and suggests that they may have a more recent common ancestor; they have a wider gladius (~10% GL) and a shorter secondary conus (~20–35% GL).

The structure of the gladius is also very useful in differentiating some species. Within local mastigoteuthids, the gladius structure, and especially the cross-sections, can be

used for species identification. However, the differences in gladius structure of *Mg.* sp. nov. and the closely related species *Mg. magna* and *Mg. microlucens* were not compared. Therefore, although the gladius can be used locally for some identifications, it is not known whether any two closely related species can be differentiated in this way. Less variation was observed in the gladii of *Mastigoteuthis* species, which may limit the use of this character for species-level identification within this genus.

Photophores

Photophores are absent in several chiroteuthid families: the Magnapinnidae (Vecchione & Young, 2013), the Promachoteuthidae (Young & Vecchione, 2003), and the Joubiniteuthidae (Young, 2009). In addition, the single batoteuthid species, *Batoteuthis skolops*, has photophores on the tips of Arms IV (Young & Roper, 2009). Within the Chiroteuthidae, photophores are absent in *Planctoteuthis* (Young, Vecchione, & Roper, 2008) and *Grimalditeuthis*, except for the arm tips on mature female *Grimalditeuthis* (Young & Roper, 2011b). However, eye photophores are present in both *Asperoteuthis* (Young & Roper, 2011c) and *Chiroteuthis*, while integumental photophores are present only in *Chiroteuthis* (Roper & Young, 2013). Some mastigoteuthids have integumental, eye sinus, and/or eye photophores, while photophores are entirely absent in a few species. The presence of similar types of photophores may indicate a recent common ancestor between species, while differences in photophore structure may indicate that they arose independently. Integumental photophores are present in *Mg. microlucens* (but absent from all other *Magnoteuthis* species), all *Mastigoteuthis* species, and '*Mastigoteuthis*' *pyrodes* (whose generic status is currently uncertain); however, these three groups have different photophore size and structure, which could indicate that they were gained independently, or present in a distant common ancestor, lost in the most recent common ancestor for this family, and then regained in some lineages. Eye photophores are present in *Idioteuthis*, *Mastigopsis*, and one species of *Mastigoteuthis*. In addition, there is some indication of a vestigial (or possibly arising) eye photophore present in *Mg*. sp. nov. (Fig. 50). Since eye photophores are also present in some chiroteuthid species, this could indicate that their most recent common ancestor possessed eye photophores, which were then lost in some genera and species, and likely regained in *Mt*. sp. Y. The presence of eye-sinus photophores indicates a recent common ancestor shared between *Mastigoteuthis* and *Echinoteuthis*, because these structures are absent in *Idioteuthis*, *Mastigopsis*, and *Magnoteuthis*. However, the eye-

sinus photophores in *Echinoteuthis* are relatively large compared to those in *Mastigoteuthis*.

Local mastigoteuthid species can be distinguished based on photophore location, size, and patterns. Eye photophores are found in three forms in mastigoteuthids: hemispherical (*Mp. hjorti*, *I. okutanii, fide* Salcedo-Vargas, 1997), photogenic patch (*I. cordiformis*), and a band around the entire eye circumference (*Mt.* sp. Y). The relatively large size of the eye-sinus photophore can be used to distinguish *E. famelica* from other locally occurring *Mastigoteuthis* species, which have integumental photophores of a similar size to their eye-sinus photophore. Locally, integumental photophores are present in *Mt. dentata*, *Mt. psychrophila*, *Mt.* sp. X, and *Mt.* sp. Y. The photophore pattern on Arms IV can be used to differentiate *Mt. dentata* (Fig. 7E), *Mt. psychrophila* (Fig. 14A), and *Mt.* sp. X (Fig. 20F); however, the complete Arms IV pattern on *Mt.* sp. Y is unknown (Fig. 28B). Unfortunately, photophore presence and location should not be heavily relied upon for species identification because mastigoteuthids are so frequently damaged during capture.

Skin tubercles

Within the Mastigoteuthidae, skin tubercles are present in *Idioteuthis*, *Mastigopsis*, and juvenile *Echinoteuthis*. The skin tubercles of both *I. cordiformis* (Fig. 31I) and *Mp. hjorti* (Fig. 41G) are conical tubercles of elastic/fibrocartilage tissue with overlying epidermis (Roper and Lu, 1990). Skin tubercles are also present in paralarval *Echinoteuthis*, but they are morphologically unique because they are small and multicuspid (Young, 1991). However, the skin tubercles found in *Asperoteuthis acanthoderma* are morphologically distinct from those found in the mastigoteuthids and by their hyaline-like tissue composition (Roper & Lu, 1990). The similar tubercles of *Idioteuthis* and *Mastigopsis* to each other indicate a possible recent common ancestor; however, it appears that other skin tubercles arose independently based on their different morphology.

Skin tubercles have been used in the past for classifications within the Mastigoteuthidae. The genus *Echinoteuthis* was distinguished from *Mastigoteuthis* based on the presence of skin tubercles. Additionally, Salcedo-Vargas and Okutani (1994) used skin-tubercle morphology as part of their new classification of four

subgenera within the Mastigoteuthidae. Because Salcedo-Vargas (1997) used the presence of skin tubercles in his diagnosis of *Idioteuthis*, *E. famelica* was therein included in that genus. However, the skin tubercles found in *E. famelica* are distinct from those found in *Idioteuthis*. Skin tubercles appear absent from *Magnoteuthis* and *Mastigoteuthis*. Therefore, it appears that tubercles can be used for species identification, and also hold some value for higher classifications.

CONCLUSION

This family appears to comprise five genera in New Zealand waters: *Mastigoteuthis*, *Idioteuthis*, *Mastigopsis*, *Echinoteuthis*, and *Magnoteuthis*. Comparison of the morphological characters of these genera to those of other chiroteuthid families, supports this division. It seems likely that the most recent common ancestor for the Chiroteuthidae and the Mastigoteuthidae had integumental photophores, eye photophores, ear-shaped funnel-locking cartilage, a narrow gladius, and lacked skin tubercles. It is likely that integumental photophores were lost early in the evolution of the Mastigoteuthidae, and subsequently regained in some genera. Some characters show a close relationship between *Idioteuthis*, *Mastigopsis*, and *Magnoteuthis*: broad gladius, absence of eye-sinus photophore, absence of funnel pocket, and arm suckers that are adentate or possess blunt teeth. In contrast, *Echinoteuthis* and *Mastigoteuthis* share the following characters: narrow gladius, presence of eye-sinus photophore, presence of funnel pocket, and arm suckers with sharp teeth. Therefore it is possible that a recent common ancestor was shared by *Idioteuthis*, *Mastigopsis*, and *Magnoteuthis*, and another for *Mastigoteuthis* and *Echinoteuthis*.

A high biodiversity of mastigoteuthids has been found in New Zealand waters. Five previously known species have been identified: *Mt. dentata*, *Mt. psychrophila*, *I. cordiformis, Mp. hjorti*, and *E. famelica*. In addition, three potentially new species have also been found: *Mg.* sp. nov., *Mt.* sp. X, and *Mt.* sp. Y. With eight locally occurring species, Mastigoteuthidae is the second most diverse squid family found in this region. These species have been identified using a combination of genetic data (see Chapter 3) and morphological characters. Tentacles and photophore pattern have been heavily relied upon in the past for species identification; however, because these are the two characters most often damaged during capture, other characters are needed. Herein, beak morphology and funnel-locking cartilage have been found to be helpful for species

identifications, although some variation was observed within. While photophore distribution and morphology are useful for species identification, they should not be relied upon.

CHAPTER 3: Molecular phylogenetic analysis of the squid family Mastigoteuthidae (Mollusca, Cephalopoda) based on three mitochondrial genes

INTRODUCTION

Morphological description and identification of this group are particularly difficult since specimens are often badly damaged and are only caught in small numbers (Young, 1972). Characters that are frequently used for identification, such as skin photophores and tentacles, are usually lost or damaged during capture, hindering identification. Most species have been described from single and/or badly damaged specimens. In addition, many descriptions were written prior to the guidelines set forth by Roper and Voss (1983), and lack reference to characters since identified as important.

The 652 bp 'DNA barcode' region of the mitochondrial 5′ end of cytochrome *c* oxidase subunit I (COI) gene (Hebert et al., 2003) has been widely used for species identification and discovery (Hebert et al., 2004; Allcock et al., 2011; Rosso et al., 2012). Barcode reference sequence libraries derived from expert-identified reference specimens have greatly extended our ability to accurately identify juveniles (Victor et al., 2009), badly damaged specimens (St-Onge et al., 2008) and fragmentary remains, such as prey items from dietary analysis (Clare et al. 2009; Dunn et al., 2010; Braid et al., 2012). Although DNA barcoding has been proposed for cephalopods, it has been suggested that additional genes should be sequenced as well to ensure the adequacy of COI for species identification (Strugnell & Lindgren, 2007). DNA barcodes were used by Allcock et al. (2011) to study cryptic speciation in octopus in the genus *Pareledone* from the Southern Ocean. Recently, Dai et al. (2012) found DNA barcodes to be effective in the differentiation of coleoid cephalopods from Chinese waters. They used 16S rRNA in addition to COI to test the effectiveness of the DNA barcode region and identified a potentially cryptic species. The description for the most recent new mastigoteuthid species, *Mg. microlucens*, included DNA sequences for several closely related species for COI, 16S rRNA, and 12S rRNA (Young et al., 2008).

Mitochondrial DNA sequences for COI, 16S rRNA, and 12S rRNA were analysed herein for eight species of mastigoteuthid squids from the Pacific and Atlantic oceans, seeking independent corroboration of the morphological identifications to explore the genetic diversity among species. The resulting combined phylogeny, based on the three

mitochondrial genes, is used to test the morphology-based hypothesis of a generic division between *Mastigoteuthis*, *Idioteuthis*, *Mastigopsis*, *Echinoteuthis*, and *Magnoteuthis* from Chapter 2.

MATERIALS & METHODS

Specimens

The outgroup species, *Joubiniteuthis portieri,* was included in both individual gene trees and the combined phylogeny. This outgroup species was chosen following Young et al. (2008) because it is a member of the chiroteuthid group of families, to which the Mastigoteuthidae and the Chiroteuthidae also belong, but it is more distantly related than these to each other. In addition, species representing both the Mastigoteuthidae and the Chiroteuthidae were included to verify that the current morphological divisions between the families were supported molecularly. This was necessary because historically, species have been occasionally described or placed in the incorrect family. This is especially important for *Asperoteuthis nesisi*, which has been described from a single adult specimen lacking tentacles (Arkhipkin & Laptikhovsky, 2008) and shares many morphological characters with mastigoteuthids.

Four specimens of the species *I. cordiformis*, nine of *Mt. psychrophila*, one of *Mg.* sp. nov., and one of *Chiroteuthis cf. mega* were obtained during sampling efforts around New Zealand (Table 14); tissue samples were preserved in 100% EtOH prior to analysis. A further 16 tissue samples were obtained from the Smithsonian National Museum of National History (USNM), representing the species *Mt. agassizii*, *Mp. hjorti*, *E. atlantica*, and *Mg. magna*. These had been stored in 95% EtOH. Additional sequences were obtained from GenBank in the interest of presenting the most complete analysis possible. This material included additional sequences for *Mt. agassizii*, *Mp. hjorti*, *Mg. magna*, and *Mg. microlucens*, and the chiroteuthid squids *A. nesisi*, *C. veranyi*, *C. mega*, and *C. calyx* (fresh material was limited or not available for these species—see Table 14). The sequences for the outgroup species, *J. portieri*, were also obtained from GenBank.

Table 14—Specimen information for sequences used in this study (generic affiliations are those suggested by genetic information herein). Specimens sequenced in this study have BOLD ID numbers.

Species	Specimen ID	BOLD ID	GenBank number:			Reference
			COI	16S rRNA	12S rRNA	
Mastigoteuthidae						
Mastigoteuthis						
Mt. agassizii	USNM 1191203	MPMTG006-12	KC860965	KC860996	KC861182	Present study
Mt. agassizii	USNM 1191206	MPMTG009-12	KC860966	KC860997	KC861183	Present study
Mt. agassizii	USNM 1191208	MPMTG011-12	KC860967	KC860998	KC861184	Present study
Mt. agassizii	USNM 1191209	MPMTG012-12	KC860968	KC860999	KC861185	Present study
Mt. agassizii	USNM 1191207	MPMTG010-12	KC860969	KC861000	KC861186	Present study
Mt. agassizii	DE0409 (Stat. 12)		EU201162	EU201151	EU2001140	Young et al. 2008
Mt. agassizii	M8, DE0409 (Stat. 12)			EU201157	EU201146	Young et al. 2008
Mt. agassizii	USNM 1191205	MPMTG008-12	KC860980	KC861007	KC861193	Present study
Mt. agassizii	USNM 1191204	MPMTG007-12	KC860981	KC861008	KC861194	Present study
Mt. psychrophila	NIWA 44302_1	MPMTG031-12	KC860971			Present study
Mt. psychrophila	NIWA 44293_1	MPMTG024-12	KC860972	KC861002	KC861188	Present study
Mt. psychrophila	NIWA 44303_1	MPMTG025-12	KC860973	KC861003	KC861189	Present study
Mt. psychrophila	NIWA 44300_1	MPMTG030-12	KC860974			Present study
Mt. psychrophila	BAY312.1_1	MPMTG032-12	KC860975			Present study
Mt. psychrophila	NIWA 44301.2_1	MPMTG026-12	KC860976	KC861004	KC861190	Present study
Mt. psychrophila	NIWA 44301.3_1	MPMTG027-12	KC860977	KC861005	KC861191	Present study
Mt. psychrophila	NIWA 44304_1	MPMTG028-12	KC860978	KC861006	KC861192	Present study
Mt. psychrophila	239MPS_1	MPMTG029-12	KC860979			Present study
Idioteuthis						
I. cordiformis	NMNZ M.306356	MPMTG018-12	KC860952	KC860983	KC861169	Present study
I. cordiformis	NIWA 84390	MPMTG023-12	KC860953	KC860984	KC861170	Present study
I. cordiformis	NMNZ M.306358	MPMTG019-12	KC860954	KC860985	KC861171	Present study
I. cordiformis	NMNZ M.306355	MPMTG017-12	KC860955	KC860986	KC861172	Present study
Mastigopsis						
Mp. hjorti	USNM 1191213	MPMTG013-12	KC860956	KC860987	KC861173	Present study
Mp. hjorti	USNM 1191201	MPMTG004-12	KC860957	KC860988	KC861174	Present study
Mp. hjorti	USNM 1191202	MPMTG005-12	KC860958	KC860989	KC861175	Present study
Mp. hjorti	USNM 1191215	MPMTG015-12	KC860959	KC860990	KC861176	Present study
Mp. hjorti	USNM 1191214	MPMTG014-12	KC860960	KC860991	KC861177	Present study
Mp. hjorti	DE0506 (Stat.5)		EU201169	EU201159	EU201148	Young et al. 2008
Mp. hjorti	DE0304 (Stat.14)		EU201170	EU201160	EU201149	Young et al. 2008
Echinoteuthis						
E. atlantica	USNM 1191216	MPMTG016-12	KC860970	KC861001	KC861187	Present study
Magnoteuthis						
Mg. magna	USNM 1191200	MPMTG003-12	KC860961	KC860992	KC861178	Present study
Mg. magna	USNM 1191199	MPMTG002-12	KC860962	KC860993	KC861179	Present study
Mg. magna	USNM 1191198	MPMTG001-12	KC860963	KC860994	KC861180	Present study
Mg. magna	DE0506 (Stat. 1)		EU201164	EU201156	EU201145	Young et al. 2008
Mg. magna	DE0506 (Stat. 19)		EU201168	EU201155	EU201144	Young et al. 2008

Table 14 (continued)

Species	Specimen ID	BOLD ID	GenBank number:			Reference
			COI	16S rRNA	12S rRNA	
Mg. magna	Mar-Eco (44:369)		EU201167	EU201152	EU201141	Young et al. 2008
Mg. microlucens	Keahole Pt., Hawaii		EU21163	EU21153	EU21142	Young et al. 2008
Mg. sp.nov.	NIWA 76653	MPMTG021-12	KC860964	KC860995	KC861181	Present study
Chiroteuthidae						
Chiroteuthis						
C. cf. mega	NIWA 76669	MPMTG022-12	KC860951	KC860982	KC861168	Present study
C. mega			EU735362	EU735225		Lindgren, 2010
C. calyx			EU735372	EU735237		Lindgren, 2010
C. veranyi			EU735383	EU735246		Lindgren, 2010
Asperoteuthis						
A. nesisi			EU421718	EU421719	EU421720	Arkhipkin & Latikhovsky, 2008
Joubiniteuthidae						
Joubiniteuthis						
J. portieri	DE0304 (Stat. 14)		EU201163	EU201153	EU201142	Young et al., 2008

Table 15—Primer sequences for each gene region and reaction profiles for the PCR.

Gene region	Primer pair	Primer sequence (5′ to 3′)	Reaction profiles
16S rRNA	16Sar (Simon et al. 1994)	CGCCTGTTTATCAAAAACAT	Hot start of 94°C for 2 min; 35 cycles of 94°C for 30s, 52°C for 40s, 72°C for 1 min; extension of 72°C for 10min, hold 4°C indefinitely.
	16Sb (Xiong & Kocher, 1991)	CTCCGGTTTGAACTCAGATCA	
12S rRNA	12Sai (Simon et al. 1994)	AAACTAGGATTAGATACCCTATTAT	Hot start of 94°C for 2min; 35 cycles of 94°C for 30s, 52°C for 40s, 72°C for 1 min; extension of 72°C for 10min, hold 4°C indefinitely.
	12Sbi (Simon et al. 1994)	AAGAGCGACGGGCGATGTGT	
COI (DNA barcode)	LCO1490_CephF	TTTCAACAAATCATAAAGATATTGG	Hot start of 94°C for 1 min; 5 cycles of 94°C for 40s, 45°C for 40s, 72 for 1min; 35 cycles of 94°C for 40s, 51°C for 40s, 72°C for 1min; extension at 72°C for 5 min, hold 4°C indefinitely.
	HCO2198_CephR (modified from Folmer et al., 1994)	ACTTCTGGGTGACCAAAAAATCA	

DNA extraction and sequencing

DNA was extracted using a glass-fibre extraction technique (Ivanova, deWaard, & Hebert, 2006) or Xytogen Animal Extraction Kit (Xytogen, Perth, Australia), following manufacturer's instructions, except that ethanol was evaporated from the tissue prior to extraction rather than rinsing with water. DNA extracted using Xytogen was diluted with ddH_2O to 1:10 and 1:20 before use in PCR. Three mitochondrial gene regions (COI, 16S rRNA, and 12S rRNA) were amplified using the primers and reaction profiles listed in Table 15. The 652 bp DNA-barcode region of COI (Hebert et al. 2003) was amplified using primers modified slightly from universal invertebrate primers (Folmer et al., 1994) to be cephalopod specific based on whole mitochondrial sequences downloaded from GenBank. PCR amplification was carried out in 12.5µl reaction volumes with 6.25µl 10% trehalose, 2µl ddH_2O, 1.25µl 10X buffer, 0.625µl $MgCl_2$ (50mM), 0.1µl forward primer (10µm), 0.1µl reverse primer (10µm), 0.0625µl 10mM dNTPs, 0.06µl Platinum Taq polymerase (5U/µl), and 2µl of DNA. PCR products were visualised using 2% Agarose E-gels (Invitrogen). Sequencing reactions for PCR products used BigDye v3.1. PCR products were bidirectionally sequenced using an ABI 3730 DNA Analyzer (Applied Biosystems). Bi-directional sequence contig assemblies were created and edited using Sequencher v. 4.9 (Gene Codes) and multiple sequence alignments were generated manually using BioEdit v. 7.0.5.3 (Hall, 1999). Sequences were uploaded to the Barcode of Life Data System (BOLD; Ratnasingham & Hebert, 2007) public project titled 'Molecular Phylogeny of Mastigoteuthidae' (project code: MPMTG) (Table 14) and subsequently submitted to GenBank via BOLD.

Phylogenetic analysis

To test the ability of 16S rRNA, 12S rRNA and COI to separate morphologically hypothesised species, maximum-likelihood phylogenies were constructed separately for each gene. The sequences were run through FINDMODEL (Tao et al., 2005) under the Akaike information criterion (AIC); the general time-reversible model (GTR) was determined to be the best model for COI and Tamura–Nei (TN) was the best model for16S rRNA and 12S rRNA. Phylogenies were constructed using PhyML (Guindon & Gascuel, 2003) as implemented in Geneious Pro 5.1.7 (Biomatters). Edited sequences were aligned using ClustalW (Thompson et al., 1994) in Geneious.

A combined phylogeny from all three mitochondrial loci was created for mastigoteuthid sequences as well as representatives from two genera in Chiroteuthidae, a closely related family, with *Joubiniteuthis portieri* as the outgroup. Bayesian MCMC phylogenetic analyses were performed in BEAST 1.7.3 (Drummond et al., 2012). A stepping-stone analysis (Xie et al., 2011) was performed to determine whether data should be partitioned into protein-coding and rRNA genes, for which different substitution models and clock models could vary. Stepping-stone analyses produce estimated marginal likelihoods that are penalised for model complexity and can be directly compared (Baele et al., 2012). The partitioned model (marginal likelihood = -5828.4) was preferred to the unpartitioned model (marginal likelihood = (-6068.8) and was selected for the remaining analysis. For the two partitions, Bayes factors were calculated in Tracer 1.5 to determine optimal substitution and clock models, and the tree prior. For the protein-coding partition, the SRD06 substitution model (Shapiro et al., 2006) was selected, which applies a HKY+Γ model to the first and second codon position, and a separate HKY+Γ model to the third codon position. The rRNA partition used a HKY+I+ Γ model. Both data partitions used uncorrelated exponential clocks and assumed a birth–death tree prior. Three independent runs of 10,000,000 iterations were performed, with the first 1,000,000 iterations removed as burn-in. The runs were inspected for convergence and then concatenated in LogCombiner 1.7.3. The maximum clade credibility tree was then selected from the combined output in TreeAnnotator 1.7.3.

The effectiveness of DNA barcodes for separating species was assessed using the Barcode Index Number (BIN) system, which algorithmically forms clusters of barcode sequences that can be used to document taxonomic diversity (Ratnasingham & Hebert, 2013). The barcode gap, which is the smallest interspecific distance (Meier, Zhang, & Ali, 2008), was calculated for the four species of Mastigoteuthidae that had multiple representatives (*Mt. agassizii, I. cordiformis*, *Mp. hjorti*, and *Mg. magna*). Intraspecific differences could not be calculated for species that were only represented by one individual (*Mt. psychrophila*, *E. atlantica, Mg. microlucens*, and *Mg.* sp. nov.). The barcode gap and the average intra- and interspecific distances were calculated from aligned sequences using the K2P model (Kimura, 1980) in MEGA 5.05 (Tamura et al., 2011).

RESULTS

Sequences were successfully recovered from all 31 specimens for COI. For *Mt. psychrophila*, only one bidirectional sequence could be obtained; even after three attempts, the reverse direction of COI could only be recovered from one specimen out of nine. Therefore, only the COI sequence for this specimen was included in the analysis. COI sequences ranged from 560 bp to 658 bp and did not contain stop codons or indels. For 16S rRNA and 12S rRNA, a maximum of five individuals per species were attempted; therefore, 27 individuals were sequenced, all successfully. 16S rRNA and 12S rRNA sequences included indels and ranged from 509 to 518 bp, and 403 to 406 bp, respectively. The GC content was higher in COI compared to 16S rRNA and 12S rRNA (Table 16).

All species where multiple individuals were sequenced (*Mt. agassizii, I. cordiformis*, *Mp. hjorti,* and *Mg. magna*) formed distinct species clusters on the maximum-likelihood trees (Figs 52–54). The four species represented by single individuals (*Mt. psychrophila*, *E. atlantica*, *Mg. microlucens*, and *Mg.* sp. nov.) were also well separated from all other species. Species from the same genus consistently grouped together where more than one species were represented (*Mastigoteuthis*, *Magnoteuthis*) and separate from the other genera where there was only one representative species (*Idioteuthis*, *Echinoteuthis*, *Mastigopsis*) for each of the individual gene trees (Figs 52–54), as well as the consensus tree (Fig. 55). The three species in *Magnoteuthis* (*Mg. magna*, *Mg. microlucens*, and *Mg. sp. nov.*) grouped together, including an apparently new species of *Magnoteuthis* (‘*Mg*. sp. nov.’). This individual grouped together with the two most morphologically similar species in the *magna* group; however, it was genetically distinct from both *Mg. magna* and *Mg. microlucens* at all three loci. The combined phylogeny showed a posterior probability of 1 for the division between *Mastigoteuthis* and *Echinoteuthis*, and 0.98 for *Magnoteuthis* and *Mastigopsis*. The remaining species, *I. cordiformis*, grouped separately from other mastigoteuthids in the COI and 12S rRNA maximum-likelihood trees. Additionally, in the combined phylogeny, *I. cordiformis* grouped separately from other mastigoteuthids, as a sister group to *Asperoteuthis* and *Chiroteuthis,* with a posterior probability of 0.75. The minimum genetic distances between the proposed genera for the Mastigoteuthidae (mean 9.1%) were larger than the distance found between *Asperoteuthis* and

Table 16—Sequence composition of three mitochondrial genes for Mastigoteuthidae. Percentage of each nitrogenous base in COI, 16S rRNA, and 12S rRNA based on the sequences of 27 individuals for seven species of Mastigoteuthidae based on the sequences generated for this study.

Base	COI	16S rRNA	12S rRNA
G %	16.61	18.95	17.99
C %	22	10.22	8.71
A %	28.1	33.2	31.21
T %	33.14	37.62	42.08

Table 17—Estimates of evolutionary divergence between COI sequences. Eight mastigoteuthid species are included in this analysis. Intra-Sp stands for intraspecific divergence; NN is the nearest sequence of another species. Analyses were conducted using K2P parameters and included all codon positions. Positions containing missing data or gaps were eliminated.

Species	Mean Intra-Sp	Max Intra-Sp	Nearest Species	Distance to NN
I. cordiformis	0	0	*Mg. magna*	15.03
Mg. magna	0	0	*Mg.* sp. nov.	9.94
Mg. microlucens	N/A	N/A	*Mg.* sp. nov.	9.90
Mg. sp. nov.	N/A	N/A	*Mg. microlucens*	9.90
Mp. hjorti	0.37	0.77	*Mt. psychrophila*	11.88
Mt. agassizii	0.29	0.61	*Mt. psychrophila*	6.93
Mt. psychrophila	N/A	N/A	*Mt. agassizii*	6.93
E. atlantica	N/A	N/A	*Mt. psychrophila*	10.97

Table 18—Intra- and interspecific percent divergences for COI, 16S rRNA, and 12S rRNA, for eight species of Mastigoteuthidae.

Distance		COI	16S rRNA	12S rRNA
Intraspecific				
	Mean	0.12	0.04	0.10
	Min	0	0	0.00
	Max	0.37	0.14	0.20
Interspecific				
	Mean	13.67	5.19	5.72
	Min	6.93	2.23	2.37
	Max	17.16	8.02	8.31

Table 19—Minimum intergeneric percent divergences for COI, 16S rRNA, and 12S rRNA combined, for five genera of Mastigoteuthidae.

Genus	*Mastigoteuthis*	*Idioteuthis*	*Mastigopsis*	*Echinoteuthis*
Magnoteuthis	8.5	8.8	7.7	9.0
Echinoteuthis	8.3	10.5	8.7	–
Mastigopsis	9.2	9.7	–	–
Idioteuthis	10.1	–	–	–

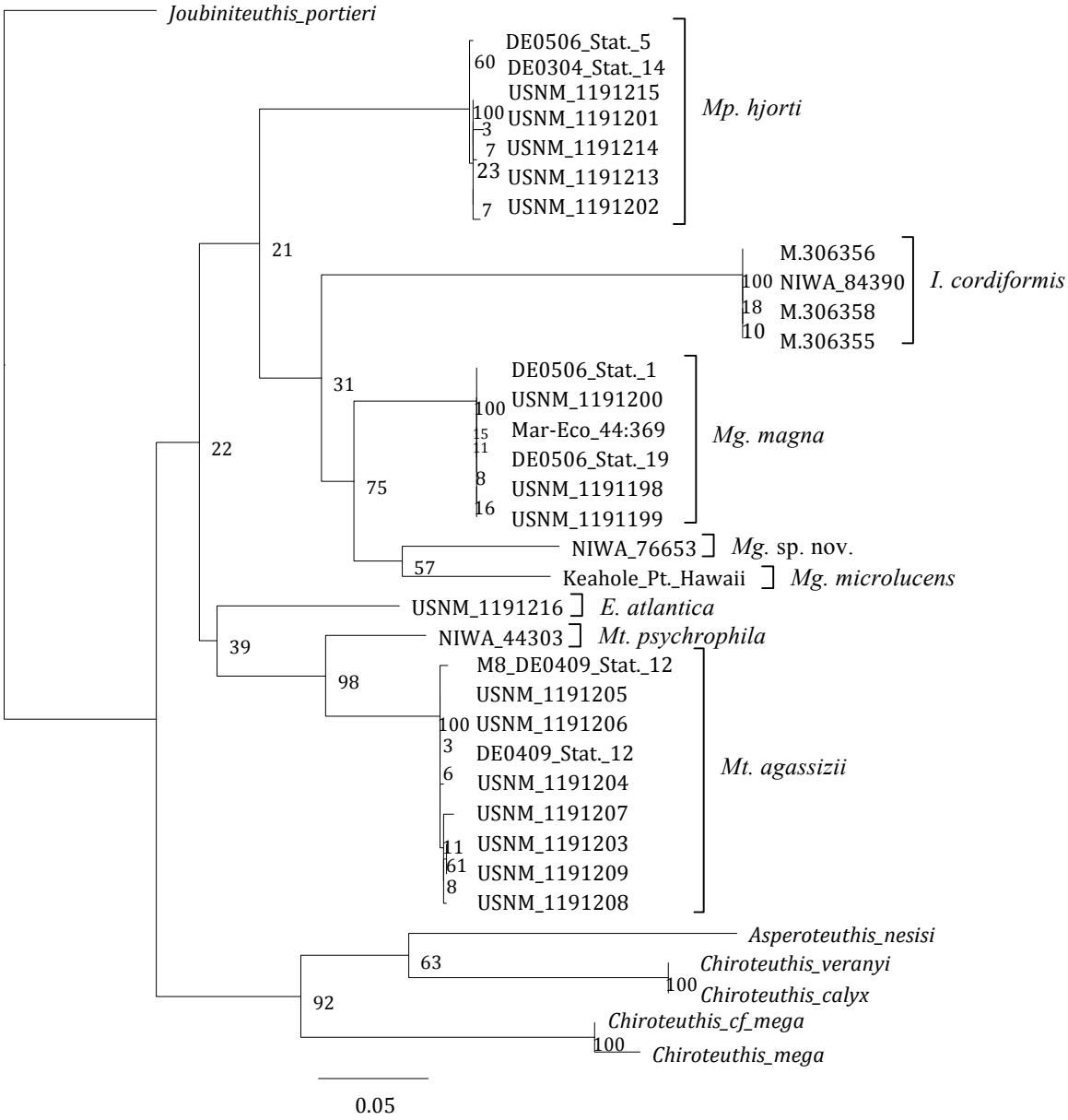

Fig. 52—Maximum-likelihood tree for Mastigoteuthidae based on COI sequences with GTR for eight mastigoteuthid species. Sample names correspond to Table 14; bootstrap support values are based on 100 replicates.

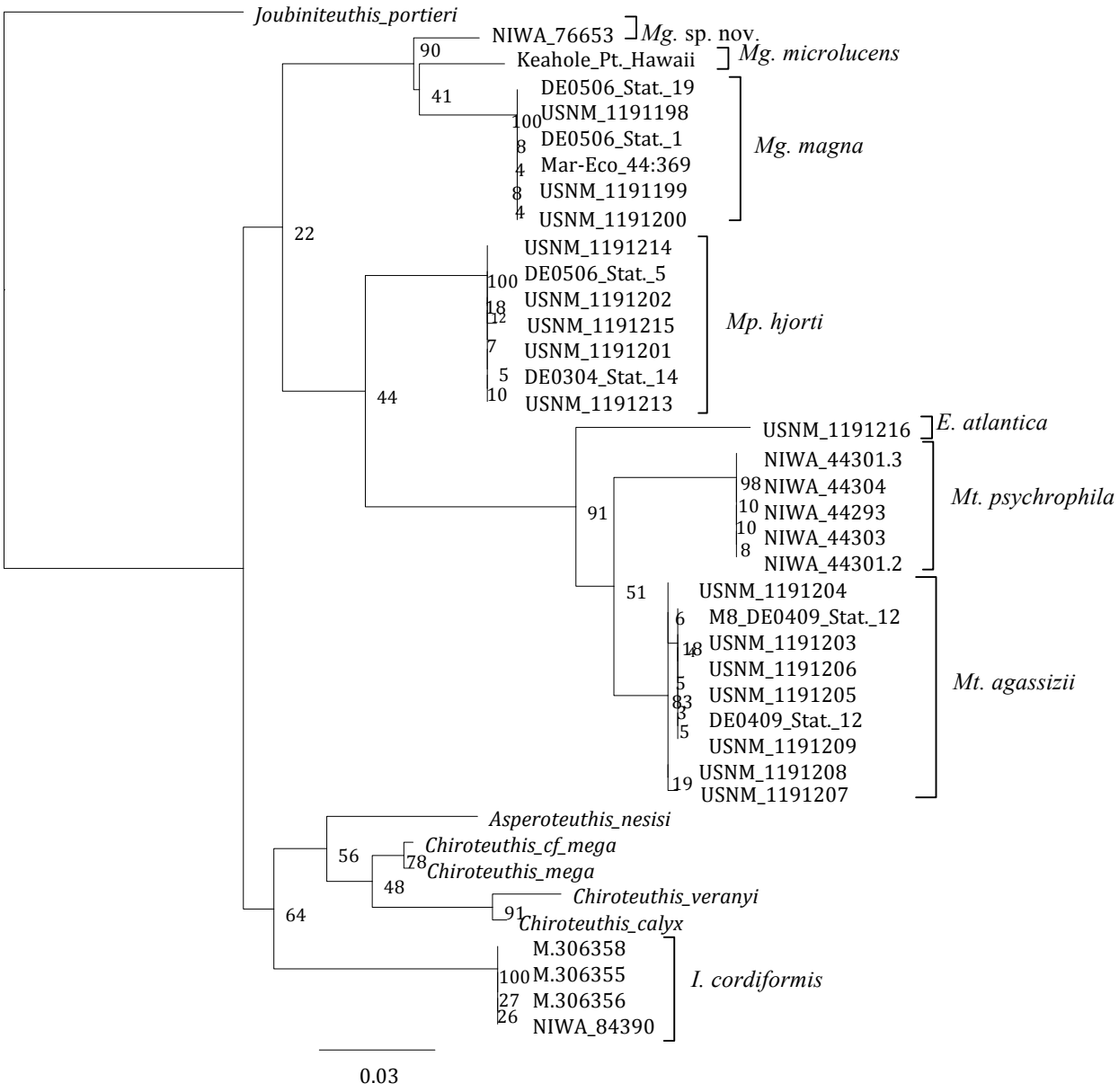

Fig. 53—Maximum-likelihood tree for Mastigoteuthidae based on 16S rRNA sequences with TN93 for eight species. Sample names correspond to Table 14; bootstrap support values are based on 100 replicates.

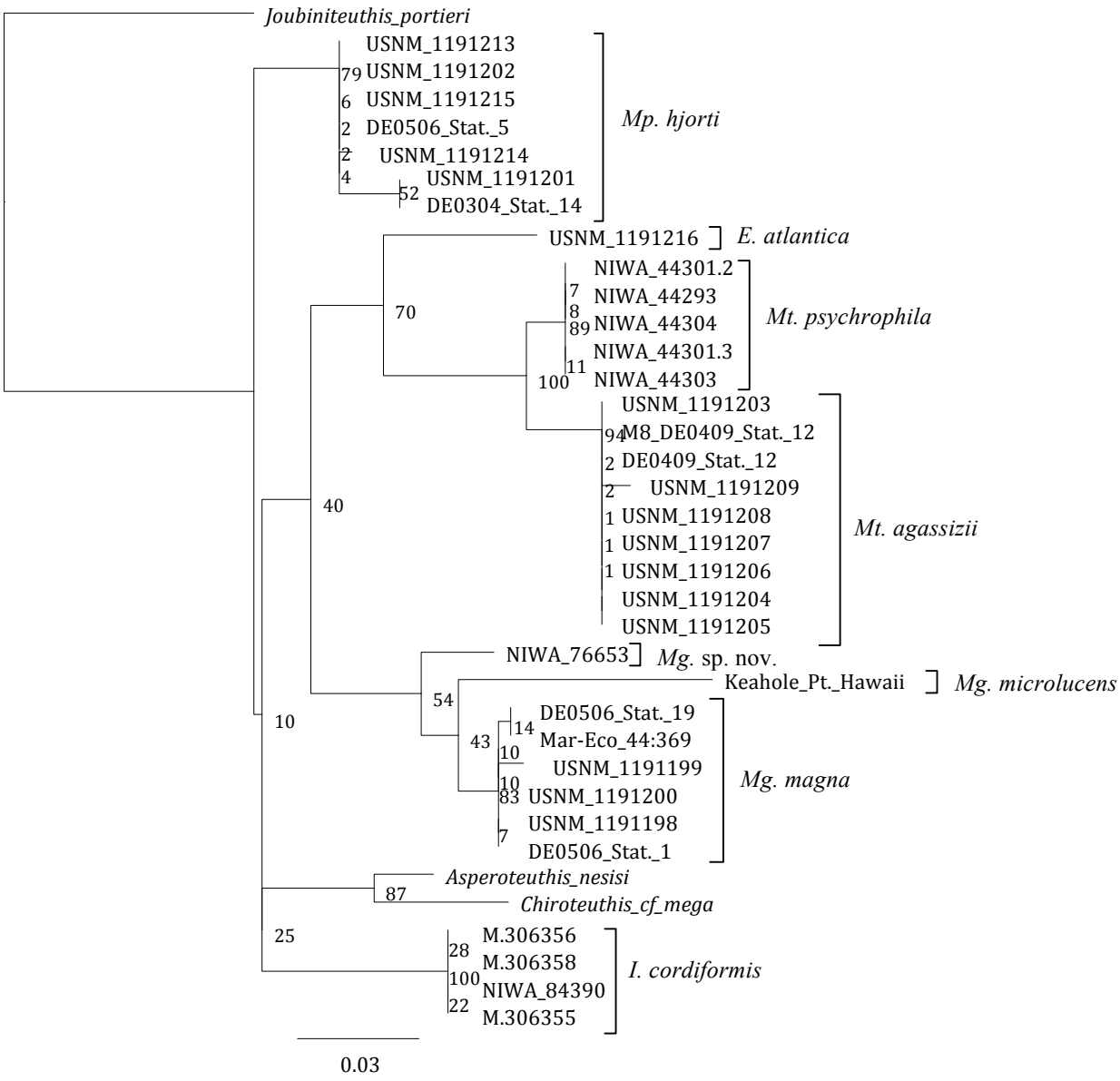

Fig. 54—Maximum-likelihood tree for Mastigoteuthidae based on 12S rRNA sequences with TN93 for eight species. Sample names correspond to Table 14; bootstrap support values are based on 100 replicates.

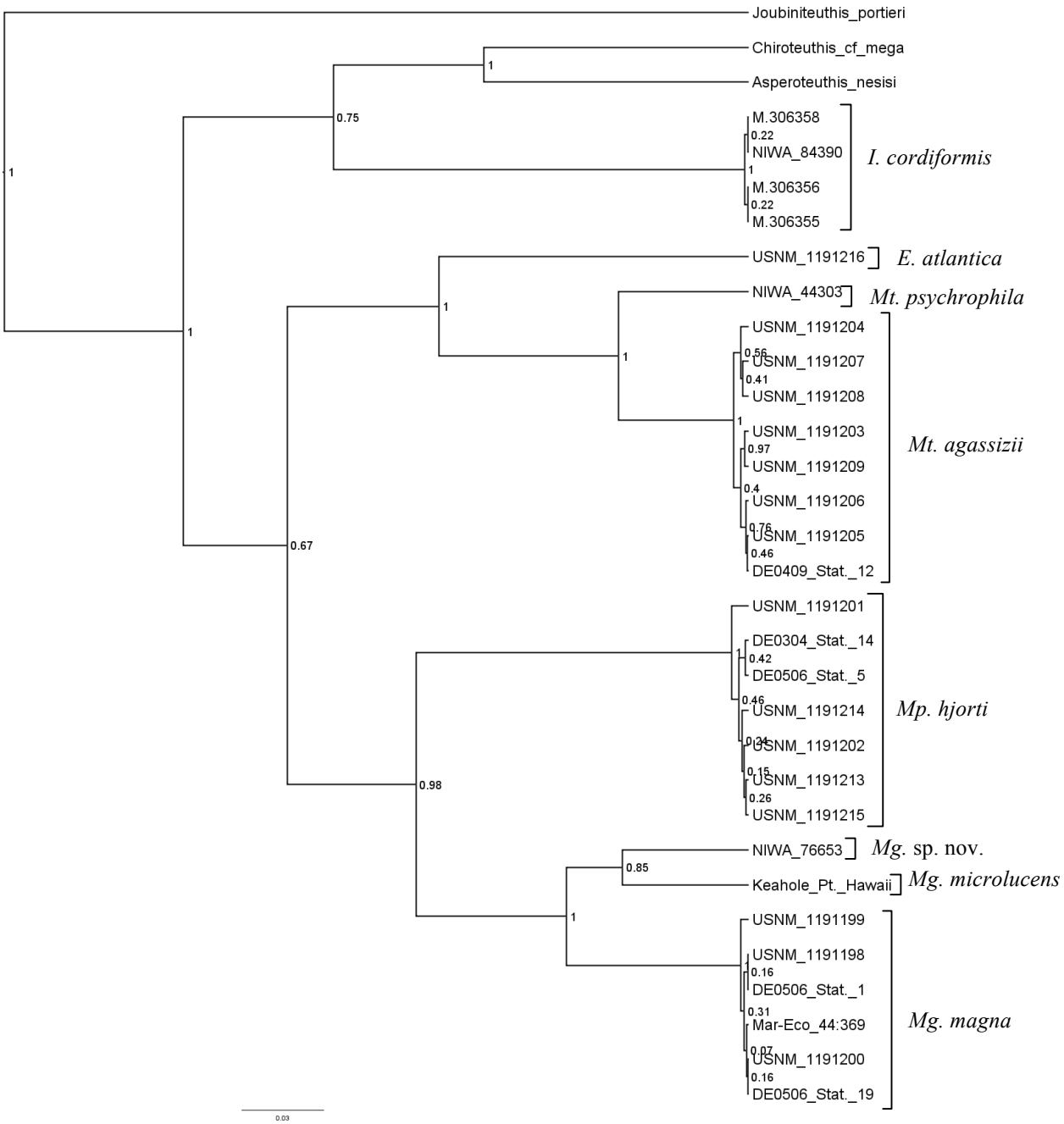

Fig. 55—Bayesian MCMC phylogenetic analysis for Mastigoteuthidae based on COI, 16S rRNA, and 12S rRNA. Sample names correspond to Table 14; values beside internal nodes are posterior probabilities.

Chiroteuthis (7.9%), the only exception was the distance between *Mastigopsis* and *Magnoteuthis* (7.7%) (Table 19).

Barcode Index Numbers (BINs) were assigned to all barcode clusters generated in this study using a spectral clustering method implemented in BOLD 3.0 (Ratnasingham & Hebert, 2013). The resulting BIN clusters corresponded to morphological species and were supported by the species groupings for COI on the maximum-likelihood trees. Three singleton sequences were identified by the BIN analysis for *E. atlantica, Mg. microlucens*, and *Mg*. sp. nov., which also formed branches that were separate from all other species in the maximum-likelihood trees. Divergences within and between species, as well as the distance to the nearest neighbour for COI, were determined for the eight mastigoteuthid species examined (Table 17). The barcode gap analysis revealed that the highest intraspecific divergence within COI was 0.77%, found in *Mp. hjorti*, and the lowest interspecific divergence was 6.93%, between *Mt. psychrophila* and *Mt. agassizii.* The mean intra- and interspecific divergences were calculated for all three genes (Table 18). COI has the highest mean interspecific divergence (13.67%) compared to 16S rRNA (5.19%) and 12S rRNA (5.72%). For all three loci, the maximum intraspecific divergences are smaller than the minimum interspecific divergences. DNA barcodes had marginally higher mean intraspecific divergence than 16S rRNA and 12S rRNA; however, COI mean interspecific divergences were more than twice those of the other two loci.

DISCUSSION

Herein, the morphological recognition of the five genera in the Mastigoteuthidae (*Mastigoteuthis, Idioteuthis, Mastigopsis, Echinoteuthis,* and *Magnoteuthis*) from Chapter 2 is strongly supported by the partitioned Bayesian phylogeny created using COI, 16S rRNA and 12S rRNA (posterior probabilities of 0.98–1; Fig. 55). Members from two well-established genera from the closely related family Chiroteuthidae were included in this phylogeny to ensure that these loci were appropriate for showing divisions in genera. Consistent with the generic subdivision of Mastigoteuthidae proposed here, there was mostly greater sequence divergence between each genus proposed for the Mastigoteuthidae than between *Asperoteuthis* and *Chiroteuthis*; (7.7–*9.1*–10.5% and 7.9% respectively). Although the use of subgenera have been proposed

for this family, due to the great genetic divergence and distinct morphological characters, previously used subgenera appear to require full genus status. In the combined phylogeny, *I. cordiformis* formed a sister taxon to the chiroteuthid outgroups; however, morphological analysis supports the current recognition of *I. cordiformis* as a mastigoteuthid.

All of the COI sequences generated in this study were free of indels and stop codons, which indicates that they were not likely to be Numts (nuclear mitochondrial DNA). Numts are mitochondrial sequences that have been translocated to the nucleus, and could be found when amplifying any mitochondrial gene (Song et al., 2008; Buhay, 2009), possibly affecting DNA barcoding (Buhay, 2009). However, it is easier to identify Numts from coding genes, like COI; BOLD sequences containing stop codons are flagged, and indels can be identified when the sequences are aligned manually. Both stop codons and indels may be present in non-coding genes like 16S rRNA and 12S rRNA, making Numts more difficult to identify, which makes the DNA barcode region more reliable.

The maximum intraspecific divergences for all three loci were lower than the minimum interspecific divergences. This indicates that COI, 16S rRNA, and 12S rRNA can all be used to separate species in the family Mastigoteuthidae. The barcode gap was found in the present study; the smallest distance between two individuals of different species was 6.93%, while there was low intraspecific variation (highest divergence of 0.77%). BIN numbers have shown a high congruence with species delimitation (Ratnasingham & Hebert, 2013), which is consistent with the present results; morphological species delimitations were supported by the BIN clusters and species groupings found for all three mitochondrial loci. The BIN system, and the maximum-likelihood trees for all three genes, also supported the recognition of a new species, *Mg.* sp. nov. that has been consistently misidentified as the morphologically similar species *Mg. magna*. Similarly, Rosso et al. (2012) found that BIN clusters aided in the discrimination of cryptic species of Neotropical fishes.

DNA barcoding of cephalopods has raised several concerns (Strugnell & Lindgren, 2007); for example, mitochondrial DNA evolves faster than nuclear DNA and may 'oversplit' species. However, all three mitochondrial genes show low intraspecific variation and high interspecific differences. Dai et al. (2012) found that DNA barcodes

and16S rRNA could be used effectively for distinguishing 33 species of coleoid cephalopods; they also found that 16S rRNA could be used to successfully separate species, although COI was much more divergent. COI divergences between species in this study were higher than those reported by Toussiant et al. (2012), who found that two clades of giant Pacific octopus, *Enteroctopus dofleini*, had interspecific differences of 3–4% for COI. In contrast, Allcock et al. (2011) found overlap between the amount of intra- and interspecific variation in octopuses of the genus *Pareledone*; however, it appears that there is recent speciation in this genus and that *P. aequipapillae* may be a ring species.

Within the boreal specimens of *Mt. agassizii*, a form with thicker skin has been recognised (Vecchione & Young, 2007b); however, this trait has not been quantified. One specimen identified as having 'thick skin' was included in this study (USNM 1191205), but appears to be genetically identical with other boreal specimens of *Mt. agassizii* that had typical skin thickness (Figs 52–55). It is possible that the variation in skin thickness is due to phenotypic plasticity and influenced by environmental conditions. Environmentally influenced phenotypic plasticity has been found to be the main cause of population variability in cephalopods that exhibit low levels of genetic diversity (Boyle & Boletzky, 1996).

DNA barcoding has been successfully used for identifying cryptic cephalopod species (Allcock et al., 2011), and more specifically to identify squid species that are morphologically similar (Sin, 2009). Genetically, three species of *Magnoteuthis* sequenced herein (*Mg. magna, Mg. microlucens* and *Mg.* sp. nov.) show high divergences between species for COI (9.90–9.94%), 16S rRNA (2.8–2.3%), and 12S rRNA (2.3–2.7%), while *Mg. magna* shows low intraspecific variation (0%, 0%, and 0.25% respectively). These species all share the same flask-shaped funnel-locking cartilage, largest arm suckers in the middle of the arms, and microscopic tentacular suckers. The species *Mg. magna* occupies the North and South Atlantic (Vecchione & Young, 2010a); *Mg. microlucens* appears restricted to the North Pacific, south of Hawaii (Young et al., 2008); and *Mg.* sp. nov. is currently known only from nine New Zealand specimens, with only one available for sequencing in this study. The distinguishing feature of *Mg. microlucens* is the microscopic photophores in the skin (Young et al., 2008). The most distinctive feature of *Mg.* sp. nov. is that the largest suckers—which are twice as large as the largest suckers on other arms—are located

distally on Arms II, while in *Mg. magna* the largest suckers are on Arms IV (Vecchione & Young, 2010a). The dentition of the arm suckers in these three species also differs: *Mg. microlucens* has blunt teeth, *Mg. magna* is adentate, and *Mg.* sp. nov. has intermediate dentition with indistinct blunt teeth. It now appears that three morphologically similar species occupy different geographic regions and can also be separated by COI, 16S rRNA, and 12S rRNA.

CHAPTER 4: Preliminary attempts to extract DNA from formalin-fixed museum squid specimens

INTRODUCTION

Museum collections hold specimens that are essential to taxonomy. Unfortunately, most museum specimens are formalin-fixed and preserved in ethanol, which makes DNA extraction difficult or impossible (Tang, 2006). Different protocols have been devised for amplifying DNA from museum specimens, such as Fang, Wan, and Fujihara (2002) who combined gradual dehydration and critical-point drying to successfully amplify high-molecular-weight DNA from formalin-fixed vertebrate tissues. In addition, mitochondrial DNA has been amplified from museum specimens of octopus (Söller et al., 2000) and squid (Carlini, Kunkle, & Vecchione, 2006). However, there are still many challenges to overcome with formalin-fixed tissue, and failed attempts are not reported in the literature (Tang, 2006).

The Barcode of Life Data System (BOLD) is a public compilation of DNA barcodes (Ratnasingham & Hebert, 2004). BOLD contains several databases that can be used to identify unknown specimens (Ratnasingham & Hebert, 2004). Recently, the Barcode Index Number (BIN) System has been introduced, which groups together genetically similar individuals (Ratnasingham & Hebert, 2013). For taxonomy, DNA barcodes can be used to help separate species (Hebert & Gregory, 2005), and have been successful in delimitating cephalopod species (Allcock et al., 2011; Dai et al. 2012; Zheng et al., 2012). In addition, DNA barcodes can be used to identify juveniles (Victor et al., 2009) and badly damaged specimens (St-Onge et al., 2008). With the great potential for museum material to extend BOLD, DNA barcoding of formalin-fixed museum specimens has been previously attempted with limited success (Zhang, 2010).

During this review of the Mastigoteuthidae found around New Zealand, it became apparent that integrative taxonomy is necessary for working on a group represented mostly by badly damaged specimens. Therefore, some preliminary tests were conducted on the DNA extraction of formalin-fixed squid tissue. Three mitochondrial genes were chosen (COI, 16S rRNA, and 12S rRNA). Several steps were included in attempts to amplify DNA from formalin-fixed tissue: 1) critical-point drying of tissue prior to extraction; 2) two different DNA extraction protocols: alkaline lysis and a silica-gel column-based extraction; and 3) DNA purification to eliminate PCR inhibitors.

MATERIALS & METHODS

Samples

Due to limited material and time constraints, the same individuals were not used for all tests, but were used in several tests when possible. Specimen details are available in Table 20. Mastigoteuthids were the focus of this study, but one sample of *Taningia danae* was included because tissue samples were available from pre- and post-fixation for comparison of sequences. In addition, a potentially new species of *Asperoteuthis* was included. Sequences from an ethanol-fixed specimen of *Mastigoteuthis* sp. 'X' (NIWA 86556, see Chapter 2) was included for comparison with the sequences generated from formalin-fixed material. Additional DNA sequences for the three mitochondrial genes for *Mt. agassizii* and *Mt. psychrophila* were taken from Chapter 3. Tests involved different combinations of tissue treatment, DNA extraction, and DNA purification (Table 21).

Critical-point drying

The protocol from Fang, Wan, and Fujihara (2002) was used with the following modifications. Gradual dehydration of tissue samples was accomplished through 24h at 80% EtOH, followed by 24h at 90% EtOH, and finally 100% EtOH for at least 24h prior to critical-point drying. Individual samples were folded into filter paper for critical-point drying. Samples were immersed in liquid CO_2 and washed for 3 min, then left in liquid CO_2 for 1h, and finally washed for another 3 min. Then, the temperature was increased to 34°C before the gaseous CO_2 was gradually released. DNA extraction followed immediately.

Extraction

Two methods of DNA extracted were attempted. The silica-gel column-based method used a Qiagen DNeasy Blood and Tissue Kit (Qiagen) following manufacturer's instructions, except that the elution volume was 100µl, and the eluate was re-eluted

Table 20—Collection details for formalin-fixed specimens used for DNA extraction trials. All specimens were formalin-fixed except for NIWA 86556, which was ethanol-fixed. Test number which corresponds to the tests in Table 21; buccal muscle indicates tissue taken from the buccal musculature.

Species	Specimen ID	Collection date	Additional collection data	Test	Tissue type	Sequence recovered
A. sp. nov.	N/A	no data	New Zealand, no data	**1, 3, 4**	fin	None
I. cordiformis	NIWA 71663	28/03/2000	37.24°S, 177.23°E, 800m, Stn Z10079	**1, 3, 4**	fin	None
I. cordiformis	NIWA 71668	no data	New Zealand, no data	**1**	ovary	None
Mp. hjorti	NMNZ M.172986	15/05/2003	29.53°S, 167.63°E, 200–1200m, RV *Tangaroa*, NORFANZ, Stn 23	**1**	arm	None
?Magnoteuthis	N/A	no data	From Tasmania, coll. G. Jackson	**3, 6**	buccal muscle	None
Mt. dentata	CH-LIA-01	no data	No data	**1, 6**	buccal muscle	12S rRNA
Mt. dentata	NIWA 75806	28/11/2011	44.8°S, 173.9°E, 899–973m, bottom trawl, TRIP3415/31	**6**	arm	16S rRNA
Mt. dentata	NMNZ M.172944	30/05/2003	32.61°S, 167.84°E, 1303–1313m, RV *Tangaroa*, NORFANZ Stn 120	**5**	buccal muscle	None
Mt. dentata	NMNZ M.287214	24/10/1988	41.22°S, 176.70°E, 918–970m, RV *James Cook*, Stn J12/56/88	**5**	buccal muscle	None
Mt. dentata	NMNZ M.172936	24/05/2003	32.07°S, 159.88°E, 1920–1934m, RV *Tangaroa*, NORFANZ Stn 71	**5**	buccal muscle	None
Mt. sp. ?	NMNZ M.091609	9/12/1985	44.43°S, 178.03°E, 1185m, RV *James Cook*, Stn J21/05/85	**1**	arm	None
Mt. sp. X	NMNZ M.100817	19/09/1989	39.97°S, 177.92°E, 1105–1110m, RV *James Cook*, Stn J09/29/89	**1, 6**	buccal muscle	COI
Mt. sp. X	NIWA 48864	30/06/1993	39.46°S, 178.37°E, 883m, MWT, TAN9306/181	**1**	buccal muscle	None
Mt. sp. X	NMNZ M.172950	12/05/2003	32.54°S, 169.73°E, 1275m, RV *Tangaroa*, NORFANZ Stn 10	**1**	tentacle	None
Mt. sp. X	NMNZ M.94101	14/10/1988	43.05°S, 168.40°E, 1092m, FV *Arrow*, Stn A03/23/83	**1**	buccal muscle	None
Mt. sp. X	NIWA 86556	17/06/2010	42.80°S, 179.97°W, 1015–1005m, Stn TAN1008/14	**1**	Arm	COI, 12S rRNA, 16S rRNA
Mt. sp. Y	NIWA 71721	13/04/1997	44.82°S, 173.05°E, 44.82°S, 173.04°E, 1053–1052m, Stn TAN9705/3	**1, 3, 4**	arm	None
T. danae	NMNZ M.305062	31/01/2012	34.57°S, 175.27°E	**1, 2, 5**	fin	None

through the column. The alkaline-lysis method used a Xytogen Animal Extraction Kit (Xytogen, Perth, Australia) following manufacturer's instructions, except that ethanol was evaporated from the tissue prior to extraction rather than rinsing with water. DNA from the Xytogen extraction was diluted with ddH_2O to 1:10 and 1:20 before use in PCR.

DNA purification

Sodium dioxide suspension purification used the following protocol: 10µl of N-phenacylthiazolium bromide (PTB) was added to 50µl extracted DNA and incubated at room temperature for 20 min. Then 20µl frozen SiO_2 was vortexed for ~20 sec and allowed to stand for 30 sec. DNA was added to the SiO_2 solution and vortexed gently. The solution was incubated at 21°C for 30 min in a shaking incubator, then centrifuged at 6000xg for 3 min and the supertenant was discarded. The sample was washed with 200µl AW1 buffer, vortexed for 5–10 sec, until resuspended, then centrifuged at 6000xg for 3 min and the supertenant was discarded. The sample was washed with 200µl AW2, and then centrifuged at 17000xg for 5 min. The wash step with AW2 was repeated, and any remaining supertenant was removed. The sample was incubated in a heat block at 56°C for 15 min to dry the DNA pellet. The DNA was eluted with 50µl AE buffer and incubated at room temperature for 1 min, then centrifuged at 6000xg for 3 min. The supertenant, containing the DNA, was removed and centrifuged at 6000xg for 2 min.

Ethanol precipitation used the following protocol: 10µl of PTB was added to 50µl extracted DNA and incubated at room temperature for 20 min. Then, 6µl sodium acetate (pH 5.2) was added and the sample was vortexed. 175µl cold 100% EtOH was added, and incubated on ice for 20 min. The sample was centrifuged at 17000xg for 10 min. The supertenant was removed and 1ml of 70% propanol was added, and the sample vortexed. The sample was centrifuged at 6000xg for 5 min, and the supertenant was discarded. The sample was allowed to air dry and DNA was eluted with 20µl AE buffer.

Amplification

Amplification for the three mitochondrial genes (COI, 16S rRNA, and 12S rRNA) used primers and reaction profiles listed in Table 15 (Chapter 3). Internal primers for COI were designed based on mastigoteuthid COI sequences downloaded from GenBank and

Table 21—Trials used to extract DNA from formalin-fixed specimens. DNA extraction was either with alkaline lysis (Xytogen) or silica-gel column-based extraction (Qiagen) with different DNA purification protocols and tissue preparation.

DNA extraction method	**Xytogen**	**Qiagen**
	Test 1	**Test 2**
Purification	None	None
Tissue prep	None	None
Result	12S rRNA, contamination, no amplification	no amplification
	Test 3	**Test 4**
Purification	None	None
Tissue prep	Critical-point dried	Critical-point dried
Result	Contamination, no amplification	Contamination, no amplification
	Test 5	**Test 6**
Purification	EtOH precipitation	SiO_2
Tissue prep	Critical-point dried	Critical-point dried
Result	Contamination, no amplification	COI, 16S rRNA, contamination/no amplification

made to amplify COI in two overlapping halves (mCephF: 5′GAGCACCAGATATAG CATTCCCACG3′; mCephR: 5′GCTCCTCTTTCTACAGCTGA3′). PCR amplification followed protocols outlined in Chapter 3. Amplification success of PCR products was ascertained visually using 2% Agarose E-gels (Invitrogen). Successful amplification showed as a clear band on the gel. Secondary amplification was performed using the protocol above, except that 1µl of PCR product and 1µl of ddH_2O was used in place of DNA. PCR products were unidirectionally (bidirectionally for the fresh sample NIWA 86556) sequenced using BigDye v3.1 and analysed on an ABI 3730 DNA Analyzer (Applied Biosystems). Sequences were edited using Sequencher v. 4.9 (Gene Codes) and identified using the Barcode of Life Data Systems (BOLD) database and GenBank.

Phylogenies

Edited sequences were aligned using ClustalW (Thompson et al., 1994) in BioEdit. Maximum-likelihood phylogenies were constructed separately for COI, 16S rRNA, and 12S rRNA using MEGA 5.05 (Tamura et al., 2011). General time-reversible (GTR) was used for COI and Tamura–Nei (TN) was used as the model for16S rRNA and 12S rRNA. Distances were calculated using the K2P model (Kimura, 1980) in MEGA 5.05 (Tamura et al., 2011).

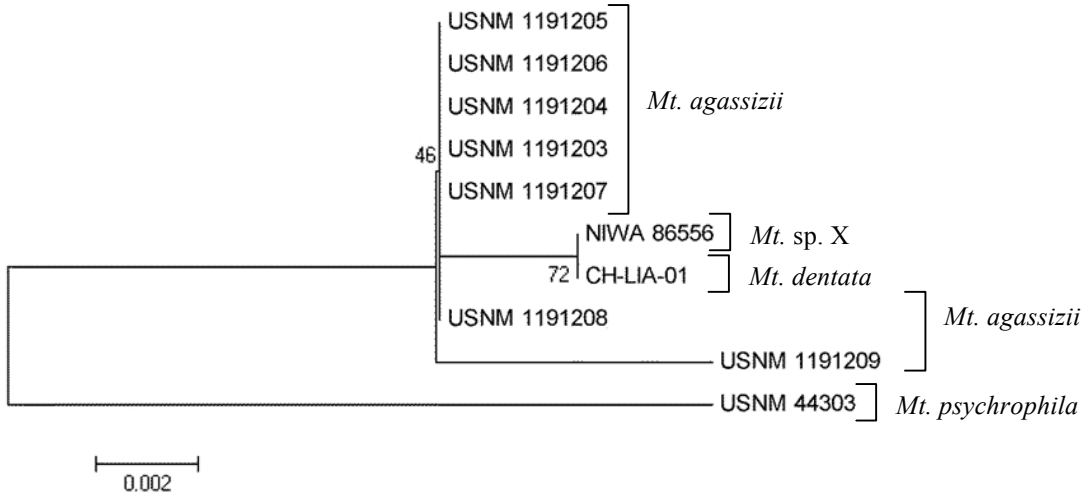

Fig. 56—Maximum-likelihood tree for four *Mastigoteuthis* species based on 12S rRNA sequences with TN. Sample names correspond to Table 20; bootstrap support values are based on 100 replicates.

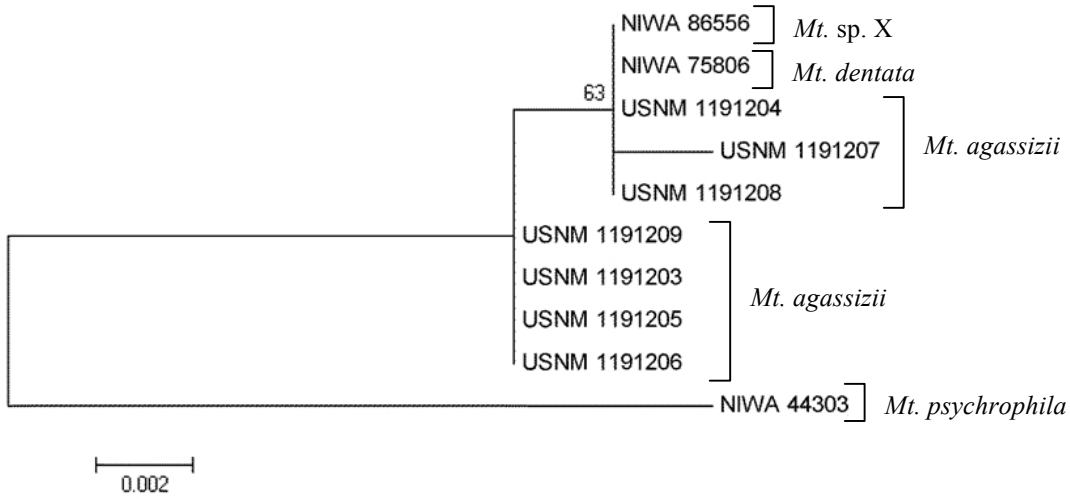

Fig. 57—Maximum-likelihood tree for four *Mastigoteuthis* species based on 16S rRNA sequences with TN. Sample names correspond to Table 20; bootstrap support values are based on 100 replicates.

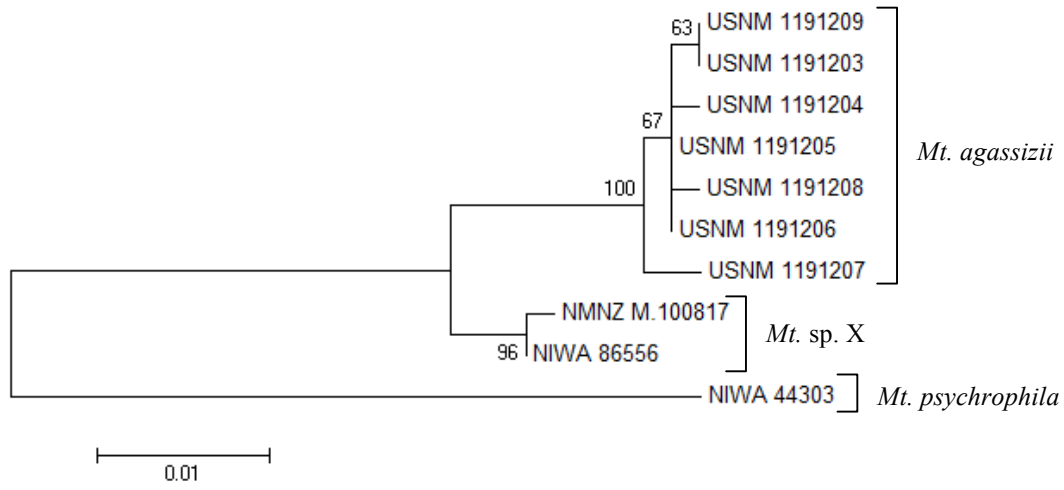

Fig. 58—Maximum-likelihood tree for three *Mastigoteuthis* species based on COI sequences with GTR. Sample names correspond to Table 20; bootstrap support values are based on 100 replicates.

RESULTS & DISCUSSION

Two sequences out of eight were recovered using a silica-gel column-based extraction, but only with critical-point-dried tissue and when combined with a DNA purification protocol. A third sequence was recovered from alkaline lysis extraction from tissue that was not critically-point dried, but this method seemed to have a very low success rate (one out of 12 samples). Critical-point drying alone is not sufficient to obtain DNA sequences; with a DNA purification step, to remove impurities and increase the DNA concentration, DNA recovery was possible. Although sequences were successfully recovered from three specimens, only one sequence was recovered from each and attempts to sequence other genes for those individuals failed. It is not clear why different genes amplified for different specimens; however, this indicates that there is the potential for other genes to be obtained from all three individuals. Tissue type may affect the success of DNA extraction (Tang, 2006), but it appears that DNA extracted from the buccal mass muscle can be successfully amplified. Buccal mass tissue is an ideal source of muscle tissue because it is removed during the extraction of beaks during morphological examination.

Internal primers were designed based on conserved regions in mastigoteuthid COI sequences, but it appears that mCephF can be used to amplify a variety of taxa, which unfortunately resulted in the amplification of contamination. The specimen that had been sequenced previously from ethanol-fixed tissue failed to amplify from the formalin-fixed tissue, so it was not possible to examine any potential DNA mutations caused by formalin within a single sample. However, Fang et al. (2002) reported that formalin-fixed rat tissue, subjected to critical-point drying prior to DNA extraction, produced sequences that were identical to those from fresh tissue.

Formalin-fixed tissue did not seem to break down during lysis, while after critical-point drying, samples lysed readily. Therefore, it seemed possible that if critical-point drying made the tissue easier to break down, then mechanical grinding might be equally effective. Vollossiouk, Robb, and Nazar (1995) found that grinding samples in liquid nitrogen was effective for cell lysis. Unfortunately, attempts to grind tissue samples herein did not produce powder effectively because the tissue still contained ethanol (data not shown). For future attempts, samples should be dried prior to grinding.

The sequences obtained from fresh and formalin-fixed tissue for 12S rRNA (Fig. 56) and 16S rRNA (Fig. 57) indicate a very close relationship between *Mt. dentata*, *Mt.* sp. X (genetically identical to *Mt. dentata*), and *Mt. agassizii* (0.27% for 12S rRNA and 0.2% for 16S rRNA). The divergences observed in these genes falls within the natural sequence variation found in *Mt. agassizii*. However, both *Mt. dentata* and *Mt.* sp. X have an insertion in 12S rRNA that separates them from *Mt. agassizii*. In addition, for COI, *Mt.* sp. X is 1.99% divergent from *Mt. agassizii* (Fig. 58). Although *Mt. dentata* and *Mt.* sp. X are both from New Zealand waters and appear to be genetically identical for 12S rRNA and 16S rRNA, they can be distinguished morphologically; *Mt. dentata* is distinguished from *Mt.* sp. X by the photophore pattern on Arms IV, funnel-locking cartilage, and beak shape. *Mt. dentata* has two main series of photophores on Arms IV, while *Mt.* sp. X has a scattered pattern proximally and two main series distally. *Mt. dentata* and *Mt.* sp. X both have ear-shaped funnel-locking cartilage, but the antitragus is stronger in *Mt.* sp. X. The lower rostrum of the *Mt.* sp. X beak forms an approximate right angle with the baseline, while the angle is smaller in *Mt. dentata*. The type locality of *Mt. dentata* is the Pacific (Hoyle, 1904), while *Mt. agassizii* was described from the Atlantic (Verrill, 1881). Currently, there are no reliable morphological characters to separate these two species (Young & Vecchione, 2007g).

Overall, it seems that critical-point drying of tissue prior to DNA extraction and DNA purification seems to assist in sequence recovery from formalin-fixed tissue. In addition, tissue sampling is a destructive process, but this can be minimised by using muscle tissue that is removed from the buccal mass during beak extraction. The DNA sequences indicate that *Mt. dentata* and *Mt.* sp. X are distinct from *Mt. agassizii*, but they are all very closely related. More genes should be investigated in future studies to determine whether there is a genetic distinction between *Mt. dentata* and *Mt.* sp. X.

CHAPTER 5: Ecology of *Idioteuthis cordiformis* (Cephalopoda, Mastigoteuthidae): Stable isotope analysis and DNA barcoding of gut contents

INTRODUCTION

The largest species in the family Mastigoteuthidae is *Idioteuthis cordiformis*; many times larger than any other species in this family, it attains more than 1m ML and 75kg (Steve O'Shea, pers. comm.). It is known from the Pacific, and has also been reported from Sumatra (Chun, 1908), Japan (Sasaki, 1929), the Philippines (Voss, 1963), and New Zealand, where it was recently listed as nationally endangered (Hitchmough et al., 2005). However, after the re-evaluation of the threat classification system, the status for *I. cordiformis* was elevated to 'nationally critical' (Freeman et al., 2010), meaning that it is considered to be within the top 10 species in New Zealand in the greatest danger of local extinction. Its occurrence on seamounts makes it vulnerable to deep-sea fishing activities that target these structures. Although fishing is believed to have greatly affected the New Zealand *I. cordiformis* population (Freeman et al., 2010), the actual impacts are not known due to limited data.

A variety of different marine species are known to consume *I. cordiformis*. It has been found in the diets of blue marlin, *Makaira nigricans* (Shimose et al., 2012); sperm whales, *Physeter macrocephalus* (Evans & Hindell, 2004); swordfish, *Xiphias gladius* (Watanabe et al., 2009); and neon flying squid, *Ommastrephes bartramii* (Watanabe et al., 2008). Very little is known of the diet of any mastigoteuthid, but one species (*Mt. psychrophila*) has been reported to consume euphausiids (Kear, 1992). Tentacular morphology (unexpanded clubs with microscopic suckers) suggests that most mastigoteuthids are passive predators, dangling their tentacles in search of prey (Dilly, Nixon, & Young, 1977; Roper & Vecchione, 1997; Vecchione et al., 2002). However, the diet of *I. cordiformis* (a species with unusually large tentacle suckers, for this family) remains completely unknown.

A variety of methods can be used to analyse the trophic ecology of a species; gut content analysis in particular is often used to determine prey. Morphological analysis of the gut contents from large squids has been previously used successfully (Bolstad & O'Shea, 2004; Ibáñez, Arancibia, & Cubillos, 2008; Stewart et al., 2012), but this approach relies on identifiable hard parts, which are often lacking in squid gut contents,

since any items that successfully traverse the oesophagus have been finely masticated by the beak (Jackson et al., 2007). However, DNA analysis can identify squid prey from even fragmentary remains and soft tissue (Deagle et al., 2005; Braley et al., 2010; Braid et al., 2012), although this approach is limited because it cannot yet be reliably used for museum material that has been formalin-fixed (see Chapter 4).

Examining the gut contents can give insight into the specific prey that a predator has consumed recently, while stable isotopes can give a more general, long-term view of the trophic role of a species; they have been used to study the trophic interactions of other squids (*e.g.,* Cherel & Hobson, 2005; Cherel et al., 2008). Stable isotopes for nitrogen can be used to infer trophic position because the tissue of predators is enriched with ^{15}N compared to their prey, while carbon, which remains relatively constant, can be used to geographically pinpoint sources of primary productivity. Fresh material gives more accurate results than museum specimens because formalin fixation alters the stable isotope composition of tissue (Edwards et al., 2002).

This aspect of the project was based on opportunistically collected samples. Several fresh specimens were available, augmented by additional gut contents from preserved museum specimens. The purpose of this study is to gain insight into the ecology of *I. cordiformis*, by (1) analysing gut contents from fresh and fixed specimens using morphology and DNA barcoding, and (2) analysing food sources and trophic position using stable isotopes ^{13}C and ^{15}N.

MATERIALS & METHODS

Specimens

Four frozen individuals of *Idioteuthis cordiformis*, and one of *Mg.* sp. nov. from New Zealand, were available for gut content and stable isotope analysis. These individuals were caught between 2003 and 2010 and kept frozen until analysis; their gut contents were preserved in 100% EtOH (Table 22). In addition, the stomach contents from one formalin-fixed *I. cordiformis* specimen (NIWA 84684, Table 22) was included for morphological examination.

Table 22—Specimen data for *Idioteuthis cordiformis* and *Magnoteuthis* sp. nov. used in this study. No collection data were available for NIWA 84390. All specimens were frozen except for NIWA 84684, which was formalin-fixed and therefore not used for DNA or stable isotopes.

Specimen ID	Species	Sex	ML (mm)	Latitude	Longitude	Date
NIWA 76653	*Mg*. sp. nov.	♂	180	39.96°S	178.18°E	23/03/2010
NIWA 84390	*I. cordiformis*	♀	820	–	–	–
NIWA 84684	*I. cordiformis*	♀	730	35.97°S	166.18°E	29/05/1998
NMNZ M.306358	*I. cordiformis*	♂	549	33.78°S	167.49°E	29/05/2003
NMNZ M.306356	*I. cordiformis*	indet.	405	34.24°S	168.35°E	3/06/2003
NMNZ M.306355	*I. cordiformis*	♂	513	34.57°S	168.94°E	3/06/2003

Morphological prey identification

Gut contents were rinsed with ethanol in a 1mm^2-mesh sieve and visually sorted into potentially identifiable items, including hard parts and tissue fragments that retained structure.

DNA barcoding prey

Individual prey items (pieces of scale, bone, or tissue) were removed and stored individually in 100% EtOH. Eight items were chosen from each gut for analysis based on morphological differences (different tissue types or colours). DNA was extracted using Xytogen Animal Extraction Kit (Xytogen, Perth, Australia), following manufacturer's instructions, except that tissue was allowed to air dry to evaporate the ethanol, rather than rinsed with water. DNA was diluted with ddH_2O to 1:10 and 1:20 before use in PCR. The DNA barcode region (Hebert et al. 2003) was amplified using primers following Braid et al. (2012); however, these samples were only sequenced in the forward direction using Folmer et al. (1994) primers. Edited sequences were compared against the Barcode of Life Data Systems (BOLD) COI Species Database (Ratnasingham & Hebert 2007; in January 2013). Species-level identifications were made using a tree-based identification method by examining neighbour-joining trees.

Stable isotopes

Muscle from the fins of five squids (four *I. cordiformis*, one *Mg.* sp. nov.) were used for stable isotope analysis for carbon and nitrogen. Approximately 700 mg of fin tissue was dried at 60°C for 48 hours. The tissue was submerged in liquid nitrogen and ground

using a mortar and pestle. Samples were sent to the Waikato Stable Isotope Unit, University of Waikato, Hamilton, New Zealand. Analysis was performed using a fully automated Europa Scientific 20/20 isotope analyser. The $\delta^{13}C$ was calculated using precalibrated C4 sucrose that is cross-referenced to Pee Dee belemnite. The $\delta^{15}N$ was calculated using a urea standard traceable to atmospheric nitrogen. Graphs were created and statistical analyses were performed using Windows Excel 2010. Trophic levels were calculated according to the equation Trophic Level = $[(\delta^{15}Nx - 3.4)/3.2] + 2.0$ from Cherel et al. (2008).

RESULTS & DISCUSSION

Morphological prey identification

No beaks or otoliths were present for species identification. The majority of prey remains in the gut contents were not identifiable. Bones and scales were found that belong to the class of bony fishes, Actinopterygii, but more precise identifications could not be made (Fig. 59A), and one unidentifiable marine organism was found that could not be identified to phylum (Fig. 59B).

Although morphological identification has been successfully used for squid gut contents previously in several studies (*e.g.,* Bolstad & O'Shea, 2004; Ibáñez, Arancibia, & Cubillos, 2008; Stewart et al., 2012), only class-level identification of prey was possible herein using morphology. Lu and Williams (1994) experienced similar difficulties in examining *Mt. psychrophila* for gut contents: out of 19 specimens, 12 had empty guts

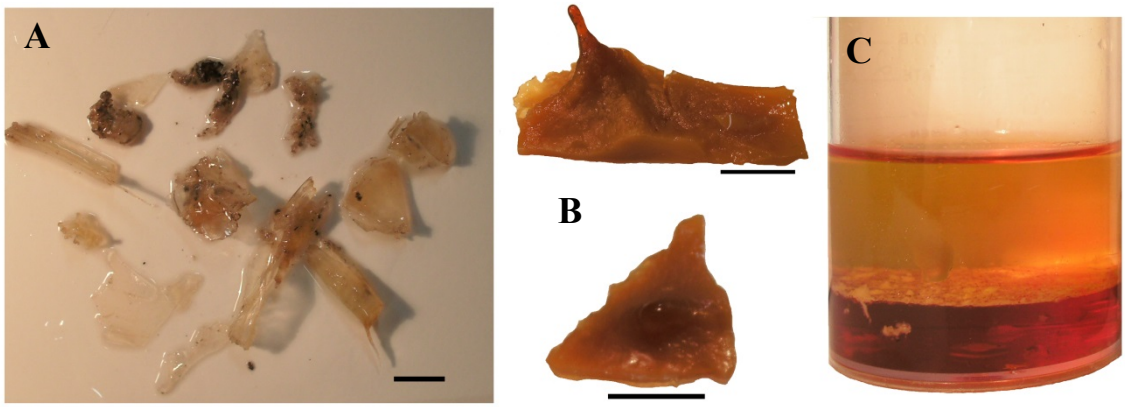

Fig. 59—Gut contents of *Idioteuthis cordiformis*. A) NMNZ M.306356, sex indet., ML 405mm; B, C) NIWA 84684, ♀, ML 730mm. A) hard parts and tissue; B) unidentifiable organism; C) orange and red oil from stomach. Scale bars = 5mm.

and the rest were missing their viscera. Gut contents are rarely found in *I. cordiformis* (Steve O'Shea, pers. comm.), so it is unsurprising that, apart from the bones and scales (likely belonging to the *Lutjanus* sp. that was identified using DNA barcoding), no visually identifiable prey items were present among the few specimens available here. Anecdotally, the only other known recognisable gut contents for *I. cordiformis* were observed in one earlier specimen that contained orange roughy (*Hoplostethus atlanticus*) otoliths (Darren Stevens, pers. comm.). A large amount of orange and red oil was found in the stomachs (Fig. 59C). Similarly, Philips, Jackson, and Nichols (2001) found a high oil content in the gut fluid of *Moroteuthis ingens*. Their fatty acid analysis of this fluid suggested that it was from myctophid fishes, which are known to contain a high level of oil (Phleger et al., 1999). Verrill (1881) also found bright orange oil in the viscera of *Mt. agassizii*, and fragments of small crustaceans in the stomach.

DNA barcoding of prey

Out of the four *I. cordiformis* individuals, only two contained gut contents suitable for DNA analysis, while the others contained only orange and red oil. Out of the 16 samples extracted, only ten samples amplified in the PCR, which is indicated with a clean band on the agarose gel. Eight of the ten sequences were not usable because they either failed or were contaminated (human or *I. cordiformis*). Two sequences were obtained that could be used for identification (Table 23). One sequence was a 100% match to the shark *Deania calcea*. The other sequence was a 100% match to *Lutjanus* sp. (three species have a 100% match: *L. lemniscatus*, *L. erythropterus*, and *L. fulvus*).

DNA barcoding successfully identified two prey species from the gut contents, while the majority of sequences recovered were contaminated. Contamination from both predators and humans are common, especially with the use of universal primers (Braid et al. 2012). Although two prey sequences were recovered from the gut contents, definitive species-level identifications could only be made for one.

Shark was an unexpected prey item because mastigoteuthids are generally believed to be passive predators (Dilly et al., 1977) who consume euphausiids (Kear, 1992). The sequence of the birdbeak dogfish, *D. calcea*, matched most closely with specimens that were from the Tasman Sea, which is near the capture location for these *I. cordiformis* specimens (Norfolk Ridge). *Deania calcea* is relatively abundant in the same depths

Table 23—Sequences from the gut contents of two individuals of *Idioteuthis cordiformis* obtained through DNA barcoding.

>M.306355_Sample1 GCTGTTTCCTGTTCTGATTTTTTGGTCACCCTGTAAGTTTAAACGACCAGATTTATAATGTAA TTGTTACAGCACATGCGTTCGTAATAATTTTCTTTATAGTAATGCCAATTATGATCGGAGGAT TTGGAAACTGACTAATCCCACTAATGATCGGAGCCCCTGACATGGCATTCCCCCGAATGAAC AACATAAGCTTTTGACTCCTCCCCCCATCATTCCTGCTGCTACTAGCCTCCTCAGGGGTAGAA GCCGGCGCTGGAACTGGGTGGACAGTGTACCCCCCTCTAGCAGGAAACCTTGCGCACGCAG GAGCATCTGTTGACCTAACTATCTTCTCCCTTCATCTGGCAGGTGTTTCTTCAATTCTGGGGG CCATTAATTTTATTACAACAATTATTAATATGAAACCCCCTGCTATCTCTCAATACCAAACAC CTCTGTTCGTCTGAGCCGTTCTAATTACCGCGGTCCTGCTTCTTCTCTCTCTCCCAGTCCTAGC TGCCGGAATTACAATGCTTCTCACAGATCGAAACCTAAACACTACTTTCTTTGACCCTGCAG GAGGAGGAGACCCCATCCTCTACCAACAC
>M.306356_Sample2 ACACTTCTGGGGGATGATCAAATCTACAATGTTATTGTAACCGCTCACGCTTTTGTAATAATC TTTTTTATAGTTATGCCCGTAATAATCGGCGGGTTCGGGAATTGATTAGTACCTTTAATAATT GGTGCACCGGATATAGCTTTTCCACGAATAAATAACATAAGCTTTTGACTATTGCCACCATC TCTTCTATTACTTTTAGCCTCTGCTGGCGTCGAAGCAGGGGCCGGAACCGGATGAACGGTTT ATCCCCCTCTTGCAGGTAATATAGCCCATGCTGGAGCATCCGTGGACTTAGCCATCTTCTCAC TCCATTTAGCCGGTATTTCCTCAATTTTAGCCTCTATTAACTTTATTACTACTATTATTAATAT AAAACCACCTGCAATTTCTCAATACCAAACCCCACTCTTTGTTTGATCTATTCTTGTGACCAC TGTCCTTCTACTACTTGCTCTCCCTGTCCTTGCCGCTGCAATTACAATACTATTAACTGACCGT AATTTAAATACAACATTTTTTGATCCAGCAGGAGGTGGGGACCCCATTCTTTACCAACATTT A

where *I. cordiformis* occurs (Zintzen et al., 2011). While surprising, it is not unreasonable to find sharks as prey of a cephalopod. There is anecdotal evidence that the giant Pacific octopus, *Enteroctopus dofleini*, has eaten the spiny dogfish, *Squalus acanthias* (Cowles, 2005). Because the gut contents here were so macerated, it was not possible to estimate the size of the prey; however, a large squid could consume a small shark or the shark may have been scavenged. Scavenging would seem unlikely as most cephalopods are active predators; however, the vampire squid, *Vampyroteuthis infernalis*, has recently been revealed as a detritivore (Hoving & Robison, 2012). Another possibility is that the squids were feeding on sharks that were caught within the net during the trawl; other large squids, such as *Dosidicus gigas*, are known to feed within the net during capture (Ibáñez et al., 2008).

The snapper sequence (*Lutjanus* sp.) was also unexpected because it is a shallow-water reef species (Newman & Williams, 1996). However, the three potential species matches for the sequence from *I. cordiformis* gut contents—*L. lemniscatus*, *L. erythropterus*, and *L. fulvus*—are all found in the Great Barrier Reef (Newman & Williams, 1996), which is west of the Norfolk Ridge. Some deep-sea fishes, such as rattails (*Coryphaenoides armatus* and *C. yaquinae*), have been shown to scavenge shallow-water carrion (Drazen et al., 2008). However, more research is needed to conclusively determine the feeding behaviour of *I. cordiformis*. The presence of

Table 24—Stable isotope results for carbon and nitrogen from *Idioteuthis cordiformis* and *Magnoteuthis* sp. nov. from New Zealand. Stable isotope δ^{15}N ‰ and δ^{13}C ‰ for each specimen are shown along with the trophic level estimated based on the equation from Cherel et al. (2008).

Species	Specimen ID	δ^{15}N ‰	δ^{13}C ‰	Estimated trophic level
Mg. sp. nov.	NIWA 76653	14.97874	-19.08108	5.6
I. cordiformis	M.306358	15.53752	-18.28440	5.7
I. cordiformis	M.306356	16.12116	-18.15976	5.9
I. cordiformis	M.306355	16.25770	-18.04250	6.0
I. cordiformis	NIWA 84390	16.60209	-17.83064	6.1

snapper could also be due to a different kind of sampling bias: secondary predation can be a significant source of error with molecular prey detection (Harwood et al., 2001; Sheppard et al., 2005), and could potentially explain the *Lutjanus* sequence.

Stable isotopes

The stable isotope values for both mastigoteuthid squids, *I. cordiformis* and *Mg.* sp. nov., correlated together and the relationship between δ^{15}N and δ^{13}C was linear, positive, and significant ($p = 0.013$, Fig. 60). The relationship between mantle length and δ^{15}N showed some correlation but is not statistically significant ($p = 0.095$, Fig. 61). Both species showed high trophic levels between 5.7 and 6.1 (Table 24).

As nitrogen passes through the food chain, it becomes enriched so it can be used to determine the trophic level at which animals are feeding (Fry, 2006). Here, there was a general trend for larger specimens to have more enriched nitrogen, and the large *I. cordiformis* were more enriched than the smaller *Mg.* sp. nov. Similarly, Cherel and Hobson (2005) found a significant linear relationship between δ^{15}N and squid size, which indicates that larger squid occupy a higher trophic position. *Idioteuthis cordiformis,* rather unexpectedly, had an estimated trophic level comparable to that of the colossal squid, *Mesonychoteuthis hamiltoni*, and higher than that of the giant squid, *Architeuthis dux* (Cherel et al., 2008), which indicates that it is a top predator in the system. Another mastigoteuthid, *Mt. psychrophila*, which is relatively small, was previously found to also have higher δ^{15}N values than the giant squid (Cherel & Hobson, 2005).

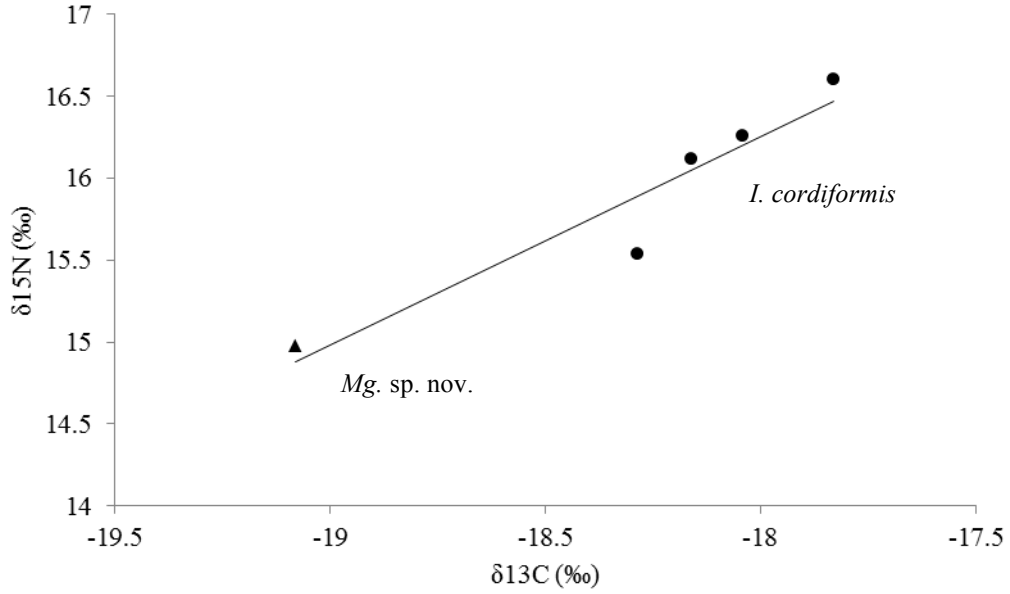

Fig. 60—Stable carbon and nitrogen isotope values of fin samples from *Idioteuthis cordiformis* (circles) and *Magnoteuthis* sp. nov. (triangle) from around New Zealand. $\delta^{15}N$ values for these squids are positively and linearly correlated with their $\delta^{13}C$ values ($y = 1.2757x + 39.218$, $R^2 = 0.902$, $p = 0.013$).

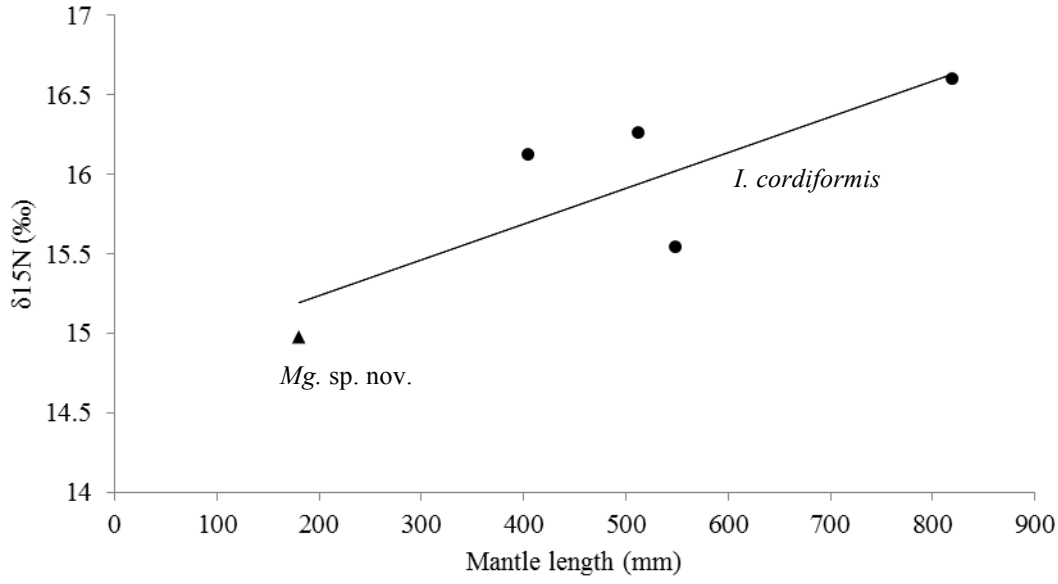

Fig. 61—Stable nitrogen isotope values from fin tissue and mantle lengths of squid *Idioteuthis cordiformis* (circles) and *Magnoteuthis* sp. nov. (triangle) from New Zealand. There is a slight positive relationship between $\delta^{15}N$ values and mantle length ($y = 0.0022x + 14.792$, $R^2 = 0.6604$, $p = 0.095$).

Unlike nitrogen, the isotope value for carbon remains relatively constant as it moves through the food chain, making carbon a helpful tool for tracing the origin of primary production for a system (Fry, 2006). Here, there was a significant correlation between the carbon and nitrogen values, which has also been found for the colossal squid (Cherel & Hobson, 2005). This correlation agrees with the latitudinal variation that has been found in the Southern Ocean in carbon and nitrogen values from particulate organic matter, which is at the bottom of food chains (François et al., 1993; Altabet & François, 1994). The markedly different carbon values for *I. cordiformis* and *Mg.* sp. nov. indicate that they occur in different regions and therefore have different sources of primary production, which means they are parts of different food webs. Carbon and nitrogen stable isotope values have been previously identified for *Deania calcea* specimens from south-eastern Australia (Pethybridge, 2010). These isotope values place *D. calcea* one trophic position lower than *I. cordiformis*, with a similar carbon value (Pethybridge, 2010), which supports it as potential prey of *I. cordiformis*.

CONCLUSION

This is the first investigation into the ecology of *I. cordiformis* using stable isotopes and DNA barcoding for gut content analysis. DNA barcoding successfully identified prey items, and stable isotope values showed that this species is a top predator. Cephalopod trophic interactions in the Southern Ocean are poorly known (Cherel & Hobson, 2005); however, it is important to study the ecological role that this species plays in order to assess the impacts that its impending disappearance could have on other deep-sea species around New Zealand. Future research should investigate the stable isotope values and gut contents of other organisms within the local ecosystem.

CHAPTER 6: General discussion and conclusions

New Zealand mastigoteuthid diversity had been previously underestimated. The species checklists by Spencer et al. (2011) listed three mastigoteuthid species in New Zealand waters: *I. cordiformis*, *Mg. magna*, and *Mt. agassizii*. Spencer et al. (2009) identified five species based on specimens in collections and published records of species. They identified *I. cordiformis*, which was confirmed in the present study. The specimen they identified as *Mg. magna* was actually *Mg.* sp. nov., which is morphologically similar but genetically distinct. The specimen they identified as *Mt.* 'sp. 1' was identified herein as *Mt. dentata*. They also listed *Mt. agassizii*, which is a closely related species found in the Atlantic, but some generic evidence suggests that local specimens may be distinct (Chapter 4). The specimen identified as *Mt.* 'sp. 2' was identified herein as *Mp. hjorti*. Herein, the following species have been identified from New Zealand waters: *Mt. dentata*, *Mt. psychrophila*, *Mt.* sp. X, *Mt.* sp. Y, *I. cordiformis*, *Mp. hjorti*, *Mg.* sp. nov., and *E. famelica*. This makes the Mastigoteuthidae the second most diverse squid family in New Zealand waters.

Genetically, all of the individuals of *I. cordiformis* sequenced here had nearly identical sequences for COI, 16S rRNA, and 12S rRNA; however, the beaks of sequenced individuals displayed extreme morphological variation (Figs 35–37). The extent of variation in beak morphology for other mastigoteuthids is not known due to limited material; however, intraspecific beak variation was also observed in *Mt. dentata* (Fig. 9) and *Mt*. sp. X (Fig. 22E–I). Variation in beak morphology has implications for dietary studies that rely on identifying prey from predator gut contents.

While *I. cordiformis* beaks can be readily distinguished from those of other mastigoteuthids by their large size, there are other giant-sized squids (ML > 1m) that occur locally. Other large squid have been identified from stomach contents of sperm whales stranded in New Zealand waters (*Architeuthis dux*, *Kondakovia longimana*, *Lepidoteuthis grimaldii*, *Mesonychoteuthis hamiltoni*, and *Taningia danae* [Gomez-Villota, 2007]), but *I. cordiformis* beaks can be readily distinguished from the beaks of these species. Ecologically, *I. cordiformis* occupies a higher trophic position than previously suspected, similar to that of the colossal squid, *Mesonychoteuthis hamiltoni* (Cherel et al. 2008). This was additionally supported by the identification of birdbeak dogfish (*Deania calcea*) from the gut contents. Further studies on the ecology of *I.*

cordiformis should be undertaken to determine the consequence of its local population decline in New Zealand waters.

Based on morphology, we consider *Mt. agassizii*, *Mt. dentata*, *Mt. psychrophila*, *Mt*. sp. X, and *Mt*. sp. Y as members of *Mastigoteuthis*; *E. famelica* and *E. atlantica* as *Echinoteuthis*; *I. cordiformis* as *Idioteuthis*; *Mp. hjorti* as *Mastigopsis*; and *Mg. magna*, *Mg. microlucens*, and *Mg*. sp. nov. as *Magnoteuthis*. These genera were supported by genetics (Fig. 55), although genetically *I. cordiformis* consistently fell outside Mastigoteuthidae and grouped with Chiroteuthidae (posterior probability of 1). However, *I. cordiformis* has morphological features that place it in Mastigoteuthidae. Chiroteuthids are characterised by tentacles with up to six series of suckers, a paralarval doratopsis stage, and a 'decorated tail' (Young & Roper, 2011a). In contrast, *I. cordiformis* has more than six series of suckers distally where the tentacle club is covered by minute, densely set suckers (resembling those of all other mastigoteuthid tentacle clubs). In addition, it seems that *I. cordiformis* does not undergo a doratopsis stage; Voss (1963) described six juvenile (ML 36–92 mm) *I. cordiformis* caught around the Philippine Islands and did not note any as doratopsis, which can reach up to ML 90 mm (Young & Roper, 2011a). Although no tail damage was noted, the gladius was not examined, and the doratopsis tail is almost always broken off on capture. Moreover, *I. cordiformis* has some characters in common with *Magnoteuthis* and *Mastigopsis*: its broad gladius, adentate or blunt-toothed arm suckers, and the absence of a funnel pocket or eye sinus photophore. Its morphological characters align it most closely with *Mp. hjorti* (although *Mp. hjorti* is genetically closest to *Mg. magna*), in that both have large fins (length ~85% ML), eye photophores, skin tubercles, and a similar mantle shape. These morphological similarities suggest that *Mp. hjorti* and *I. cordiformis* may have shared a recent common ancestor.

Other studies have found unexpected placement of mastigoteuthid species with relation to true chiroteuthids. In Lindgren's (2010) phylogenetic analysis on a wide range of Decapodiformes using both mitochondrial and nuclear genes, *Mp. hjorti* fell within the other chiroteuthid families, rather than with *Mt. agassizii* and *Mg. magna*. The Bayesian analysis of the combined phylogeny indicated that *Mt. agassizii* had a close relationship with *Mg. magna*, while *Mp. hjorti* surprisingly grouped with the Batoteuthidae. Mastigoteuthidae grouped closely with the other chiroteuthid families, but the Chiroteuthidae grouped separately and as a sister group to the chiroteuthid families.

This separation of *Mp. hjorti* from other mastigoteuthids further supports the division of this family into five genera, because although the combined phylogeny herein shows *Mastigopsis* as a sister group to *Magnoteuthis*, they should not be included in the same genus. However, since there are many morphological similarities between *I. cordiformis* and *Mp. hjorti*, and only two chiroteuthids were available to include in this study, it is too early to rearrange the classification of the chiroteuthid families.

Salcedo-Vargas & Okutani (1994) divided the Mastigoteuthidae into *Idioteuthis* and *Mastigoteuthis* based on presence/absence of integumental photophores and eye-sinus photophores, gladius width, olfactory papilla shape, and arm-sucker dentition. Although the morphological analysis herein found some support for this division, our genetic analysis was not consistent with their findings. Their use of integumental photophores for separating the genera are not in agreement with the present results. Although integumental photophores are found in many mastigoteuthids, they are not consistently present or absent in closely related species. For example, *Mg. microlucens* is genetically and morphologically similar to *Mg.* sp. nov., but integumental photophores are present in the former and absent in the latter. In addition, mastigoteuthid integumental photophores are often structurally different between species, such as *Mastigoteuthis* species and *Mg. microlucens*. The olfactory papilla of *Mt. dentata* was found in this study to be broad and short, while it is slim and long in the closely related species *Mt.* sp. Y, which does not support the use of this character for generic divisions. Arm-sucker dentition has also been suggested as a useful character for separating the genera (Salcedo-Vargas & Okutani, 1994; Salcedo-Vargas, 1995), with *Mastigoteuthis* arm suckers having sharp teeth and *Idioteuthis* arm suckers being adentate or possessing weak teeth; this is partially supported by the results of this study (Table 3). Salcedo-Vargas & Okutani (1994) additionally proposed that *Idioteuthis* and *Mastigoteuthis* should each be divided into two subgenera based on arm- and tentacle-sucker morphology, skin tubercles, gladius morphology, and funnel-locking cartilage shape. Although funnel-locking-cartilage morphology was found herein to be helpful in generic divisions, the other characters have been less consistent. In addition, some of the species placed in each subgenus by Salcedo-Vargas & Okutani conflict with the results herein. They placed *Mt. psychrophila* into *Echinoteuthis* and *Mp. hjorti* in *Idioteuthis*, which is not consistent with the molecular or morphological results herein.

The combined data also partly contradict the morphological classification of *Idioteuthis* and *Mastigoteuthis* proposed by Salcedo-Vargas (1997). Among other characters, Salcedo-Vargas (1997) used the presence of the eye-sinus photophore, presence of an antitragus in the funnel-locking cartilage, and sharp teeth on the arm suckers to diagnose *Mastigoteuthis*. However, he placed *Mg. magna* within *Mastigoteuthis*, which is inconsistent with that study's proposed criteria: in *Mg. magna*, the eye-sinus photophore is absent, the funnel-locking cartilage lacks an antitragus, and the arm suckers are adentate. The present genetic data concur that *Mg. magna* is closely related to *Mp. hjorti*, but suggest that they represent members of distinct genera. Salcedo-Vargas (1997) also classified *Idioteuthis* by the presence tubercles and *Mastigoteuthis* by their absence. In this study, the presence of skin tubercles is not a consistent generic character: they are present in *E. famelica* and *I. cordiformis,* but absent in *E. atlantica* (Vecchione & Young, 2007c), and *I. latipinna* (Sasaki, 1929). Because of inconsistencies within the Salcedo-Vargas & Okutani (1994) and Salcedo-Vargas (1997) classifications, and due to many poorly known species within the Mastigoteuthidae, Vecchione et al. (2007) only recognised the genus *Mastigoteuthis*. Although Vecchione et al. (2007) also identified the funnel pocket and eye-sinus photophore as characteristic of some species, they proposed that the former may be a pleisiomorphy, which is consistent with the results of this study.

Many different methods have been proposed for grouping species within the Mastigoteuthidae. Salcedo-Vargas & Okutani (1994) proposed two subgenera within each genus. However, in the reclassification by Salcedo-Vargas (1997), subgenera were removed and each genus was divided into three 'groups'. Vecchione et al. (2007) also divided the Mastigoteuthidae into groups based on morphological characters but retained all groups within the genus *Mastigoteuthis*. The groups that Salcedo-Vargas (1997) formed within *Mastigoteuthis* were based on funnel-locking cartilage, eye size, and eye-sinus photophore size; however, some of these groupings conflict with the current genetic results. Neither the genera proposed by Salcedo-Vargas & Okutani (1994) nor the group divisions set forth by Salcedo-Vargas (1997) were supported by the morphological examination or the combined phylogeny in this study. While Salcedo-Vargas (1997) classified *Mt. psychrophila* in the same group with *E. atlantica*, here *Mt. psychrophila* grouped more closely with *Mt. agassizii* in both individual and combined phylogenies, which is in agreement with the *Mt. agassizii* group proposed by Vecchione et al. (2007). Furthermore, Vecchione et al. (2007) classified *E. famelica* and

E. atlantica in the *glaukopis* group, which is supported by our morphological analysis; genetically, the distinction between the *Mt. agassizii* group (herein *Mastigoteuthis*) and the *glaukopis* group (herein *Echinoteuthis*) is supported by the combined phylogeny. In addition, species recognised here as *Magnoteuthis* (*Mg. magna*, *Mg. microlucens*, and *Mg. sp. nov*) with the characteristics of the *magna* group recognised by Vecchione et al. (2007) all group closely on all trees.

For some species in this family, placement remains unclear. *Mastigoteuthis pyrodes* has several unusual morphological features, including: larger tentacular suckers and eye-sinus photophore than are seen in members of the *Mt. agassizii* group, the lack of antitragus in the funnel-locking cartilage, the presence of skin tubercles, the integumental photophore placement and morphology, and the abundant chromatophores (Young & Vecchione, 2007). Unfortunately, no specimens of this species were examined or available for genetic analysis, and therefore its generic placement remains unclear. Additionally, several species (*e.g. Chiroteuthoides hastula*, *Idioteuthis okutanii*, and *Idioteuthis tyroi*) are only known from paralarval type specimens and cannot be assigned to a genus without adult specimens or material for genetic analysis.

CONCLUSIONS

Until now, the diversity of New Zealand mastigoteuthids has been underestimated; checklists have listed three (Spencer et al., 2011) to five (Spencer et al., 2009) species in New Zealand waters, while this review has identified eight. Three mitochondrial genes, 12S rRNA, 16S rRNA, and COI can all be used to separate species; of these, COI shows the greatest divergence rate (minimum distance of 6.93% for COI; Table 18). The morphological separation of these species into five genera (*Mastigoteuthis*, *Idioteuthis*, *Mastigopsis*, *Echinoteuthis*, and *Magnoteuthis*) proposed in Chapter 2 is supported by the combined phylogeny (Chapter 3). In addition, *Mg.* sp. nov. was previously reported from New Zealand as the morphologically similar species *Mg. magna*. DNA was vital in identifying this species as distinct from other *Magnoteuthis* species. This suggests that there is potentially a greater diversity of mastigoteuthids than previously suspected. Because specimens are often juvenile, badly damaged, or prey remains, it is crucial that an integrative approach to this family's systematics is applied in future reviews, and that techniques are refined for recovering DNA can be recovered from museum mastigoteuthid specimens (Chapter 4).

The threat classification for *I. cordiformis* was based on decreasing bycatch incidence in commercial fishing nets (Freeman et al., 2010), which was possible because it is large and easily recognised; threat assessment has not been possible for the smaller, less distinctive species that are less frequently encountered, but these smaller species could be similarly impacted by human activities (particularly if, as new species are identified, many existing mastigoteuthid species prove to have narrower geographic ranges than previously thought). Stable isotopes and gut contents suggest that *I. cordiformis* is a top predator (Chapter 5); the implications of its potential loss from the local waters around New Zealand remain to be seen.

REFERENCES

Adam, W. (1954). Cephalopoda. 3E Partie. IV – Céphalopodes à l'exclusion des genres *Sepia*, *Sepiella* et *Sepioteuthis*. *Siboga Expedition*, *55*, 121–199.

Allcock, A. L., Barratt, I., Eleaume, M., Linse, K., Norman, M. D., Smith, P. J., … Strugnell, J. M. (2011). Cryptic speciation and the circumpolarity debate: A case study on endemic Southern Ocean octopuses using the COI barcode of life. *Deep-Sea Research II, 58*, 242–249.

Altabet, M. A., & François, R. (1994). Sedimentary nitrogen isotopic ratio as a recorder for surface ocean nitrate utilisation. *Global Biogeochemical Cycles, 8,* 103–116.

Arkhipkin, A. I., & Laptikhovsky, V. V. (2008). Discovery of the fourth species of the enigmatic chiroteuthid squid *Asperoteuthis* (Cephalopoda: Oegopsida) and extension of the range of the genus to the South Atlantic. *Journal of Molluscan Studies*, *74*, 203–207.

Baele, G., Lemey, P., Bedford, T., Rambaut, A., Suchard M. A., & Alekseyenko, A. V. (2012). Improving the accuracy of demographic and molecular clock model comparison while accommodating phylogenetic uncertainty. *Molecular Biology and Evolution, 29*, 2157–2167.

Berry, S. S. (1909). Diagnoses of new cephalopods from Hawaiian Islands. *Proceedings of the United States National Museum 37*, 407–419.

Berry, S. S. (1920). Preliminary diagnosis of new cephalopods from the western Atlantic. *Proceedings of the United States National Museum, 58*, 293–300.

Bester, A. J., Priddel, D., & Klomp, N. I. (2010). Diet and foraging behaviour of the Providence petrel *Pterodroma solandri*. *Marine Ornithology*, *39*, 163–172.

Bolstad, K. S. R. (2010). Systematics of the Onychoteuthidae Gray, 1847 (Cephalopoda: Oegopsida). *Zootaxa, 9626* [186 pp].

Bolstad, K. S., & O'Shea, S. (2004). Gut contents of a giant squid *Architeuthis dux* (Cephalopoda: Oegopsida) from New Zealand waters. *New Zealand Journal of Zoology, 31*, 15–21.

Boyle, P. R., & Boletzky, S. V. (1996). Cephalopod populations: Definition and dynamics. *Philosophical Transactions of the Royal Society of London. Series B: Biological Sciences*, *351*(1343), 985–1002.

Braid, H. E., Deeds, J., DeGrasse, S. L., Wilson, J. J., Osborne, J., & Hanner, R. H. (2012). Preying on commercial fisheries and accumulating paralytic shellfish toxins: a dietary analysis of invasive *Dosidicus gigas* (Cephalopoda: Ommastrephidae) stranded in Pacific Canada. *Marine Biology 159*, 25–31.

Braley, M., Goldsworthy, S. D., Page, B., Steer, M., & Austin, J. J., 2010. Assessing morphological and DNA-based diet analysis techniques in a generalist predator, the arrow squid *Nototodarus gouldi. Molecular Ecology Resources, 10*, 466–474.

Buhay, J. E. (2009). 'COI-like' sequences are becoming problematic in molecular systematic and DNA barcoding studies. *Journal of Crustacean Biology, 29*, 96–110.

Carlini, D. B., Kunkle, L. K., & Vecchione, M. (2006). A molecular systematic evaluation of the squid genus *Illex* (Cephalopoda: Ommastrephidae) in the North Atlantic Ocean and Mediterranean Sea. *Molecular phylogenetics and evolution*, *41*(2), 496–502.

Cherel, Y., Ducatez, S., Fontaine, C., Richard, P., & Guinet, C. (2008). Stable isotopes reveal the trophic position and mesopelagic fish diet of female southern elephant seals breeding on the Kerguelen Islands. *Marine Ecology Progress Series, 370*, 239–247.

Cherel, Y., & Hobson, K. A. (2005). Stable isotopes, beaks and predators: a new tool to study the trophic ecology of cephalopods, including giant and colossal squids. *Proceedings of the Royal Society B, 272*, 1601–1607.
Cherel, Y., Weimerskirch, H., & Trouvé, C. (2002). Dietary evidence for spatial foraging segregation in sympatric albatrosses (*Diomedea* spp.) rearing chicks at Iles Nuageuses, Kerguelen. *Marine Biology*, *141*(6), 1117–1129.
Chun, C. (1908). Über Cephalopoden der Deutschen Tiefsee-Expedition. *Zoologischer Anzeiger 33*, 86–89.
Chun, C. (1910). Die Cephalopoden. I. Oegopsida. *Wissenschaftliche Ergebnisse der Deutschen Tiefsee-Expedition auf dem Dampfer 'Valdivia' 1898–1899*. [English Translation, Israel Program for Scientific Translations, 1975, 18, 1–552, 92 plates.]
Chun, C. (1913). Cephalopoda. *Report on the Scientific Results of the 'Michael Sars' North Atlantic Deep-Sea Expedition, 1910*, *3*, 1–28.
Clare, E., Fraser, E. E., Braid, H. E., Fenton, M. B., & Hebert, P. D. N. (2009). Species on the menu of generalist predator, the eastern red bat (*Lasiurus borealis*): Using a molecular approach to detect prey. *Molecular Ecology, 18*, 2532–2542.
Clarke, M. R. (1966). A review of the systematics and ecology of oceanic squids. *Advances in Marine Biology, 4*, 91–300.
Clarke, M. R. (1980). Cephalopoda in the diet of sperm whales of the southern hemisphere and their bearing on sperm whale biology. *Discovery Reports*, *37*, 1–324.
Clarke, M. R. (1986). *A Handbook for the Identification of Cephalopod Beaks*. Oxford, United Kingdom: Clarendon Press.
Clarke, M. R., & Roper, C. F. E. (1998). Cephalopods represented by beaks in the stomach of a sperm whale stranded at Paekakariki, North Island, New Zealand. *South African Journal of Marine Science*, *20*, 129–133.
Clarke, M. R., & Trueman, E. R. (1988). Paleontology and neontology of cephalopods. *The Mollusca*, *12*, 331–340.
Cowles, D. (2005). Enteroctopus dofleini *(Wülker, 1910)*. Retrieved January 15 2013, from http://www.wallawalla.edu/academics/departments/biology/rosario/inverts/Mollusca/Cephalopoda/Enteroctopus_dofleini.html
Cruz, J. B., Lalas, C., Jillett, J. B., Kitson, J. C., Lyver, P. O. B., Imber, M., ... & Moller, H. (2001). Prey spectrum of breeding sooty shearwaters (*Puffinus griseus*) in New Zealand. *New Zealand Journal of Marine and Freshwater Research*, *35*, 817–829.
Dai, L., Zheng, X., Kong, L., & Li, Q. (2012). DNA barcoding analysis of Coleoidea (Mollusca: Cephalopoda) from Chinese waters. *Molecular Ecology Resources, 12*, 437–447.
Deagle, B. E., Jarman, S. N., Pemberton, D., & Gales, N. J. (2005). Genetic screening for prey in the gut contents from a giant squid (*Architeuthis* sp.). *Journal of Heredity, 96*, 417–423.
Degner, E. (1925). Cephalopoda. *Report on the Danish Oceanographical Expeditions 1908–10 to the Mediterranean and Adjacent Seas*, *2*(9), 1–94.
Dell, R. K. (1959). Some additional New Zealand cephalopods from Cook Strait. *Zoology Publications from Victoria University of Wellington*, *25*, 1–12.
Dilly, P. N., Nixon, M., & Young, J. Z. (1977). *Mastigoteuthis* – the whip-lash squid. *Journal of Zoology, London, 181*, 527–559.
Drazen, J. C., Popp, B. N., Choy, C. A., Clemente, T., De Forest, L., & Smith, K. L. (2008). Bypassing the abyssal benthic food web: Macrourid diet in the eastern

North Pacific inferred from stomach content and stable isotopes analyses. *Limnology and Oceanography, 53*, 2644–2654.
Drummond, A. J., Suchard, M. A., Xie, D., & Rambaut, A. (2012). Bayesian phylogenetics with BEAUti and the BEAST 1.7. Molecular Biology and Evolution 29: 1969–1973.
Dunn, M. R., Szabo, A., McVeagh, M. S., & Smith, P. J. (2010). The diet of deepwater sharks and the benefits of using DNA identification of prey. *Deep-Sea Research I, 57*, 923–930.
Edwards, M. S., Turner, T. F., & Sharp, Z. D. (2002). Short- and long-term effects of fixation and preservation on stable isotope ratios ($\delta^{13}C$, $\delta^{15}N$, $\delta^{34}S$) of fluid-preserved museum specimens. *Copeia*, *2002*, 1106–1112.
Evans, K., & Hindell, M. A. (2004). The diet of sperm whales (*Physeter macrocephalus*) in southern Australian waters. *ICES Journal of Marine Sciences*, *61*, 1313–1329.
Fang, S. G., Wan, Q. H., & Fujihara, N. (2002). Formalin removal from archival tissue by critical point drying. *BioTechniques*, *33*, 604–611.
Fischer, H., & Joubin, L. (1907). Céphalopodes. *Expeditions Scientifiques du 'Travailleur' et du 'Talisman'*, *8*, 313–353.
Folmer, O., Black, M., Hoeh, W., Lutz, R., & Vrijenhoek, R. (1994). DNA primers for amplification of mitochondrial cytochrome *c* oxidase subunit I from diverse metazoan invertebrates. *Molecular Marine Biology and Biotechnology*, *3*, 294–299.
François, R., Altabet, M. A., & Goericke, R. (1993). Changes in the $\delta^{13}C$ of surface water particulate organic matter across the subtropical convergence in the SW Indian Ocean. *Global Biogeochemical Cycles*, *7*, 627–644.
Freeman, D. J., Marshall, B. A., Anyong, S. T., Wing, S. R., & Hitchmough, R. A. (2010). Conservation status of New Zealand marine invertebrates, 2009. *New Zealand Journal of Marine and Freshwater Research, 44*, 129–148.
Fry, B. (2006). *Stable Isotope Ecology*. New York, NY: Springer.
Gomez-Villota, F. (2007). Sperm whale diet in New Zealand (Unpublished doctoral thesis, Auckland University of Technology, Auckland, New Zealand). Retrieved from http://hdl.handle.net/10292/172
Grimpe, G. (1922). Systematische Übersicht der europäischen Cephalopoden. *Sitzungsberichte der Naturforschenden Gesellschaft zu Leipzig*, *45*, 36–52.
Guindon, S., & Gascuel, O. (2003). A simple, fast, and accurate algorithm to estimate large phylogenies by maximum likelihood. *Systematic Biology*, *52*, 696–704.
Hall, T. A. (1999). BioEdit: a user-friendly biological sequence alignment editor and analysis program for Windows 95/98/NT. *Nucleic Acids Symposium Series*, *41*, 95–98.
Harwood, J. D., Phillips, S. W., Sunderland, K. D., & Symondson, W. O. C. (2001). Secondary predation: quantification of food chain errors in an aphid-spider-carabid system using monoclonal antibodies. *Molecular Ecology*, *10*, 2049–2057.
Hebert, P. D. N., Cywinska, A., Ball, S. L., & deWaard, J. R. (2003). Biological identifications through DNA barcodes. *Proceedings of the Royal Society of London, Series B: Biological Sciences*, *270*, 313–321.
Hebert, P. D. N., & Gregory, T. R. (2005). The promise of DNA barcoding for taxonomy. *Systematic Biology*, *54*, 852–859.
Hebert, P. D. N., Penton, E. H., Burns, J. M., Janzen, D. H., & Hallwachs, W. (2004). Ten species in one: DNA barcoding reveals cryptic species in the neotropical skipper butterfly *Astraptes fulgerator*. *Proceedings of the National Academy of Sciences of the United States of America*, *101*, 14812–14817.

Hitchmough, R., Bull, L., & Cromarty, P. (2005). New Zealand Threat Classification Systems List. *Department of Conservation*, Wellington.
Horn, P. L., & Dunn, M. R. (2010). Inter-annual variability of the diets of hoki, hake, and ling on the Chatham Rise from 1990 to 2009. *Ministry of Fisheries*, Wellington.
Hoving, H. J. T., & Robison, B. H. (2012). Vampire squid: detritivores in the oxygen minimum zone. *Proceedings of the Royal Society of London, Series B: Biological Sciences*, 279, 4559–4567.
Hoyle, W. E. (1904). Reports on the Cephalopoda. *Bulletin of the Museum of Comparative Zoology, Harvard*, *43*(1), 1–72.
Ibáñez, C. M., Arancibia, H., & Cubillos, L. A. (2008). Biases in determining the diet of jumbo squid *Dosidicus gigas* (D'Orbigny 1835) (Cephalopoda: Ommastrephidae) off southern-central Chile (34°S–40°S). *Marine Research*, 62, 331–338.
Ivanova, N. V., deWaard, J. R., & Hebert, P. D. N. (2006). An inexpensive, automation-friendly protocol for recovering high-quality DNA. *Molecular Ecology Notes*, *6*, 998–1002.
Jackson, G. D., Bustamante, P., Cherel, Y., Fulton, E. A., Grist, E. P. M., Jackson, C. H., ... & Xavier, J. C. (2007). Applying new tools to cephalopod trophic dynamics and ecology: Perspectives from the Southern Ocean Cephalopod Workshop, February 2–3, 2006. *Reviews in Fish Biology and Fisheries*, *17*, 79–99.
James, G. D., & Stahl, J. C. (2000). Diet of southern Buller's albatross (*Diomedea bulleri bulleri*) and the importance of fishery discards during chick rearing. *New Zealand Journal of Marine and Freshwater Research*, *34*, 435–454.
Jokela, J., Niederegger, S., Negovetic, S., & Mutikainen, P. (2001). Mode of reproduction, ploidy and fluctuating asymmetry: Comparison of co-existing sexual and asexual freshwater snails. *Evolutionary Ecology Research*, *3*, 969–984.
Joubin, L. (1895). Contribution à l'étude des céphalopodes de l'Atlantique nord. *Résultats des campagnes scientifiques accomplies sur yacht par Albert 1er Prince souverain de Monaco*, *9*, 1–63.
Joubin, L. (1913). Éstudes préliminaires sur les céphalopodes recueillis au cours des croisières de S.A.S. le Prince de Monaco. 3e Note: *Mastigoteuthis magna* nov. sp. Bulletin de l'Institut Océanographique 275: 1–11.
Joubin, L. (1924). Résultas sur campagnes scientifiques de Prince de Monaco accomplies sur son yacht par Albert 1er Prince souverain de Monaco. *Contribution à L'Étude des Céphalopodes de l'Atlantique nord*, *4*, 1–113.
Joubin, L. (1933). Notes préliminaires sur les Céphalopodes des croisières du Dana (1921–1922), 4e Partie. *Annals de l'Institut Océanographiques*, *13*, 1–49.
Kear, A. J. (1992). The diet of Antarctic squid: comparison of conventional and serological gut contents analyses. *Journal of Experimental Marine Biology and Ecology*, *156*(2), 161–178.
Kimura, M. (1980). A simple method for estimating evolutionary rate of base substitutions through comparative studies of nucleotide sequences. *Journal of Molecular Evolution*, *16*, 111–120.
Lindgren, A. R. (2010). Molecular inference of phylogenetic relationships among Decapodiformes (Mollusca: Cephalopoda) with special focus on the squid Order Oegopsida. *Molecular Phylogenetics and Evolution*, *56*, 77–90.
Lönnberg, E. (1896). Notes on some rare Cephalopoda. *Öfversigt af Kongl. Vetenskaps-Akademiens Förhandlingar*, *53*, 603–612.

Lormann, K. B. (2008). Subcutaneous photophores in the jumbo squid *Dosidicus gigas* d'Orbigny, 1835) (Cephalopoda: Ommastrephidae). *Revista de Biología Marina y Oceanografía*, *43*, 275–284.
Lu, C. C., & Williams, R. (1994). Contribution to the biology of squid in the Prydz Bay region, Antarctica. *Antarctic Science*, *6* (2), 223–229.
MacDonald, R., & Clench, W. J. (1934). Descriptions of a new genus and two new species of squids from the North Atlantic. *Occasional Papers of the Boston Society of Natural History*, *8*, 145–152.
Mattern, T., Houston, D. M., Lalas, C., Setiawan, A. N., & Davis, L. S. (2009). Diet composition, continuity in prey availability and marine habitat–keystones to population stability in the Snares Penguin (*Eudyptes robustus*). *Emu*, *109*, 204–213.
Meier, R., Zhang, G., & Ali, F. (2008). The use of mean instead of smallest interspecific distance exaggerates the size of the 'barcoding gap' and leads to misidentification. *Systematic Biology*, *57*, 809–813.
Mensch, R. (2010). A systematic review of the squid genus *Chiroteuthis* (Mollusca: Cephalopoda) in New Zealand waters (Unpublished master's thesis, Auckland University of Technology, Auckland, New Zealand). Retrieved from http://hdl.handle.net/10292/1041
Mintzer, V. J., Gannon, D. P., Barros, N. B., & Read, A. J. (2008). Stomach contents of mass-stranded short-finned pilot whales (*Globicephala macrorhynchus*) from North Carolina. *Marine Mammal Science*, *24*, 290–302.
Naef, A. (1921–1923). Cephalopoda. *Fauna and Flora of the Bay of Naples*, *35*, 1–917.
Nesis, K. N. (1977). *Mastigoteuthis psychrophila* sp. n. (Cephalopoda, Mastigoteuthidae) from the Southern Ocean. *Zoologichesky Zhurnal*, *56*(6), 835–842.
Nesis, K. N. (1980). Taxonomic position of *Chiroteuthis famelica* Berry (Cephalopoda, Oegopsida). *Byulleten Moskovskogo Obshchestva Ispytatelei Prirody (Otdel Biologicheskii)*, *85*(4), 59–66.
Nesis, K. N., 1987. *Cephalopods of the World; Squids, Cuttlefishes, Octopuses, and Allies*. Neptune City, NJ: TFH Publications.
Newman, S. J., & Williams, D. M. (1996). Variation in reef associated assemblages of the Lutjanidae and Lethrinidae at different distances offshore in the central Great Barrier Reef. *Environmental Biology of Fishes*, *46*(2), 123–138.
Nigmatullin, C. M., Nesis, K. N., & Arkhipkin, A. I. (2001). A review of the biology of the jumbo squid *Dosidicus gigas* (Cephalopoda: Ommastrephidae). *Fisheries Research*, *54*, 9–19.
Nixon, M. (1998). The radulae of cephalopoda. *Smithsonian Contributions to Zoology*, *586*, 39–53.
Palmer, A. R., & Strobeck, C. (1986). Fluctuating asymmetry: Measurement, analysis, patterns. *Annual Review of Ecology and Systematics*, *17*, 391–421.
Parsons, P. A. (1992). Fluctuating asymmetry: a biological monitor of environmental and genomic stress. *Heredity*, *68*, 361–364.
Pethybridge, H. R. (2010). Ecology and physiology of deepwater chondrichthyans off southeast Australia: mercury, stable isotope and lipid analysis (Unpublished doctoral thesis, University of Tasmania, Australia). Retrieved from ori-oai.u-bordeaux1.fr/pdf/2010/PETHYBRIDGE_HEIDI_2010.pdf
Pfeffer, G. (1900). Synopsis der oegopsiden Cephalopoden. *Mitteilungen aus dem Naturhistorischen Museum Hamburg*, *17*, 147–198.
Pfeffer, G. (1912). *Die Cephalopoden der Plankton-Expedition: Zugleich eine monographische Übersicht der Oegopsiden Cephalopoden*. Kiel, Germany: Verlag von Lipsius & Tischer.

Phillips, K. L., Jackson, G. D., & Nichols, P. D. (2001). Predation on myctophids by the squid *Moroteuthis ingens* around Macquarie and Heard Islands: Stomach contents and fatty acid analyses. *Marine Ecology Progress Series*, *215*, 179–189.

Phleger, C. F., Nelson, M. M., Mooney, B. D., & Nichols, P. D. (1999). Wax esters versus triacylglycerols in myctophid fishes from the Southern Ocean. *Antarctic Science*, *11*(4), 436–444.

Rancurel, P. (1971). *Mastigoteuthis grimaldii* (Joubin, 1895) Chiroteuthidae peu connu de l'Atlantique tropical (Cephalopoda-Oegopsida). *Cahiers ORSTOM. Série Océanographie*, *9*, 125–145.

Rancurel, P. (1972). *Mastigoteuthis inermis* espèce nouvelle de Chiroteuthidae du Golfe de Guinée (Cephalopoda, Oegopsida). *Extrait du Bulletin de la Société Zoologique de France*, *97*, 25–34.

Rancurel, P. (1973). *Mastigoteuthis hjorti* Chun 1913 description de trios échantillons provenant du Golfe de Guiée (Cephalopoda, Oegopsida). *Cahiers ORSTOM. Série Océanographie*, 11, 27–32.

Ratnasingham, S., & Hebert, P. D. N. (2007). BOLD: The Barcode of Life Data System (http://www. barcodinglife. org). *Molecular Ecology Notes*, *7*(3), 355–364.

Ratnasingham, S., & Hebert, P. D. N. (2013). A DNA-based registry for all animal species: The Barcode Index Number (BIN) System. *Public Library of Science One*, *8*(7): e66213.

Roper, C. F. E., & Lu, C. C. (1990). Comparative morphology and function of dermal structures in oceanic squids (Cephalopoda). *Smithsonian Contributions to Zoology*, *493*, 1–40.

Roper, C. F. E., & Vecchione, M. (1997). *In situ* observations test hypothesis of functional morphology in *Mastigoteuthis* (Cephalopoda, Oegopsida). Vie et Milieu, *47* (2), 87–93.

Roper, C. F. E., & Voss, G. L. (1983). Guidelines for taxonomic descriptions of cephalopod species. *Memoirs of the National Museum Victoria*, *44*, 48–63.

Roper, C. F. E., & Young, R. E. (2013). Chiroteuthis *Orbigny, 1841*. Retrieved September 28, 2013 from http://tolweb.org/Chiroteuthis/19462

Roper, C. F. E., Young, R. E., & Voss, G. L. (1969). An illustrated key to the families of the order Teuthoidea (Cephalopoda). *Smithsonian Contributions to Zoology*, *13*, 1–32.

Rosecchi, E., Tracey, D. M., & Webber, W. R. (1988). Diet of orange roughy, *Hoplostethus atlanticus* (Pisces: Trachichthyidae) on the Challenger Plateau, New Zealand. *Marine Biology*, 99, 293–306.

Rosso, J. J., Mabragana, E., Gonzalez Castro, M., & Diaz De Astarloa, J. M. (2012). DNA barcoding Neotropical fishes: recent advances from the Pampa Plain, Argentina. *Molecular Ecology Resources*, *12*, 999–1011.

Salcedo-Vargas, M. A. (1993). *Revision of the Squid Family Mastigoteuthidae (Mollusca: Cephalopoda) from the Northwest Pacific* (Unpublished doctoral thesis). Tokyo University of Fisheries, Tokyo, Japan.

Salcedo-Vargas, M. A. (1995). Systematic value of the ultrastructure of the sucker surface in the squid family Mastigoteuthidae (Mollusca: Cephalopoda). *Contributions to Zoology*, *65*, 65–77.

Salcedo-Vargas, M. A. (1997). Cephalopods from the Netherlands Indian Ocean Programme (NIOP)-II. Mastigoteuthid lineage and related forms. *Beaufortia*, *47*, 91–108.

Salcedo-Vargas, M. A., & Okutani, T. (1994). New classification of the squid family Mastigoteuthidae (Cephalopoda: Oegopsida). *Venus*, *53*, 119–127.

Salcedo-Vargas, M. A., & Young, R. E. (2007). Mastigoteuthis tyroi *Salcedo-Vargas, 1997*. Retrieved May 1, 2013 from http://tolweb.org/Mastigoteuthis_tyroi/19526

Santos, M. B., Pierce, G. J., Herman, J., Lopez, A., Guerra, A., Mente, E., & Clarke, M. R. (2001). Feeding ecology of Cuvier's beaked whale (*Ziphius cavirostris*): A review with new information on the diet of this species. *Journal of the Marine Biological Association of the United Kingdom*, *81*, 687–694.

Sasaki, M. (1916). Notes on oegopsid cephalopods found in Japan. *Annotationes Zoologicae Japonenses*, 9, 89–120.

Sasaki, M. (1929). A monograph of the dibranchiate cephalopods of the Japanese and adjacent waters. *Journal of the College of Agriculture*, *20*, 1–357.

Shapiro, B., Rambaut, A., & Drummond, A. J. (2006). Choosing appropriate substitution models for the phylogenetic analysis of protein-coding sequences. *Molecular Biology and Evolution*, *23*, 7–9.

Sheppard, S. K., Bell, J., Sunderland, K. D., Fenlon, J., Skervin, D., & Symondson, W. O. C. (2005). Detection of secondary predation by PCR analyses of the gut contents of invertebrate generalist predators. *Molecular Ecology*, *14*, 4461–4468.

Shimose, T., Yokawa, K., Saito, H., & Tachihara, K. (2012). Sexual difference in the migration pattern of blue marlin, *Makaira nigricans*, related to spawning and feeding activities in the western and central North Pacific Ocean. *Bulletin of Marine Science*, *88*, 231–250.

Simon, C., Frati, F., Beckenbach, A., Crespi, B., Liu H., & Flook, P. (1994). Evolution, weighting, and phylogenetic utility of mitochondrial gene sequences and a compilation of conserved polymerase chain reaction primers. *Annals of the Entomological Society of America*, *87*, 651–701.

Sin, Y. W., Yau, C., & Chu, K. H. (2009). Morphological and genetic differentiation of two loliginid squids, *Uroteuthis (Photololigo) chinensis* and *Uroteuthis (Photololigo) edulis* (Cephalopoda: Loliginidae), in Asia. *Journal of Experimental Marine Biology and Ecology*, *369*, 22–30.

Söller, R., Warnke, K., Saint-Paul, U., & Blohm, D. (2000). Sequence divergence of mitochondrial DNA indicates cryptic biodiversity in *Octopus vulgaris* and supports the taxonomic distinctiveness of *Octopus mimus* (Cephalopoda: Octopodidae). *Marine Biology*, *136*, 29–35.

Song, H., Buhay, J. E., Whiting, M. F., & Crandall, K. A. (2008). Many species in one: DNA barcoding overestimates the number of species when nuclear mitochondrial pseudogenes are coamplified. *Proceedings of the National Academy of Sciences of the United States of America*, 105, 13486–13491.

Spencer, H. G., Marshall, B. A., & Willan, R. C. (2009). Phylum Mollusca: Clams, snails, chitons, squids, octopuses and their kin. In D. P. Gordon (Ed.) *The New Zealand Inventory of Biodiversity: A Species 2000 Symposium Review* (pp. 196–219). Christchurch, New Zealand: University of Canterbury Press.

Spencer, H. G., Willan, R. C., Marshall B. A., & Murray, T. J. (2011). Checklist of the recent Mollusca recorded from the New Zealand exclusive economic zone. Retrieved April 30, 2013, from http://www.molluscs.otago.ac.nz/

Stewart, J. S., Field, J. C., Markaida, U., Gilly, W. F. (2012). Behavioral ecology of jumbo squid (*Dosidicus gigas*) in relation to oxygen minimum zones. *Deep-Sea Research II* in press http://dx.doi.org/10.1016/j.dsr2.2012.06.005

St-Onge, M., LaRue, B., & Charpentier, G. (2008). A molecular revision of the taxonomic status of mermithid parasites of black flies from Quebec (Canada). *Journal of Invertebrate Pathology*, *98*, 299–306.

Strugnell, J. M., & Lindgren, A. R. (2007). A barcode of life database for the Cephalopoda? Considerations and concerns. *Reviews in Fish Biology and Fisheries*, 17, 337–344.

Tamura, K., Peterson, D., Peterson, N., Stecher, G., Nei, M., & Kumar, S. (2011).

MEGA5: Molecular evolutionary genetics analysis using maximum likelihood, evolutionary distance, and maximum parsimony methods. *Marine Biology and Evolution*, *28*, 2731–2739.

Tang, E. P. Y. (2006). *Path to effective recovering of DNA from formalin-fixed biological samples in natural history collections: Workshop summary*. Washington, DC: National Academies Press.

Tao, N., Bruno, W. J., Abfalterer, W., Moret, B. M. E., Leitner, T., & Kuiken, C. (2005). FINDMODEL: a tool to select the best-fit model of nucleotide substitution. Retrieved October 20, 2012 from http://hcv.lanl.gov/content/sequence/findmodel/findmodel.html.

Taylor, J. D., & Lewis, A. (1995). Diet and radular morphology of *Peristernia* and *Latirolagena* (Gastropoda: Fasciolariidae) from Indo-Pacific coral reefs. *Journal of Natural History*, *29*, 1143–1154.

Thiele, J. (1935). *Handbook of Systematic Malacology Part 3*. English translation by J. S. Bhatti, 1998. Washington, DC: Smithsonian Institution Libraries.

Thompson, J. D., Higgins, D. G., & Gibson, T. J. (1994). CLUSTAL W: Improving the sensitivity of progressive multiple sequence alignment through sequence weighting, position specific gap penalties and weight matrix choice. *Nucleic Acids Research*, *22*, 4673–4680.

Toussiant, R. K., Scheel, D., Sage, G. K., & Talbot, S. L. (2012). Nuclear and mitochondrial markers reveal evidence for genetically segregated cryptic speciation in giant Pacific octopuses from Prince William Sound, Alaska. *Conservation Genetics*, *13*, 1483–1497.

Vecchione, M., Roper, C. F. E., Widder, E. A., & Frank, T. M. (2002). In situ observations on three species of large-finned deep-sea squids. *Bulletin of Marine Science*, *71*(2), 893–901.

Vecchione, M., Roper, C. F. E., Sweeney, M. J., & Lu, C. C. (2001). *Distribution, relative abundance and developmental morphology of paralarval cephalopods in the Western North Atlantic Ocean.* A Scientific Paper of the Fishery Bulletin, NOAA Technical Report NMFS 152.

Vecchione, M. ,& Young, R. E. (2006a). Magnapinna talismani *(Fischer and Joubin, 1907)*. Retrieved April 15, 2013 http://tolweb.org/Magnapinna_talismani/52212

Vecchione, M., & Young, R. E. (2006b). Mastigoteuthis agassizii: *Type description with notes on the syntype and squid from type locality*. Retrieved April 30, 2013 from http://tolweb.org/notes/?note_id=4004

Vecchione, M., & Young, R. E. (2007a). Mastigoteuthis danae *(Joubin, 1933)*. Retrieved April 5, 2013 from http://tolweb.org/Mastigoteuthis_danae/19511/2007.11.19

Vecchione, M., & Young, R. E. (2007b). Mastigoteuthis agassizii *Verrill, 1881*. Retrieved April 16, 2013 from http://tolweb.org/Mastigoteuthis_agassizii/19508

Vecchione, M., & Young, R. E. (2007c). Mastigoteuthis atlantica *Joubin, 1933*. Retrieved April 5, 2013 from http://tolweb.org/Mastigoteuthis_atlantica/19509/2007.11.19

Vecchione, M., & Young, R. E. (2007d). Mastigoteuthis hjorti *Chun, 1913*. Retrieved May 17, 2013 from http://tolweb.org/Mastigoteuthis_hjorti/19517

Vecchione, M., & Young, R. E. (2010a). Mastigoteuthis magna *Joubin, 1913*. Retrieved April 5, 2013 from http://tolweb.org/Mastigoteuthis_magna/19520/2010.08.15

Vecchione, M., & Young, R. E. (2010b). Mastigoteuthis magna: *Description continued.* Retrieved April 5, 2013 from http://tolweb.org/notes/?note_id=3917

Vecchione, M., & Young, R. E. (2013). *Magnapinnidae Vecchione and Young, 1998.* Magnapinna *Vecchione and Young, 1998. Bigfin squid*. Retrieved Sept. 28, 2013 from http://tolweb.org/Magnapinna

Vecchione, M., Young, R. E., & Lindgren, A. (2007). *Mastigoteuthidae Verrill, 1881.* Mastigoteuthis *Verrill, 1881. Whip-lash squid.* Retrieved April 5, 2013 from http://tolweb.org/Mastigoteuthis/19453/2007.11.19

Verrill, A. (1881). Report on the cephalopods and on some additional species dredged by the U.S. Fish Commission Steamer 'Fish-hawk', during the season of 1880. *Bulletin of the Museum of Comparative Zoology, Harvard*, *8*, 99–116.

Victor, B. C., Hanner, R. H., Shivji, M., Hyde, J., & Caldow, C. (2009). Identification of the larval and juvenile stages of the Cubera Snapper, *Lutjanus cyanopterus*, using DNA barcoding. *Zootaxa*, *2215*, 24–36.

Vollossiouk T., Robb E. J., & Nazar, R. N. (1995). Direct DNA extraction for PCR-mediated assays of soil organisms. *Applied and Environmental Microbiology*, *61*, 3972–3976.

Voss, G. L. (1956). A review of the cephalopods of the Gulf of Mexico. *Bulletin of the Marine Science of the Gulf and Caribbean*, *6*, 85–178.

Voss, G. L. (1963). *Cephalopods of the Philippine Islands*. *United States National Museum Bulletin*, *234*, 1–180.

Voss, G. L. (1977). Present status and new trends in cephalopod systematics. *Symposia of the Zoological Society of London*, *38*, 49–60.

Watanabe, H., Kubodera, T., Ichii, T., Sakai, M., Moku, M., & Seitou, M. (2008). Diet and sexual maturation of the neon flying squid *Ommastrephes bartramii* during autumn and spring in the Kuroshio–Oyashio transition region. *Journal of the Marine Biological Association of the United Kingdom*, *88*, 381–389.

Watanabe, H., Kubodera, T., & Yokawa, K. (2009). Feeding ecology of the swordfish *Xiphias gladius* in the subtropical region and transition zone of the western North Pacific. *Marine Ecology Progress Series*, *396*, 111–122.

West, J. A., & Imber, M. J. (1986). Some foods of Buller's mollymawk *Diomedea bulleri*. *New Zealand Journal of Zoology*, *13*, 169–174.

Wienecke, B., & Robertson, G. (2006). Comparison of foraging strategies of incubating king penguins *Aptenodytes patagonicus* from Macquarie and Heard islands. *Polar Biology*, *29*(5), 424–438.

Xavier, J., Croxall, J., Trathan, P., & Rodhouse, P. (2003). Inter-annual variation in the cephalopod component of the diet of the wandering albatross, *Diomedea exulans*, breeding at Bird Island, South Georgia. *Marine Biology*, *142*(3), 611–622.

Xie, W., Lewis, P. O., Fan, Y., Kuo L., & Chen, M. H. (2011). Improving marginal likelihood estimation for Bayesian phylogenetic model selection. *Systematic Biology*, *60*, 150–160.

Xiong, B., & Kocher, T. D. (1991). Comparison of mitochondrial DNA sequences of seven morphospecies of black flies (Diptera: Simuliidae). *Genome*, *34*, 306–311.

Young, R. E. (1972). The systematic and areal distribution of pelagic cephalopods from the seas off southern California. *Smithsonian Contributions to Zoology*, *97*, 1–159.

Young, R. E. (1991). Chiroteuthid and related paralarvae from Hawaiian waters. *Bulletin of Marine Science*, *49*, 162–185.

Young, R. E. (2009). *Joubiniteuthidae Naef, 1922.* Joubiniteuthis portieri *Joubin, 1916*. Retrieved September 28, 2013 from http://tolweb.org/Joubiniteuthidae/19450

Young, R. E. (2010). Mastigoteuthis famelica *(Berry, 1909)*. Retrieved April 15, 2013 from http://tolweb.org/Mastigoteuthis_famelica/19513

Young, R. E., Lindgren, A., & Vecchione, M. (2008). *Mastigoteuthis microlucens*, a new species of the squid family Mastigoteuthidae (Mollusca: Cephalopoda). *Proceedings of the Biological Society of Washington*, *121*, 276–282.

Young, R. E., & Roper, C. F. E. (2009). *Batoteuthidae Young and Roper, 1968.* Batoteuthis skolops *Young and Roper, 1968*. *The Bush-club Squid.* Retrieved September 28, 2013 from http://tolweb.org/Batoteuthidae/19452
Young, R. E., & Roper, C. F. E. (2011a). *Chiroteuthidae Gray, 1849.* Retrieved April 5, 2013 from http://tolweb.org/Chiroteuthidae/19451/2011.11.22
Young, R. E., & Roper, C. F. E. (2011b). *Grimalditeuthis Joubin, 1898.* Grimalditeuthis bonplandi *(Verany, 1839)*. Retrieved September 28, 2013 from http://tolweb.org/Grimalditeuthis/19463
Young, R. E., & Roper, C. F. E. (2011c) Asperoteuthis *Nesis, 1980*. Retrieved September 28, 2013 from http://tolweb.org/Asperoteuthis/19461
Young, R. E., & Vecchione, M. (2003). *Promachoteuthidae Naef, 1912.* Promachoteuthis *Hoyle, 1885*. Retrieved September 28, 2013 from http://tolweb.org/Promachoteuthidae/19454
Young, R. E., & Vecchione, M. (2004). *Mastigoteuthidae: Doubtful and questionable species.* Retrieved April 15, 2013 from http://tolweb.org/notes/?note_id=2643
Young, R. E., & Vecchione, M. (2006). Mastigoteuthis schmidti: *Description from Degner, 1925.* Retrieved April 15, 2013 from http://tolweb.org/notes/?note_id=3932
Young, R. E., & Vecchione, M. (2007a). Mastigoteuthis agassizii *group*. Retrieved April 28, 2013 from http://tolweb.org/Mastigoteuthis_agassizii_group/65306
Young, R. E., & Vecchione, M. (2007b). Mastigoteuthis pyrodes *Young, 1972.* Retrieved April 15, 2013 from http://tolweb.org/Mastigoteuthis_pyrodes/19523
Young, R. E., & Vecchione, M. (2007c).Mastigoteuthis glaukopis *group*. Retrieved April 16 2013, from http://tolweb.org/Mastigoteuthis_glaukopis_group/65305
Young, R. E., & Vecchione, M. (2007d). Mastigoteuthis magna *group.* Retrieved April 5, 2013 from http://tolweb.org/Mastigoteuthis_magna_group/65303
Young, R. E., & Vecchione, M. (2007e). Mastigoteuthis *type beta.* Retrieved April 15, 2013 from http://tolweb.org/Mastigoteuthis_type_beta/65357
Young, R. E., & Vecchione, M. (2007f). Mastigoteuthis agassizii*: Description of beaks*. Retrieved May 1, 2013 from http://tolweb.org/notes/?note_id=4484
Young, R. E., & Vecchione, M. (2007g). Mastigoteuthis dentata *Hoyle, 1904*. Retrieved April 15, 2013 from http://tolweb.org/Mastigoteuthis_dentata/19512
Young, R. E., & Vecchione, M. (2008). *Chiroteuthid families*. Retrieved April 15, 2013 from http://www.tolweb.org/Chiroteuthid_families/19410
Young, R. E., & Vecchione, M. (2010). Mastigoteuthis psychrophila *Nesis, 1977*. Retrieved April 15, 2013 from http://tolweb.org/Mastigoteuthis_psychrophila/19522
Young, R. E., Vecchione, M., & Lindgren, A. (2008). Mastigoteuthis microlucens *Young, Lindgren & Vecchione 2008*. Retrieved April 28, 2013 from http://tolweb.org/Mastigoteuthis_microlucens/65304
Zhang, J. (2010). Exploiting formalin-preserved fish specimens for resources of DNA barcoding. *Molecular Ecology Resources*, *10*, 935–941.
Zheng, X., Lin, X., Lu, C., & Ma, R. (2012). A new species of *Cistopus* Gray, 1849 (Cephalopoda: Octopodidae) from the East and South China Seas and phylogenetic analysis based on the mitochondrial COI gene. *Journal of Natural History*, *46*, 355–368.
Zintzen, V., Roberts, C. D., Clark, M. R., Williams, A., Althaus, F., & Last, P. R. (2011). Composition, distribution and regional affinities of the deepwater ichthyofauna of the Lord Howe Rise and Norfolk Ridge, south-west Pacific Ocean. *Deep Sea Research Part II: Topical Studies in Oceanography*, *58*, 933–947.